



City Research Online

City, University of London Institutional Repository

Citation: Fneer, M. K. (1997). Development of Fibre Optic Based Ammonia Sensor For Water Quality Measurement. (Unpublished Doctoral thesis, City, University of London)

This is the accepted version of the paper.

This version of the publication may differ from the final published version.

Permanent repository link: <https://openaccess.city.ac.uk/id/eprint/30824/>

Link to published version:

Copyright: City Research Online aims to make research outputs of City, University of London available to a wider audience. Copyright and Moral Rights remain with the author(s) and/or copyright holders. URLs from City Research Online may be freely distributed and linked to.

Reuse: Copies of full items can be used for personal research or study, educational, or not-for-profit purposes without prior permission or charge. Provided that the authors, title and full bibliographic details are credited, a hyperlink and/or URL is given for the original metadata page and the content is not changed in any way.

Development of Fibre Optic Based Ammonia Sensor For Water Quality Measurement

By

Mohamed K. Fneer

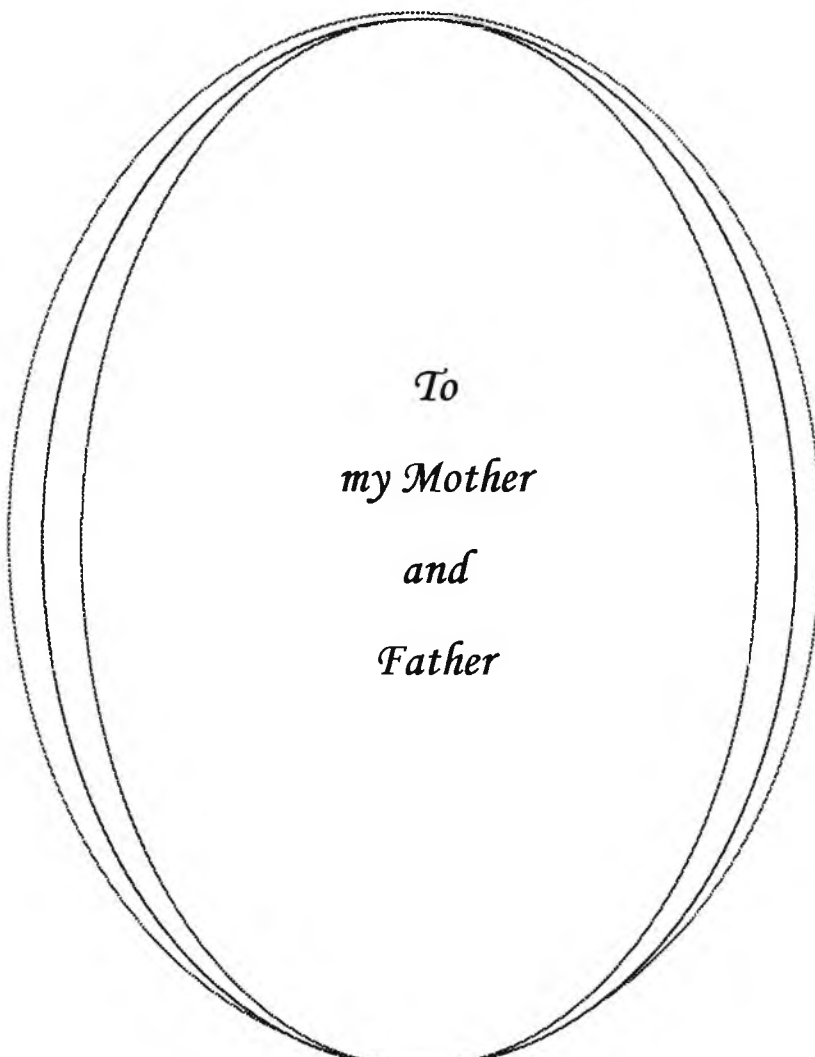
**A thesis submitted to City University for the Degree of Doctor of Philosophy
in Electrical and Electronic Engineering**

**City University
Measurement and Instrumentation Centre
Department of Electrical, Electronic and Information Engineering
Northampton Square, London EC1V 0HB**

June 1997

*Knowledge is proud that he has learn'd so much; Wisdom
is humble that he knows no more.*

William Cowper 1731-1800



To
my Mother
and
Father



The construction of the Fibre Optic Ammonia-Based Sensor Experiment

List Of Headings

Table of Contents	i
List of Tables and Figures	ix
Acknowledgement	xii
Declaration	xiii
Abstract	xiv
List of Units	xv

Chapter 1 Introduction and Background

1.1 Introduction	1
1.1.1 Analytical Instrumentation	1
1.1.2 Sensors and Chemical Sensors	2
1.2 Aim and Objective of this Work	6
1.3 Structure of the Thesis	8
1.4 Analytical Methods for Chemical Species	10
1.4.1 Electrochemical Analysis of Water	10
1.4.2 Chromatographic Methods of Analysis	11
1.4.3 Optical Methods of Analysis	12
1.4.3.1 Absorption Methods	13
1.4.3.2 Ultraviolet Spectrophotometry	14
1.4.3.3 Infrared Spectrophotometry	15
1.5 Fibre Optic Sensor Systems	16
1.5.1 Sensor Definition	16
1.5.2 Fibre Optic Sensors	17
1.5.3 Advantages of FOS Technology	18
1.5.4 Fibre Optic Limitations in Sensing	19
1.5.5 Fibre Optic Sensor Instrumentation	19

1.5.5.1 Fibre Optic Sensor Configuration	20
1.6 The Reagent Phase	22
1.6.1 Absorption-based Sensors	23
1.6.2 Fluorescence-based Sensors	23
1.6.3 Phosphorescence-based Sensors	24
1.6.4 Chemiluminescence-based Sensors	24
1.7 Examples of Fibre Optic Chemical Sensors	24
1.7.1 pH (Hydrogen ion Concentration)	24
1.7.2 Ammonia Sensors	27
1.8 Application Fields and Sensors Markets	28
1.9 Summary	30
1.10 References	32

**Chapter 2 The General Theory of Chemical Sensors
and Implementation of Fibre Optic Systems**

2.1 Abstract	35
2.2 Design and Specification of the Chemical Sensors	36
2.2.1 Outline of the Model	36
2.2.2 Behaviour of the Model	37
2.2.3 Thermodynamic and Kinetic Considerations	40
2.2.3.1 Thermodynamics	41
2.2.3.2 Kinetics	43
2.2.3.3 Transport	44
2.3 Fibre Optics	45
2.3.1 Multimode Fibres	46
2.3.2 Single Mode Fibres	47
2.4 Fibre Optic Parameters and Characteristics	48
2.4.1 The Numerical Aperture	48
2.4.2 The V Number	49
2.5 The Structure of the Fibres	50

2.5.1 Step-Index Fibre	51
2.5.2 Graded Index Fibre	52
2.5.3 Loss Mechanisms Within Fibre	52
2.5.3.1 Absorption	52
2.5.3.2 Scattering	53
2.5.3.3 Bulk and Wavelength Imperfections	55
2.5.4 Fibre Bending	55
2.5.4.1 Fibre Coupling	57
2.5.5 Mechanical Effects	58
2.6 Fibre Reliability	58
2.7 Optical Emission and Detection Systems	59
2.7.1 Light Sources	59
2.7.2 LED Technology	60
2.7.3 Characteristics of LEDs	60
2.7.4 Temperature Effects on LEDs	61
2.8 LEDs and Chemical Sensing	62
2.9 Light Detectors	64
2.9.1 Junction Diode	64
2.9.2 Photomultiplier	65
2.9.3 Avalanche Photodiode	66
2.10 Summary	67
2.11 References	68

Chapter 3 pH Measurement With Dyes Preliminary Investigation on Optical re Ammonia Based Sensor Using Colorimetric Techniques

3.0 Abstract	71
3.1 Introduction	72
3.1.1 Theoretical Considerations	72
3.1.2 Measurement of hydrogen-ion Activity	73
3.1.3 pH Concept	74
3.2 The Measurement of pH	74
3.2.1 pH Measurement Using Colorimetric Techniques	76

3.2.3 Focusing in Fibre Optic pH Sensor	77
3.3 Colour Indicators	78
3.4 Spectral Properties of Dyes	79
3.4.1 Phthalein	80
3.4.2 Sulphonphthalein	80
3.4.3 Azo Indicators	80
3.5 Choice of the Acid-Base Indicator	80
3.5.1 Phenol red Indicator Dye	81
3.5.2 The Blue LEDs Intensity	82
3.5.3 Effect of other Solvents to Indicators	83
3.6 Relationship between Light Absorbance and pH	85
3.6.1 Choice of the Parameters to be Determinated	87
3.6.2 Referencing Scheme	89
3.7 Summary	90
3.8 References	92

Chapter 4 Design and Implementation of a Computer Controlled Fibre Optic pH Sensor

4.0 Abstract	93
4.1 Time Multiplexed Wavelength Fibre Optic pH Sensor	94
4.2 Referencing Scheme	95
4.3 Design of the Sensor	96
4.3.1 Optical Arrangement	96
4.3.1.1 Optical Link	96
4.3.1.2 The Probe Head Design and Construction	97
4.3.1.3 Light Sources	98
4.3.2 Electronic System	100
4.3.2.1 Clock Signal Generation	101
4.3.2.2 Detection and Signal Processing Circuits	103
4.3.2.3 Optical Detector	106
4.3.2.4 Amplifier	108
4.3.2.5 Interference Rejection	108

4.4 Output Signal Separation	110
4.4.1 Error Considerations	113
4.5 Summary	114
4.6 References	115
<i>Chapter 5 Feasibility Study for The Design of a Fibre Optic Ammonia Sensor Based on Absorption of the Green Light and Changes of the Indicator Dye Colour</i>	
5.0 Abstract	116
5.1 Ammonia Nitrogen	117
5.2 Environmental Significance of Nitrogen Data	117
5.2.1 Water Quality Treatments	117
5.2.2 Nutritional and Related Problems	118
5.3 Established Analytical Methods for Ammonia Measurements	118
5.3.1 Colorimetric Methods	119
5.4 Electrochemical Methods.	121
5.4.1 The Potentiometric Method.	122
5.4.2 The Glass Membrane pH Sensor as Ammonia Sensor.	123
5.4.3 Cation Ammonia Sensor.	124
5.4.4 Ammonia Gas-Permeable-Membrane Sensing Electrode.	125
5.4.5 Conductimetric Sensor.	126
5.4.6 Amperometric Ammonia Sensor.	127
5.4.7 Semiconductor Based Ammonia Sensor.	129
5.4.8 IR Methods for Ammonia Analysis.	130
5.5 General Comparison of the Analytical Techniques.	131
5.6 New Optical Techniques for ammonia Analysis.	132
5.7 Theoretical Aspects of Membrane Based Ammonia Sensor.	133
5.7.1 Chemical Equilibrium Model.	135
5.7.2 Modelling Diffusion in the Sensor Cell.	139
5.7.3 Modelling the Absorbance of Light.	141
5.8 Simulation of the Membrane-Based Ammonia Sensor.	142
5.8.1 Main Aspects of the Simulation Model.	142

5.8.2 Values for Diffusion Constants in the Membrane and the Cell. ...	144
5.8.3 Initial Results of Model.	145
5.9 Summary.	149
5.10 References.	151

Chapter 6 Design Construction and Evaluation of a Multi-Wavelength-Based Optical Fibre Ammonia Sensor for Water Quality Measurements.

6.0 Abstract.	154
6.1 Data Sampling in the Measurement Process.	155
6.1.1 Performance Specification.	155
6.2 Measurement Scheme.	156
6.2.1 Referencing Signal.	156
6.2.2 Error in the System.	156
6.3 The Description of the Ammonia Sensor.	157
6.3.1 Optical System.	159
6.3.2 Light Source.	159
6.3.3 Computer Based Controller.	160
6.3.4 Chemical Aspects of the Optorode.	161
6.4 Design of the Fibre Optic Probe.	161
6.4.1 Sensor Response Function.	162
6.4.2 Path Length.	163
6.4.3 The Acid Dissociation.	163
6.4.4 Molar Absorptivity of the Indicator Dye.	164
6.4.5 Temperature Effect.	164
6.5 Mathematical Model Simulation.	165
6.5.1 Model Assumption.	167
6.5.2 Simulation Results.	167
6.6 Manufacturing The Sensor Head.	170
6.7 Experimental Procedure.	170
6.7.1 Sample Preparation.	170
6.7.1.1 pH Adjuster.	172
6.7.1.2 The Internal Filling Solution.	172

6.8 The Electronic System.	173
6.9 Sensor Calibration.	173
6.10 Experimental Validation.	175
6.10.1 Assessment of the original.	175
6.11 Assessment of the modified design.....	179
6.12 Validation of the new sensor head.....	180
6.13 Separation of the optical dye.	181
6.14 Long term running and dynamic response.	184
6.15 Summary.	185
6.16 References.	186

Chapter 7 Conclusions

7.1 The Thesis Summary.	187
7.2 Further Work.	191
7.3 References.	193

<u>List of Publications</u>	194
--	-----

Appendix 1 Design Drawings and Notes for Fibre Optic Probe

General Drawings.	195
Tooling.	196
Cell Dimensions.	196
Head Drawing.	196

Appendix 2 Calculation of the Inflexion Point

Calculation of the Inflexion Point.	203
--	-----

Appendix 3 Figure 6.17 Experimental data.

Data of Figure 6.17.	206
---------------------------	-----

Appendix 4 Sensor Software

Sensor Software program. 208

Appendix 5 Cost Estimation of The FOBAS.

Cost Estimation of The Fibre Optic Based Ammonia Sensor(FOBAS). 216

Appendix 6 Some of publication papres out of this thesis

List of Tables and Figures

Tables

- Table 1.1** Major Instrumental techniques for chemical analysis.
Table 1.2 Typical application fields for chemical & biochemical sensors.
Table 1.3 World-wide demand of sensors for medical applications 1988-2000 in UK £.
Table 1.4 World-wide demand of sensor for environmental protection 1990-2000.
Table 3.1 Example of dyeindicators used for acid base titration.
Table 3.2 Dissociation constant of the acidic forms of some indicators in ethyl alcohol.
Table 5.1 Activity constants for the chemical reactions in the simulated ammonia sensor.
Table 5.2 Values of diffusion constant in the model.
Table 6.1 The set of ammonia samples.

Figures.

Chapter 1.

- Fig. 1.1** Range of wavelengths for different types of radiant energy.
Fig. 1.2 Basic components for measurement of absorption.
Fig. 1.3 Instrumentation of a typical fibre optic sensing system.
Fig. 1.4 (a) and (b) Possible configuration of FOS.
Fig. 1.4 (c) and (d) Possible configuration of FOS.
Fig. 1.5 pH sensor of Peterson.
Fig. 1.6 Ammonia sensor of Shahriari and Zhou.
Fig. 1.7 Ammonia vapour waveguide sensor of Giuliani.

Chapter 2.

- Fig. 2.1** Schematic representation of an equilibrium state fibre optic sensor.
Fig. 2.2 Relationship between analyte concentration and reagent phase.
Fig. 2.3 The change in free energy associated with the reaction between analyte and reagent.
Fig. 2.4 Graph showing the relationship between diffusion coefficient and diffusion distance, for three time periods.
Fig. 2.5 Schematic of fibre optic.
Fig. 2.6 The angle of acceptance of fibre using ray propagation theory.
Fig. 2.7 The light propagating through different types of fibre.
Fig. 2.8 Ray light scattering.
Fig. 2.9 Types of fibre losses.
Fig. 2.10 Broadening due to temperature (-153 to +25 °C) occurring in the emission of GaP LED with an acceptor concentration of 10^{+18} cm^{-3} .

Chapter 3.

- Fig. 3.1** pH scale.
Fig. 3.2 Schematic drawing of a pH electrode based on potentiometric techniques.

Fig. 3.3 Absorption spectra of phenol red in a sample of distilled water at different pH values: 4, 7 and 11.

Fig. 3.4 Absorption of indicator as a function of wavelength for pH values.

Fig. 3.5 The blue LEDs Intensity at a various current in mA.

Fig. 3.6 Variation of the ratio (p/p_{ref}) calculated as a function of $pH-pK_{ind}$ with different values of m.

Chapter 4.

Fig. 4.1 Set-up of the time multiplexed dual wavelength fibre optic pH meter.

Fig. 4.2 Positioning of the emitter and receiver fibres in the probe head.

Fig. 4.3 Schematic design of the probe head for the first configuration.

Fig. 4.4 Spectrum of the green LED at various driving current intensities.

Fig. 4.5 Block diagram of the electronic circuit used in the implementation.

Fig. 4.6 Schematic diagram of the timing signals.

Fig. 4.7 Perturbation which appears as an overshoot as a result of the limited frequency response of the detector.

Fig. 4.8 Schematic diagram of the electronic circuit used for the emitter.

Fig. 4.9 Block diagram of the detector and signal processing circuit.

Fig. 4.10 Schematic diagram of the electronic circuit used for the receiver.

Fig 4.11 Spectral response of the detector amplifier module.

Fig 4.12 Frequency response of the detector-amplifier module.

Fig 4.13 Sample signal through the separation stage using sample and hold devices.

Fig. 4.14 Calibration curve for the pH sensor.

Chapter 5.

Fig. 5.1 A typical set up for potentiometric system.

Fig. 5.2 Schematic of FET Sensor

Fig. 5.3 One dimensional model of sensor showing array of elements used in the..

Fig. 5.4 Dependence of the concentration of the various species in the sensor ..

Fig. 5.5 Finite element used for analysis in equation 5.11.

Fig. 5.6 Absorbance spectra of phenol red (2.5%) for various pH values.

Fig. 5.7 Flow Chart for sensor simulation model.

Fig. 5.8 Simulated response of the 'small volume sensor using unbuffered indicator.

Fig. 5.9 Simulated response of the 'small volume sensor using buffer Ind.

Fig. 5.10 Simulated response of sensor to step change in ammonia concentration..

Fig. 5.11 Concentration profiles for the four species after 0.8 second.

Fig. 5.12 Simulated response of the concentration profile of the two indicator species to prolonged exposure to ammonia.

Chapter 6.

Fig. 6.1 Schematic diagram of the experiment set-up.

Fig. 6.2 Spectra of the green LEDs at a various current.

Fig. 6.3 Software flow chart.

Fig. 6.4 Schematic Design of the fibre optic sensor head

Fig. 6.5 Effect of indicator Pk_a on the simulation response.

Fig. 6.6 Mathematical simulation module for the design of optical fibre probe.

Fig. 6.7 Received power by the receiving fibre in proposed probe.

- Fig. 6.8** Simulation results of received power.
Fig. 6.9 Contour map of received power.
Fig. 6.10 Ammonia sensor calibration to pH as an early procedure to ammonia analysis.
Fig. 6.11 Optical fibre ammonia sensor response to different NH_3 concentrations.
Fig. 6.12 Electrochemical ammonia electrode response to different concentrations.
Fig. 6.13 Calibration of the fibre optic sensor
Fig. 6.14 Calibration of the electrochemical sensor
Fig. 6.15 The new sensor after several modifications.
Fig. 6.16 The new Optical fibre sensor response to ammonia without buffer.
Fig. 6.17 The new Optical fibre sensor response to ammonia using buffer.
Fig. 6.18 Camcorder recording the ammonia diffusion through the membrane wall.
Fig. 6.19 Long time running and sensor recovery.

Chapter 7.

- Fig. 7.1** The New Fibre Optic Ammonia Sensor after several modifications.
Fig. 7.2 Shape recognition and hydrophobic bound in biological system.

Appendices

Appendix 1 Design Drawing

- Fig. A1.1** Exploded views of components.
Fig. A1.2 Assembly views.
Fig. A1.3 Sensor Jacket (Material: clear acrylic).
Fig. A1.4 Fibre Holder (Material: rigid polyurethane).
Fig. A1.5 Window screw (Material: rigid polyurethane).
Fig. A1.6 Mirror (Material: A2 Stainless steel).
Fig. A1.7 Sealing plug (Material: A2 Stainless steel)
Fig. A1.8 O-rings (Material: Medium nitride)

Appendix 3

- Table. A5.1** Ammonia Samples of 1ppm, 10ppm, and 100ppm.

Acknowledgements

First and foremost, I would like to express my appreciation to my supervisor, Professor K.T.V. Grattan for his guidance and steadfast support and to my co-supervisor, Dr. W.J.O. Boyle, for his encouragement and advice, during the course of this thesis. I shall remain deeply indebted to both for their patience and perseverance which has enabled me to progress to this stage of my educational development.

I wish to acknowledge the support of the Libyan Ministry of Higher Education whose financial support provided me with the opportunity to study. Their financial support is highly appreciated.

I would like to thank the secretarial and the technical staff, for their help especially Mr. R. A. Valsler, Mr. B. Orrin, Mr. L. Frampton and Mr. B. Burns. I much appreciate the help of my colleagues, Mr. M. Belz, Mr. J. Bourilkov, Mr. W. Zgallai, Mr. Dan. Valsler, Mr. J. El-shawish and all other researchers at the Instrumentation Centre.

The many suggestions made by Dr. Z. Mouaziz were extremely productive. I am grateful for his meticulous reviewing of the manuscript. His friendship and support has been invaluable.

I am indebted to Dr. Junichi Kurata of Kansai University Japan for his help to monitor ammonia diffusion using video camera and image processing techniques. His friendship shall always be valued.

My appreciation extends to Dr. N. Kelly of SouthBank University who assisted in the chemistry experimental work especially, in the membrane behaviours. His help has enabled me to overcome many problems.

I am grateful to my wife and daughter for their enduring patience and their support without which I could not achieve this goal.

Finally, I would like to pay a special tribute to my parents, sisters and brothers who have supported me in many ways throughout the course of my studies and to whom this thesis is dedicated.

Declaration

I grant powers of discretion to the University Librarian to allow this thesis to be copied in whole or in part without further reference to the author. This permission covers only single copies made for study purposes, subject to normal conditions of acknowledgements

Abstract

The feasibility and the design of a fibre-optic based sensor for measurement of the concentration of molecular species dissolved in aqueous solutions has been investigated. The use of optical fibres as an alternative approach to the use of conventional optical procedures has been demonstrated to show significant advantages in terms of cost and flexibility in design as well as sensitivity and reliability in the measurement.

Apart from the first two chapters, which review the field and outline the theoretical background to the sensor operation, the work reported is experimentally based with an appropriate theoretical foundation, culminating in the construction of a fibre-optic sensor for the detection of dissolved ammonia in water. The sensor is based upon an absorption technique in which the change in the optical spectrum with the concentration of ammonia dissolved in water is monitored. This technique is used with a small volume of indicator dye mixed with an ammonia buffer solution, which is injected into the sensor chamber. This dye is linked into a optical fibre and the optical absorptivity at an absorption peak of the indicator dye is determined via the transmission through the optical fibre.

The construction of the sensor is described, it consisting of two major parts: (a) the production of the sensor head, and (b) the interfacing of this head into a computer-based controller. The sensor head consists of three major components, a mixture of the indicator dye with a buffer solution, the optical fibre and the membrane mechanism. The sensing material includes the pH-indicating dye phenol red, ammonium chloride (NH_4Cl) as a buffer and distilled water. This mixture was injected into the small sensor chamber which was sealed and surrounded by an ion selective membrane for ammonia detection, then interfaced into a fibre optic bundle. This enables the sensing material to be in direct contact with the end of the fibres, and hence penetrated by the ammonia samples.

The operation of the sensor is thus that ammonia gas, to be detected, dissolved in to the water contained in the samples, changes the pH of the dye. This induces a change in the optical absorption of the dye mixture because of the change in the colour of the phenol red. This change is probed, via the fibre optic, in terms of the light propagating along the transmitting fibres. The resultant decrease in transmitted intensity can be related to ammonia gas concentration. In the case of pH, an accuracy of ± 0.05 pH units was achieved and for the ammonia monitor $\pm 100 \mu\text{g/l}$ ammonia concentration was obtained with a reproducibility in the order of $\pm 3\%$.

Finally the sensor is evaluated for its overall suitability for ammonia detection. The best sensor constructed can detect dissolved ammonia gas concentration over the range 0 to 2 %, to an accuracy and lower detection limit potential in the parts per million region. The sensor has an extremely rapid response, less than 0.2 seconds

List of Units

γ_i	Coefficient of activity.
ψ	Proportionality constant between light sources.
ϵ	Coefficient of extinction.
ϵ	Molar absorptivity in chapter 6 (equ. 6.1).
Δ	Error symbol.
ν	Wave number.
λ	Wavelength.
ω	Angular of frequency.
Ω	Resistance units.
β	Reflected and incident angle at a core cladding interface.
θ	Angle of the lunched beam.
A	Absorption.
LED	Light Emitting Diode.
L, L	Path length.
[Ind]	Concentration of the dissociated part of the chemical dye.
[Hind]	Concentration of undissociated part of the dye.
FOS	Fibre Optic Sensors.
NA	Numeric aperture of the fibre.
pH	Logarithm of concentration of hydrogen ion.
pK_{ind}	Logarithm of the equilibrium constant of dye,
K	Equilibrium constant of indicator.
N_o	Index of refraction of air.
V	Volume.
R	Reagent phase (chapter 2).
A	Analyte phase (chapter 2).
C	Constant physical in AR (chapter 2 equ. 2.3).
C	Concentration.
ΔG^{++}	Energy barrier.
T	Temperature.
IR	Infrared.
ϕ	The angle between the receiving fibre and the transmitter fibre (chapter 6).
dm	The distance between the transmitted fibre and the mirror.
ppm	Parts per million.
NH_3	Chemical symbol for ammonia.
dB	Decibel.
κ	Boltzman constant.
L_f	Fresnel losses.
m	Constant of the pH meter.
n_w	Refractive index of water.
H_2O	Chemical symbol for the water.
X	Small distance in the sensor cell (chapter 5).

D	Diffusion rate of ammonia in and out of the sensor cell.
M	Molar
X_m	The maximum distance in the sensor cell.
X_0	The minimum distance in the sensor cell.
[]	Symbol brackets for the ion concentrations.
{ }	Symbol brackets for the ion activity.
H_3O^+	Hydronium ion.
PC	personal computer.
AR	The bound reagent-analyte species (chapter 2).
P	pressure.
n_1	Refractive indices of the fibre core.
n_2	Refractive indices of the fibre cladding.
SNR	Signal to noise ratio.
N_T	Total concentration of ammonia species (chapter 5).
J_i	Flow of species I.
pK_a	Acid dissociated constant.

Chapter 1

Introduction and Background

1.1 Introduction

1.1.1 Analytical Instrumentation

A variety of sensitive instruments have been developed in recent years, which has increased considerably the engineer's ability to measure and cope with determining and quantifying pollution material of increasing complexity. Instrumental methods of analysis are finding wide usage for routine monitoring of air quality, groundwater and surface water quality, and soil contamination, as well as during the course of water flow in waste treatment. Such methods have often allowed analytical measurements to be made immediately at source, and have permitted the recording of such data to be made at some distance from the place of actual measurement. In addition, they have extended considerably the range of inorganic and organic chemicals that can be monitored and the concentrations that can be detected and quantified. A variety of sensing methods are now routinely used both for investigation the extent of contamination and for routine monitoring of treatment effectiveness.

The electrochemical pH meter and spectrophotometer are analytical instruments that were developed several decades ago, and have now become seemingly indispensable in environmental control. However, these instruments have been reduced in size and modified over the years in shape and configuration but still they are expensive and require careful handling. Today, environmental analysis engineers looking for a wider variety of sensors and instruments that can be reliable, easy to use and overall are cheap in price, also having a long life, accuracy in operation and ideally being maintenance free. This gap in analytical instrumentation between expectation and reality needs to be filled by the further development of sensors that bring with them a greater sensitivity and reliability to meet the new legislation driving pollution control.

However, these targets are not easy to achieve in one single instrument and the market need is to fill this gap and cope with the rising requirements of chemical pollution monitoring. The measurement of ammonia is of great importance not only in medical science but also in environmental, forensic, food science as well as in enzyme-based assays where ammonia serves as an indicator species for many enzymatically-degradable nitrogenous compounds.

Numerous methods of ammonia determination for this purpose have been introduced, and some of them are available commercially. However, so far none of these methods satisfies all the commonly specified needs for a simple, reliable, cheap and stable ammonia sensor. At the same time, for example similar basic needs for a glucose sensor have been fulfilled by the development of a device based on the use of the amperometric method. This kind of sensor is now commercially available as a disposable sensor strip, equipped with a pen-sized potentiostat^[1].

1.1.2 Sensors and Chemical Sensors

Sensors can be classified into two main categories for the purpose of this work sensors of physical parameters such as temperature, pressure, light intensity, magnetic field strength, and chemical sensors, for the detection of various atomic, molecular and ionic species.

An example of the former type is a thermocouple, which generates a voltage dependent upon the temperature of the junction, and an example of the latter is the pH electrode, which generates a voltage dependent upon the concentration of hydrogen ions in solution. These two classes of sensor are very different in that the number of chemical parameters in which there is interest is almost infinite, but they are often very similar in nature, as opposed to sensors for physical parameters where there are far fewer, but distinctively different parameters to determine.

This thesis is concerned with chemical sensors, (and more specifically fibre optic chemical sensors). The word 'sensor' is to be taken as synonymous with 'chemical sensor'. In addition, so called 'sensors' have been devised that are irreversible.

Ideally a sensor should have the following characteristics: continuous reading of the measurand over a wide range with accuracy and high sensitivity, be selective to the measurand of interest, respond rapidly, having long term stability, and be of low cost. Meeting all these criteria in one device may prove to be impossible, particularly regarding selectivity and lifetime.

However, depending upon the application a reasonable compromise should be possible for many situations. Sensors are required for many uses, and currently there is a great demand for simple and inexpensive devices for applications as diverse as industrial process control and use in life support systems. This demand has spurred a world-wide research effort in the field of sensors, both in academic circles and industry.

In medicine, significant interest exists in the area of medical diagnostics with low cost sensors replacing the traditional laboratory analytical techniques, leading to more widespread monitoring of patients, and thus obvious health benefits^[2]. Also in this field there is a growing interest in applying sensors to intensive care monitoring, to assess and optimise a patient's biochemical condition and hence increase the chance of survival of critically ill patients^[3].

Industry has a great interest in the use of sensors for the control of the manufacturing process in order to maximise productivity and optimise product quality^[4]. Sensors are also required for industry to meet increasingly stringent safety requirements, e.g. for the detection of toxic and explosive gases. The environment, and man's effect upon it, is currently of great concern, and here too sensors are finding application. Examples include the use of sensors to optimise the combustion process in automobile engines to reduce the emission of toxic gases^[5], and in sensors to monitor water quality^[6].

Longer term research is also being undertaken into more ambitious applications of sensors, such as the construction of an 'artificial nose' consisting of a matrix of various sensors linked to a signal processor^[7], which is able to sense the subtle

chemistry of flavours and smell, for example differentiating between fresh and stale food. Another sensor application is to produce an artificial pancreas, consisting of an implantable glucose sensor linked to an insulin pump^[8].

Such a device could improve the quality of life for millions of diabetics it has even been proposed that such a system could be incorporated into a wrist watch. Beside these examples where sensors are specifically required, there are many other situations where, if a suitable sensor were available, it could be applied to the advantage of the user. The realisation of sensors suitable for applications such as the above is by no mean an easy task. Chemical sensors can be said essentially to consist of two parts:

(i) A zone of selective chemistry (the reagent phase or sensing material) which interacts with the measurand selectively.

(ii) A more or less non-specific transducer which produces useful output signal dependent upon the state of the sensing material.

However, the distinction between these two regions is not always clear. It is the reagent phase where the actual chemistry involved in the operation of the sensors occurs, where major progress is required, and where the research effort is being concentrated. There are many approaches which have been taken in constructing chemical sensors; excellent reviews cover the area in detail^[9,10,11]. Briefly, some of the more common sensing methods include:

(a) conductance-based devices in which the measurand interacts with the surface of a material oxide (or organic semiconductors) to induce a change in bulk conductance.

(b) electrochemical devices where the measurand takes an active role in an electrochemical system, e.g. ion-selective electrodes.

(c) chemically sensitive field effect transistors (Chem-FETs) whose characteristics are altered by the presence of the chemical species being adsorbed on to the surface of the device.

(d) mass-sensitive devices consisting of a piezoelectric resonator whose resonant frequency is changed by the measurand absorbing on to the surface of a reagent coating material.

(e) optically-based devices in which the measurand interacts with a sensing material changing its optical properties, which is then detected by some optical system. In the final category of devices, by far the most common type of sensor is the fibre optic sensor.

Low attenuation optical fibres, generally forming part of fibre optic cables were introduced in the mid-1970s and have revolutionised communications technology. However, in recent years, fibre optic technology has started to enter the field of chemical and biochemical sensors. The advantages of such technology make it highly desirable for application to such sensors. Optical fibre technology has offered substantial advantages, often incorporating spectroscopic analytical methods in the ultraviolet-visible and infrared parts of the spectrum which were also well suited to the design of the sort of quantitative measuring instruments which can solve many of the problems of existing instruments.

In this work, the author has studied the use of the absorption of electromagnetic radiation in the visible part of the spectrum as a quantitative technique which lies at the heart of the design of an optical fibre-based instrument. These techniques were intended for the measurement of parameters associated with various substances dissolved in aqueous solutions, such as ammonia gas.

Fibre optics have proven to be a promising technology for use in the development of such sensors, for several reasons. Optical fibres are insensitive to electromagnetic interference (EMI) and can be configured to sense a variety of chemical and physical

effects, including temperature, pressure, electric field strength, magnetic field strength, stress and strain^[12]. Their small size allows optical fibres to be integrated with various composite systems without compromising the structural integrity of the part involved. Integration can be either internal or external. However, the advantages of this technology will be illustrated in greater detail later in this chapter.

1.2 Aim and Objectives of this Work.

This research work has aimed specifically to investigate optical fibre-based techniques for sensing ammonia gas dissolved in water. This can be used as a basis for the development of a simple, reliable, selective, sensitive and cheap sensor for ammonia concentration monitoring.

One of the primary objectives of this research work was to investigate a possible solution to the problems associated with existing instrumentation and to provide a scientific basis for the design and production of cost-effective sensing systems. In this thesis, a practical implementation of the absorption characteristics of light was investigated to relate to the concentration of chemical species using optical fibre systems and this activity may be summarised as follows:

- Analysis of the basic physical phenomena underlying the process of light absorption by the chemical molecules and establishing a quantitative relationship, through the use of several approaches, termed as direct and indirect measurements.
- Investigation of the use of colorimetric techniques as a means of an indirect measurement of the concentration of the chemical species and to consider their advantages as well as their limitations for a fibre optic implementation.
- Design of a simple fibre optic-based colorimetric instrument to measure the pH, in this case using phenol red indicator dye.

- Analysis of the application of a direct method carried out on a widely used and important chemical species i.e. ammonia, and of its optical characteristics to employ the visible part of the spectrum in the analysis.
- Design and implementation of a fibre optic based ammonia sensor which can also be used for other chemical species detection, by changing the sensor selective-membrane involved or with a small modification in the system software program.
- Discussion of the direct analytical method in conjunction with the fibre optic approach in order to design and build a sensor with potentially wider industrial applications.
- General comparison of the experimental results of this work with the characteristics of literature devices and commercially available conventional sensors, such as the Orion ammonia electrode.

The work which is subsequently described has been divided in two parts:

In the first part of this research work, colorimetric techniques were employed, having been modified to suit optical fibre use and comprising the monitoring of the change of colour of organic dyes, mainly with the use of phenol red for the quantitative measurement of the concentration of the hydronium ion (H_3O^+), expressed in terms of pH units.

In this approach, for example using the colorimetric method, one scheme was mainly deployed in order to provide the appropriate optical reference signal. This signal was used to optimise the measurement of the sensor system. In this option, the reference signal was generated externally using a Light Emitting Diode (LED) which emits light at a wavelength where the absorption profile of the dye remains unchanged with the change of the absorption as a function of pH values.

In this work, the measurement of the ammonia concentration proceeded using the same principle that was used for the measurements of pH, the difference being that an ammonia selective membrane was incorporated with an ammonium chloride as a buffer solution in the sensor cell. In this approach, the ammonia was detected by direct measurement without adding other chemical species to the sensor system or the indicator dye. This research was conducted using the same wavelengths as were used in the pH measurements. However, this approach required a modification to the data analysis which relates the measurement of the pH of the sample to the concentration of ammonia, contrast to the pH measurements.

A fibre optic-based ammonia sensor system was designed, constructed and evaluated in light of the published water industry specifications and providing the requisite control commands, e.g. a display of the analytical data which could be plotted graphically. Furthermore, the sensor was controlled by using a computer where the data could be analysed and stored for a long periods of time, providing valuable information for further system implementations and research into appropriate data analysis.

1.3 Structure of the Thesis

This thesis describes several developments of a fibre optic sensor based upon the use of absorption of light by the chemical species under investigation, but also providing development work on optical devices reported in the literature. This is achieved by using the fibre optic approach with the intention to produce a practical device that utilises cheap and reliable optoelectronic technology, e.g. LEDs as opposed to gas lasers, and photodiodes as opposed to more complex photomultipliers (PMTs). It is also intended that the design be suitable for further development, as unfortunately many of the fibre optic sensors developed to date, such as the CO₂ sensor of Hirschfeld et al^[13] and the pH sensor of Peterson et al^[14], do not appear to have been developed beyond that in the early literature reports.

The project is largely experimentally based. The structure of the thesis is designed with Chapter 1 as an introduction to the subject with aims and objectives clearly stated and the structure itself spelt out. Chapter 2 and the early part of Chapter 3 are used to outline the essential theory and the essence of the sensor materials involved. In Chapter 3, in considering the subject of pH measurement with dyes, this covers the interaction between light in the visible range and dyes in general, and phenol red as the selected dye in particular.

This is discussed with the implication that it has for a fibre optic system theoretically, reflecting what is implemented experimentally in Chapter 4. The major experimental part of the project is described in Chapter 4, this covering the electronic design of the sensor and a description of the methods and components used is given. An analysis of the results detailed on the sensor performance is provided and error considerations are discussed. Chapter 5 reports a feasibility study on the design of a fibre optic-based ammonia sensor that uses the same principle of measurement as electrochemical sensors.

The major new implementation is through the use of a fibre optics incorporating a computer-based controller. A mathematical model for the ammonia measurement study, well established and scientifically valid and the results of a simulation were developed and compared. Chapter 5 also describes the full manufacturing parameters of the system and the sensor head design steps.

A mathematical model and simulation of the ammonia sensor are described in Chapter 5. In Chapter 6 the author's report on the evaluation of the fibre optic based-ammonia sensor as well as on the conventional electrode sensor and the results are analysed and discussed. Finally the work is summarised and conclusions are drawn in Chapter 7, with suggestions as to possible directions for further work.

1.4 Analytical Methods for Chemical Species

There are several methods and techniques regularly employed for the detection of chemical species in aqueous solutions. However, these techniques can be grouped in to four major categories, as shown in Table 1.1, although other methods beyond these exist.

These methods of analytical analysis are often applied to chemical species in general and here seen in relation to ammonia in particular. However, its worth giving a brief outline of the general analytical methods employed in chemical analysis.

<i>Major Instrumental Methods of Analysis</i>			
Spectroscopy	Electrochemical	chromatography	Miscellaneous
Absorption and emission spectroscopy.	Conductometry.	Gas chromatography.	Thermal analysis.
Fluorimetry.	Potentiometry.	liquid chromatography	Mass spectroscopy.
Polarimetry.	Voltametry.		Kinetic techniques.
Refractometry.	Electrogravimetry.		Hybrid.
Raman effect.	Coulometry.		
Electron spin resonance.			

Table 1.1 Major Instrumental techniques for chemical analysis

1.4.1 Electrochemical Analysis of Water

Electrical methods of analysis make use of the relationships between electrical and chemical phenomena. Such methods are particularly useful in water chemistry, as they lend themselves to continuous monitoring and recording. The method on which the conventional pH meter is based is probably the most widely used method of analysis. In this case a glass electrode and a reference electrode are inserted in a solution, and the electrical potential or voltage across these electrodes is a measure of the concentration of the hydrogen ions in the solution. Methods based upon this principle are said to be *potentiometric*.

In other electrical methods, suitable electrodes are introduced into a solution and a small measured voltage is applied. The current which flows is dependent upon the composition of the solution and so may be used to make analytical measurements.

Methods based upon this principle are said to be *polarographic*. There are many modifications to the different electrical methods of analysis, and the distinctions between them are not always readily apparent.

However, there are other electroanalytical methods that have not been discussed in any detail in this thesis, because this work is primarily concerned with a *fibre optic* method of analysis. *Conductimetry*, which measures the ability of a solution to carry a current, and *coulometry*, which is a measure of the equivalence relationship between the quantity of electricity required to effect a given quantity of chemical charge are often methods frequently used. More detailed information can be obtained from any text book on physical chemistry.^[15]

1.4.2 Chromatographic Methods of Analysis

Chromatography is the general term used to describe the set of different procedures used to separate components in a mixture based upon their relative affinity to partitioning between different phases. For example, carbon dioxide is more soluble in water than methane, so that if both gases were present in a sample of air that was brought into contact with water, carbon dioxide would partition more strongly into the water than would methane.

This property, which is different for different molecules, can be used to bring about their separation. Chromatography comes in two different types one being the stationary phase and the other the moving phase. The stationary phase may be either a liquid or a solid, and the moving phase may be either a liquid or a gas. When the mobile phase is a gas, the procedure is termed *gas chromatography*, and when it is a liquid it is called *liquid chromatography*. Although chromatography is reported to be widely used and can provide results in the sub-ppm range, it is expensive, and is difficult to employ as a basic method of an on-line measurement system such as the system deployed in this work.

1.4.3. Optical Methods of Analysis

Optical methods of analysis measure the results of an interaction between radiant energy and matter. The first class of instruments that were developed were for use in the visible region and were thus called *optical instruments*. Now this term is used for instruments measuring a much broader range of radiant energy, although such broad usage is not strictly correct. The radiant energy used in such measurements may vary from that in the X-ray region, through visible light, to radio waves. The parameter most frequently used to characterise radiant energy is the wavelength, usually measured in nanometers (nm).

Figure 1.1 indicates the normal range of wavelength for various types of radiant energy used in instrumental analysis.

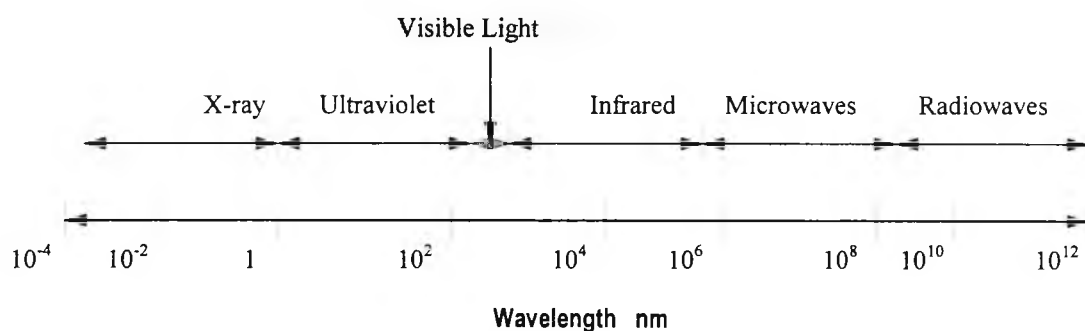


Fig 1.1 Range of wavelengths for different types of radiant energy (graph not to scale)

Radiant energy may also be considered to consist of *photons* or packets of energy that can interact with matter. The energy of a photon is related to its wavelength λ as follows:

$$E = \frac{hc}{\lambda} \quad \text{equ (1.1)}$$

where h is Planck's constant and is equal to $6.6 \times 10^{-34} \text{ Js}^{-1}$ and c is the velocity of light in vacuum, which is equal to $3 \times 10^8 \text{ ms}^{-1}$. This equation indicates that in the X-ray region, wavelengths are short but carry relatively high energy and for this reason

they can cause marked changes in matter. Microwaves and radio waves, on the other hand, have longer wavelength values and are relatively low in energy contents. The changes that they cause upon interaction with matter are quite small and difficult to detect. The use of radiation of different energy content at these wavelengths permits the determination of different properties of materials using the range of interactions region.

Optical methods of analysis may be designed to measure the ability of a material or solution to *absorb* radiant energy, to *emit* radiation when excited by an energy source, or to *disperse* or *scatter* radiation. Methods based upon these three principles are described below:

1.4.3.1 Absorption Methods

When a source of radiant energy, such as beam of white light, is passed through a solution, the emergent beam will inevitably be lower in intensity than that entering. If the solution does not contain suspended particles that scatter light, then the reduction in intensity is due primarily to *absorption* by the solution. The extent of absorption of white light is generally greater for some colours (wavelength bands) than for others, with the result that the emerging beam is coloured due to its absorption of some of the spectral content of white light. The overall intensity of the emergent beam is also affected by the type of elements present in the sample some chemical species absorb light in such a way that identifies the type of chemical species and its concentration.

The use of a spectrophotometer to determine the extent of absorption of various wavelengths of visible light by a given solution is discussed in detail in section 5.4.1 of Chapter 5, and the result of such a measurement are illustrated. Colorimetry, of course, strictly refers to the visible region of the spectrum, but the same principles apply to other regions. Thus, analytical methods based on absorption of ultraviolet or infrared radiation are also in very common usage, and represent a major means of instrumental analysis.

All instruments designed to measure the absorption of radiant energy have the basic components indicated in figure 1.2, (confirmed in one of several ways) which include an energy source to provide radiation of the desired wavelength, an energy spreader which permits separation of radiation of the desired wavelength from other radiation, and an energy detector which measures the portion of radiation that passes through the sample.

Spectrophotometers for such measurements may vary from the simple and relatively inexpensive to highly complicated and expensive instruments that automatically scan the ability of a solution to absorb radiation over a wide range of wavelengths and automatically record the results of these measurements.

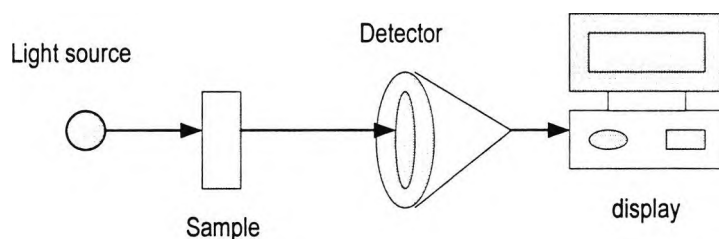


Fig 1.2 Basic components for measurement of absorption.

One single, simple instrument cannot be used to measure absorbance at all wavelengths because a given energy source, energy spreader, and energy detector is suitable for use over only a limited range of wavelengths. Instruments that measure the absorption of visible light are widely used in water analysis. However, instruments measuring the absorption of ultraviolet or infrared radiation are finding increasing usage and will be briefly discussed.

1.4.3.2 Ultraviolet Spectrophotometry

When a molecule absorbs radiant energy in either the ultraviolet or the visible region, valence or bonding electrons in the molecule are raised to higher energy levels. Some smaller molecular changes can also take place, but these are usually masked by the above electronic excitations. The result is that fairly broad absorption bands are usually observed in both the ultraviolet and the visible regions.

Many instruments are designed to make measurements in both regions. A typical simple instrument of this type is the diode array spectrophotometer e.g. HP 5428A, known as ultraviolet and visible (UV-Vis) spectrophotometer. The ultraviolet region is of more limited general usage than the infra-red for species identification although it is particularly suitable for selective measurement of low concentrations of organic compounds such as benzene-ring-containing compounds or unsaturated straight-chain compounds containing a series of double bonds.

1.4.3.3 Infrared Spectrophotometry

Nearly all organic compounds show marked selective absorption in the infrared region. However, infrared spectra are exceedingly complex compared to ultraviolet or visible spectra. Infrared radiation is of low energy and its absorption by a molecule causes a variety of subtle change in the vibrational or rotational energy of the molecule, not discussed in detail here but information on this available elsewhere^[16].

An experienced analyst with a library of known spectra available, if necessary, can readily use infrared spectra to identify particular atomic groupings that are present in an unknown molecule. To illustrate this principle, for example, the absorption of short-wavelength 0.8 μm infrared radiation causes vibrations of hydrogen atoms in molecules, longer wavelengths 1000 μm cause vibrations of triple bonds, while still longer wavelengths cause vibrations of double bonds. Because of the complexity of infrared spectra, it is highly unlikely that any two different compounds will have identical signatures. This fact has made infrared spectrophotometry a valuable aid in the identification of pesticides and other complex organic chemicals that have been extracted from waterways.

While infrared analysis gives much more information about a molecule than either ultraviolet or visible analysis, it is less sensitive, and thus a relatively high concentration (10^{-4} to 10^{-5} M) of the substance to be analysed is needed. Another problem stemming from the complex infrared spectra produced by even simple molecules is that when many materials are present in a solution, interference between their individual spectra makes the use of infrared analysis for identification or

quantification almost impossible. For this reason an extensive separating procedure is often required to isolate compounds of interest from interfering sources prior to analysis. In principle, quantitative infrared analysis occurs in the same way as that in the ultraviolet or visible spectral regions.

By examining the spectrum of a pure substance, a wavelength may be found at which the absorption is considerably greater than for other compounds present in the mixture. For analysis it is simply necessary to measure absorbance at the selected wavelength. Use is made of this principle in some instruments designed for the rapid measurement, for example, of total organic carbon or TOC, when only small quantities of organic carbon are present in water.

Here a liquid sample is injected into a furnace, where the water is evaporated and the organic carbon catalytically burned to carbon dioxide. The carbon dioxide is then carried by a stream of oxygen through an infrared analyser that is specifically designed to measure and record the concentration of the carbon dioxide present. Actually, total carbon is measured by this procedure, but if the sample is first prepared by acidification and aeration to remove inorganic carbon, then a selective measurement of the organic carbon present can be obtained.

1.5 Fibre optic sensor systems

1.5.1 Sensor Definition

For many applications a sensor is a device that can be inserted into a sample and will display the result of a chemical analysis within a few seconds with sufficient precision and selectivity. No sample dilution (with its inherent drawbacks), or reagent addition would be required, and the results may be displayed continuously and in real time. While such kinds of sensors are rare at present, there is growing interest, by virtue of their real-time nature, in achieving a wide range of such devices. Increasing concern about environmental quality in an increasingly cost-conscious world, promotes their application in water monitoring.

Considerable personnel cost savings in comparison with manual off-line methods can further contribute to the desirability of such sensors. Hence, tremendous efforts have been devoted to the development of various sensing devices for use in analytical and clinical chemistry to meet these objectives. By definition, an on-line sensor in this context may be defined as a device that is able to indicate continuously and reversibly the concentration of an analyte or a physical parameter.

Thus, a pH meter and a 'non-bleeding' pH paper strip may be called true sensors, since they act continuously and are fully reversible. However, certain devices that are able to measure the concentration (or activity) of biomolecules have also been called sensors although they do not sense continuously but rather allow only a single determination event. Some of these "sensors" have been included in this Chapter, but they have usually been referred to as probes rather than as sensors. However, such definitions vary widely from context to context and with different authors in their texts.

1.5.2 Fibre Optic Sensors

Fibre optic sensors are also known as 'optodes' or 'optrodes' in analogy with the term 'electrode' as applied to electrically-based sensors. However, in this thesis the less ambiguous term fibre optic sensor will be used, often abbreviated to FOS. As with other types of sensors, fibre optic chemical sensors usually consist of two regions:

1. the sensing material or reagent phase, which is in optical contact with measurand.
2. the optical fibre which carries the optical signal from the light source to the detector.

Radiation from an optical source is launched into the fibre where it interacts with the reagent phase, being modified in some manner to an extent dependent upon the state of the sensing material, which is in turn dependent upon the concentration of the measurand. The state of the returning light is then measured by an optical detector,

measurand. The state of the returning light is then measured by an optical detector, from which the measurand concentration is may be deduced. A number of fibre optic sensors are based on a type of chemical analysis method relying on spectroscopy that simply utilises an optical fibre to carry the absorption spectrum of a measurand from the end of a fibre to a spectrometer^[17].

1.5.3 Advantages of FOS Technology Described in the Literature

There are several advantages of using FOS, as opposed to electrically based devices, which are often given and in summary these are.^[18]

- No reference electrode is required in the measurement
- Measurements can be made in potentially explosive environments as there is no risk of spark generation.
- FOS are free from electrical and cross-talk interference problems. They are often mechanically flexible.
- They offer electrical isolation which is an advantage in environments where safety is of primarily concern.
- Often two or more chemical parameters can be measured simultaneously by the use of multiple wavelengths.
- FOS can detect chemical species where conventional sensors are at present inappropriate such as highly explosive chemical and temperature where a glass electrode cannot be used.
- Often only low energy radiation is required for operation, typically a few milliwatts.

1.5.4. Fibre Optic limitations in Sensing

These include the possibility of fibre losses and degradation of the fibre in the sub-200nm wavelength range which results from the higher level energy photons interacting with the medium. However, most manufacturers have not produced analytical data to confirm or reject this long term effect.

- ◇ Large diameter fibre cannot be bent easily without creating micro-cracks which probably are invisible to the naked eye but which can reduce the light transmission of the fibre and hence diminish the durability of the fibre and sensor.
- ◇ No standards regarding interfacing or communications are yet established in the field of sensing which could enable FOS to be more portable.
- ◇ More selective indicators have to be found for various important analytes and the immobilisation chemistry has to be improved so as to achieve both better reproducibility, selectivity, and sensitivity.

There are other minor disadvantages in their use, such as the fact that ambient light can cause interference. However, good design can eliminate or reduce this effect. Other problems include possible leakage from the reagent phase, low signal-to-noise ratios, the lack of long term stability and a limited dynamic range, most of which are not problems unique to FOS.

The above advantages have made FOS well suited to medical and environmental applications, particularly with respect to their ability to be inserted *in vivo* into human tissue and their inherent electrical isolation.^[19,20]

1.5.5 Fibre Optic Sensor Instrumentation

Instrumentation involved in a typical FOS system is shown schematically in Figure 1.3^[21]. Optical radiation of the required wavelength is launched into the sensing fibre, where it interacts with the reagent phase, and the returning light signal may be

detected in its modified form. Depending upon the light source used, filters, monochromators, and lenses may be required to facilitate effective instrument design. In many such sensors the detected signal is amplified, possibly undergoes some signal processing, and is converted to a useable output which is related to the measurand concentration.

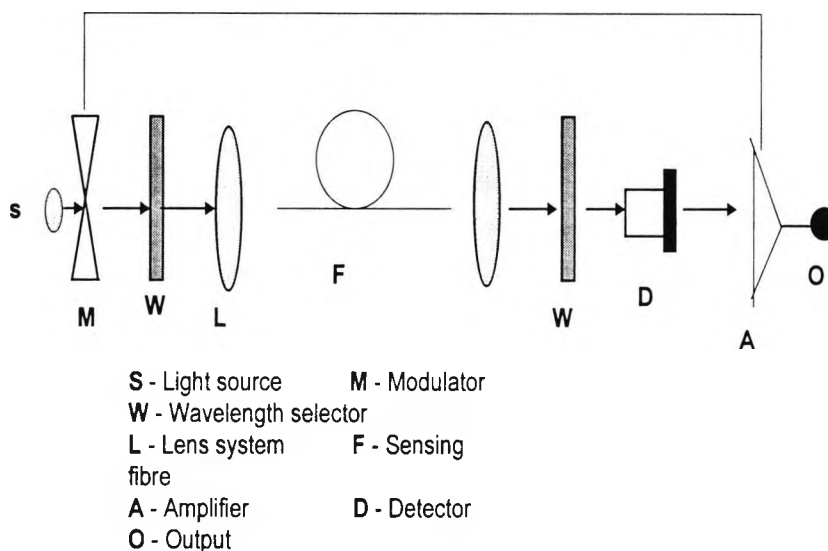


Fig 1.3 Instrumentation of a typical fibre optic sensing system

In any practical system a modulation of the input signal would be required, and achieved either mechanically or electronically, in order to separate the signal from any background optical noise, i.e. such as any ambient light present.

1.5.5.1 Fibre Optic Sensor Configurations

The configuration of a typical FOS in general falls into one of four categories^[22], as shown schematically in Figure 1.4. Figure 1.4 (a) shows the case where the radiation is carried to the reagent phase immobilised onto the end of the fibres, and returned for its detection by separate fibres. There may be only one fibre and a coupler, or two fibres, or two bundles of fibres. The sensing head must incorporate a scattering phase or an end mirror, in order to scatter or reflect the modified radiation back along the fibres.

The second case (Fig. 1.4 (b)) is similar except that the same fibres are used to carry both the launched and returning radiation, which, as before, must be scattered or reflected. A bundle of fibres may be used but a single fibre is more common if the signal is sufficiently strong. With this configuration, a device is required to separate radiation in the two light paths, such as a semi-silvered mirror or a 'Y' coupler.

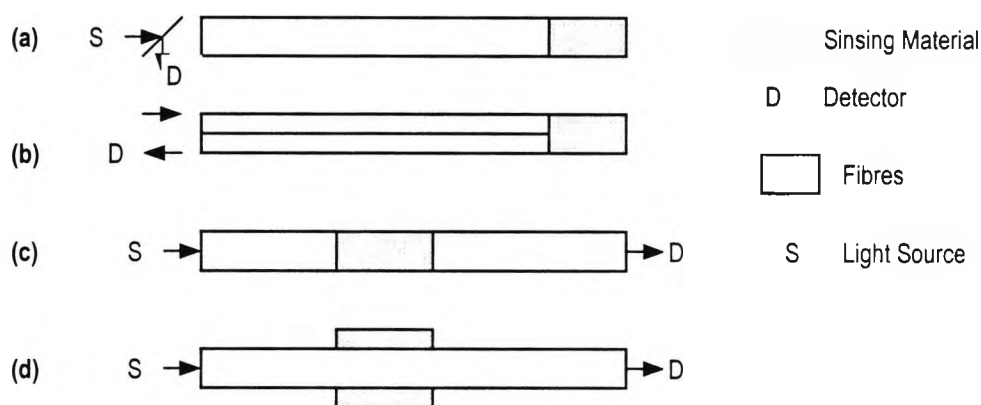


Fig 1.4: Possible configurations of FOS.

Figure 1.4 (c) is a linear arrangement whereby radiation is carried to the reagent phase by one fibre, passes directly through it, and is collected by another fibre. Finally, Figure 1.4 (d) shows a somewhat different configuration involving only a single fibre, with the sensing material coated along the fibre.

For the reagent phase to interact with the optical radiation it must be in contact with the core of the fibre, i.e. often the cladding must be removed within the sensing region to expose the core. The interaction between the radiation and the sensing material occurs via the evanescent field, i.e. the region of the field propagating for a small distance outside of the fibre core.

In the case of the first two configurations, the type of optical fibre used is not critical as it is merely acting as a light pipe. Multimode plastic or glass fibres are normally used as these are easy to handle and to launch light into, as well as being readily available. However, if transmission of radiation in the ultraviolet (UV) spectral

region is required, more expensive quartz fibres must be utilised. The situation is very different in the case of the fourth configuration as both the geometry of the fibre and the refractive index of the core (and sensing material) are critical, since the degree of interaction between the radiation and reagent phase is dependent upon these factors.

1.6 The Reagent Phase

There are a vast number of chemical species in existence which respond in some way to changes in their chemical environment; however only a very small number of these can be utilised in sensing due to limitations in areas other than their ability to detect chemical species. Ideally, for application in optical fibre sensing, the reagent phase should satisfy four general criteria^[23],

1. It should change its optical property of interest only in response to the measurand of interest, i.e. it should be selective.
2. It should respond in a reversible and reproducible fashion to an extent which enables the required degree of precision to be obtained from the sensor.
3. The material must be optically compatible with the optical system (i.e. the optical fibre) in terms of refractive index or absorptivity.
4. Finally the material should be durable and stable over its intended lifetime. In general, it must not bleach into its environment or affect its stability, or be affected by radiation, e.g. photobleached. In reality, meeting all of these criteria is very difficult, but the majority must be satisfied for a practical sensor for sufficient time for measurement to be taken.

To date, the majority of sensing materials for use in FOSs are based upon existing organic or biochemical molecules immobilised in some way into a solid (usually an organic polymer), and /or contained within a membrane.^[24]

The use of a membrane can also add to the selectivity of a sensor by only allowing certain molecules to the reagent phase, selecting, for example, specific characteristics in as much as size or polarisation chosen. Looking towards the future it seems likely that there will be a trend towards engineering materials which specifically detect certain measurands through the 'design' of new molecules or the use of composite materials.^[25] The change in the optical properties of the reagent phase, which is exploited by the fibre system, in general falls into one of the following possibilities:^[26,27,28]

- ◆ Absorbance
- ◆ Fluorescence
- ◆ Phosphorescence
- ◆ Chemiluminescence
- ◆ Refractive index.

1.6.1 Absorption-Based Sensors

Absorption devices are based upon materials which change their spectral transmission in the presence of the measurand species (e.g. pH indicating dyes). The wavelength of the absorption peak is used to probe the state of the dye, and usually a second wavelength at some point which remains unaffected by the species is used as a reference. This enables the compensator of losses due to factors other than the dye absorption, e.g. fibre bending losses, to be allowed for.

1.6.2 Fluorescence-Based Sensors

Fluorescence-based sensors utilise molecules whose fluorescence intensity is dependent upon analyte concentration. The technique is particularly well suited for optical sensing, as the emitted fluorescence wavelength is different (i.e. longer) from that of the excitation wavelength, thus enabling easy separation of the two signals. Back-scattered excitation radiation can be used as a reference signal. In addition, fluorescence is an inherently sensitive technique capable of measuring very low concentrations of analyte, against a 'zero' background light level.

1.6.3 Phosphorescence-Based Sensors

Phosphorescence is similar to fluorescence but has a potential advantage, due to the longer decay lifetimes of the emitted radiation, in that high power pulsed sources (e.g. lasers) can be used, and the returning signal detected separated in time.

1.6.4 Chemiluminescence-Based Sensors

Chemiluminescence uses reactions between an analyte and reagent that emit optical radiation, the intensity being proportional to the analyte concentration. In principle it is a very simple technique that requires no external radiation input.

However, in a practical system a reference source would be required to allow for other losses in the system. To date this method has found little application. The techniques discussed, using fluorescence, phosphorescence and chemiluminescence have the disadvantage in that the returning radiation is often very weak. Finally, the use of materials which change their refractive index has been exploited by coating them onto the outside of fibres, and changing their transmission characteristics with measurand variations.

1.7 Examples of Fibre Optic Chemical Sensors.

This section contains some specific examples of various fibre optic chemical sensors that have been devised, and their intended application. It is not intended to be an exhaustive literature review, but to give a broad illustration of the types of sensors that have been developed and the way in which the issues raised are featured in 'real' sensors. The examples are categorised by the chemical species they detect.

1.7.1 pH (Hydrogen Ion Concentration)

Sensors for the detection of pH are based upon pH-indicating reagents, either of the colorimetric or fluorescent type. The first reported practical fibre optic pH sensor was that made by Peterson et al.^[14], shown schematically in figure 1.5.

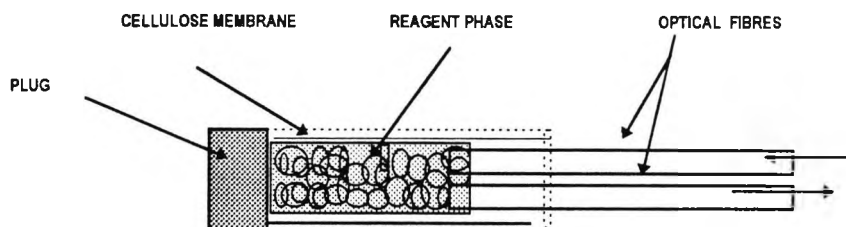


Figure 1.5: pH sensor of Peterson et.al.

The operation is based upon the change in the optical absorption spectra of the pH-indicating dye phenol red, over the pH range 6.6 to 8.4. The dye is covalently bound onto polyacrylamide micro-spheres and contained within a *cellulose membrane*, which is porous to hydrogen ions (H^+). Polystyrene micro-spheres are also used to scatter light. Two multimode plastic fibres of diameter of $150\mu m$ were used, one for delivering white light from a tungsten lamp to the reagent, and the other for collecting the back-scattered radiation.

The returning radiation intensity was measured at two wavelengths using a single photodetector and rotating filter wheel arrangement. Green light of 560 nm, which is the peak of the absorption curve for phenol red, was used to detect the state of the dye, and red light of wavelength greater than 600 nm (which not absorbed by the dye) was used as reference. The ratio of the two signals gives a reading of the pH.

The device was calibrated over the physiological pH range of 7.0 to 7.4, giving an accuracy of ± 0.01 pH, with a response time of tens of seconds. The device was evaluated *in vivo* in an anaesthetised sheep, performing well in comparison with a conventional pH electrode and a blood sampling gas analyser.

Since this pioneering work many other workers have constructed devices along similar lines, but often using different combination of dyes, immobilisation procedures, and membranes. Notable in early fibre optic sensors is the work of Kirkbright et.al.^[29], whose device utilised bormothymol blue immobilised on to the end of a fibre bundle in a styrene-divinylbenzene copolymer, giving a rugged yet accurate sensor, and the

work of Boide et.al.^[30], who constructed a range of devices to cover the pH range 1 to 11.

One of the main disadvantages of devices based upon colorimetric pH indicators is that such dyes typically only cover a range of 2 pH units. The use of fluorescent pH indicating dyes i.e. dyes which fluoresce upon excitation to a degree dependent upon their pH, can give a wider dynamic range (but still not cover the range from pH 1 to pH 12 as electrode-based pH sensors do).

The first such fluorescent based device was reported by Sari and Seitz^[31] utilising the dye fluoresceinamine immobilised onto the end of fibre bundle either within porous glass or cellulose. Excitation was at 480 nm from a filtered white light source, and fluorescence at 520nm. Due to the low fluorescent intensity of this dye, the device was not very accurate. Much better results have since been obtained for example from the dye hydroxyrene trisulphonic acid (HOPSA)^[32], which has a much more intense fluorescence and has been shown to be very specific to pH.

As with fluoresceinamine, HOPSA is excited at 480nm which enables an argon-ion laser to be used as a powerful illumination source, enabling, reasonable fluorescence signal to be obtained from very small amounts of reagent. In one particularly simple device a monolayer of HOPSA is covalently bound on to the end of a single silica fibre^[33], giving the device a rapid response time of less than a second, since the H⁺ ions do not need to diffuse through membranes etc.

A further device has been reported with rapid response of about 5 seconds, which utilises the fluorescent dye immobilised into silica gel which is coated on to the outside of a fibre optic core to a thickness of $\approx 0.3\mu\text{m}$ using the sol-gel process^[34]. Excitation of the material is from an Ar-ion laser coupled in via the evanescent field, the fluorescence signal being detected using a monochromator and PMT (Photo Multiplier Tube) This device has an unusually wide dynamic range for a fibre optic pH sensor - pH 3 to 8.

Finally, there is another type of pH FOS, from Attridge et al., based on a novel co-axial coupler optical fibre^[35]. The transmission characteristics of the fibre are dependent on the refractive index of a coating material which consists of phenol red bound into an ion exchange resin. The change in refractive index of this material is induced by the change in absorption peak of the dye, according to the Karma's Curing relations. The device responded rapidly over the pH range 6 to 8, but problems existed with the rigidity of the fibre, which was only about 15 μ m in diameter.

1.7.2 Ammonia Sensors

The detection of ammonia, a basic gas either as a vapour or in aqueous solution, typically is carried out in a similar manner to the pH, i.e. based on pH indicators. Shahriari et al.^[36] and Zhou et al.^[37] have constructed sensors as shown in figure 1.6, based upon optical absorption by the indicator bromocresol purple.

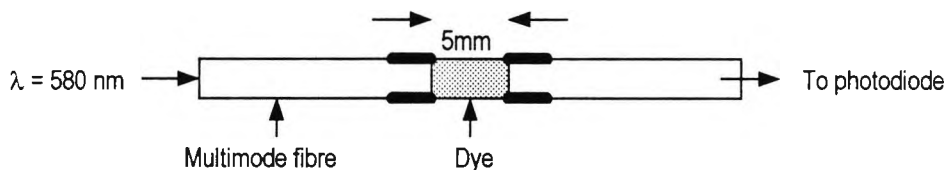


Fig. 1.6 : Ammonia sensors of Shahriari et. al.Zhou et.al.

The dye is absorbed into a section of porous fibre, into which the NH_3 enters and interacts with dye. For this reaction to occur adsorbed water must be present, and so the devices are sensitive to humidity as well as ammonia. Shahriari's device uses porous glass made by heat treating and etching borosilicate glass, giving a pore size of 80 - 150 nm. It can detect ammonia level down to 0.7ppm, and has a linear relationship between absorbency and concentration up to 3ppm.

Zhou's sensor is less sensitive, working in the range of 10 - 90ppm, utilising a porous plastic (a treated polymethylmethacrylate) with a pore size of $\approx 10 \text{ nm}$. Besides the sensitivity to humidity, both devices have the major disadvantage of very long response time, typically 20 minutes. Another ammonia sensor made by Giuliani et al.^[38], whilst not a FOS as such, demonstrates the use of practical instrumentation.

Shown schematically in figure 1.7, it consists of a capillary tube (0.8mm inner diameter, 1.1mm outer diameter and 90mm long) used as a waveguide, the outside of which is coated with the pH indicator oxazine perchlorate.

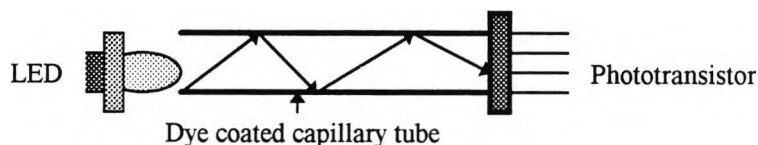


Fig. 1.7: Ammonia vapour waveguide sensor of Giuliani et.al

Radiation of wavelength 560nm from a blue LED is multiply reflected along the capillary, interacts with the dye via the evanescent field, and is detected by a phototransistor at the other end. All the associated electronic circuitry, LED modulator, amplifier, demodulator etc., occupy only a few square cm on a printed circuit board. The device has a sensitivity in the range 10 to 1000ppm, and a response time of 1 - 2 minutes. However these ammonia sensors suffer from a short life and need periodic servicing and calibration to ensure that the measurement remain accurate.

1.8 Application Fields and Sensor Markets

Typical application fields of chemical and biochemical sensors are summarised in Table 1.2. Future markets are extremely difficult to predict with any real precision. Following one of the many recent predictions on future markets for the two specific examples, “environmental protection” and “medical application”, the world-wide increasing demand (in million £) is listed for the years 1988 - 2000 in Tables 1.3 and 1.4. The data are obtained from sensor trend sources and for further details, see for example the work of Schroder.^[39]

Environmental and emission control (air, water, soil,)
 Working area measurements (work place, household, car,)
 Emission measurements (car, car exhaust, waste water,)
 Fire warning and safety control (household, mining, laboratory, tunnel, hotel, ...)
 Breathing gases: control and regulation (living rooms, diving or medical equipment, airlines)
 Household appliance: control and regulation
 Car engines: control and regulation
 Process control and regulation (biotechnological and chemical plants, fermentation processes, general chemical processes, drying,)
 Chemical and biochemical analysis
 Medical applications (clinical diagnostic, prosthetics, anaesthetics, veterinary, ...)
 Agriculture (analysis in agriculture and gardening, detection of pesticides,)

Table 1.2 Typical application fields for chemical & biochemical sensors^[40, 41]

Sensor types	1988	1990	1995	2000
<i>Diagnostics:</i>				
ultrasound sensors	£2.2	£2.61	£3.9	5.7
optical sensor	£3.5	£4.8	£8.7	15.3
electrochemical sensors	£17.4	£23.8	£47.8	73.9
biosensors	£27.8	£132.6	£213.0	308.7
total value	£50.9	£163.81	£273.5	403.6
<i>Control</i>				
transcutaneous electrodes	£44.4	£53.5	£78.7	115.7
breathing gas sensor for O ₂ and CO ₂	£58.7	£72.2	£113.5	169.6
optical sensors	£60.9	£70.9	£94.8	120.9
pH - sensor (electrodes)	£7.8	£10	£17.4	29.2
pressure sensors	£17.4	£21.0	£33.5	47.8
temperature sensors	£10.9	£11.7	£18.7	23.9
electrochemical and fluorescence sensors	£7.8	£9.2	£13.0	16.9
ion-sensitive sensors (ISFETs)	£3.5	£5	£10	17.4
flow-through sensors	£0.87	£1.30	£2.20	3.05
biosensors	£13.04	£145.22	146.96	195.65
total value	£225.31	£400.02	528.76	740.10

Table 1.3: World-wide demand of sensors for medical applications 1988 -2000 in UK(millions of £).^[42]

The market aspect of fibre optic sensors systems has sharply risen as can be seen from Table 1.3. There is great interest in this field of exploration into the development of fibre optic sensors because their application can be applied to many aspects of human need i.e. medical aspects, pollution control, etc. The predicted

value of £120 M in year 2000 is for spending on medical applications only. However, in case of the environmental issues, as illustrated in Table 1.4, the growing demand for sensors systems in the field of environmental analysis can be seen.

Application	1990	1995	2000
<i>Emission and imission measurement in gases and air</i>			
electrochemical sensors	17.4	37.4	70.5
semiconducting sensors	6.5	34.8	87.0
phys. - chem. sensors	54.7	65.2	78.3
biosensors	----	1.74	3.5
total value	78.6	139.14	239.30
<i>Waste water and environmental control</i>			
electrochemical sensors	10.43	28.26	56.52
semiconducting sensors	2.17	6.52	56.52
phys. - chem. sensors	4.78	8.71	15.22
biosensors	21.74	56.52	126.1
fibre optic sensors	12.50	15.74	135.5
total value	51.62	115.75	389.86

Table 1.4 : World-wide demand of sensors for environmental protection 1990 - 2000^[42].

Numbers denote units of 10^6 UK £.

1.9 Summary

This thesis discusses sensors and their applications and concentrates upon one particular implementation of sensors - that using fibre optics. Perhaps one of the most important messages which the thesis serves to emphasise, but which is also general to the entirety of sensor technology, is that the conversion of one type of signal into another via a sensing element is a very multidisciplinary science involving electronics, mechanical engineering, chemistry, packaging and, in this case, fibre optic as well. The combination presents a considerable challenge and perhaps this explains why the sensor is often described the "Cinderella of the information age" - the design problems are simply very difficult.

In this chapter a general introduction and background to sensors and their applications were presented. In the next chapter several points are discussed which need to be taken into account before the complete implementation of the sensor system is established. The theory of chemical sensors and the fibre optic implementation will be discussed in some detail.

1.10 References

1. L.S. Clesceri, A.E. Greenberg, and R.R. Trussell, eds., "Selected Physical and Chemical Standard Methods for Student", 17th ed., American Public Health Association, New York (1990).
2. P.A. Payne, "Transducers, sensors and instrumentation in clinical biomechanics", *J. Biomed. Eng.* 11, 180 (1989).
3. P. Rolfe, "In vivo chemical sensors for intensive care monitoring", *Med. and Biol. Eng. & Comput.* 28, B34, (1990)
4. A. Jones, et. al., "The chemistry of solid state gas sensors", *Chem. Brit.* 23, 147 (1987).
5. D. E. Williams and P. McGeehin, "Solid state gas sensors and monitors", *Electrochemistry* 9, 247 (1984), (RSC specialist periodical report).
6. R. Briggs, K.T.V. Grattan, "The measurement and sensing of water quality: a review", *Trans. Inst. MC.* 12, 65 (1990).
7. J.W. Gardner, et.al., "The design of an artificial olfactory system", in 'Chemosensory Information Processing', (ed:D. Schild), NATO, ASI Series, Vol. H39, pp-131-173 Springer - Verlag (1990).
8. G.D. Velho, et.al., "The design and development of in vivo glucose sensors for a artificial endocrine pancreas", Chapter 22 in, 'Biosensors - Fundamentals and Applications', (eds: A.P.F. Turner, I. karube, and G.S. Wilson), Oxford University Press (1987).
9. J. Janata, "Principles of Chemical Sensors", Plenum (1989).
10. T.E. Edmonds, "Chemical Sensors", Chapter 13, Blackie (1988).
11. C. Nylander, "Chemical and biological sensors", *J. Phys. E: Sci. Instrum.* 18, 736 (1985).
12. J. Palais "Fibre optic communications" third edition., Chapter 5, Prentice Hall, Inc. (1992).
13. T. Hirschfeld et.al., "Laser - Fiber optic 'optrode' for real time in vivo blood carbon dioxide level monitoring", *J. Lightwave Tech.* LT-5, 1027 (1987).
14. J.I. Peterson and R.V. Fitzgerald, *J. Biomed. Eng.*, 102 pp141 (1980).

15. P. W. Atkins "Physical Chemistry" 2nd Edition, Oxford University Press, (1982).
16. A Tebo "Fibre optic sensing in medicing - an exploding field", SPIE, Reports, No. 86, 11 (1991).
17. W.R. Seitz, "Optical sensors based on immobilised reagents", chapt. 30 in: 'Biosensors - fundamentals and applications', (eds. A.P.F. Turner, I. Karube, & G.S. Wilson), Oxford University Press (1987).
18. M.J. Martin, et.al., "Fibre optics and optical sensors in medicine", Med. and Biol. Eng. & Comput., 25, 597 (1987).
19. J.I. Peterson, G.G. Vurek, "Fibre optic sensor for biomedical applications", Science, 224, 123 (1984).
20. W.R. Seitz, "Chemical sensors based on fibre optics", Anal. Chem. 56, 16A (1984).
21. G. Keiser, "Optical Fibre Communications", chapters 4 and 6, McGraw-Hill (1983)
22. A.M. Smith, "Materials interactions in optical fibre sensors", chapter 6 in: 'Optical Fibre Sensors: Principles and Practice', (eds: J. Dakin & B. Culshaw), Artch House (1988).
23. S.A. Barker, "Immobilisation of the biological component of biosensors", chapter 6in: Biosensors - Fundamentals and Applications, (eds: A.P.F. Turner, I. Karube and G.S. Wilson), Oxford University Press (1987).
24. K. Takahashi, "Sensor materials for the future intelligent materials", Sensor and Actuators 13, 3 (1988).
25. D.A. Krohn, "Fibre Optic Sensors - Fundamental and Applications", chapter 12 Instrument Society of America (1988).
26. J. I. Peterson, et.al., "Fibre optic pH probe for physiological use", Anal. Chem. 52 pp-864 (1980)
27. S.A. Barker, "Immobilisation of the biological component of biosensors", chapter 6 in: Biosensors - Fundamentals and Applications, (eds: A.P.F. Turner, I. Karube and G.S. Wilson), Oxford University Press (1987).
28. K. Takahashi, "Sensor materials for the future intelligent materials", Sensor and Actuators 13, 3 (1988).

29. G.F. Kirkbright, et.al., "Fibre optic pH probe based on the use of an immobilised colorimetric indicator", *Analyst* 109, pp-1025 (1984).
30. G. Boisdé, et.al., "Comparisons between two dye - immobilisation techniques on optodes for pH measurement by absorption and reflectance", *SPIE vol. 1172 (Chemical, biochemical and environmental sensors)*, 239 (1989).
31. L.A. Sari and W.R. Seitz, "pH sensor based on immobilised fluoresceinane", *Anal. Chem.* 54, pp-821 (1982).
32. O.S. Wolfbeis, "Fibre optic fluorosensors in analytical and clinical chemistry", in: 'Molecular Luminescence Spectroscopy: Methods and Applications', part II, (ed: J.S. Schulmen), pp-129-281, Wiley- New York (1988).
33. Y. Kawabata, et.al., "Fibre optic pH sensor based on fluorimetry", *Int. Conf. Optical Fibre Sensors, Tokyo, Japan, (1986)* pp-139.
34. McCraith et. al., "Fibre optic sensors based on sol-gel entrapped dyes", *SPIE vol. 1510, (Chemical and medical sensors)*, (1991).
35. J.W. Attridge, et. al., "Design of a fibre optic pH sensor with rapid response", *J. Phys. E: Sci. Instrum.*, 20, pp-548 (1987).
36. M.R. Shahriari, et. al., "Porous optical fibre for high - sensitivity ammonia vapour sensor", *Op. Lett.* 13, 407, (1988).
37. Q. Zhou, et. al., "Porous plastic optical fibre sensor for ammonia measurement ", *Appl. Op.* 28, pp-2022 (1989).
38. J.F. Giuliani, et. al., "Reversible optical waveguide sensor for ammonia vapours", *Opt. Lett.* 8, pp-54 (1983).
39. Schroder, N., Zerressen, A., *Sensortechnik 2000. Prognos Weltreport, Technologieanalyse und prognose der sensoren bis zum jahr 2000*, Basel, Switzerland: Prognos, (1988).
40. Infratest Industria, *Chemische und Biochemisch Sensoren, Marketübersicht*, Infratest Industria, Munchen (1989).
41. Oehme F., Gopel W., "Chemische Feldeffekt - Sensoren", *Hard and soft, Fachbeilage Mikro peripherik*, Dusseldorf: VDI - Verlay, (1987).
42. to 44 Tritank, J.W., "Sensors and Fibre Optic Sensors Market Trend" Graz (1996).

Chapter 2

The General Theory of Chemical Sensors and Implementation of Fibre optic Systems

2.1 Abstract

Several workers have attempted to construct an all-encompassing 'general theory' of sensor operation and behaviour. Various approaches have ranged from modelling sensors as a 'black-box' using control engineering theory, to studying their fundamental operational limitations due to quantum effects and thermal fluctuations. The development of such a general, yet simple sensor theory is unlikely to be successful, however, because of the diverse range of sensors, and the fundamentally different principles upon which different types of sensor operate. For instance, from a thermodynamic point of view sensors may be divided into two groups: equilibrium and non-equilibrium state sensors, which operate in fundamentally different ways.

The approach taken in this chapter is to describe the theoretical underpinning of only one type of sensor, using the most general thermodynamic and kinetic descriptions, this sensor being the reversible fibre optic sensor based upon the absorption of transmitted light. It should be noted that the description given in this chapter is essentially simplistic, yet effective to describe sufficiently adequately the system, and the conclusions derived are thus of an approximate nature. Some of the description is based upon the foundationS of Ylilammi^[1], Janata^[2], and Seitz^[3]. A basic knowledge of the thermodynamics and kinetics of chemical reactions is also assumed, this can be found in any standard text on chemistry, e.g. Eggers^[4] or Buttle et.al.^[5].

2.2 Design and Specification of the Chemical Sensor

The relationship between the species under investigation and the energy of the input light wave is mathematically determined using the Beer-Lambert Law which, when used under specific conditions, linearly relates the loss in energy of the light beam travelling through the sample to the concentration of the chemical parameter.

The visible and ultraviolet region of the spectrum are considered in the investigation of both the theoretical and practical feasibility of a measuring instrument based on the spectral properties of the chemical parameter. The construction is aided by the advantages seen in the use of fibre optic cables as a light carrying medium from the sensor head through the many interfaces of the instrument.

2.2.1 Outline of the Model

The objectives behind the use of the model is to establish a general description of the sensor system on which its design will be based. The parameters of the model will change with the specific chemical species to be considered. As outlined in the Introduction to the thesis, a fibre optic sensor consists of a sensing material or reagent phase, which interacts with the environment to be investigated, in contact with a transducing fibre; and this is shown schematically in figure 2.1.

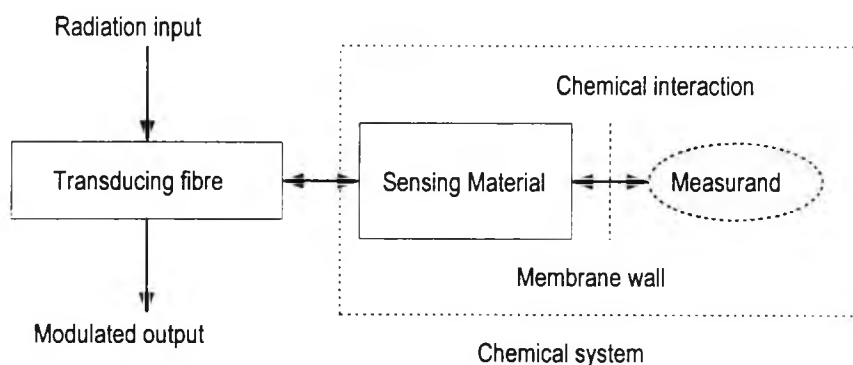


Figure 2.1 : Schematic representation of an equilibrium state fibre optic sensor.

The transducing fibre is essentially an inert device which allow the state of the reagent phase to be optically probed. The reagent phase interacts with the measurand, reaching an equilibrium dependent upon the measurand concentration. The chemical interaction that is central to the operation of the sensor is described schematically here, (indicated by the shaded area in figure 2.1).

Obviously the transducing fibre and its coupling to the sensing material are of vital importance, but these details are dependent upon the exact structure of the sensor head and not of the *fundamental* importance to its operation. It is the function of the transducer to modulate the state of the optical radiation supplied to it in order to give a reading of the measurand state; the sensor cannot generate this signal itself and be in reversible equilibrium with its environment.

The act of probing the system by the optical radiation results in the perturbation of the state of the system, but this effect is assumed to be practically negligible, (the ultimate limitation is of course the Heisenberg Uncertainty Principle) for macroscopic sensors. It is common for sensors to have a membrane which separates the reagent phase from the measurand. Its function is either simply to contain the reagent phase or to exclude certain chemical species (either to increase selectivity or exclude pollutants), or to act with a combination of both purposes.

Again this is a detail of construction that is not of fundamental importance. If it is to act as a selectively permeable membrane, it is merely restricting the nature of the chemical system to be considered.

2.2.2 Behaviour of the Model

The above method of analysis is very useful when the reagent is in the solid form and immobilised to the fibre optic. However, in this research work a liquid indicator was employed but it is worth giving a brief outline of the measurement technique employed and its limitations.

Representing the bound reagent phase by R, and the analyte (i.e. measurand) by A, and assuming a stoichiometry for the reaction of 1:1 for simplicity, the reaction upon which the fibre optic sensor is based can be described thus:



Where AR is the bound reagent-analyte species.

Assuming concentrations to be equal to activities, the equilibrium constant may be written:

$$K = \frac{[AR]}{[A][R]} \quad \text{equ. (2.2)}$$

where $[A]$ is the analyte concentration and $[R]$ and $[AR]$ are the concentrations of free and combined reagent molecules in the immobilised phase. The concentration (or total number) of reagent molecules in the sensor is fixed:

$$C = [R] + [AR] \quad \text{equ. (2.3)}$$

i.e. C is a constant. Physically it is $[R]$ or $[AR]$ (or sometimes both) that is probed by the optical signal, and so it is the variation of these with $[A]$ that is of interest. Combining equations 2.2 and 2.3 gives the relations:

$$[AR] = \frac{K[A]}{1 + K[A]} C \quad \text{equ. (2.4)}$$

$$[R] = \frac{1}{1 + K[A]} C \quad \text{equ. (2.5)}$$

These relationships are shown plotted in figure 2.2. If the transducer has a linear relationship, (as is often the case), then these will be the fundamental response curves

of the sensor. The rate of change of $[AR]$ and $[R]$ with $[A]$ is maximum for low values of $[A]$, i.e. the sensor is most sensitive at low concentrations. This is one of the most useful features of this type of sensor. An alternative mode of operation is to compare the ratio of $[R]$ and $[AR]$. Combining equations 2.4 and 2.5 gives the relationship:

$$\frac{[AR]}{[R]} = K[A] \quad \text{equ. (2.6)}$$

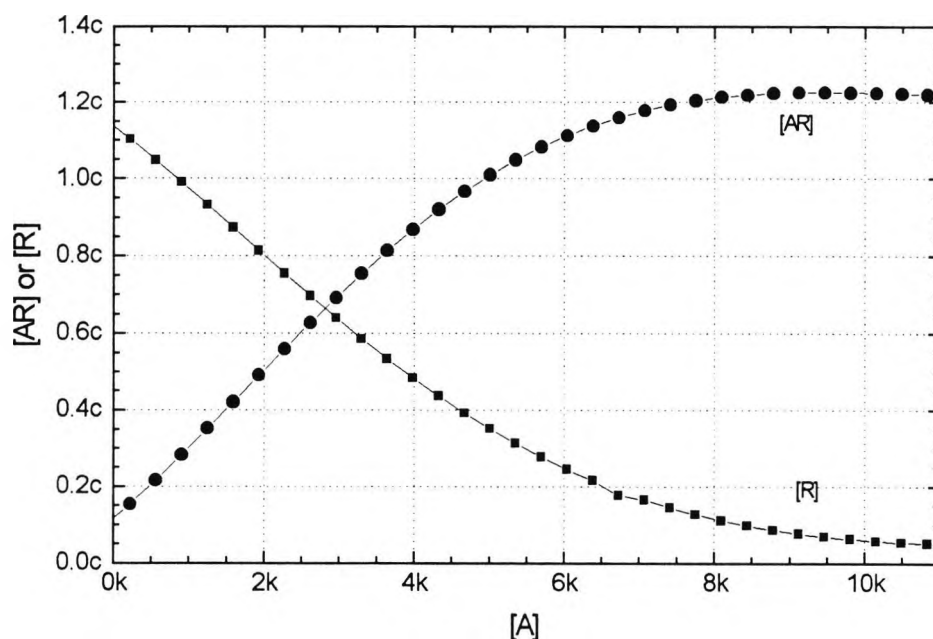


Figure 2.2: Graph showing the relationship between analyte concentration and proportion of reagent phase in the bound and unbound states

If both $[R]$ and $[AR]$ are measured by the transducer, (e.g. using two different wavelengths), and the ratio of the two signals is taken, the response of the device is linear. This mode of operation has the added advantage that compensation for bending losses etc. is automatically allowed, i.e. no separate reference is required. In this analysis it is assumed that the amount of analyte combining with the reagent is small compared to the amount of analyte in the sample, i.e. the sensor has a negligible effect upon its environment. This is frequently the case as the amount of reagent in the sensor head is usually very small ($\ll 1\text{ml}$), and the sample usually very large in

large in concentration in comparison ($\gg 1$ ml). However, it may be the case in some examples medical analysis that a very small volume of analyte is available, and so the above equations would not be valid.

It can be seen in figure 2.2 that for $K[A] \gg 1$, $[AR] \rightarrow 1$ and $[R] \rightarrow 0$. Physically this represents all of the reagent sites available for bonding to the analyte molecules being full, i.e. the sensor is *saturated*. This is the upper limit of the sensor dynamic response range, i.e. :

$$[AR]_{\max} = C \quad \text{equ. (2.7)}$$

for the case where it is $[AR]$ being measured. The total dynamic range of the sensor is given by:

$$\text{Dynamic response range} = C - [AR]_{\min} \quad \text{equ. (2.8)}$$

Here $[AR]_{\min}$ is theoretically limited by either the total number of binding sites available for the analyte, or the measurement limits due to number of photons available for detection by the transducing system. Practically, however, these limits are rarely approached and $[AR]_{\min}$ is determined by the accuracy of the instrumentation, as a common problem with a fibre optic sensor is noise in the optical signal. However, with careful design of instrumentation and the use of modulation, sensors can be constructed having a dynamic range of several decades.

2.2.3 Thermodynamic and Kinetic Considerations

In the thermodynamic and kinetic considerations of the system under investigation, ideally the only variable is the concentration of the analyte, i.e. it is only this change that causes the equilibrium position to shift (equation 2.1); all other factors such as temperature, concentration of the reagent phase etc. are assumed to remain constant. From a thermodynamic point of view, the equation of importance is the change in the measurand concentration to be detected which will produce a significant shift in equilibrium position, (and hence $[AR]$ and $[R]$), to produce a useful sensor scheme.

A second and vitally important point is whether or not this equilibrium is reached in a reasonable time, i.e. are the kinetics of the reaction sufficiently rapid to ensure a “rapid” response in the sensor. Finally, before any reaction can occur the reagent and analyte molecules must come into contact, and so the transport kinetics of the analyte molecules in the reagent phase must also be similarly rapid. Using simple thermodynamic and kinetic considerations, the following sections illustrate approximate quantitative factors, for any sensing system, upon which a sensor is to be based. These represent a good starting point when considering the potential chemical systems on which to base a sensor scheme.

2.2.3.1 Thermodynamics

The driving force for any chemical reaction is the reduction in the free energy, G , for the system. This is shown diagrammatically in figure 2.3, where ΔG represent the difference in free energy of the products and reactants for equation 2.1.

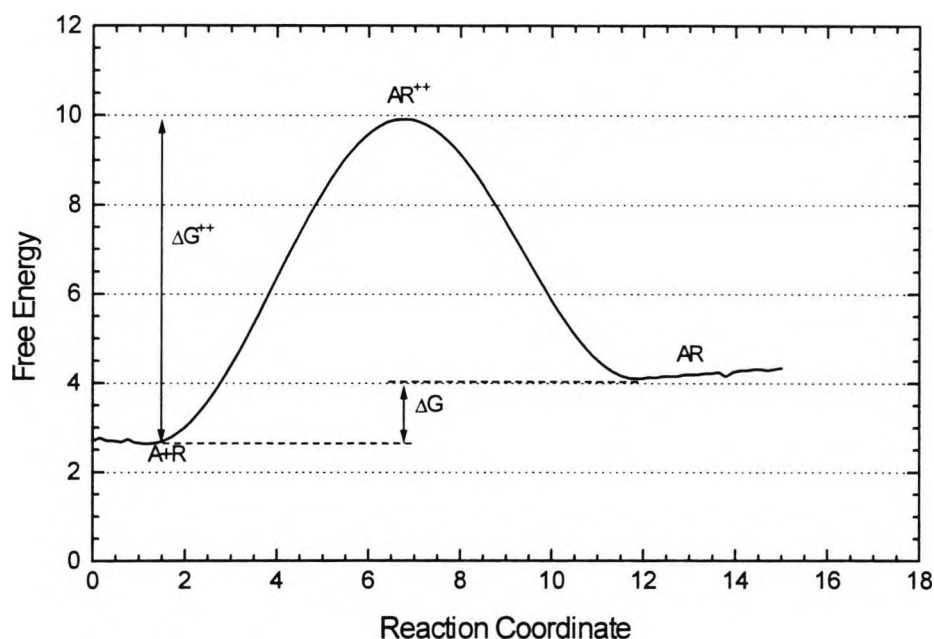


Figure 2.3 : Diagram showing the changes in free energy associated with the reaction between analyte and reagent

It is necessary to know how the free energy changes with the analyte concentration. Considering the case of a gas sensor for example, from the second law of thermodynamics:

$$\left(\frac{dG}{dP}\right)_T = V \quad \text{equ. (2.9)}$$

Where P is pressure, V, the volume, and T indicates a constant temperature. For a change in the pressure, from P₁ to P₂, integration of this expression gives:

$$\Delta G = \int_{P_1}^{P_2} V dP \quad \text{equ. (2.10)}$$

or, expressing the volume as a function of pressure (for an ideal gas), gives for one mole:

$$\Delta G = RT \int_{P_1}^{P_2} \frac{dP}{P} \quad \text{equ. (2.11)}$$

where R is the gas constant and T the absolute temperature. Thus the change in free energy per mole for a gas undergoing a change in pressure from P₁ to P₂, at constant temperature, is :

$$\Delta G = RT \ln\left(\frac{P_2}{P_1}\right) \quad \text{equ. (2.12)}$$

Thus each decade change in the concentration of the analyte gas, (i.e. P₂/P₁ = 0.1), typically gives $\Delta G \cong 6$ kJ/mole, at room temperature. Since a typical gas sensor requires a dynamic range of the order of a few decades, the free energy change of the chemical reaction upon which it is based should be of the order of kJ/mole.

2.2.3.2. Kinetics

There are no simple rules to relate the rate of a reaction to the reaction formula. Experimentally it is usually found that the rate of reaction is proportional to the concentration of one or more of the reactants, or powers of their concentrations. For instance, for a second order reaction of the type shown in equation 2.1, it is commonly found that:

$$\text{Reaction rate} = k [A].[R] \quad \text{equ. (2.13)}$$

where k is termed the rate constant and is a function of reactant that is used (per unit time). If one of the reactants is in molar excess compared to the other, the rate of reaction is approximately proportional to the concentration of the lower concentration reactant, and the reaction is termed a pseudo-first order. Thus, for simplicity, taking $[R]$ to be large compared to $[A]$, (not entirely justifiable, e.g. at near the upper limit of the dynamic range), then first order kinetics can be assumed, for which:

$$t_{1/2} = (\ln 2)/k \quad \text{equ. (2.14)}$$

where $t_{1/2}$ is termed the half time of the reaction and is equal to the time required to use up half of the reactant. Using transition-state theory^[4] it is possible to relate k to an energy barrier, ΔG^{++} , which must be overcome for a reaction to occur. Transition state theory says that a chemical reaction proceeds via an unstable intermediate complex of a higher energetic state than that for either of the reactants or products:



From figure 2.3 it is clear that overcoming this barrier is the rate limiting step in the reaction. This can be expressed numerically:

$$k = \kappa T/h \cdot \exp(\Delta G^{++}/RT) \quad \text{equ. (2.16)}$$

where κ is Boltzman's constant, and h is Plank's constant. The factor kT thus equals the frequency (per mole) at which reactant molecules 'hit' the barrier. Thus k is the fraction of molecules per unit time overcoming the barrier.

It is now possible to calculate a minimum value of ΔG^{++} which will allow for a reasonable reaction rate. Typically a sensor should respond in a few seconds, i.e. $t_{1/2} \cong 1$ second., and also $k \cong 1 \text{ s}^{-1}$.

Thus putting in the values into equation 2.15 yields $\Delta G^{++} \cong 70 \text{ kJ/mole}$.

2.2.3.3 Transport

Before any of the above can occur, the analyte must diffuse into the immobilised reagent phase. The diffusion of a gas or liquid into another phase is described by Fick's law, which in one dimension is:

$$\frac{\partial c}{\partial t} = D \frac{\partial^2 c}{\partial x^2} \quad \text{equ. (2.17)}$$

where c is the concentration at a point x and time t , and D is termed the diffusion coefficient. The solution of this equation for a real sensor geometry is not straightforward. For example, solving for the relatively simple situation of diffusion into a uniform film results in a very complex equation which is not easy to apply.^[4] As only an order of magnitude solution is required, a simpler situation is to consider the time taken for a molecule (or small element) of the analyte to diffuse a distance x in to the sensing material. This gives the expression:

$$x^2 = 2.Dt \quad \text{equ. (2.18)}$$

This expression is plotted in figure 2.4 for values of $t = 0.1, 1,$ and 10 seconds. Thus if the sensing material is in the form of a thin film of thickness $1 \mu\text{m}$, D can be as low

as $\sim 10^{-8} \text{ cm}^2 \text{ s}^{-1}$, but on the other hand if it is in bulk form and $x \sim 1 \text{ cm}$, then $D < 1 \text{ cm}^2 \text{ s}^{-1}$. (i.e. unrealistic).

Polymers are commonly used as an immobilising material for the reagent phase. The diffusion coefficient of molecules in polymers can be as high as $10^{-5} \text{ cm}^2 \text{ s}^{-1}$, (depending upon the molecular size and polymer).

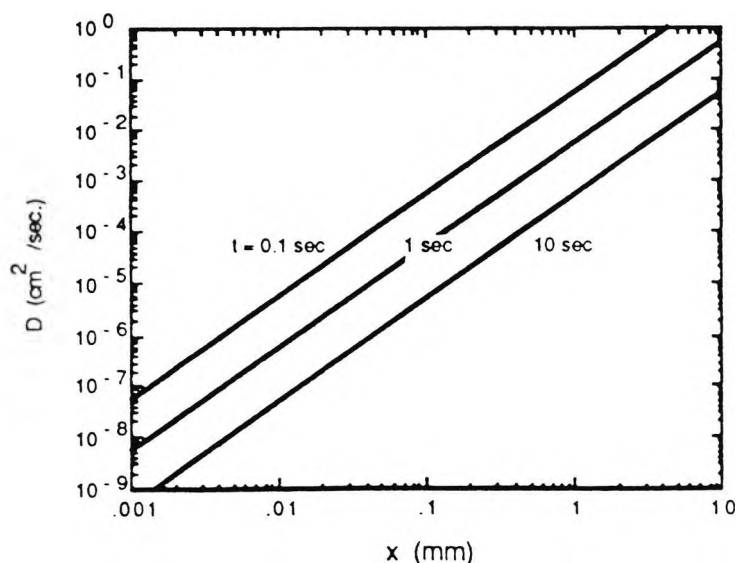


Fig 2.4: Graph showing the relationship between diffusion coefficient and diffusion distance, for three time periods

This is a rapid response which can be obtained from a sensor, if the sensing material has dimensions of say, tens of μm . On the other hand, if the sensing material is large, (say several mm/s) or the diffusion coefficient lower, then the response time will be correspondingly longer; hence the slow response of many of the devices described in Chapter 1, due to their comparatively large bulk.

2.3 Fibre Optics

An optical fibre cable consists a glass core that is completely surrounded by a glass cladding. The core performance the function of transmitting the light waves, while the purpose of the cladding is to minimise surface losses and to guide the light waves. The glass used for both the core and the cladding must be of very high purity since any impurities present will cause some scattering of light to occur. Two types of glass are commonly employed: silica-based glass (silica with some added oxide)

and multi-component glass (e.g. sodium borosilicate). (Some alternative optical fibres do not use glass at all, but special types of plastic; these are usually cheaper to make than very pure glass but introduce greater attenuation.). Cables made from optical fibres are cheaper, lighter and easier to install than copper cables. Furthermore, they are completely free from electromagnetic interference since data on a light beam cannot be corrupted by emission from electrical machinery, thunderstorms and 'noisy' power lines.

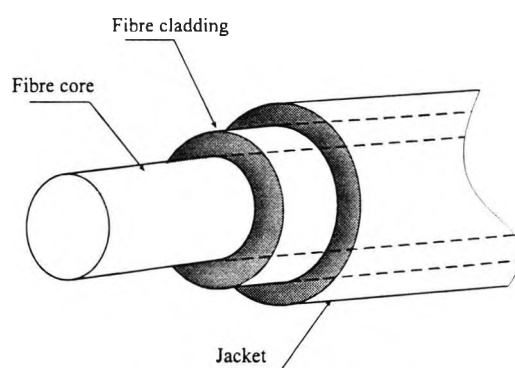


Fig. 2.5 Schematic of fibre optic

Proper choice and proper utilisation of optical fibres require a deep understanding of their characteristics. With this in mind, the major types of fibres and the properties of waves propagating through them should be considered.

2.3.1 Multimode Fibres

The multimode fibres normally are fabricated with a large core diameter e.g. 50 to 1000 μm , the different light beams that enter the glass guide travel at the same speed for different distances inside the fibre. This results in the delayed arrival of some of the modes. As a consequence, the intermodal dispersion in the fibre is increased. Although these fibres are not used in communications because they are a major source of bandwidth limitations, they are very useful in applications where simple light power transmitted is more important than intermodal dispersion and speed^[6], such as in chemical sensors.

This is the case where light from visible indicator type LEDs is used to provide an optical light source. As a result of the spreading of the light beam generated in these types of sensors i.e. due to diverging beams, it is more difficult to launch the light into the fibre unless the core diameter is large. This is often the case for amplitude modulation techniques where the optical intensity is the main measured variable. This type of fibre is mostly used in instrumentation and sensor applications where the speed of modulation of optical signals is very low (i.e. 0 to 100 KHz) which is the case in the work described in this thesis.

2.3.2 Single Mode Fibres

The single mode fibres normally have a core of 5 to 10 μm , so better bandwidth capacity is achieved through the propagation of a single mode, and thus this fibre is known as single mode fibre.

As a result, the intermodal dispersion is eliminated because there is no delay between the modes travelling in the fibre since there is only one mode propagating along it. The modal dispersion is then mainly caused by the material dispersion which cannot be avoided since it is inherent in the material used in the fabrication process. This type of fibre is used in most communication networks since it can achieve a very high bandwidth capacity and where data rates of Gbit/s^{-1} (gigabits per second) have been implemented in practice^[7].

Conventional interferometry is another field where single mode fibres are effectively the only fibre that can be used because these fibres can protect the phase and polarisation information of the light, especially in sensors such as current, pressure and temperature sensors^[8]. However, launching light from general purpose light sources can be a tedious problem because of the small cross section dimensions of the fibres. On the other hand, the output from laser light sources can be easily coupled to fibre since the divergence of the light beam emitted from the laser source is maintained within the acceptance angle of the fibre.^[9]

2.4 Fibre Optic Parameters and Characteristics

An important characteristic of an optical system is its ability to collect light incident over a wide range of angles. The optical fibres are characterised by a number of parameters, mainly the Numerical Aperture (NA) and V number of the fibre, as discussed below.

2.4.1 The Numerical Aperture

The numerical aperture of a given fibre is a measure of the maximum acceptance angle that the beam entering can be guided by way of multiple internal reflections along its length. It is independent of the dimensions of the fibre and is only a function of the refractive indices of the core and cladding and the medium from which the beam is launched i.e. in most case it is air, where $n_{\text{air}} = 1$. (where n is the sample medium e.g. for air is 1.).

However, in the case of the light source and the fibre both being immersed in the liquid, as often occurs in optical chemical sensing the numerical aperture value is seen to change according to the refractive index of the liquid, and, usually decreases since the refractive indices of liquids are larger than that of air. This may also result in a decrease in the divergence of the beam of light at the exit end of the fibre depending on conditions there. In order to obtain an accurate calculation of this parameter, the numerical aperture may be calculated from Eq. 2.19 by changing the value of the index of refraction of air by the corresponding value for the liquid.

As a result of applying Snell's law to :

$$n_w \sin(\theta) = n_1 \sin(\alpha) \text{ and } n_1 \sin(\beta) = n_2 \sin(\gamma).$$

The condition of the critical angle results in $\gamma = \pi/2$. Hence, the numerical aperture (NA) may be expressed as a function of the largest launch angle (θ) as follows:

$$NA = \arcsin \theta = \frac{1}{n_w} \sqrt{n_1^2 - n_2^2} \quad \text{equ. (2.19)}$$

where θ, β, γ are as shown in Figure 2.6 and n_w, n_1, n_2 are the refractive indices of the liquid sample, core and cladding of the fibre respectively. This can be expressed as a function of the numerical aperture with respect to air and is given by the following:

$$NA = \frac{NA_{air}}{NA_{water}} \quad \text{equ. (2.20)}$$

For instance, in the case of silica fibre used in this work, the Numerical Aperture (NA), as defined by the manufacturer at the air-glass interface, is 0.4. Consequently, the maximum acceptance angle for an air-glass interface is approximately 23° .

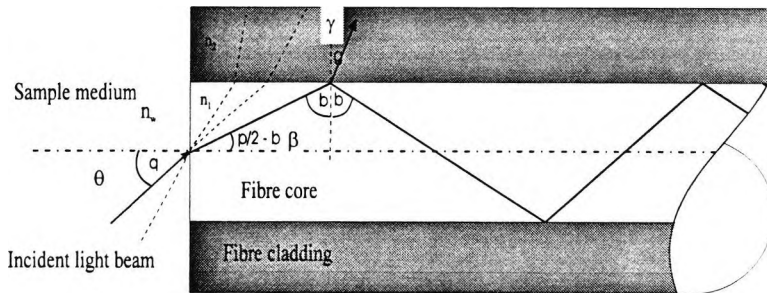


Fig 2.6 Figure showing the angle of acceptance of a fibre using ray propagation theory.

However, this value decreases when the fibre is immersed in water (index of refraction, around 1.3) where the $NA = 0.3$ giving a maximum acceptance angle of 18° (the index of refraction of most common species used in fibre can vary from 1.4 to 1.6 hence giving a relative NA as low as 0.28 and $\theta_{max} = 16^\circ$ or $NA = 0.25, \theta_{max} = 14^\circ$ respectively)^[10]. This effect has the advantage of reducing the spread of the beam leaving the fibre when used in water and hence allows for a stronger optical signal to be guided or collected by the returning fibre.

2.4.2 The V Number

The V number is a fibre parameter which gives an indication of the number of modes that can propagate along the fibre. It relates to the low cut off frequency for which no mode can propagate in the core of the fibre. Some other modes whose frequencies are below the cut off frequency can still propagate in the core for a short distance and

then exit the core of the fibre to be guided in the cladding before leaving the fibre completely. However, these modes are not important since they do not contribute to the total amount of light that reaches the end of a “realistic” length of fibre. This parameter (V) is also a function of the numerical aperture and is inversely proportional to the wavelength i.e. $V = \frac{2\pi}{\lambda} r(NA)$ where λ is the wavelength, r the radius of the core and NA the numerical aperture of the fibre. An optical fibre consists of an inner core of light-conducting material and a surrounding cladding with a refractive index which must be less than that of the core. In practical applications, both materials are surrounded by a protective sheath. The light propagates through the core through a total reflection at the core-sheath boundary. Figure 2.6 illustrates light propagation behaviour for different optical fibres

2.5 The Structure of Fibres

If the diameter of the light-conducting core is much greater than the wavelength of the light and if there is little change in refraction over an interval of one wavelength, then the propagation of the light waves can be described in terms of the so-called geometric optical approximation. However, there is the limitation that only a finite number of angles of inclination to the fibre axis are permitted. The number of modes thus propagating depends both on the wavelength of the light and on the geometry and distribution of refractive indices of the waveguide^[10].

In a multimode optical fibre V has a value of between 30 and 50. From figure 2.6 it is immediately clear that beams with different incident angles will require a different time to travel a given distance. This is important in communications technology, as a focused input pulse spreads during travel. This *mode dispersion*, limits the bandwidth of the transmission signals in stepped-index fibres, is of little significance for most chemical sensors where such a rapid response is not needed.

As discussed mode dispersion can be completely eliminated if a monomode fibre is used. From the technical point of view, it is much easier to produce multimode fibre^[12]. While monomode fibres with core diameters of between 2 and 10 μm are

manufactured from quartz (core and cladding), multimode fibres with core diameters of between 50 and several hundred μm s can be produced from a variety of material combinations, for example:

- cladding and core of quartz glass;
- cladding and core of normal glass;
- plastic cladding and quartz glass core, i.e. Plastic-Cladding Fibre (PCFs)
- plastic core and cladding.

The appropriate correct type of fibre should be selected for the intended application. Fibre optic bundles are also used for applications which require a particularly large light-conducting cross-section as well as a high degree of flexibility. Monomode fibres are rarely used in a fibre optic chemical sensor for the reasons mentioned above.

2.5.1 Step-Index Fibres

The Step-Index Fibre (SIF) consists of a fibre where the profile of the index of refraction of the core across the section varies as a step function as shown in figure 2.7 (1) and figure 2.7 (3). The manufacturing process is easy and hence cost is low. The mechanism of interfacing the fibre to a light source is not very critical i.e. The error of positioning of the light source especially large ones can be relatively high.

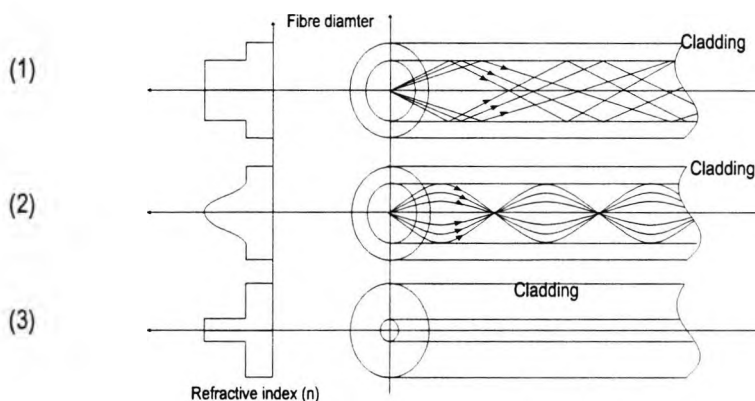


Fig. 2.7 :The light propagation through different types of optical fibres.
 (1) Step-index multimode fibre (2) Graded-index multimode fibre.(3) Step-index single mode fibre.

Step-index fibres have three common forms: a glass core, clad with a glass having a slightly lower refractive index; a silica glass core, clad with plastic; and a plastic core, clad with another plastic. Generally, the refractive index step is smallest for all glass fibres, a little larger for the plastic clad silica (PCS) fibres, and largest for the all plastic construction. This is due to the limited range of refractive indices available for glasses and the somewhat larger range for plastics.

2.5.2. Graded Index Fibre

This is a fibre whose profile of the index of refraction varies as a sinewave function, as is shown in figure 2.7 (2). This type of fibre is more difficult to manufacture and hence is more expensive. It is usually used where large diameter fibres and high bandwidth requirements are both needed at the same time.

2.5.3 Loss Mechanisms Within Fibres

The attenuation of light travelling inside a silica fibre can be attributed to three major sources which have been conveniently summarised in the literature^[13].

- Absorption
- Scattering
- Mechanical effects

2.5.3.1 Absorption

Absorption results from the interaction of the light as an electromagnetic wave with the constituents of the glass fibre, with the associated impurities and defects, and this can be classified into three types:

1. **Intrinsic**: in this case the losses are attributed to the stimulation of electron transition in the glass structure caused by higher energy excitations that occur in the ultraviolet part of the spectrum. This results in an exponential decay which increases with decreasing wavelength. A second phenomenon occurring in the infrared region is due to the molecular vibrations which result in fundamental and overtone absorption bands such as Si-O (9.2 μm) or Ge-O (11.0 μm).

2. **Extrinsic:** This type of absorption is caused by impurities deposited in the core and cladding material during the fabrication process. Their concentration can be in the low part per billion range (ppb). Nevertheless, they can cause attenuation throughout the UV and visible range which may be as high as 2 dB/km^{-1} . For example, Fe^{3+} absorption occurs at 400 nm with an attenuation of 0.15 dB. km^{-1} , Cu^{2+} , (685nm and 0.1 dB. km^{-1}) and Fe^{2+} , (1100nm , 0.68 dB. km^{-1}). Another source of attenuation is related to the hydroxyl ion (OH^-) which can be present as water vapour dissolved in the glass. As opposed to the other impurities, (OH^-) effects occur in the near infrared and infrared, and are thus far removed from the spectral range where UV and visible light are utilised.
3. **Defects :** These defects are usually generated by material vacancies within the crystalline structure of the glass. They can also be induced thermally or by means of radiation.

2.5.3.2 Scattering

The most common scattering effect which causes attenuation of light in the fibre is Rayleigh scattering. Molecules move randomly through the glass in the molten state during manufacture. The heat applied provides the energy for the motion. As the liquid cools, the motion ceases. Upon reaching the solid state, the random molecular locations are frozen within the glass.

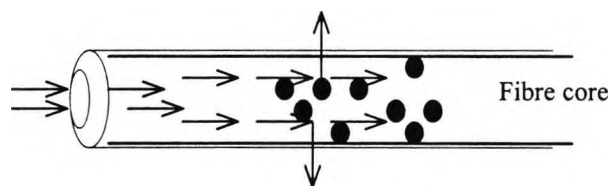


Figure 2.7: Rayleigh scattering showing attenuation of an incident stream of photons owing to localised variations in refractive index.

This results in localised variations in density and thus, local variations in refractive index throughout the glass. These variations may be modelled as small scattering objects embedded in an otherwise homogeneous material. The size of these objects is much smaller than the optical wavelengths. A beam of light passing through such a

structure will have some of its energy scattered by these objects, as illustrated in figure 2.7. This type of loss is known as Rayleigh scattering, which applies whenever a wave travels through a medium having scattering objects smaller than a wavelength of light. Because Rayleigh scattering is proportional to λ^{-4} , it becomes increasingly important as the wavelength diminishes.

A further cause of scattering loss must be considered. When a fibre material consists of more than one oxide, concentration fluctuations of the constituent oxides may occur. This is not a problem of imperfect chemical bonding of the various components. In this case the actual glass composition varies from place to place within the glass. Again, the localised refractive index variation resulting in Rayleigh loss follows the λ^{-4} dependence. The Rayleigh scattering loss (L) can be estimated by the expression

$$L = 1.7 (0.85/\lambda)^4 \quad \text{equ. (2.21)}$$

where λ is in micrometers and the loss L is in dB/km.

It is clear that scattering severely restricts the use of fibres at short wavelengths. Below 0.8 μm , the loss owing to this effect alone builds to a prohibitive value for long distance propagation. On the other hand, as the wavelength increases, the scattering loss diminishes. This effect provides an incentive to work at wavelengths beyond 0.8 μm . In fact, if fibre losses less than 0.05 dB/km are ever to be attained, the wavelength of operation will have to be greater than 2 μm .

Glasses composed of materials other than silica will be required to improve the fibre flexibility. Glasses based on the light and heavy metal halides (such as fluoride glasses) are candidates for this purpose but require further development. The density and compositional losses just described are intrinsic losses. They cannot be removed by any processing techniques other than changing the material composition. The scattering losses introduced by these two phenomena are considered to be a minimum

below which a fibre cannot be manufactured for a given glass. Other types of scattering, such as Raman scattering, of light by atoms and molecules may occur. When the photon energy is comparable with or greater than the resonance energies in the scatterer, there may be a quantum interchange of energy, so that a photon emerges from a collision with a different energy. This phenomenon is used in some physical optical sensors e.g. in temperature monitoring.

2.5.3 Bulk and Wavelength Imperfections

The physical irregularities generated during the fabrication process especially at the core cladding interface provide a means of reducing the transmission by total internal reflection since the latter is no longer sustained because of the resultant variations in the angle of incidence of the light on the interface. Scattering due to bubbles and cracks in the core of the fibre can also contribute to the loss of the light, especially when the dimensions of the irregularities are comparable to the wavelength. This effect is known as Mie scattering.

2.5.4 Fibre Bending

Bending a fibre causes attenuation. Two types of bends are *macroscopic* and *microscopic*. Macroscopic refers to large-scale bending, such as that which occurs intentionally when wrapping the fibre on a spool or pulling it around a corner. As a practical example, 125 μm diameter fibres can be bent with radii of curvature as small as 25 mm with negligible loss.

Typically, breaking will not occur unless the bend radius is much smaller. For example, the fibre will not fracture unless the bend radius is less than 10 mm. This example illustrates the great flexibility of glass fibres, allowing them to be installed where frequent bending is required. Loss is not the only adverse effect of bending. In addition, bending reduces the fibre tensile strength.

A fibre's strength depends on microscopic flaws located on its surface. These flaws will grow over time if the fibre is subjected to stress (or moisture), weakening the fibre. Thus, the stress due to bending may cause early failure of a fibre. For

commercial 125 μm diameter fibres, the minimum bend radius of 25 mm that assures negligible loss also ensures negligible strength loss.

Bending loss can be explained in several ways in Figure 2.9 (a). When the fibre is bent, the angle of incidence changes. The beam then propagates through the cladding since the angle of incidence becomes larger than the critical angle. This effect, as can be seen in Equ.2.22, is a function of the critical curvature radius. It is also a function of wavelength and results in different loss values for different wavelengths, especially if the gap difference between the wavelengths is large. In a sensor system using two different wavelengths, one as the sensing wavelength and the other as the reference wavelength, a non systematic error is introduced during the measurement process when the guiding fibre is bent, especially for systems where each fibre is used to guide one particular wavelength.

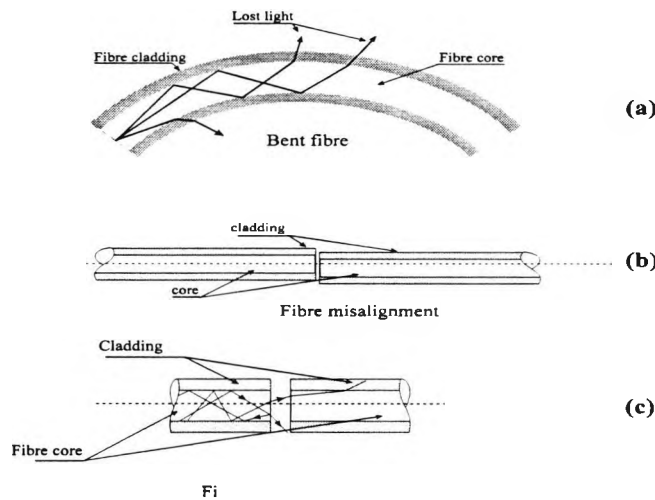


Figure 2.9 : Types of fibre losses: (a) losses caused by fibre bending (b) losses from fibre misalignment and (c) Fresnel losses at the fibre-fibre connection

$$R_c \approx \frac{3 n_2^2 \lambda}{4\pi (n_1^2 - n_2^2)^{3/2}} \quad \text{equ. (2.22)}$$

where n_1 and n_2 are the refractive indices of core and cladding, R_c is the curvature radius and λ is the wavelength.

For small scale sensors care must be taken not to bend fibre optic excessively to avoid such losses. The design of a fibre optic must be such as to allow fibre to have a sufficiently large bend radius to maximise transmission.

2.5.4.1 Fibre Coupling

A change in the refractive index in the connecting part of the fibres is usually the source of the losses at the fibre-fibre interface. The most common is the gap between fibres. As can be seen in fig 2.9 (b), there is always a gap between the two fibres however, well polished and flat the fibre ends are. Hence, there is a gap made of air which has a different refractive index to that of the glass and will result in a loss of light power.

Other effects such as fibre misalignment tend also to produce a loss of light power since the total area of the core of the fibres are not in line, hence part of the energy is transmitted into the cladding of the second fibre. This effect, although very important for small diameter fibre e.g. 10 to 100 μm , is usually insignificant in large diameter fibre e.g. 500 to 1000 μm diameter since the control of the positioning of the fibres is easier. A second source of energy loss within fibres is due to Fresnel effects as depicted in Figure 2.9(c).

These losses are inherent in the process of light guidance in a fibre. Similar to the reflection of light inside a fibre, the air (or water sample), and fibre interface behave in the same way as the core cladding interface. Because the index of refraction of air is smaller than that of the fibre core, the light is partially reflected back into the fibre. This effect is used in Optical Time Domain Reflectometers (OTDR) as a mean of locating splices and fibre break. Fresnel losses calculated from Equ. 2.23.

$$L_{\text{Fresnel}} = -10 \log_{10} \left(1 - \left\{ \frac{n_1 - n_2}{n_1 + n_2} \right\}^2 \right) \quad \text{equ. (2.23)}$$

where n_1 and n are the refractive indices of fibre core and medium (usually air or index matching gel) respectively. The losses are smaller when the interface is made of water and glass since the difference in their respective refractive indices is small.

2.5.5 Mechanical Effects

According to ray theory, the multiple internal reflection principle can only be sustained if the reflected light beam falls within the acceptance angle along the fibre as shown in fig 2.9 (a). When the fibre is bent, the angle of incidence changes and the beam can propagate through the cladding. In sensor systems using two different wavelengths, one as the sensing wavelength and the other as the reference wavelength, a non systematic error is introduced during the measurement process when the guiding fibre is bent, especially for systems where each fibre is used to guide one particular wavelength.

2.6 Fibre Reliability

Much emphasis has been placed on fibre reliability for acceptability of fibres in sensors and long term effects depend upon on three major factors. These are related to fibre strength, changes in attenuation due to radiation and finally the effect of hydrogen on the increase in the OH^- absorption profile.

(1) The fibre strength is related to the appearance of micro-cracks caused by fibre bending and fibre stress. These are believed to be generated by chemically or mechanically induced flaws, usually at the surface of the fibre, and result in a local failure. Coating the fibre with different polymer and appropriate materials to prevent moisture damage to the fibre surface has been proposed as a feasible solution to these problems.^[14]

(2) The effect of strong ionising radiation on the attenuation profile of the fibre has been found to be an important factor in the design of instruments using fibre links. The radiation can affect the chemical bonds in the glass matrix. These are then disrupted giving rise to absorption in the visible and infrared parts of the spectrum.

This structural damage is seen to affect multicomponent fibres (e.g. silica doped with GeO_2) more than fibres made out of pure silica.^[15] This structural damage is found to be caused by the removal of the oxygen atom from the glass matrix, thus generating defect sites.

(3) Finally, the increase of attenuation in the fibre is related to the hydrogen induced losses. This is the result of the reaction of hydrogen, dissolved in the glass, with the rest of the matrix. Although the phenomenon which causes this absorption is understood, the mechanism of reaction of non-dissolved hydrogen with the glass lattice is still not clear^[16]. It has been observed also that these OH^- absorption losses occur in the red and infrared part of the spectrum. Most of the above problems can be avoided, with care, in practical sensor systems.

2.7 Optical Emission and Detection Systems

In optical instrumentation, two important stages form the basis of the measurement, once the sensing principle has been chosen. These consist of the light source and the light detection systems. In addition to the correct choice of these devices, the influence of the various sources of noise in the detected optical signal must be considered.

2.7.1 Light Sources

Traditionally, sources for chemical sensing are broad-band light sources with filters or narrow-band lasers. There are inherent problems associated with these sources. For example, laser sources are often bulky and expensive. Incandescent filament sources have stability problems, they generate a lot of heat and are generally bulky and movement of the actual filament within the bulb can cause change in the optical alignment of the system.

The interference filters often used with these sources are also very temperature sensitive and the layers forming the filter can separate over a period of time (i.e. delamination), causing a change in the optical transmission characteristics of the

device. Light emitting diode (LED) sources can overcome a number of these problems. Their narrow bandwidth means that they can often be used without filters. They are small in size, have a low power consumption, they have a stable output and they are inexpensive.

2.7.2 LED Technology

Light emitting diodes (LEDs) often have been used in the design and the implementation of the optical fibre chemical sensors. These have been chosen because of the light power/cost ratio, have a long life and the fact that they are small in size, hence do not present a major problem in the minimisation of the overall dimensions of the instrument. Additionally, they can be electronically modulated so that the effect of noise and ambient perturbations can be filtered out electronically. The operating principles of LEDs and how these principles give rise to the advantage features of these sources are discussed in several standard texts ^[17].

2.7.3 Characteristics of LEDs

The output spectrum of an LED is centred around the energy of the main recombination process for that particular p-n junction. This feature gives rise to two of the most important characteristics of LEDs as a light sources. The first is the narrow bandwidth of the output spectrum compared with broad-band sources. The emitted photons arise from a single recombination process and hence have a narrow band of energies centred around this transition level.

The second feature is that LED output covers almost the entire visible band and near-infrared (NIR) spectrum. By selection of semiconductor material, dependent impurities, dopant concentrations and manufacturing techniques, LEDs can be made to emit in specific wavelength bands. Because of the finite number of semiconductor materials, (e.g. E_g values), not every wavelength region is available with LEDs. However, new materials and processes are constantly being discovered. For example until quite recently high intensity blue LEDs were not available. Early designs involved doping silicon carbide with aluminium, but these had low output powers.

More recently gallium nitride has been doped to p-type production a new range of high intensity LEDs which emit in the near ultra-violet and blue regions^[18], which will clearly have an impact upon fibre optic sensors. Each emitted photon is generated by an injected electron from the external circuit. Hence the output intensity is easily modulated by controlling the externally supplied current. As the majority of semiconductor materials used in LEDs are of the direct band-gap type, there is no heat released in the recombination process and hence no electrical heating in the device. As a result LEDs have very large mean time between failures, (e.g. 10000 hrs), compared with incandescent sources.

Advances in semiconductor manufacturing technology have improved the quality and reduced the cost of LEDs. Large numbers of p-n junctions can be produced from a single wafer and this results in low costs for most commercial LEDs. They are also easily manufactured to specific shapes and orientations which enables more efficient coupling to fibre ends.

2.7.4 Temperature Effects on LEDs

A disadvantage of light emitting diode is that their output is temperature sensitive. The peak wavelength of the output spectrum shifts to longer wavelengths with increasing temperature by typically 0.3 nm/K^[19]. The output intensity also decreases with increasing temperature and aging^[19]. The intensity L , at a particular wavelength λ and temperature T , is governed by the following equations^[20].

$$L(\lambda, T) = P_o / 0.6 \lambda_w (\pi)^{1/2} \cdot \exp(k\Delta T) \cdot \exp\{-2.78[\lambda - \lambda_o(T)]^2 / \lambda_w(T)^2\} \quad \text{equ.(2.24)}$$

$$\text{and } \lambda_o(T) = \lambda_o + k_o \Delta T \quad \text{equ.(2.25)}$$

$$\lambda_w(T) = \lambda_w + k_w \Delta T \quad \text{equ.(2.26)}$$

$$\Delta T = T_\lambda - 25 \quad \text{equ.(2.27)}$$

where P_o is the radiant power, λ_o is the peak wavelength, λ_w is the spectral bandwidth, k_I is the temperature coefficient of light intensity (usually $-0.001/\text{K} \rightarrow -0.02/\text{K}$), k_s is the temperature coefficient of spectral shift (usually $0.1 \text{ nm/K} \rightarrow 0.6 \text{ nm/K}$), k_B is the temperature coefficient of spectral bandwidth (usually assumed to be 0) and k_A is the ambient temperature (25°C). The characteristics of the peak wavelength and the width of the emission are both sensitive to temperature, especially over the large temperature range as shown in Fig 2.10.

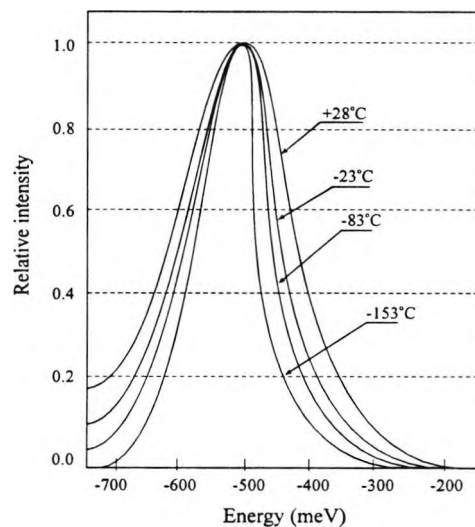


Fig. 2.10: Broadening due to temperature (-153 to $+25^\circ\text{C}$) occurring in the emission of GaP LED with an acceptor concentration of 10^{+18} cm^{-3} . [21]

Although there is a shift of the peak wavelengths towards higher wavelength and also width broadening, this effect is not practically important in normal use since absorption in UV-visible part of the spectrum is broad and the range of temperatures covered is significantly smaller. Additionally, these LEDs can be easily electronically driven which reduces the complexity of the drive instrumentation circuitry normally employed.

2.8 LEDs and Chemical Sensing

A recent review paper by Taib and Narayanaswamy^[22] details a number of LED-based systems for chemical sensing, several examples of which are given. The most common use of LEDs in chemical sensing has been with photometric methods, i.e. measurement of spectral attenuation of LED radiation by a sample.

Traditionally, incandescent sources and filters have been used for these tests. However this sort of arrangement has inherent stability problems associated with filter degradation and pulse stability. Recently LEDs, have been favoured, as alternative light sources, for the reasons outlined in section 2.7.3. Some examples of the use of LEDs in various chemical sensor arrangements, are described here. Worsfold et al. have produced numerous papers outlining the incorporation of LEDs into on-line flow injection analysis (FIA) systems^[23-25].

The stability, long life and low power consumption of LEDs make them ideal sources for much on-line systems. Worsfold documents a nine month field trial of an on-line FIA system testing for nitrate in river water^[26]. No problems were reported from the green LED used in this system. Kraus et al. utilise LEDs in their photometric comparator^[27]. This is a hand-held device providing a binary output which indicates if a sample is above or below a certain threshold. Several LEDs can easily be incorporated into a single FIA system to allow dual analyte detection, e.g. zinc and aluminium^[27], dual wavelength referencing^[28], and dual wavelength compensation for turbidity and refractive index effects^[29].

Grattan et al have also used dual wavelength referencing for their fibre optic based pH sensor^[30]. Small size and low power consumption, make LEDs an ideal source for a portable pH sensor for process control. Also entero-gastric reflex detection outlined by Baldini et al^[31]. This fibre based device is inserted into the patients stomach via the nasal cavity. The small size and low power consumption of the source allows the necessary instrumentation to be strapped to the patient's body.

Recently LEDs have been used in a fluorometric process^[32]. Here the LED excites fluorescence of a particular dye and then the concentration of analyte in the sample affects the intensity or lifetime of the emitted fluorescent intensity. Lasers were previously favoured for fluorimetric techniques because of the high intensity and narrow bandwidths required. However, new high intensity LEDs are now proving suitable and this allows considerable simplification of the necessary instrumentation.

2.9 Light Detectors

There are three type of light detectors that are commercially valuable and can be used in fibre optic related instrumentation:

- Junction photodiodes.
- Avalanche diodes.
- Photomultipliers.

2.9.1 Junction Diode

The junction photodiode is basically a diode whose junction is only covered by a glass window to allow light to penetrate the device and interact with the carriers in the depletion region to produce free electrons. When the electron absorbs the light energy, it jumps from the valence band into the conduction band. As a result, a hole is liberated and a pair (electron-hole) is generated. These are attracted to opposite sides of the junction by the electrical field thus generating a flow of current. This current is proportional to the intensity of the incident light on the diode e.g. photodiode. Devices such as current converters transform this signal into a different form without loss of information. The most common material used is silicon which has a varying sensitivity to light as a function of wavelength. The peak of sensitivity is reached in the 900nm region.

However, silicon is used in visible region with good results and when the glass window is replaced by quartz window, the same device can used to detect ultraviolet energy to a maximum wavelength of 250nm although with a much reduced sensitivity e.g. 1.5 to 2 compared to 6 at 900nm. Different materials having enhanced optical properties such as germanium (Ge) and indium gallium arsenide (InGaAs) are used in the design of photodetectors. These are mainly used for the detection of infrared and far infrared wavelengths. Hence they are not suitable for ultraviolet and visible light detection.^[33]

A major factor which affects the response of the photodiode is the dark current which represents the current flowing without illumination. This effect can be superposed onto the main detected signal and reduces the signal to noise ratio. Large values are obtained with germanium e.g. 100nA, but are low in the case of silicon (e.g. 1nA). Additionally the dark current is sensitive to temperature and can reach values as large as 1 μ A at 40 °C for germanium. These photodiodes have a response in the order of 10^{-9} s. Performance is enhanced when an intrinsic layer is sandwiched between the p and the n regions creating a longer depletion region where most of the photons are absorbed to produce an electron hole pair and this is known as a positive-intrinsic-negative (PIN) device. As a result of this layer, longer wavelengths can be detected and the sensitivity of the diode is increased.

When speed is not major requirement e.g. below the μ s range, a phototransistor which relies on the same physical effect, can be used to measure the light. The collector-based junction is used as the photon converting part and the generated carrier is amplified in the same device. A Darlington structure can also be used to amplify the current to the required level.

2.9.2 Photomultiplier

A different type of detector could be used but is usually avoided because of its fragility and power supply requirements. This device is the photomultiplier. It uses a different mechanism in order to detect and amplify the signal. When light falls on a thin layer of conducting material such as cesium, an electron is extracted from the metal. The latter is accelerated through an electric field generated by a difference of voltage of the order of 100V applied to a successive number of dynodes. On impact on the collecting dynode, more electrons are extracted which in turn are accelerated through by the light voltage existing between these dynodes.

The gain in the detection process is also that this device is sensitive to light power in the 10^{-12} W range. It has a flat response especially in the ultraviolet part of the spectrum and is widely used. This device is very sensitive to the fluctuation of the bias voltage since the gain is a function of the high voltage value and hence requires

a very stable power supply. Recently, robust and miniaturised devices have become available, particularly in Japan ^[34] (Hamamatsu Corp.), and in future research could prove to be valuable.

2.9.3 Avalanche Photodiode

Avalanche photodiodes are similar devices to the photodiode with improved carrier amplification which occurs by impact ionisation. This is the result of an intense electric field created by the high reverse bias voltage (e.g. 100 to 400V). Amplification as high as 10^{+4} can be achieved in defect-free material.

This is very useful especially in conditions where the detected light is very weak as is the case in certain type of instrumentation. However, both the random nature of the gain mechanism and its sensitivity to temperature tend to increase the noise level. Additionally, the high gain which is reverse bias voltage dependent is not constant over the optical spectrum since it is a function of the wavelength. Finally, this device is targeted towards communication type wavelengths and hence their cost tends to be high when developed for use in the visible and ultraviolet part of the spectrum for instrumentation use.

Finally, the detection of the returning radiation is usually undertaken in one of two ways.^[35]

- (i) - Semiconductor photodiodes (or their avalanche and PIN variations), are the most commonly used, being sensitive, small, cheap, and available for directly coupling to fibres.
- (ii) - Silicon devices are utilised for detection in the visible and near IR regions, with other narrower band gap semiconductors such as germanium and indium-gallium-arsenide for detection further into the IR.
- (iii) - If the signal to be detected is particularly weak and in the blue end of the visible or UV, it is necessary to use a photo-multiplier tube PMT. (However, these are bulky, expensive, and require a high voltage power supply).

2.10 Summary

The use of optical fibres as part of the optical set-up can only provide more flexibility for the design of such a practical sensors. It has been shown in this chapter that there is not one set of rules to use to devise and build a measuring instrument but the development is rather case dependent, so that the choice of the light source and the detector system is carefully studied.

Beer's law was discussed and a method derived for determination of analyte concentration in a sample when using a colorimetric process. The availability of LEDs are a great advantage as their narrow bandwidth, long stability compared to incandescent sources, also their small size, long lifetime and low power consumption make it very easy for the designer. The main features of the LEDs that they are increasing used in favour of the traditional sources in chemical sensing applications. The next Chapter will deal with sensor theory in general and outline the fibre optic chemical sensor specifically in great detail.

2.11 References

1. M. Ylilammi, "Thermodynamics of Sensors", *Sensors and Actuators* 18, 167 (1989).
2. J. Janata, "Principles of Chemical Sensors", Ch. 1, Plenum Press, (1989).
3. W.R. Seits, "Chemical sensors based on fibre optics", *Anal.Chem.* 56, 16A, (1984).
4. D.F. Eggers, "Physical Chemistry", John Wiley and Sons Inc., (1964).
5. J.W. Buttle, et al., "Chemistry : Aunified Approach", Butterworth and Co., (1981).
6. B. Culshaw, "Optical Fibre Sensing and Signal Processing", Peter Peregrinus, London (1984).
7. J. Comyn, "Polymer Permeability", Ch. 1. Elsevier Applied Science Publishers (1985).
8. P.V.P. Yupapin, "Optical Pressure Sensing using Interferometry techniques" PhD. thesis, City University chapter 1, (1993).
9. R.C. Weast, and J. Astle, *Handbook of Chemistry and Physics*, ed. 62. CRC press Inc. Boca Raton, Florida. USA, (1982).
10. D. Marcuse, "Principles of Optical Fibre Measurements", Academic Press New York (1981).
11. R.T. Kersten, "Physik in unserer", *Zeit* 15, 5, 139, (1984).
12. B.P. Pal, K. Thyagrajan, and A. Kumar, "Characterisation of optical fibres for telecommunication and sensors Part 1: Multimode fibre", *Inter J. Optoelec.*, vol. 3 No. 1, pp 45 - 47 (1993).
13. B.P. Pal, K. Thyagrajan. and A. Kumar, "Characterisation of optical fibres for telecommunication and sensors Part 2: Single mode fibre", *Int. J. Optoelec* vol. 3, No., 2, pp 153 - 176, (1994).
14. S.R. Nagel, "R&D Direction of optical fibre" *IEEE*, vol. 3, No 4 pp 26-34, (1992).
15. J. Gowar, "Optical Communication Systems" Prentice Hall Inc., London Chapter 3 (1984).
16. A. Iino, M. Kuwabara and K. Kokura, "Mechanisms of hydrogen - induced losses in silica-based optical fibre", *J. Light tech.*, vol 8, No 11, p-1675-79, (1990).

17. Kenneth A. Jones, "Introduction to Optical Electronics" Chapter 6, J. Wiley and Sons, Inc. New York (1987).
18. DCL Components Ltd. "New Super Bright LED, Technical information sheets.
19. B. Culshaw, "Optical Fibre Sensing and Signal Processing", Optics IEE pp 37 (1994).
20. G. Murtaza and J.M. Senior, "Wavelength selection strategies to enhance referencing in LED based optical sensors", Optic Communication, 112, pp-201-213, (1994).
21. K.A. Jones, "Introduction to Optical Electronics", John Wiley & Sons, Inc, Chapter 6, (1987).
22. M.N. Taib and R. Narayanaswamy, "Solid state instruments for optical fibre chemistry sensors" a review, Analyst, vol 120, pp-1617-1625,(1995).
23. J.R. Clinch, P.J. Worsfold and H. Casey, "An automated spectrophotometric field monitor for water quality parameters, determination of nitrate" Analytical Chimica Acta, 200 (1) pp523-531, (1987).
24. R.L. Benson, P.J. Worsfold and F.W. Sweeting "On-line determination of residual aluminium in potable and treated water by flow-injection analysis", Analytical Chem. Acta 238, 177-182, (1990).
25. JR Blundell, A Hopkins, PJ Worsfold and H. Vasey, "A portable battery powered flow injection monitor for the in-situ analysis of nitrate in natural waters", Journal of Automatic Chemistry vol. 15, pp-159-166 (1993).
26. H. Casey, R.T. Clark, S.M. Smith, J.R. Clich and P.J. Worsfold, Spectrophotometric field monitor for the determination of nitrate in river water: statistical analysis of the results from a nine-month field trial. Analytical Chimica Act, 227, 379-385 (1989).
27. P.P.R. Kraus, A.P. Wade, S.R. Crouch, J.F. Holland and B.M. Moller, "Portable double-beam, fibre optic based photometric comparator, Analytical Chemistry, 60, 1379-1390 (1988).
28. M.Trojanowicz and J. Szpunar- Lobinska, "Simultaneous flow-injection determination of aluminium and zinc using LED photometric detection 2 Anal. Chem. Acta. 230, pp-125-130, (1990).

29. J. Huang, H. Liu, A. Tan, J. Xiu and X. Zhao, "A Dual-wavelength light emitting diode based detector for flow-injection analysis process analysis", *Talanta*, vol. 39, No 6, 589 - 592 (1992).
30. K.T.V. Grattan, Z. Mouaziz and A.W. Palmer, "Dual wavelength Optical Fibre Sensor for pH measurement, *Biosensors*, (1), 17-25 (1987).
31. P.Bechi, F. Pucciani, R. Falciai, F. Baldini, F. Cosi, A. Bini and F. Milanesi, "Optical fibre bile sensor for entro-gastric reflux detection", *Sensors and Actuators B*, 7, 775-779, (1992).
32. H. Liu and K. Dasgupta Dual wavelength photometry with LED compensation of refractive index and turbidity effects in flow injection analysis., *Analytical Chimica Acta.*, 289 pp-347-535,(1994).
33. B.D. Mac Craith, G. O'Keefe, C. McDonagh and A.K. McEvoy, "LED-based fibre optic oxygen sensor using sol-gel coating", *Electronic letters*, vol. 30 No 11, pp 888-889, (1994).

Chapter 3

pH Measurement with Dyes Preliminary Investigation on Optical Fibre Ammonia-based Sensor using Colorimetric Techniques

3.0 Abstract

A rapid response, inexpensive, fibre optic pH sensor which uses a two wavelength time division multiplexed system to measure the change in absorption of an indicator dye and providing a reference channel for other losses in the light path has been constructed and described, for use in solution, with solid state LED light source and PIN photo detector being employed. The aim has been to investigate the pH measurement optically as a preliminary study for the ammonia measurements. This chapter acts as an introduction and background for the future ammonia sensor development and implementation of an optical fibre based.

3.1 Introduction

pH is a term used widely to express the strength of the acid or alkaline condition of a solution. It is a way of expressing the hydrogen-ion concentration, or more precisely, the hydrogen-ion activity, and pH is a factor that must be considered in chemical coagulation, disinfection water softening, and corrosion control. In wastewater treatment employing biological processes, pH must be controlled within a range favourable to the particular organisms involved.

Chemical processes used to coagulate wastewaters, dewater sludges, or oxidise certain substances, such as the cyanide ion, require that the pH be controlled within rather narrow limits. For these reasons and because of the fundamental relationships that exist between pH, acidity, and alkalinity, it is very important to understand the theoretical as well as the practical aspects of pH.

3.1.1 Theoretical Considerations

The concept of pH evolved from a series of developments that led to a fuller understanding of acids and bases. Acids and bases were originally distinguished by their difference in taste and later by the manner in which they affected certain materials that came to be known as indicators. With the discovery of hydrogen by Cavendish in 1766, it soon became apparent that all acids contained the element hydrogen. Chemists soon found that neutralisation reactions between acids and bases always produced water. From this and other related information, it was concluded that bases contained hydroxyl groups.

In 1887 Arrhenius announced his theory of ionisation. Since that time acid have been considered to be substances that dissociate to yield hydrogen ions or protons, and bases have been considered to be substances that dissociate to yield hydroxyl ion. According to the concepts of Arrhenius, strong acids and bases are highly ionised and weak acids and weak bases are poorly ionised in aqueous solution. Proof of these claims had to await the development of suitable devices for the measurement of hydrogen-ion concentration or activity.

3.1.2 Measurement of Hydrogen-Ion Activity

The hydrogen electrode was found to be a suitable device for measuring hydrogen-ion activity. With its use, it was found that pure water dissociates to yield a concentration of hydrogen ions equal to about 10^{-7} mol/l.



Since water dissociates to produce one hydroxyl ion for each hydrogen ion, it is obvious that about 10^{-7} mol of hydroxyl ion is produced simultaneously. By substitution in the equilibrium equation (3.1), we obtain

$$\frac{\{\text{H}^+\}\{\text{OH}^-\}}{\{\text{H}_2\text{O}\}} = K \quad \text{equ. (3.2)}$$

but, since the concentration of water is so extremely large and is diminished so very little by the slight degree of ionisation, it may be considered as constant (its activity equals 1.0), and Eq. 3.2 may be written as:

$$\{\text{H}^+\}\{\text{OH}^-\} = K_w \quad \text{equ. (3.3)}$$

and for pure water at 25°C ,

$$\{\text{H}^+\}\{\text{OH}^-\} = 10^{-7} \cdot 10^{-7} = 10^{-14} \quad \text{equ. (3.4)}$$

This is known as ion product or ionisation constant for water.

When an acid is added to water, it ionise in the water and the hydrogen-ion activity increases; consequently, the hydroxyl-ion activity must decrease in conformity with the ionisation constant. For example, if acid is added to increase the $\{\text{H}^+\}$ to 10^{-1} , the $\{\text{OH}^-\}$ must decrease to 10^{-13} . it means $10^{-1} \cdot 10^{-13} = 10^{-14}$.

Likewise, if a base is added to water to increase the $\{\text{OH}^-\}$ to 10^{-3} , the $\{\text{H}^+\}$ decreases to 10^{-11} . It is very important to remember that the $\{\text{OH}^-\}$ or $\{\text{H}^+\}$ can never be reduced to zero, no matter how acid or basic the solution may be.

3.1.3 pH Concept

The expression of hydrogen-ion activity in terms of molar concentrations is rather cumbersome. In order to overcome this difficulty, Sorenson (1909) proposed to express such values in terms of their negative logarithms and designated such values as p^+_{H} . His symbol has been superseded by the simple designation pH. The term may be represented by

$$\text{pH} = -\log \{\text{H}^+\} \quad \text{or} \quad \text{pH} = \log \frac{1}{\{\text{H}^+\}} \quad \text{equ. (3.5)}$$

and the pH scale is usually represented as ranging from 0 to 14, with pH 7 at 25°C representing absolute neutrality.

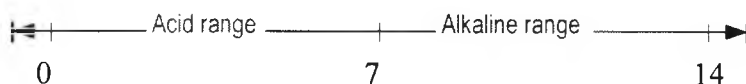


Fig 3.1: pH scale

Because K_w changes with change in temperature, the pH of neutrality changes with temperature as well, being 7.5 at 0°C and 6.5 at 60°C. Acid conditions increase as pH value decrease, and alkaline conditions increase as the pH value increase.

3.2 The Measurement of pH

The hydrogen electrode is the only absolute standard for measurement of pH until the late seventies. It is rather cumbersome and not well adapted for universal use, particularly in field studies or in solutions containing materials that are adsorbed on platinum black. A wide variety of indicators were calibrated with the hydrogen electrode to determine their colour characteristics at various pH levels. From these

studies it became possible to determine pH values fairly accurately by choosing an indicator that exhibited significant colour changes in the particular range involved. With the use of about six to eight indicators, it is possible to determine pH values in the range of interest to environmental engineers. Their use has been superseded by development of glass electrode.

About 1925 it was discovered^[6] that an electrode could be constructed of glass which would develop a potential related to the hydrogen ion activity without interference from most other ions. Its use has become the standard method of measuring pH.

However, as the technology moves faster, the interest in pH measurement is of great importance. A new techniques have been developed since the first optical fibre pH probe was reported by Peterson et al^[1]. Different methods are now available to carry out the measurement of pH under various environmental conditions. The most widely used methods are based on electrochemical or optical phenomena. In the case of electrochemical methods, potentiometric techniques are deployed to monitor the activity of the hydrogen ion based on the Nernst equation which relates the activity of the ion to the numerical value of the pH, as shown in Eq. 3.6. The resultant voltage that develops across the two electrodes, one of which is a reference electrode, provides a voltage output which represents a measurement of the pH, as is depicted in Fig. 3.2.

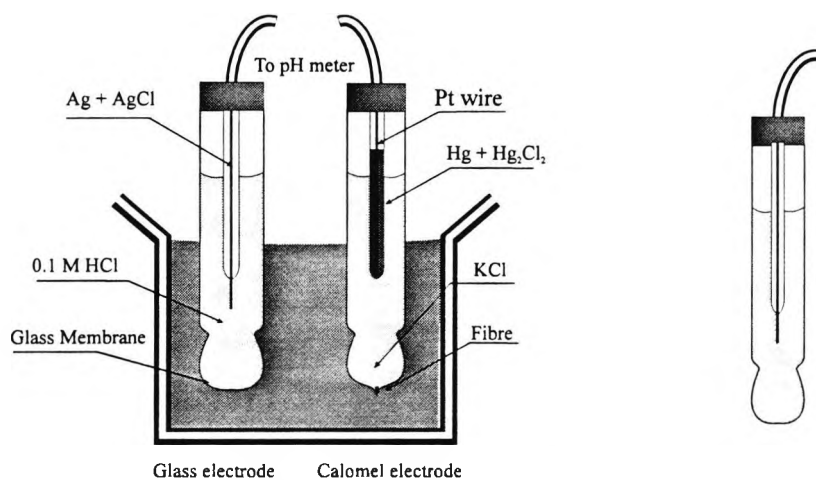


Fig 3.2 : Schematic drawing of a pH electrode based on potentiometric technique

In potentiometric measurements, this electrode could be a liquid junction whose voltage E_j is assumed to remain constant since it is generated by the solution of reference. The voltage appearing at the electrode of a system consisting of a combination of {indicator electrode/sample//reference solution/reference electrode}, can be expressed as in Eq. 3.6.

$$E_{\text{system}} = E_{\text{indicator}} - E_{\text{ref}} + E_j \quad \text{equ. (3.6)}$$

where E_{system} , $E_{\text{indicator}}$, E_{ref} and E_j are the potentials that develop for the complete system, the indicator and reference electrodes and the liquid junction respectively. To overcome the problem of liquid junction variation, salt bridges were used and different systems operating without a liquid junction were devised. For example the glass electrode pH meter has a glass membrane which is hydrogen ion selective. A voltage develops across the glass membrane and is related to the activity of the hydrogen ion. In this case the reference electrode is a calomel or Ag/AgCl electrode.

A second effect which might reduce the field of use of such a technique is the ionic strength of the sample. The activity of the ion is a function of the ionic strength and it was found that this relationship influences the activity of the ion, for an ionic strength larger than 3.^[2] Additionally, the local electrical potential is known to affect the measurement of pH value. Moreover, the pH of solutions where a current flows cannot be measured by this technique e.g. in a liquid battery.

3.2.1 pH Measurement Using Colorimetric Techniques

In the case of colorimetric techniques, the pH measurement is obtained by monitoring the change of the colour of organic dyes which are sensitive to the hydrogen ion concentration present in a given sample. Conventionally, the numerical value of the pH of a substance is approximately estimated by comparing the intensity of the colour, most simply of a “universal indicator” paper on which specific dyes have been adsorbed, with a calibrated reference. Furthermore, colorimetric techniques can be used in a variety of situations, even in liquids, where other electrical effects are taking place, as is the case for electroplating plants. This results from the fact that the

transducing effect has completely an optical characteristic. However, the major drawback of colorimetric techniques resides in the fact that the interaction of light with the dyes results in obtaining a measure of the concentration of the dye which has reacted with the species, in this case H_3O^+ . Hence the change of colour is related to the concentration of either the dissociated or the undissociated part of the dye. This, in turn, is related to the concentration of the hydrogen ions present in the sample. Approximations in the relationship between the hydronium ion concentration and its activity are made so that the measurement of pH value is obtained^[2].

This technique, in combination with spectrometry, provided a sound base for the development of a mathematical technique which can be used to overcome the problem of comparative insensitivity of the naked eye. Furthermore, with the advances of optoelectronic and fibre optic methods, colorimetry could be made to suit the requirement of the medical and industrial fields. The chemistry of these indicators is well established and has been extensively discussed in the literature^[4]. It is not the aim of this work to develop these indicators, but it is to develop appropriate fibre optic instrumentation and its implementation.

3.2.3 Focusing in Fibre Optic pH Sensor

Fibre optic pH sensors were at the centre of attention of early fibre optic based sensor development and work in this area has been focusing on the important chemical aspect of some measurement^{[3], [5], [6]}. Some of these early systems were bulky, and used costly and powerful optical light sources. Additionally, spectrometers were used to monitor the change in colour of the dye.

In this work, the aim is concentrated on the use of simple techniques for improving the electrical and electronic aspects of the sensors, for instance, indicator type LEDs were used as light sources and modulation techniques were used to guide the combined light from such sources into the same fibre and also the system was designed to provide a simple detection method, without having to resort to expensive and additional components such as optical filters and a mechanical chopper.

3.3 Colour Indicators

Colour indicators, which consist of large organic molecules, are weak acids or bases and interact with matter through chemical reaction^[7]. This results in a change to their particular properties, as is the case with acid-base indicators. In this instance, the pH of an aqueous solution is determined by the change in the overall intensity of the colour of the dye. When the latter is in an aqueous solution, a certain percentage of the dye reacts with the sample and dissociates while the rest remains undissociated, as is shown in Eq.3.7



where H_{Ind} and Ind^- are the undissociated and the dissociated part of the indicator respectively. These two species i.e. H_{Ind} and Ind^- are known as tautomers^{[7]®} and absorb light in the visible part of the spectrum at two different wavelengths respectively, or more precisely over two different bands of wavelength, since the absorption in the visible is broad. Hence the colour of the substance is determined by the highest concentration of either the undissociated or the dissociated part of the dye. For instance, in an acid sample, phenolphthalein is colourless ($\text{pH} < 8$) and becomes red in an alkaline sample. The constant of equilibrium of equ. 3.7 is K_{ind} and this can be given by:

$$K_{\text{ind}} = \frac{[\text{H}_3\text{O}^+][\text{Ind}^-]}{[\text{HInd}]} \quad \text{equ. (3.8)}$$

Hence the ratio of the dissociated to the undissociated parts of the dye is inversely proportional to the concentration of the hydronium ion, as is given by Eq. 3.9

$$\frac{[\text{Ind}^-]}{[\text{HInd}]} = \frac{[K_{\text{ind}}]}{[\text{H}_3\text{O}^+]} \quad \text{equ. (3.9)}$$

® Tautomer is the existence of a substance in equilibrium between two interconvertible forms. In this case, there are two absorption peaks whose total intensity remains constant while the intensity of absorption of each form varies with pH value.

It has been established that when the ratio of the concentration of the dissociated to the undissociated part is smaller than 10, the colour exhibited by the dissociated part of the dye becomes undetectable^[9].

On the other hand the colour, whose origin results from the undissociated part, becomes undetectable when the ratio of the concentration of the dissociated to the undissociated parts of the dye is larger than 10. As result of this definition, the combination of Eqs. 3.8 and 3.9 enables a determination of the practical range of pH values where the change of colour of the dye can be used to monitor the pH of the sample, i.e.

$$\text{pH} = \text{Log} (K_{\text{ind}}) \pm 1 \quad \text{equ. (3.10)}$$

Consequently the effective maximum range of pH that can be monitored by the use of a single dye is about ~ 2pH units.

3.4 Spectral Properties of Dyes

There are lots of different types of acid-base indicator, each of which operates over a limited pH range, as is shown in Table 3.1. The nature of the interaction between the electromagnetic wave and the indicator dyes is believed to be caused by structural changes. The subject is not discussed further here, the reader being referred to several texts on the subject^[10] but however, a basic illustration is given in this section and some examples are shown below. The major part of these indicators can be classified into three main groups. These are, phthalein, sulphonphthalein and azo compounds.

Common name	pH range	acid colour	base colour	type
Methyl red	4.2 - 6.3	red	yellow	sulphonphthalein
Phenol red	6.4 - 8.0	yellow	red	sulphonphthalein
Phenolphthalein	8.0 - 9.6	colourless	red	phthalein
Tymolphthalein	9.3 - 10.5	colourless	blue	phthalein
Methyl orange	3.1 - 4.4	red	yellow	azo
Methyl red	4.2 - 6.3	red	yellow	azo

Table 3.1 Example of dye indicators used for acid base titration

3.4.1 Phthalein

Phthalein indicators exhibit various colours when in alkaline samples and are colourless when the pH value is decreased to yield an acid sample. These are reported to be unstable when in strongly alkaline samples and their colour tends to fade^[10].

3.4.2 Sulphonaphthalein

This type of indicator usually has two conjugate colours which are associated with the dissociated and undissociated parts of the dye. The overall concentration of the dye remains constant and the predominant colour is a function of the highest concentration of the two parts of the dye i.e. the dissociated and undissociated parts. For instance, the phenol red dye exhibits a red colour when it is in an alkaline medium and changes to yellow in an acid sample. The spectral analysis of this dye shows an absorbing wavelength in the green and blue areas, as shown in Figure 3.3. This type of dye is known to be very stable, especially when used with low light levels.

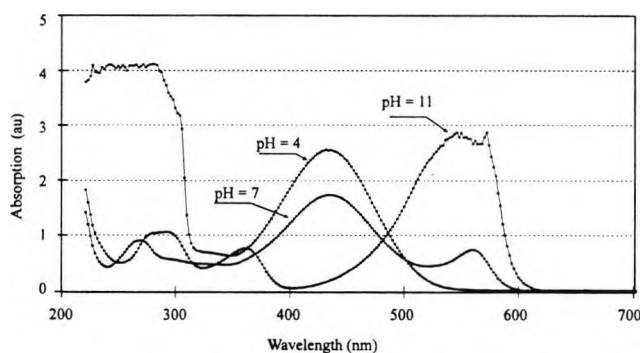


Fig 3.3 Absorption spectra of phenol red in a sample of distilled water at three different pH values: 4, 7 and 11.

3.4.3 Azo Indicators

Azo-based dyes are often associated with a change of colour as a function of pH from the yellow to the red part of the spectrum, with increasing acidity.

3.5 Choice of the Acid-Base Indicator

In this work, there was a variety of chemical acid-base indicators that had the potential to be used for the monitoring of the pH, for the “biomedical” and the “biological” range i.e. pH value between 7 and 8. The parameters that were required

for a suitable dye depended on their toxicity, stability and range of use. Phenol red suited these requirements well. It has been used widely to determine the pH of samples in the pH range of 6 to 8 which falls in the “biological” range.

Furthermore, it is known to be a non-toxic material which is also very stable. The other factor which makes it suitable for this application is the fact that one of its absorption peaks falls in the green spectral area. This coincides with the spectral emission of an ultra-bright indicator type green light emitting diode. The spectral profile of phenol red is shown in Figure 3.4, and it exhibits a strong absorption peak in the ultra violet part of the spectrum. This is complemented by the two absorption peaks which appear in the green and blue regions of the spectrum.

3.5.1 Phenol red Indicator Dye

Phenolsulfonephthalein (phenol red) was the indicator dye used in this work, as it can be used to measure pH over a wide range. It exists in two tautomeric forms, each having a significant different absorption spectrum. As the pH of the solution varies, the relative size of each tautomer's optical absorption varies in response to the changing relative concentrations of the acid and base forms of the indicator. This can conveniently be monitored at the peak of the absorption at 565 nm, corresponding to the green LED emission while the small infrared absorption is independent of that change. Figure 3.4 shows the absorption spectra of the indicator for sample solutions of varying pH, obtained in a conventional spectrophotometer in a 1cm sample cell. The arrows on the abscissa indicate the centre wavelengths of the two sources and thus the relative absorptions at those wavelengths can be seen.

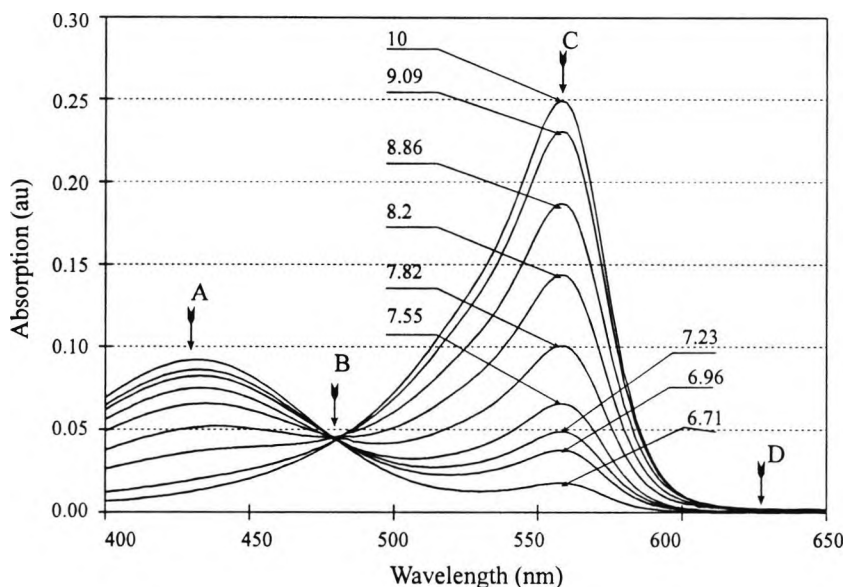


Fig 3.4: Absorption of indicator as a function of wavelength for pH values. Arrow indicate centre wavelength of LEDs used.

However, there is one particular point for which the absorption of the dye remains constant and is independent of the pH of the sample. Consequently, it can be used as a reference point. As is shown in Fig 3.4, the sensitivity of the measurement when the alkaline form is used is larger than for the acid form. As a result, a higher sensitivity for the pH measurement can be obtained.

The ratio of the acid form to the alkaline form of the dye is approximately of the order of 2.5. Consequently, the absorption peak occurring at 565 nm is more suitable for use in order to monitor the changes of concentration of the dye, since it is more sensitive to pH differences. The availability of simple and powerful light sources, detectors that are more sensitive in this region of the spectrum and fibres with excellent transmission characteristics all support the choice of 560 nm as the preferred operating wavelength of the measuring device. By comparison, the requirement for generating light in the blue part of the spectrum would lead to costly and bulky instrumentation and necessitate the use of optical filters.

3.5.2 The use of Blue LEDs

Currently it is possible to use blue LEDs as a light source but they are very expensive and may not be a close spectral match to the phenol red dye. As the blue LEDs

operate around 438nm, they can be used as a reference channel instead of the 810nm infrared LED. Again infrared LEDs are very cheap when compared to that of the blue LEDs. In this research the blue LED behaviour was studied over a range of different currents and Figure 3.5 shows the blue LEDs intensity .

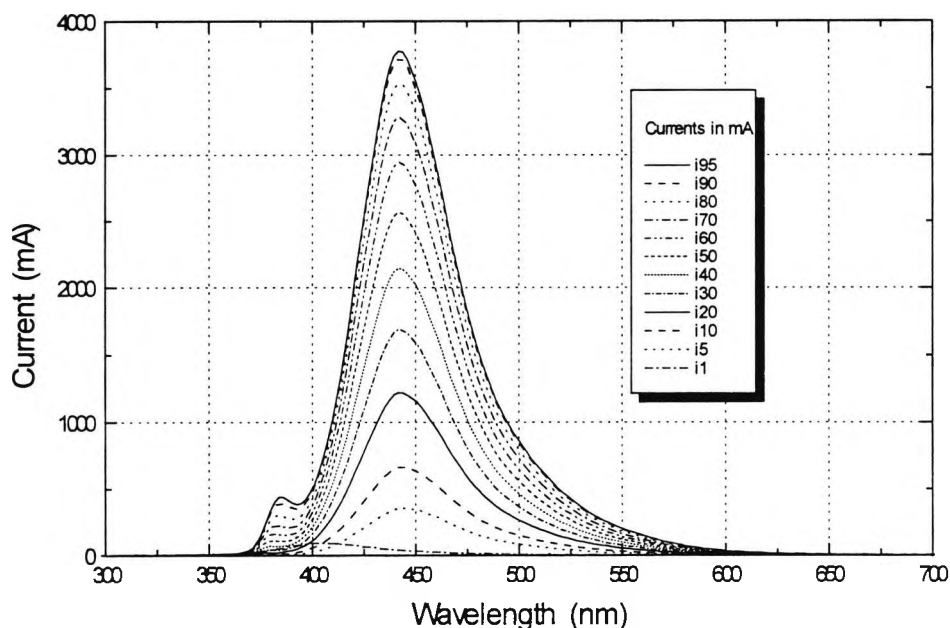


Fig. 3.5: Blue LEDs intensity at a various currents as a function of wavelength.

3.5.3 Effect of other Solvents to Indicators

Different solvents exercise different effects upon the indicator dye, so colour changes as well as indicator exponents of the indicators vary with the solvent. In aqueous methanolic or ethanolic solutions the alteration is relatively not so significant; in anhydrous alcohol, however, it becomes greater, while in other solvents a range of phenomena can be met.^[11]

It often happens in analytical practice that the aqueous solution contains alcohol. Alcohol alters the equilibrium of the indicator system, but the observed effect depends not only upon the indicator but also on the acid-base system present in the solution. The dissociation of weak acids and bases varies in the presence of alcohol, also on account of the decrease of the dielectric constant of solution. If alcohol is

added to strong acid solutions, the colour of indicator acids is shifted in the direction of the acid colour. This effect is much smaller in solutions of weak acid, whereas in buffer solution there is no change at all.

Indicator	pK(EtOH)	pK(H ₂ O)	ΔpK
Thymol blue	5.7	1.65	4.05
Dimethylaminoazobenzene	5.2	3.25	1.95
Methyl orange	2.9-3.5	3.0	-0.5
Bromphenol blue	9.1	4.1	5.0
Bromphenol green	10.3	4.9	5.4
Bromcresol purple	11.5	6.4	5.1
Bromthymol blue	12.8	7.3	5.5
Phenol red	13.4	8.0	5.4
α-Naphtholphthalein	13.8	8.3	5.5
Thymol blue (acid region)	15.1	9.2	5.9
Phenolphthalein	15.3	9.3	6.0

Table 3.2: Dissociation constant of the acidic forms of some indicators in ethyl alcohol^[12]. pK_{ind} is the logarithm of the dissociation constant of the indicator.

The behaviour of the indicator base form is just the reverse of this. One of the effects of alcohol in strong acid solutions is that the colour of indicator bases is shifted in the alkaline direction. This shift is even greater for weak acid solutions and is greatest in buffer solutions. Methyl orange, for instance, shows its transition colour in 0.01M aqueous solution of acetic acid, whereas in the presence of 40% alcohol the colour is definitely yellow.

Table 3.2 summarises the pK_a values for a set of indicators in water and ethanol solution. It will be noted that the transition ranges of pK_a values of indicators in general follow the same relative order as in water. Thus, as a first approximation, the transition intervals of indicators in water can serve as a useful guide in selecting an indicator for a particular acid-base titration in a “waterlike” organic solvent or in an aqueous-organic solvent mixture. The final selection of the indicator may have to be partly “trial-and-error”, but at least the concepts discussed should permit some “intelligent guesses”. In the presence of alcohol, the colour intensity and shade of indicators are also different. Phenolphthalein, for instance in aqueous solutions of

sodium hydroxide is cherry coloured, whereas this colour is blended in the presence of alcohol more and more with a shade of violet. The colour intensity is also less. Since the phenol red indicator dye is employed in this work it is important to guarantee that the chemical concentration of the different components in the dye are the same.

3.6 Relationship between Light Absorbance and pH

The ratio of the dissociated and undissociated parts of the dye which represent the transducing function, can be linked to the light absorption at a specific wavelength through Beer's Law. The basic considerations in this relation are as follows:

(a) The relationship between the light intensity absorption and the concentration of the dissociated part of the dye is written, in Eq.3.11, as

$$\log P/P_0 = - \epsilon L [\text{Ind}^-] \quad \text{equ. (3.11)}$$

where P , P_0 , ϵ , L , and $[\text{Ind}^-]$ are the detected light power, the initial light power, the coefficient of extinction, the path length and the concentration of the dissociated part of the dye respectively.

(b) From the chemical reaction resulting from the mixing of the dye and the sample an equilibrium is reached which can be expressed as a function of the concentration of the species involved, as

$$K_{ind} = \frac{[H_3O^+][\text{Ind}^-]}{[\text{HInd}]} \quad \text{equ. (3.12)}$$

(c) The total concentration of the dye in a given experiment, $[T]$, or in a sensor head investigation remains constant and is of the sum of the dissociated and undissociated parts i.e.

$$[T] = [\text{Ind}^-] + [\text{HInd}] \quad \text{equ. (3.13)}$$

Based on the above equation it can be shown the relation between P/P_0 and $[H_3O^+]$ is as follows. By taking the decimal logarithm of both sides in Equ. 3.12 and separating the term containing the hydronium ion concentration, Eq.3.12 becomes:

$$\log K_{ind} = \log [H_3O^+] + \log [Ind^-]/[HInd] \quad \text{equ. (3.14)}$$

Eq.3.14 may be re-written as shown in Eq.3.15.

$$pH - pK_{ind} = \log [Ind^-]/[HInd] \quad \text{equ. (3.15)}$$

The anti-logarithm of Eq.3.15 results in expressing the equation in a more convenient form, as shown in Eq.3.16 below.

$$10^{-(pH - pK_{ind}) + 1} = [T]/[Ind^-] \quad \text{equ. (3.16)}$$

The direct relationship between light intensity and the concentration of the dissociated part of the dye is introduced by using Eq.3.11 and hence Eq.3.16 may be written as follows:

$$10^{-(pH - pK_{ind}) + 1} = -\epsilon L[T]/\text{Log}(P/P_0) \quad \text{equ. (3.17)}$$

Hence, Eq.3.17 is modified to show the relationship between the variation of the light intensity as a function of concentration of the dissociated part of the dye. This relationship is described in terms of one variable only i.e. pH, which the term $\epsilon L[T]$ is a parameter which describes the sensor head and is a constant for a given implementation. Thus $\epsilon L[T] = m$ and $pH - pK_{ind} = \delta$.

The final mathematical equation for the relationship relevant to the sensor is shown in equ.3.18.

$$\text{Log}\left(\frac{P}{P_0}\right) = \frac{-m}{10^{-\delta+1}} \quad \text{or} \quad \frac{P}{P_0} = 10^{-m/(10^{-\delta+1})} \quad \text{equ. (3.18)}$$

Due to the non-linearity of the relationship between the relative light intensity and the variable δ , ($\delta = \text{pH} - \text{pK}_{\text{ind}}$), the resultant curve is an S shape with the position of the inflexion point in the middle of the S shape. In this area, i.e. approximately $\delta = \pm 1$ from either side of the point of inflexion, maximum linearity is obtained. Although this is still not enough for the curve to be linear, it can be considered as fitting a straight line whose slope is the same as the slope of the curve at the inflexion point with in a reasonable approximation, yielding a small systematic error.

3.6.1 Choice of the Parameters to be Determined

The principle parameter of the sensor to be evaluated is the factor m . This is carried out to provide a more accurate description of the required physical dimensions of the probe head and the behaviour of the sensor in various practical implementations. The choice of the value of the parameter m is dictated by two situations, these are: the largest dynamic range of pH i.e. ± 1 pH units, and the need for maximum sensitivity with minimum error over the 100% transmission range.

(1) Firstly, it can be seen that the point of inflexion is a function of the parameter m and it does not necessarily occur when $\text{pH} = \text{pK}_{\text{ind}}$ for the curves computed with different values for m . The relationship between the value of the factor m and the value of pH for which the inflexion point occurs can be calculated from the second derivative of Eq.3.18 as a function of pH. The inflexion point is defined when the second derivative is zero i.e. the slope of the curve changes sign. This is shown in Eq.3.19 (see Appendix 2 for more details).

$$\delta = -\text{Log}\left\{\frac{-m \ln 10 + \sqrt{m^2 \ln^2 10 + 4}}{2}\right\} \quad \text{equ. (3.19)}$$

Because the pK_{ind} of phenol red is 7.92^[13], and the practical range of the dye lies between 6.8 and 8.4, the optimum position of the inflexion point lies at the middle of the dynamic range of the indicator dye e.g. $\text{pH} = 7.6$.

(2) Secondly, the sensitivity of the measurement relies on a long path length through which the sensing light travels and hence, the longer it is, the more sensitive the

measurement becomes. However, this is limited by two factors, the first being the longer the path length, the smaller the signal to noise ratio, since the level of the light reaching the detector is less, and the second factor is the physical dimension of the probe head. However, limited physical dimensions and the desire for a short path length can be compensated by using a larger dye concentration which keeps overall dimension of the probe head within the desired volume.

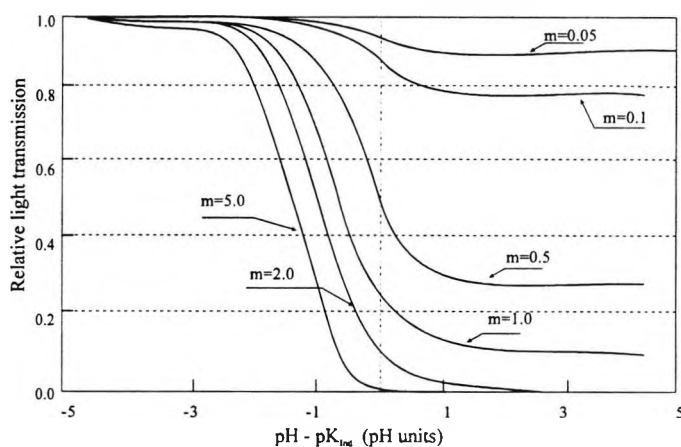


Fig. 3.6: variation of the ratio (P/P_{ref}) calculated as a function of $\text{pH} - \text{pK}_{\text{ind}}$ with different values of m

The variation of the relative light transmission as a function of δ is shown in Fig 3.6 and it can be concluded that there is a range of values of the factor, m , for which the dynamic range of the light transmission is the largest which occurs when $m > 1$. Graphically, the value of m can be obtained by moving the position of the inflexion point so that it lies at the middle of the required pH range e.g. between 7 and 8. Additionally, error analysis^[13] showed that for values of the factor m smaller than 1.2, a large error in the measurement results when the light transmission is smaller than 10%. Hence there is a “trade off” to be made so that both conditions can be satisfied i.e. minimum error and largest dynamic range.

3.6.2 Referencing Scheme

In any measurement procedure it is important to assess the value caused by any interfering process, such as ambient light, and temperature effects on the sensor systems, since it is added to the final result of the measurement.

A reference scheme can conveniently be obtained by using one of two different methods. The first consists of using the same wavelength as the sensing wavelength to monitor the value of the initial light intensity. For this, a reagent can be added to the sample to shift the pH to a value at which the dye does not absorb (i.e. in its acid form). Although this can be carried out in titrimetry, it is not a very practical situation for most sensors as this results in making the design of a sample sensor more complex.

In the second method, a second wavelength is used to monitor the level of the value of the initial light emission. Such a wavelength should only be affected by changes in absorption generated by interference sources other than the change of pH. This can also be used to monitor the background absorption and instrumental variations. The choice of this wavelength is made by assuming that the effect of the interfering species is similar for both wavelengths i.e. the sensing and the reference wavelengths.

Hence, this can only be justified when the reference wavelength is as close as possible to the sensing wavelength whilst being sufficiently removed, for the light transmission to be unaffected by the variation of the pH of the sample. In this situation, the value of the initial light power can be linearly related to the light power of the reference wavelength. This is only true in most practical situations when the wavelengths are generated from the same physical light source. Effectively, in this particular case, the problems associated with any temporary variation of the light intensity and the ageing of the light source are similar for the two wavelengths. Consequently, the ratio of the intensity of the two wavelengths can be used to eliminate this type of problem.

However, this assumption is not valid when using two different wavelength sources to generate the appropriate wavelengths, for instance, when two LEDs emitting at different wavelengths are used^[13]. In this particular example, the assumption relies on the fact that LEDs, which have a very low rate of degradation and hence are very reliable^[14], cannot differ appreciably in their spectral properties within the response time of the sensor, especially if they are used well within the manufacturer's specifications for temperature and current. As a consequence, under these circumstances, the ratio of the light intensities of the two wavelengths can be described as a constant $P_{\lambda_s}/P_{\lambda_r} = \psi$.

$$\text{Log} \frac{P}{P_o} = \frac{-\varepsilon L[T]}{10^{-\delta} + 1} \quad \text{equ. (3.20)}$$

Thus, the term P_o in Eq. 3.15 may be replaced by $P_{ref} \psi$ and can be written as follows:

$$\text{Log} \frac{P_\lambda}{P_{ref} \psi} = \frac{-\varepsilon L[T]}{10^{-\delta} + 1} \quad \text{equ. (3.21)}$$

$$\frac{P_\lambda}{P_{ref}} = \psi 10^{-m/(10^{-\delta} + 1)} \quad \text{equ. (3.22)}$$

where $m = \varepsilon L[T]$ and $\delta = \text{pH} - \text{pK}_{\text{Ind}}$ and Ψ denotes the ratio between the light intensity of the sensing and reference wavelengths. These parameters represent the factors of the sensor and can be measured for a given implementation.

3.7 Summary

In this chapter, a theoretical description of the colorimetric measurement of pH of an aqueous solution has been given. This analysis provides a basis on which a fibre optic system can be conceived even though the principle involved has a non-linear response. However, when the application is limited to a maximum range of 2 pH units, part of the instrument response can be reasonably approximated to a linear

variation as a function of pH. The limitations of the sensor are analysed and results show that it is difficult to fully estimate the error of the system without prior knowledge of the chemical composition of the sample, since other species may modify the behaviour of the dye.

Acid-base indicators are generally complex organic compounds of high molecular weight. In water or other solvents they behave as weak acids or bases and thus participate in equilibrium reactions involving the hydronium ion. Accompanying the dissociation or association reactions of these compounds are complex internal structural rearrangements that result in changes in colour. The results obtained from this chapter will be used in order to construct, and subsequently evaluate the pH monitor which is discussed in Chapter 4.

1.8 References

1. J.I. Peterson, et. al., "Fibre optic pH probe for physiological use", *Anal. Chem.* 52 pp-864-69 (1980).
2. R.Day, and A.L. Underwood, *Quantitative Analysis*, 4th Ed., Prentice-Hall, Chapter 12, (1975).
3. J. Janata, "Do Optical Sensors really measure pH", *Anal. Chem.* 59, p- 1351 - 56,(1987).
4. E. Koller, and O.S.Wolfbeis, "Sensor Chemistry", in *Fibre Optic Chemical Sensors and Biosensors vol. I*, Ed. Wolfbeis, O.S., CRC Press, USA (1992).
5. G.F. Kirkbright, R. Narayanaswamy, and N.A. Welti, "Studies with immobilised chemical reagent using flow-cell for the development of chemically sensitive fibre optic device", *Analyst*, 109, p-15-17, (1984).
6. A.L. Vogel, *Vogel's Textbook of quantitative chemical analysis*, 5th Ed. Chapter 10, Longman Scientific & Technical, (1989).
7. C.T. Collocott, and A.B. Dobson, *Chambers Dictionary of Science and Technology*, ed. by T.C. Collocott and A.B. Dobson, W&R Chambers Ltd. UK, (1976).
8. G.R. Bates, "Determination of pH; Principles and Applications, Wiley & Sons, chapter 6, (1964).
9. D.A. Skoog, and D.M. West, "Fundamentals of Analytical Chemistry", A. Holt London Edition, UK, (1971).
10. E. Bishops, *Indicators*, Chapter 3., Pergamon Press, Oxford, (1972).
11. I.A. Kolthoff, "The dissociation of acid-base indicators in ethanol with a discussion of the medium effect, *J. Phys. Chem.*, 35, pp-2632, (1931).
12. K.T.V. Grattan, Z. Mouaziz and W.A. Palmer, "Dual wavelength optical fibre pH sensor", *Biosensors*, vol.3, No.1, p-17-25, (1987).
13. H. Kressl, M. Ettenberg, J.P. Wittke, and I. Ladany, "Laser Diode and LEDs for fibre optic communication", in *Topic S in Applied Physics*, 39 Ed. by Kressel, H., P-9-60, (1982).
14. J. Janata, "Ion optodes", *Anal. Chem.* 64, 19, -921A - 927A, (1992).

Chapter 4

Design and Implementation of a Computer-Controlled Fibre Optic pH Sensor

Abstract

The design of the fibre optic pH sensor described here is based on the principle of monitoring the change of colour of an organic dye (phenol red) whose absorption of light in the visible part of the spectrum depends on the concentration of the hydronium ion (H_3O^+) present in an aqueous solution, as discussed previously. The change of absorption of light is monitored at an optimum wavelength of 560 nm which corresponded to the peak emission of an indicator type green Light Emitting Diode (LED) and was found to be linearly proportional to the variation of the pH of the sample.

External interferences may be monitored through use of a wavelength whose intensity remains largely unaffected by the change of absorption of the dye. In the first such scheme, an infrared (IR) LED emitting at a central wavelength of 840 nm was used, not only to monitor the background absorption of the sample, but also to compensate for the instrumental sources of error. The wavelength of the infrared LED falls in a region where the absorption of the dye is unaffected by pH changes (figure 3.4).

The sensor is controlled from a computer, for which software and hardware were constructed in this project. The sensing signal is modulated using a square wave technique and is time multiplexed with the reference signal. These signals are generated by software and the detected signal is also controlled and processed by the software developed. Calibration of the instrument against an electrochemical electrode-based commercial pH meter was carried out and a system characterisation and analysis of the numerous analytical and instrumental errors introduced in the two systems are appended at the end of this chapter.

4.1 Time Multiplexed Dual Wavelength Fibre Optic pH Sensor

The schematic diagram of the dual wavelength with external referencing device is depicted in Fig 4.1. The basis of the implementation relies on generating two wavelengths i.e. 565nm and 810nm, using two indicator type LEDs. The first LED was used to monitor the behaviour of the phenol red dye through the change of the transmitted light intensity and the second LED was used for the measurement of the background absorption and external interference.

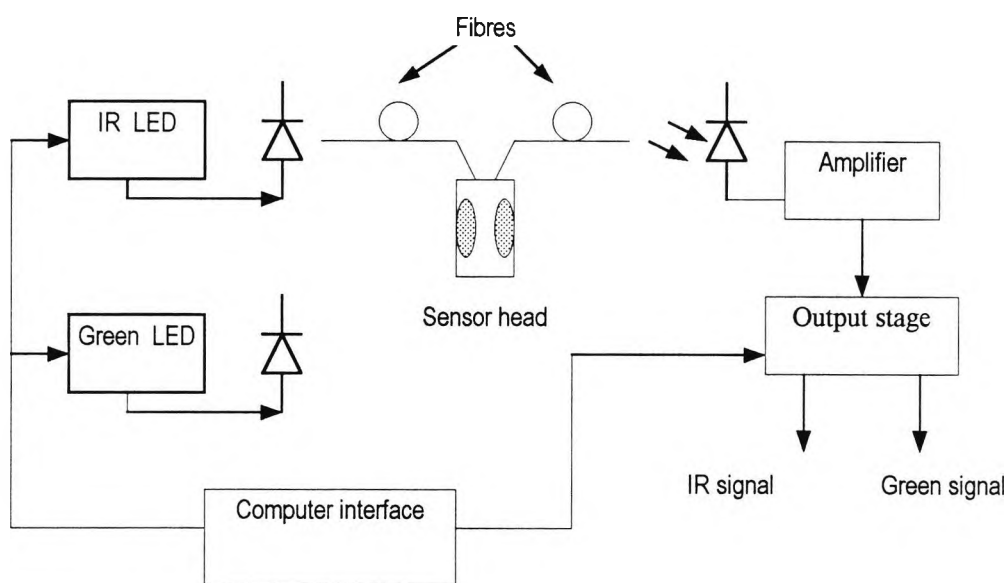


Fig. 4.1 Set-up of the time multiplexed dual wavelength fibre optic pH meter

The two optical signals i.e. those from the green and infrared LEDs were time multiplexed using a square wave modulation scheme. The optical signal thus generated was guided through two short lengths of optical fibres to the sensor head as a fibre bundle. The optical signal was then guided to the probe head. A reflecting mirror, positioned at the opposite end of the probe head facing the emitting fibre, was used to reflect the light. A bundle of fibres positioned around the emitting fibre guided the reflected light back to the detector.

Further signal processing was carried out in order to demodulate the signals corresponding to the green and infrared optical signals respectively and to remove the

effects of ambient light. Separate outputs for the two signals i.e. absorption and reference signals, were provided and a subsequent ratio was then performed.

4.2 Referencing Scheme

When external effects occur, absolute measurement of the absorbed light cannot be related to the absorption of the light by the dye unless a monitoring wavelength, whose light intensity remains unaffected by the change of absorption caused by the change in the pH value of the sample, is used. Additionally, this reference wavelength provides meaningful information about the nature of the absorption by the species present in the sample.

Moreover, losses of light which can be caused by diverse external effects such as light intensity fluctuations, losses due to the coupling of the fibres and the losses occurring in the fibre during the propagation of light, caused mainly by fibre bending were then determined quantitatively. Ideally, the wavelength of the reference light should be as close as possible to the monitoring wavelength so that most of the interfering effects would do so equally for the two wavelengths. For instance, the light transmission decreases when the fibre is mechanically bent as the resultant loss is a function of wavelength.

This type of loss is caused mainly by mode conversion and light is radiated through the cladding. In this particular implementation, phenol red absorption is unchanged for wavelengths longer than 620nm, and thus a red LED emitting at a central wavelength of 630nm could be used. However, the broad emission characteristics of the LED e.g. ± 20 nm at half height, overlaps with part of the area of the absorption curve of the dye.

Hence such an LED is not a suitable choice for generating a reference wavelength which otherwise necessitates the use of an optical filter to remove this overlap effect. The latter has the effect of complicating the optical set-up and introduces additional optical components. Hence an infrared LED whose central wavelength is far removed

from the absorbing area e.g. emitting at 810nm, was chosen as a reference light source. The error introduced is limited and constant and could be included in the systematic error of the system.^{1*}

4.3 Design of the Sensor

The fibre optic pH sensor comprises an optical arrangement and an electronic section as discussed before.

4.3.1 Optical Arrangement

The optical arrangement of the pH meter consists of a probe head, light sources, an optical link (glass fibre bundle) for guiding light from the light sources into the probe and to collect the light from the probe and guide it to the detector.

4.3.1.1 Optical Link

The optical fibre used in this implementation is a multimode type glass fibre having a numerical aperture (NA) of 0.4. Light travelling in the fibre and having an angle greater than 24° was not guided through the fibre, being coupled into the fibre but then lost through the cladding after the first few reflections. In this implementation, the losses due to the glass fibre were not significant since the fibre length was of the order of few metres. Glass fibre has a greater transmission percentage in the visible part of the spectrum than plastic fibre.

The fibres used collecting the light from the LEDs were a simple pair. This was needed since a very weak signal was detected by the detector when one LED was used. The diameter of these fibres was 600 μm , but only one of these fibres was needed for the purpose of guiding the infrared light from the IR LED since the light power of this LED was much larger than that of the green one. The fibre used to guide the optical signal from the light sources to the probe head was approximately 1.5 metres long. It was glued to the SMA type connector at one end and to a

¹ * The inequality of the light losses when the fibre is bent arises from the fact that the wavelengths of absorption and reference were farther apart e.g by 280nm

machined stainless steel connector to fit the head probe at the other end. This was larger enough to accommodate the 1mm diameter fibre and six of 600 μ m diameter fibres positioned around the large fibre to obtain an optimized light collection arrangement, as is shown in Fig 4.2.

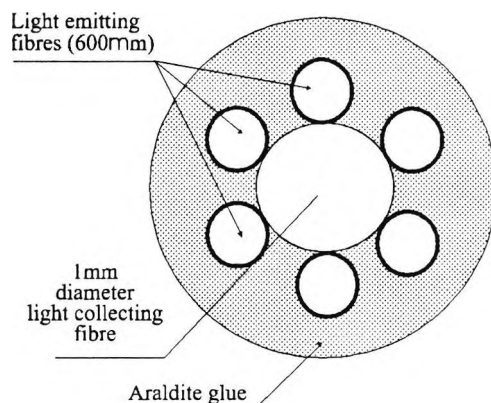


Fig 4.2 : Positioning of the emitter and receiver fibres in the probe head (bottom view)

4.3.1.2 The Probe Head Design and Construction

The probe was designed so that the fibre-probe head could be readily dipped in a sample solution, and was made of separate parts. This approach was taken to ensure ease of construction and so that it could readily be taken apart for cleaning, when necessary. Due to the acidic nature of the environment where the probe head will be used it was made from stainless steel to prevent any long term effects of corrosion.

The first part was made to connect the fibre to the probe head. The second part consisted of a hollow cylindrical body onto which large holes were machined on its longitudinal side so that the sample liquid could flow in and out, without restriction. The large diameter of the holes was also used to help reduce the chances of air bubbles being trapped inside the optical probe, which could cause larger errors in the measurement by disturbing the path of the light beam.

Consequently, under these circumstances the light intensity being reflected by the mirror and reaching the detector would not necessarily provide a true measurement of the absorption of the light by the dye. The third part of the probe head consisted of

a threaded metallic end whose front surface, facing the fibres, was well polished to produce a highly reflecting surface which was used as a mirror. Its distance from the fibre end determined the path length of the optical cell. A facility for changing this distance was provided through a thread which was machined onto the body of the mirror. The probe head is shown schematically in Fig 4.3.

The path length with such a system was twice the distance between the fibre ends and the polished mirror surface. However, there was an optimum position of the mirror where maximum light intensity was reflected. This was found experimentally to be around 20mm in this implementation.

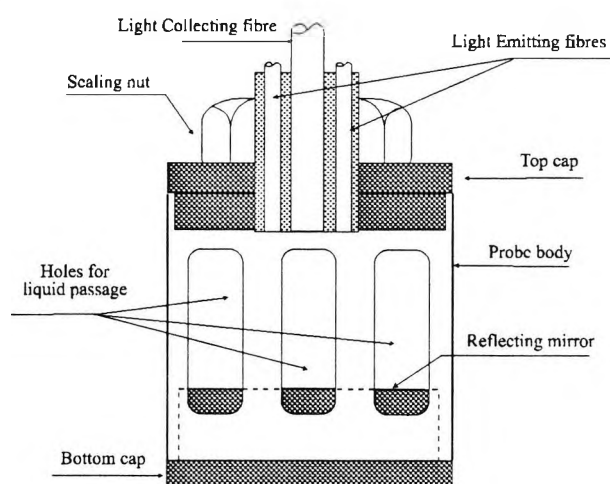


Fig 4.3 : Schematic design of the probe head for the first configuration.

4.3.1.3 Light Sources

In order to generate the appropriate wavelength needed to monitor the change in the absorption of the phenol red used, simple and inexpensive solid state LEDs were employed.

The output spectrum of the green LED, which has a peak emission at 565nm, matched the absorption spectrum of the phenol red when it was in its alkaline form and hence it was well suited to this application. The bandwidth of the LED emission is ± 20 nm at half power, and the emission spectrum of the green LED when driven at increasing dc currents changes as shown in Fig 4.4.

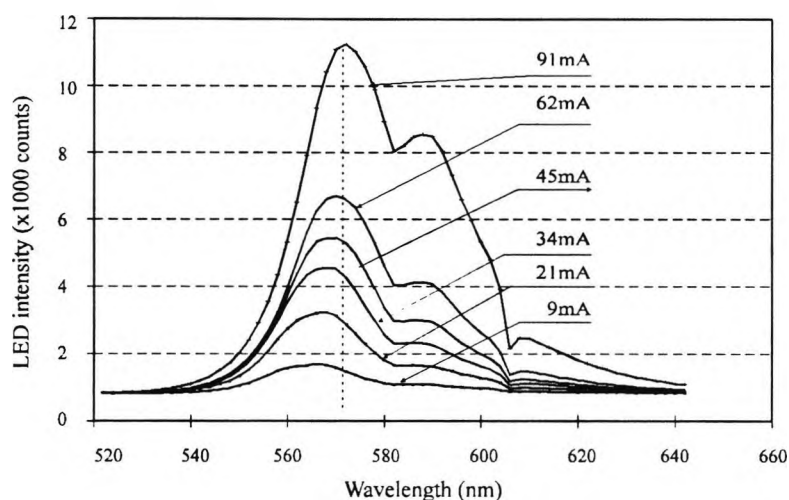


Fig. 4.4: Spectrum of the green LED at various driving current intensities.

A small shift (2 nm) of the peak of emission at 565nm was found to occur for a range of currents from 10 to 90 mA. This peak was shifted toward higher wavelengths and found to be insignificant since the envelope of the emission spectrum of the LED contained in it the absorption profile of the phenol red in its alkaline form (figure 4.4).

Although the maximum dc current specified by the manufacturer was 30mA, it was found that it was possible to drive the LED at higher current intensities provided that this occurred over a short period of time and the LED was given sufficient time to return to ambient temperature and dissipate heat caused by the passage of the current in semiconductor.

On the other hand, the infrared LED was not subjected to the same driving current conditions because of the higher quantum efficiency of infrared LEDs. For the latter the important factor was the stability of the light intensity. These LEDs have the advantage of being easily driven and electronically modulated and hence the need for a mechanical chopper was eliminated. In this particular case it was preferred to drive both LEDs sequentially by a pulse train signal. There were two reasons for choosing this type of modulation:

1. Due to nature of the processes occurring in the generation of light, these LEDs can be driven at a higher current without affecting their performance^[1]. The

limitation imposed on the driving current of an LED results from the heating of the substrate when a current passes through it. Hence, if the substrate is allowed to cool so that its temperature decreases, it can be driven at higher currents generating a more powerful optical signal since the relationship between optical power and driving current was found to be linear, within a limited range.

2. The two LEDs were driven on and off sequentially. Consequently, there was no overlap of two optical signals. An overlapping optical signal containing the two wavelengths at a ratio R_1 would not be converted into an equivalent electrical signal since the sensitivity of the detector is a function of the wavelength and was reported to be of the order of 1.72 (for $\lambda_1 = 810$ nm and $\lambda_2 = 565$ nm). Moreover, the state where the two LEDs were switched off for a certain time was purposely arranged so that it could be used for interference sampling i.e. dc level measurement and at the same time to allow the LED to dissipate most of the heat. The efficiency of light coupling between an LED and glass optical fibre was reported to be up to 15%^{[2][3]}.

4.3.2 Electronic System

The block diagram of the electronic module used to drive and construct the instrument is shown in Fig 4.5 and consisted of an emitter, receiver, amplification, demodulation and output stages. A square wave signal was used as the master clock signal and was generated using the computer timer as a network on the feedback loop of an A/D channel.

The frequency drift due to the increase of the temperature of the electronic circuit and fluctuation of the frequency was found to be smaller than 1Hz over a period of one hour. Although this drift represented 0.03%, it was not considered to be important since the rest of the circuit was synchronised on the computer based clock signal. The frequency of the clock was similar to the PC timer and was constant.

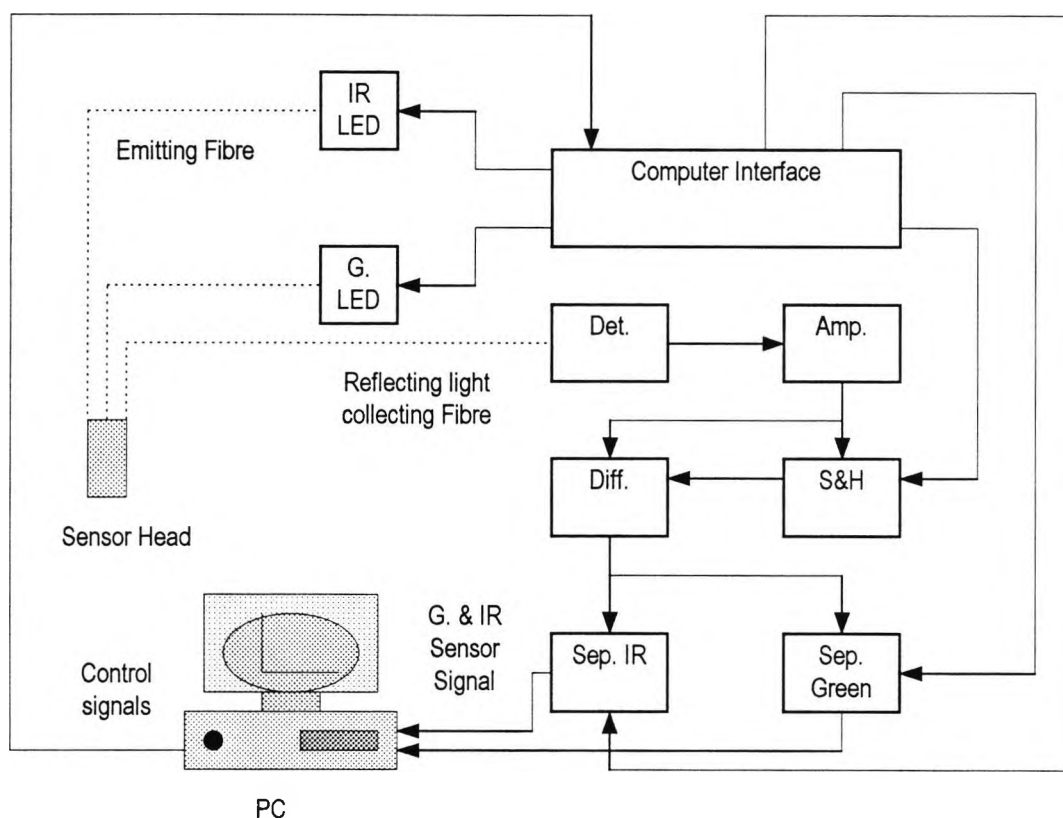


Fig. 4.5 : Block diagram of the electronic circuit used in the implementation of fibre optic pH sensor, S&H (Sample and Hold), IR LED (Infrared LED), G.LED (Green LED), Det. (Detector), Sep. IR (Separate IR Signal), G&IR (green and IR signals) Amp (Amplifire) Diff. (Differential Amplifire).

4.3.2.1 Clock Signal Generation

The generation of the various signals needed to drive the green and infrared red LEDs and the control devices was carried out by timing a series of train pulses which were output by the computer through the parallel port which was connected to the interface. This series of pulses were basically generated by software and set to be time multiplexed. These signals were needed and used:

- 1) One was used to control the green LED,
- 2) the second signal to control the infrared LED
- 3) and a third signal was used to control noise sampling devices.

Care was taken so that these three signals could not be set to have the same value namely "1" at any one time. The speed of the change of state of these signals was

relative to the speed of the computer but however, the ratio of mark to space for each was maintained constant. The electrical signals generated by the computer were optically isolated before being applied to the appropriate LED driver used to control the intensity of the driving current. Three signals were generated to perform the measurement of the pH value of a sample solution. These were:

- ◆ A signal to drive the green LED. This was carried out by a pulsed train signal having a mark to space ratio of 1:3 and was buffered using an operational amplifier connected as a voltage follower before being applied to a transistor switch circuit which controlled the current through the green LED connected between the current limiting resistor and the collector of the transistor. The rms value of the current flowing through the LED was 60mA.
- ◆ A signal to drive the IR LED using a similar transistor switch. However, a lower current value of 20mA was needed to drive this LED, also at mark to space ratio of 1:3.

Three control signals to provide the triggering pulse for controlling the timings of the sample and hold devices used to separate the signal corresponding to the green and infrared signals, and the third one which was used to sample the detected signal when both LEDs were switched off.

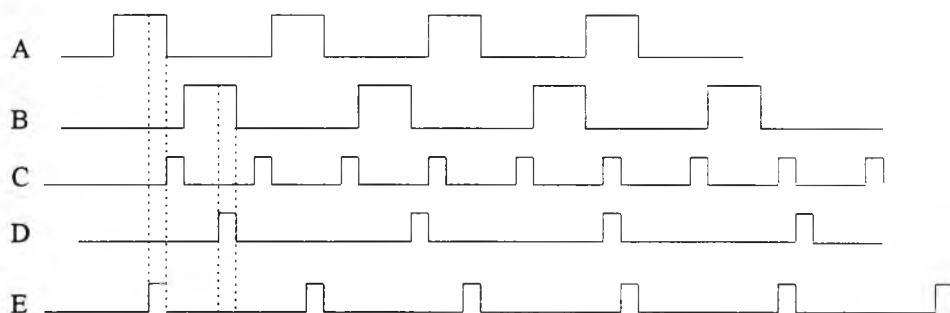


Fig 4.6 Schematic diagram of the timing signals. **A** timing of the Green LED, **B** timing of IR LED, **C** Noise sampling timing, **D** sampling of IR signal and **E** sampling of Green signal.

A dc signal resulted from the output port of the sample and hold device and was

approximately equal to the average value of the electrical background level. The timing of these signals is shown in Figure 4.6 above.

4.3.2.2 Detection and Signal Processing Circuits

The detected signal contained a large number of harmonics which were not processed in the same way due to limitation in the frequency response of the various stages i.e. of the detector and amplifiers.

Care was taken when a signal was sampled and the average value held constant until the next cycle. For this reason, the position and the length of the control pulse with respect to time did not correspond to the rise and fall of the pulse. The active time of the sampling was delayed so that sampling started after the pulse rose and the holding signal occurred before the pulse fall started.

The reason for this is shown schematically in Fig 4.7, where the detected signal is presented as a function of time. This had the effect of reducing the errors introduced by the inadequate frequency response of the components, and the output of the sample and hold element represented the average voltage of the capacitor used as a memory as shown in Eq. 4.2.

$$V_{avr} = \frac{1}{T} \int_0^T V_{input} dt. \quad \text{equ. (4.2)}$$

The energy stored in the capacitor given by Eq. 4.2 showed that if the value of the capacitor was properly chosen i.e. so that the time constant was large compared to the input signal, the energy stored was proportional to the average value of the signal.

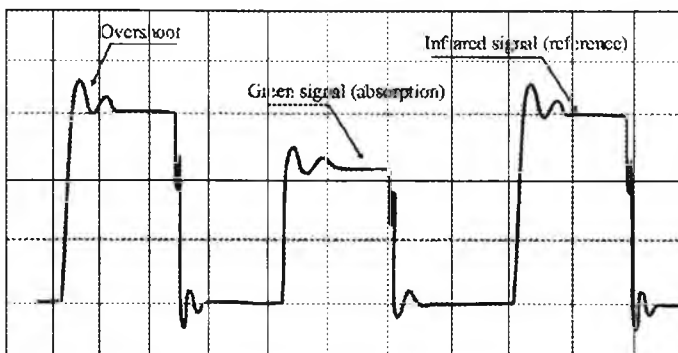


Fig. 4.7: Photograph showing the perturbation which appears as an overshoot as a result of the limited frequency response of the detector. Scale is vertical: 1Volt/Div, Horizontal: 200 μ S/Div,

Polycarbonate capacitors (10 μ F) have a very low leakage current and hence were suitable for memory applications^[4]. In this case, the time required to hold the signal in the capacitor was shorter than 1.4ms¹ and this resulted in a drop of voltage of the output signal from the sample and hold element in the order of few micro-volts (0.002%)^[5]. As the resulting error was small, the memorised signal was considered to represent the intensity of the true processed signal especially when the sampling time was kept constant.

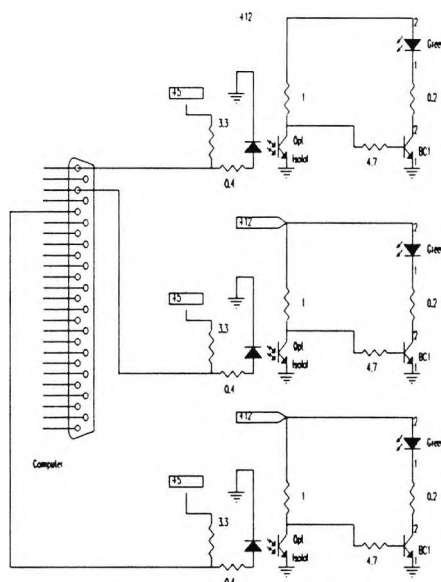


Fig. 4.8: A schematic diagram of the electronic circuit used for the emitter of the first implementation of the pH meter.

¹ Although the timing of the sample signal was dependent on the computer speed the slowest speed used was over 1KHz and therefore the drop of voltage encountered was less than 1 microvolt.

The detected optical signal containing the required information was then converted into an equivalent electrical signal prior to amplification and filtering. An output port was provided for subsequent signal measurement and the ratio of the absorption signal to the reference signal was then computed. The block diagram of the detector and signal processing stages is shown in Figure 4.9 and the electronic layout of the receiver circuit is shown in Figure 4.10 below.

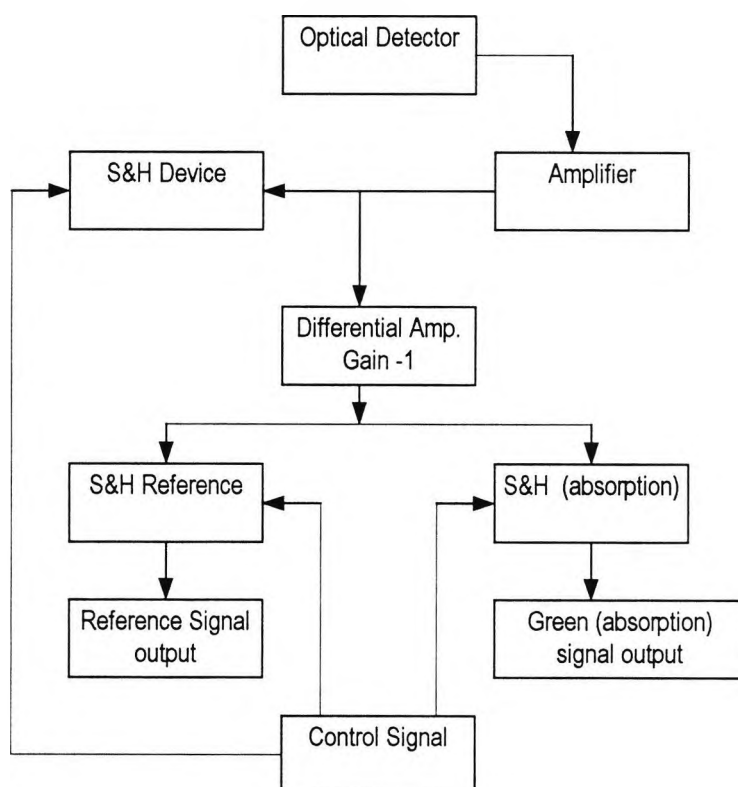


Fig. 4.9 Block diagram of the detector and signal processing scheme for the first implementation of the optical pH sensor

In order to convert the optical signal into an electrically coded signal, a combination of a silicon photodiode connected to an amplifier in a transimpedance mode was used RS(308-067). This device has the advantage of reducing the noise “pick-up” that usually occurs with weak signals since the photodiode, the amplifier and the feedback resistor were all based on the same substrate.

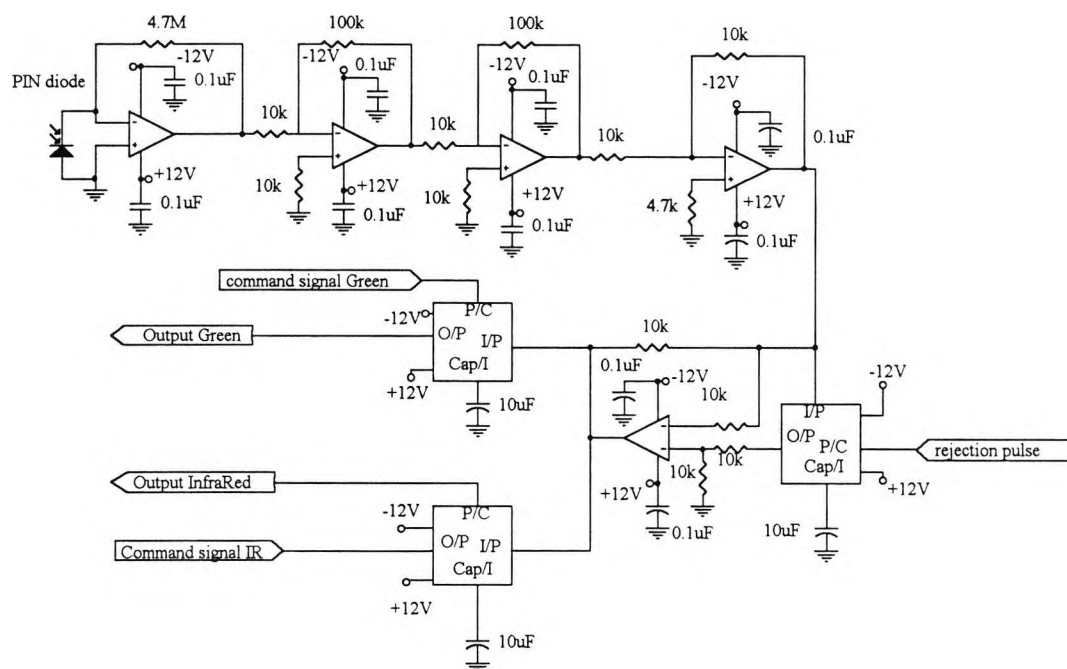


Fig. 4.10 Schematic diagram of the electronic circuit used in the receiver and signal processing section

4.3.2.3 Optical Detector

The optical and frequency characteristics of the detector are showing Fig 4.11 and Fig. 4.12. A low noise amplifier connected in transimpedance mode was used to convert the electrical current generated in the photodiode into a proportional voltage signal. A resistor of a value of $4.7\text{M}\Omega$ was used as the converting element in the circuit and was connected in the feedback loop of the amplifier.

The photocurrent generated within the photodiode was essentially the current flowing through the feedback resistor since the input impedance of the operational amplifier was very high (e.g. $10\text{M}\Omega$), because the current flowing through the inverting input of the amplifier was considered negligible.

The active area of the photodiode was 5mm^2 and the dark current output intensity average value was found to be 4nA . The intensity of the dark current was temperature dependent i.e. increasing with increased temperature. Additionally, it was of a dc nature. Hence, this effect could be minimised by either decoupling the output port of

the detector using a fairly low value electrolytic capacitor, or subtracting a dc signal which was proportional to the average value of the noise signal, from the detected signal. The bandwidth limitation of this detector e.g. 10kHz, was determined by the response of the detector to a pulse signal and overshoots appeared at the rising and falling edges of the pulse resulting from the missing or under processed higher harmonics of the pulse signal.

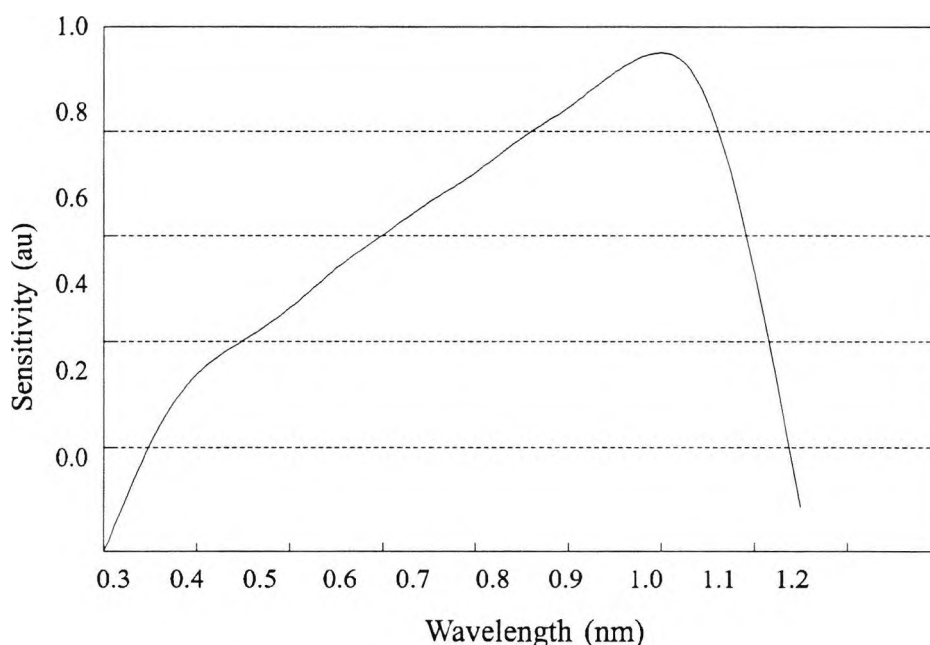


Fig 4.11 Spectral response of the detector amplifier module

The intensity of the output signal, from the detector amplifier stage was about 3mV for the pulse corresponding to the green light when the sample was acid i.e. corresponding to maximum light transmission. This represented an approximate value since the noise generated in the photodiode and elsewhere was mixed with the signal.

The detector was mounted in a standard SMA connector for ease of connection and the case was grounded. Because the can of the detector was connected to the negative supply, the detector could not be grounded although this would have reduced the noise pick-up at the detector stage.

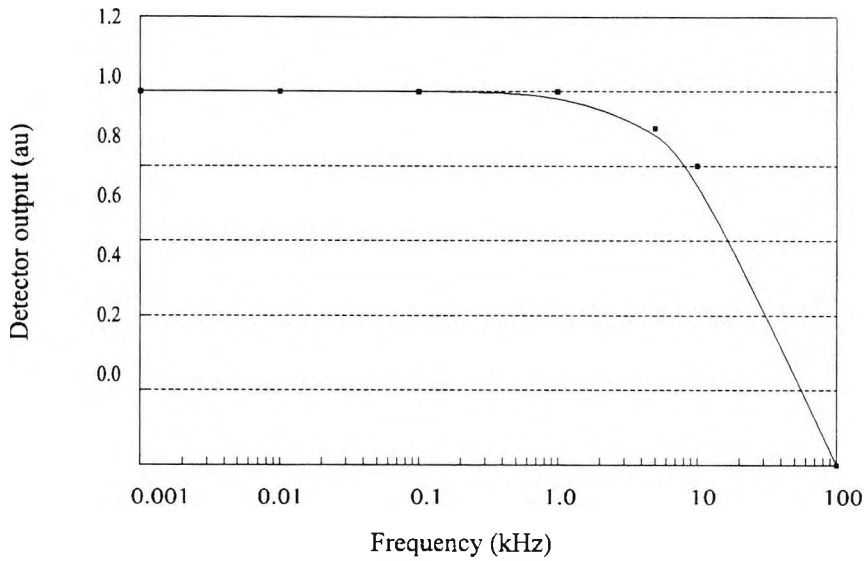


Fig. 4.12 Frequency response of the detector-amplifier module

4.3.2.4 Amplifier

Operational amplifiers type (TLO 071) were used in an inverting amplifier mode to boost the signal from the low level amplitude to a reasonable value. The noise within the range of the signal e.g. 0 to 10kHz, was also amplified. However, the limited bandwidth of the detector and the operational amplifiers was advantageously used to reduce the high frequency noise since no frequency occurring outside the frequency handling of the operation amplifiers was to be amplified, instead they were reduced.

The amplifier was made from two stages because of the limited 1MHz gain-bandwidth product of the operational amplifier which defines the upper frequency as a function of the gain. The two amplifier stages were identical, each of them having a gain of 10 so that overall gain of this stage was 100. A third amplifier having a gain of unity was used as an inverter. The noise density generated by these amplifiers was in the range of $10\text{nV}/(\text{Hz})^*$

4.3.2.5 Interference Rejection

The ambient light generated by daylight and the fluorescent tube lamps was seen to affect the baseline value of the detected signal hence resulting in an error in the measurement of the amplitude of the detected pulses. These optical signals were converted into electrical signals in the detector and appeared as a dc signal

superimposed onto the main signal. The main reasons which account for the presence of the dc signal were:

1. The ambient light, i.e. daylight and dc. powered lamps, appeared as a shift of the base line of the signal. It was noticed that a certain amount of the mains light also acts as dc. signal when the intensity is low. This could result from the long reminiscence time of the fluorescent light originating from mercury discharge lamps. These are coated with phosphor which is responsible for converting UV radiation into visible light. The wide use of this type of lighting and the lamps disposition can generate the effect of the dc light. However, this is only true in very weak signal applications.
2. A small offset was generated in the amplifier stage. This offset voltage can be reduced by balancing the path of the signal to ground. This was achieved by equalling the value of the resistor from the non-inverting input ground with the value of feedback resistor put in parallel with the resistor connected to the inverting input of the amplifier. However, this method did not eliminate the problem completely, since the offset of the amplifier affected the gain. For long standing measurements, very low temperature coefficient devices should be used.
3. The reverse current of the photodiode (which is known as dark current), was generated by the minority carriers inside the junction of the photodiode. The amplitude of the dark current was affected mainly by temperature and the reverse bias voltage of the diode. The dark level temperature coefficient for this particular photodiode was $0.5 \text{ mV}^\circ\text{C}^{-1}$.

A scheme to remove these offsets was deployed. It consisted of sampling the signal at the time where both LEDs were switched off using a sample and hold device triggered at the appropriate time by the signals generated by the computer. These were triggered to sample and then hold the signal until the next sampling time. This time, i.e. the period between two consecutive samples was approximately 1ms in the

slowest case, hence the error associated with leakage was small. The output of this sample and hold device, which represented an average value of the interfering signal and was of dc nature, was then fed to the inverting input of a differential amplifier whose gain was set to one.

The non-inverting input of this amplifier was connected to the main signal. Hence, environmental disturbances i.e. small variations in temperature, dark current and ambient light, were subtracted from the main signal. This scheme allowed for the measurement to be taken in broad background lighting and no special care was needed for the measurement. However, it was unable to discriminate against powerful ac-based light sources.

4.4 Output signal separation

Each cycle contains the information relative to the green LED and infrared LED signals. These consecutive pulses needed to be separated from each other prior to the measurement of their respective intensities. Different circuit could be used to perform the separation of the signals corresponding to the green and infrared lights. For example a set of two electronic switches could be activated, one at the time corresponding to the time where one LED is switched on and then it would be deactivated just before the falling edge of the driving pulse. This was found to be unsatisfactory because the final signal in each case would have been a pulse train signal. A further processing of these signals would have taken place so that electrical noise would have been minimised. Instead, a more appropriate method was deployed where the output of the separation stage was enhanced in terms of signal to noise ratio. This consisted of using the filtering effect of sample and hold devices.

The processed signal containing the information from the two signals was fed to the input of two sample and hold devices connected in parallel, one was triggered to sample and then hold the signal when the green LED was switched on by using a control pulse command and the second device was triggered to sample and then hold the signal at the time the IR LED was switched on with a similar control pulse. These

were originally taken from the pulses driving the LEDs and were modified to occur respectively at each specific time. The duration of these pulses was shorter than the LED driving pulses, in order not to include that part of the signal where overshoot occurred.

Consequently, signals corresponding to the absorption and the reference measurements were present at the output pin of these sample and hold devices continuously. Additionally, only the average value of the signal which was stored in the hold capacitor was provided, thus removing a large amount of noise^[4]. The computation of the ratio of the absorption signal to the reference signal was then computed and a calibration of the measuring instrument was provided. A schematic diagram of the timing of the separation stage used to separate and filter the output signals (e.g. absorption and reference) is shown in Fig. 4.13.

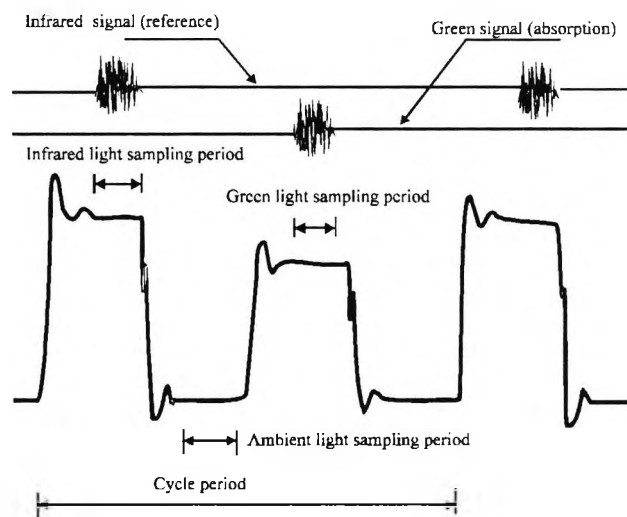


Fig. 4.13: Sample signal through the separation stage using sample and hold devices with a large polycarbonate hold capacitor $\sim 1 - 10\mu\text{F}$.

The titration was made with hydrochloric acid (HCl). Additional volumes of HCl were mixed with the sample using a magnetic stirrer. The probe was immersed and held at the same position for the rest of the experiment in order not introduce further errors. When the measurement was taken, the mixing of the sample was stopped because the latter created turbulent liquid flows which contained small air bubbles and particles,

and was affecting the transmission of the light beam. A few seconds were needed to allow for the sample to settle and any bubble movement to stop prior to recording the measurement.

The range of pH covered was from 10 to 5 pH units. Although the dye does not linearly cover this range of pH values, it was necessary to investigate the response of the fibre optic pH meter outside the linear range of light absorption by the dye. The same solution was then mixed with increasing volumes of sodium hydroxide in order to increase the pH value and cover the same range of pH as in an acid to base titration.

The volumes of acid and base were so small compared to the initial volume of the sample that the concentration of the dye remained in effect constant during the experiment. The volume of the dye phenol red was 0.5 ml and was mixed thoroughly to obtain a homogeneous mixture. The ratio of the light transmitted from both green and infrared light was calculated and plotted as function of the pH of the sample as shown in Fig. 4.14.

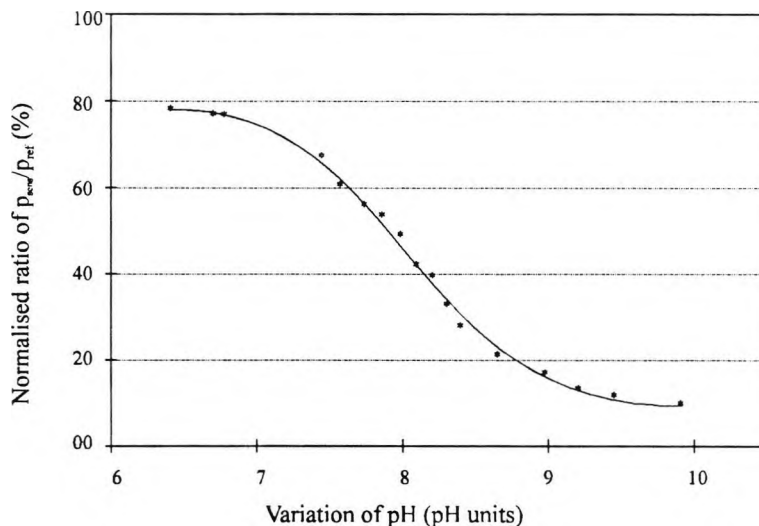


Fig 4.14: Calibration curve of the fibre optic pH sensor as a function of pH measured with a glass electrode instrument over the range of 6 to 10 pH unit values

The correlation between the calculated values and pH of the sample was carried out

using a commercial potentiometric pH meter (RS 10-450) which was calibrated with two buffered solutions (pH 7 and pH 4). The range of pH values scanned during the calibration was between 5.5 to 9 pH units. Only a portion of this range could be approximated as a linear response of the instrument which occurred around the inflexion point (i.e. pH = pK).

4.4.1 Error Considerations

The error in the measurement of pH using colorimetric techniques is related to the error in the measurement of the light intensity of the sensing signal. The relationship is not linear but varies with light level. Hence, a figure for noise performance can only be applied to a particular value of the measurement e.g. when the absorption of the dye is maximum for the particular sensing wavelength. Usually a signal to noise ratio (SNR) is a better description of the noise performance because it is related to the level of the signal and in this case a value of 54dB was obtained for a static signal.

However, for the range of pH studied the dynamic range of the signal is smaller. Consequently, the dynamic $SNR_{dynamic}$ is smaller and gave a more accurate value for the performance of the sensor. For example, the signal varied by 19% which corresponds to a $SNR_{dynamic}$ of 41dB. The noise level associated with the detected signal is $\sim 10mV$. The corresponding numerical value for the pH measurement is then computed and was found to be ± 0.05 pH units at its best value.

The results provided by the sensor when the pH of the sample was varied from the two extremes e.g. acid to alkaline sample, were compared with a commercial potentiometric pH meter and were found to be reproducible within the estimated error. The instrument was monitored for a period of an hour and it was found that the output varied by only $\sim 1\%$. The effect of temperature on the response of the instrument was found to alter the output of the sensor by 0.04 pH K^{-1} . This was carried out by heating the sample in a temperature range of 20 to 50°C and monitoring the variation in the value of the ratio of the green to infrared signals.

4.5 Summary

The design of a fibre optic pH sensor based on the principle of light absorption of a chemical dye (e.g. phenol red) was investigated using a new method based in the computer controller for generating the reference light signal.

The pH measurement approach and the implementation of this new method as an essential basis for the construction of fibre optic based ammonia sensor for the measurement of dissolved ammonia concentration in water is now discussed. In the next chapter this development and the use of fibre optic based techniques for such a sensor will be presented.

4.6 References

1. J.M. Senior, "Optical Fibre Communications; Principles and Practice", Chapter 9 Ed. By P.J. Dean, Prentice Hall International, London UK,(1980).
2. P.W. Shumate and Jr M. DiDomernico,"Lightwave Transmitters", in Topics in Applied Physics, Ed. H. Kressel, Springer-Verlag, 39, p161-200, (1982).
3. Y. Suematsu, and K. I. Iga, "Transmission sur Fibre Optic", Chapter5, Masson, Paris,(1984).
4. P. Horowitz, and W. Hill,"Horowitz and Hill: The Art of Electronics", Cambridge University Press, UK, (1994).
5. RS Components, Technical reference manual.

Chapter 5

Feasibility Study for The Design of a Fibre Optic Ammonia Sensor Based on Absorption of the Emitted Green Light

Abstract

The historical and current background to the determination of ammonia concentration in water are presented and discussed in this Chapter and a programme of research carried out is described for developing an optical analogue of the currently available electrochemical ammonia sensor. In the discussion of the process, the performance and basic design criteria are described for an optical-fibre-based dissolved ammonia sensor which requires no electrical connections between the sensor head in the analyte and the optically-based measurement system. The Chapter also presents an appropriate theoretical foundation for the physical, chemical, and optical dynamics of such sensors and the basis for the numerical simulation of later designs in the development of an appropriate ammonia sensor system.

The method of determination is based on monitoring the pH change induced by the presence of dissolved ammonia in water, due to the reaction of NH_3 with H_3O^+ (hydronium) ions and observing the resulting change in the optical absorption of a pH indicator dye. In the design, the indicator dye is separated from the analyte by a membrane barrier that selectively transports the ammonia species by diffusion, as is currently used in electrochemical ammonia sensors. In the present work, phenol red ($\text{C}_{19}\text{H}_{15}\text{O}_5\text{S}$) is used as the pH indicator dye as it has a strong absorption band centred around the 565nm wavelength, conveniently close to output of available, closely matching, ultra-bright green light emitting diodes used in the research.

5.1 Ammonia Nitrogen

Nitrogen that exists either as the ammonium ion or as the dissolved NH_3 molecule in equilibrium with NH_4^+ is considered to be ammonia nitrogen. Essentially four different methods for determining ammonia nitrogen are included in "Standard Methods"^[1]: two colorimetric procedures, a volumetric procedure, and an instrumental method using an ammonia-selective membrane probe. The NH_4^+ ion is known as the ammonium ion as stated in equation 5.1. This reaction is very well known as representing the first ammonia nitrogen form.



5.2 Environmental Significance of Nitrogen data

Data on Nitrogen potentially present in any sample, are extremely important in connection with wastewater treatment. By controlling nitrification in an aerobic treatment plant, costs of this process can be kept at a minimum. Ammonia and organic nitrogen analyses are important in determining whether sufficient available oxygen is present in the water for the biological treatment of wastewater or sewage. If not, the amount of oxygen that should be supplied from outside sources must be carefully calculated, an important point in economic considerations in many instances, for the water industry. Analyses for ammonia in its various forms have been performed on potable and polluted waters ever since water was confirmed to be a vehicle for the transmission of disease. The determination of the ammonia concentration has served as one basis of judging the sanitary quality of water for a great many years. Today ammonia analyses are performed largely for other reasons such as water purification and in the estimation of the conditions of open waters, where high ammonia levels are often indicative of the presence of decaying matter.

5.2.1 Water Quality Treatments

It has been long known that polluted waters will purify themselves, provided that they are allowed to age for sufficient periods of time. The hazard to health or the possibility of contracting disease by drinking such waters decreases markedly with

increase of time and temperature.^[1] Prior to the development of bacteriological tests for determining the quality of water, environmental engineers and others concerned with the public health were largely dependent upon chemical tests to provide circumstantial evidence of the presence of contamination.

Chemists working with wastes and freshly polluted water learned that most of the nitrogen present originates in the form of organic (protein) nitrogen and ammonia^[2]. As time progresses, the organic nitrogen is gradually converted to ammonia nitrogen, and later on, if aerobic conditions are present, oxidation of ammonia to nitrites and nitrates occurs. The waters that contained mostly organics compounds and ammonia were considered to have been most recently polluted and therefore of great potential danger. Waters in which most of the nitrogen was in the form of nitrates were judged to have been polluted a long time previously and therefore offered little threat to public health. However, it was agreed that the level of such pollution should not exceed 10mg/l of nitrogen in public water supplies^[3].

5.2.2 Nutritional and Related Problems

Most biological treatment processes employed by environmental engineers are dependent upon the reproduction of the organisms employed to break down the waste. In planning waste treatment facilities it becomes important to know whether the waste contains sufficient nutrients in the forms of ammonia and oxygen for the organisms to be viable. If not, any deficiency must be supplied from outside sources. Determinations of ammonia and organic nitrogen are normally made to obtain such data.

5.3 Established Analytical Methods for Ammonia Measurements.

As a logical consequence of the great demand for measurements of ammonia and its progenies, a large variety of techniques for sensing ammonia has been developed, some of which are available commercially. By and large, techniques for monitoring ammonia and its progenies can be classified into:

- 1 Colorimetric techniques.
- 2 Electrochemical techniques.
- 3 Semiconductor-based techniques.

In comparing these different techniques for ammonia measurement, the case for the use of colorimetric methods and the possibility of combining them with optical fibre-based methods will be explored in this research.

5.3.1 Colorimetric Methods

Colorimetric techniques for the determination of ammonia are dominated by three approaches, namely the Berthelot, ninhydrin and Nessler methods. The Berthelot method, first introduced in 1859, is based on the reaction between ammonia, phenol and calcium hypochlorite to produce the blue colour of indophenol. The procedure of this method involves mixing stock reagents, incubating for a specific time and then heating at a particular temperature for a period of time, this being specified in the text book of quantitative chemical analysis^[4]. This method has been subjected to various modifications including: (1) the substitution of hypochlorite with other oxidising agents^[5], (2) variation in temperature^[6], and the addition of catalysts^[7]. The ninhydrin method relies on the colour change observed in the reaction of ammonia and ninhydrin, similar to the reaction of ninhydrin with amino acids. Due to this similarity, determinations carried out with this method are subjected to interferences from amino acids and other amino compounds, which makes it comparatively less favoured.

Nessler's method, as discussed earlier, is also a colorimetric technique. Despite its lack of reproducibility, this method is recommended by analytical chemists in general as the method of determining ammonia in water^[8]. A review by Fleck^[9] on the various colorimetric methods of ammonia determination suggests that the technique of Berthelot is comparatively more reliable and faster to use, although it is subject to some interference from the presence of metal ions in the sample. Originally, the colour

intensity of these three methods was determined by using colour comparison tubes which rely on analysis by the naked eye. Whilst effective for use by a skilled experimenter, it is essentially subjective and has been superseded successively by photoelectric colorimeters and then by spectrophotometers.

Apart from the methods discussed above, it also has been reported by many researchers^[10] that the blood ammonia level can conveniently be measured through its reaction with α -ketoglutarate, nicotinamide adenine dinucleotide (NADH) and the enzyme glutamate dehydrogenates, where the decrease in NADH absorption directly corresponds to ammonia concentration. This is usually measured by a disposable medical sensor.

While all the traditional analytical methods for ammonia sensing discussed so far are, in principle, suitable for implementation with colorimetric sensing systems, actual sensors based on them will experience two difficulties. Firstly they will require complicated reagent handling schemes and secondly, because they involve essential irreversible chemical processes, they will require frequent replacement of the reagents, except where the measurement is made at very low concentrations, where the accumulative effect of an irreversible process can be used to advantage.

Another class of colorimetric methods for ammonia are those based on the colour change of a pH indicator dye. This class of method utilises the reaction of ammonia and water to produce ammonium and hydroxide ions thus resulting in a change of pH, the variation of which can be monitored by a conventional pH indicator.

Although this approach sounds simple and interesting, its application is limited to laboratory use where the analyte can be chemically adjusted by the addition of an indicator and buffer solution. Also it is not selective for ammonia because other species present in the sample might also cause pH changes. In addition, the amount of hydroxide ions produced will depend on the buffer capacity of the solution. However, by using a special membrane and an appropriate enzyme, this method becomes very useful for measuring ammonia-producing compounds. Some companies have used this

enzyme-membrane method for therapeutic bedside urea kits, these including Azostix (Ames Co.), Reflotest-Urea (Boehringer Mannheim), and Mercognost (E. Merck Co. Darmstadt).

In general, these commercial kits consist of a strip impregnated with a pH indicator, which is coated with a urea permeable membrane^[11]. With these kits, the measurements can be carried out by simply leaving a drop of blood on the reagent zone for one minute, after which it is washed away with water and the colour of the reagent zone is either measured by the use of a reflectance photometer or compared with the provided chart calibration block.

Another interesting approach has been reported by Status and Fridovich^[12], who developed a continual spectrophotometric assay for ammonia and urea. This method is based on the observation that the peroxidation of dianisidine by horseradish peroxides at elevated pH was enhanced as much as 160 fold by ammonium salts, and that this change of rate is directly proportional to the concentration of the ammonium salts present in the assay solution.

Despite the claim of its authors that this method is technically simple, it has a limitation of being applicable only in the alkaline pH range. This is a consequence of the fact that the stimulation of the peroxidation becomes evident only at pH values greater than 7. As an illustration, over the range from pH 9.3 to 7.8 the responsiveness of the assay decreases by a factor of twenty. As will be shown later, the use of pH indicators can lead to the possibility of essentially reversible colorimetric-based sensors when incorporated within a suitable chemical system.

5.4 Electrochemical Methods^[13]

The subject of electrochemistry is concerned with the relationships between electrical and chemical phenomena. A knowledge of electrochemistry has several applications in environmental engineering, and for example, is germane to an understanding of corrosion, for example for electrodes immersed in a range of solutions. Many

analytical procedures of interest to the environmentalist are based on electrochemical measurements.

The available electrochemical methods are particularly useful in water chemistry, as they lend themselves to continuous monitoring and recording. The pH meter is probably the most widely used electrical method of analysis in this field.

5.4.1 The Potentiometric Method.

Potentiometric is a term used to describe an electrochemical technique in which the potential is the measured quantity. This kind of device functions under equilibrium conditions and measures the potential difference generated at the sensing electrode against that at a reference electrode maintained at zero net current flow.

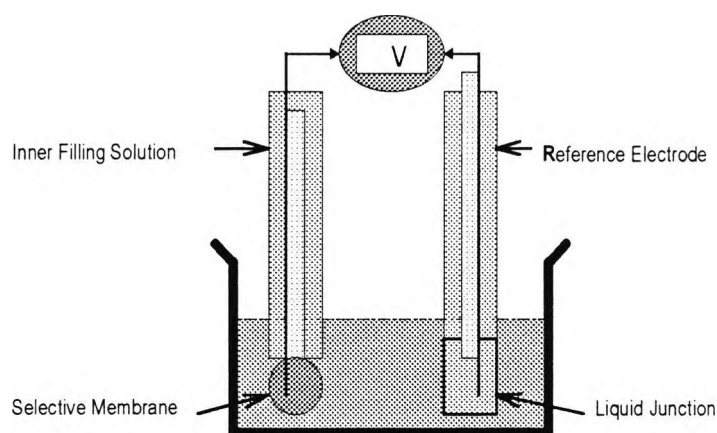


Fig. 5.1 A typical set up for Potentiometric system

Measurement using a potentiometric method is best represented by ion selective electrodes (ISEs)^[14]. In ISEs, the electrical potential difference is generated from a chemical potential difference across an ion selective membrane. A schematic diagram of an electrochemical cell used to determine a particular ion in electrolyte solution is presented in figure 5.1. A great number of various potentiometric ammonia sensors have been described based for example, on pH, cation, gas and air gap electrodes^{[15],[16]}.

5.4.2 The Glass-Membrane pH Sensor as an Ammonia Sensor.

The glass-membrane sensor forms the key component in various types of ammonia sensor. Its basic design is that of a pH sensor which incorporates a glass-membrane barrier with a composition that selectively allows the passage of hydrogen ions from the analyte into an enclosed measuring volume.

There the hydrogen ions change the ionic balance of a silver-silver chloride solution in the measuring volume which is monitored by silver - silver chloride electrode. The sensor also incorporates a reference electrode directly exposed to the analyte, as shown in figure 5.1 above.

The potential difference measured between the two sides of the membrane is related to the concentrations of the hydrogen ions present on either side of the membrane. Thus by holding the concentration of the hydrogen ion constant on one side, the concentration of the hydrogen ions on the other side can be calculated from the potential difference using the Nernst equation^[17].

The prime advantages of the glass electrode are its relative ease of use and that it can function in highly coloured solutions for which colorimetric methods are inappropriate. However, the glass electrode needs very careful handling when used in critical measurement situations, and this can be a problem in its water use.

The principle of a pH-based ammonia sensor is similar to that for ammonia from the colour change of a pH-indicator, except that the indicator is replaced with a glass pH-electrode. As with the pH-indicator based ammonia measurement, the glass pH ammonia sensor is useful only whenever it is coupled with a suitable enzyme for measuring an ammonia-producing compound. Such an arrangement has been used by some investigators to develop a urea sensor^[18]. However, these sensors have the main drawback of being sensitive to buffer capacity of samples, which is why preconditioning, i.e. dilution into a standard buffer solution, is required prior to each measurement.

The change of pH due to the reaction between ammonia and water can also be followed by an antimony pH electrode. A urea enzyme micro-sensor has been fabricated by using this approach. The sensor responds to 1 - 0.1 mM urea in 45 seconds, but since it is based on pH, any factor which alters the pH of the solution, other than the enzyme reaction, would seriously interfere with the measurement.^[19]

5.4.3 Cation Based Ammonia Sensor.

In attempts to reduce the selectivity problem associated with glass and antimony pH electrodes, a cation selective electrode has been introduced^[20]. This electrode is sensitive to the ammonium ion as well as some monovalent cations such as potassium. The construction of this electrode is similar to that of the pH electrode except that the glass membrane employed has a certain composition that is selective towards monovalent cations. For example, a commercial Beckman 39137 cation electrode has a glass composition^[20] of 27% Na₂O, 4% Al₂O₃, 69% SiO₂ and a selectivity series $Ag^+ > H^+ > K^+ > NH_4^+ > Na^+ > Li^+ > Mg^{++} > Ca^{++}$.

An enzyme electrode for measuring urea in plasma and urine has been constructed based on urea coated cationic glass electrode^[21]. In this sensor a urea-containing polyacrylamide gel is placed on the surface of cationic glass electrode. When placed in enzyme a solution containing urea, the substrate diffuses into the gel layer and reacts with the enzyme to produce the ammonium ion. This is seen at the surface of the electrode and is sensed by the cation electrode in a manner similar to pH determination with a usual glass electrode.

However, since the glass membrane employed is not specific to the ammonium ion alone, interference from other monovalent cations, particularly Na⁺ and K⁺, is inevitable. In attempts to obtain a membrane with good selectivity for the ammonium ion, Simon and Scholer^[22] constructed a liquid-membrane electrode consisting of nonactin and monactin in tri (2-ethylhexyl) phosphate. The new liquid membrane does exhibit a good selectivity over K⁺ and Na⁺, but it is not good enough to be coupled

with an ammonia generating enzyme because the organic solvent of the membrane is enzyme-incompatible.

Guilbault and Nagy^[23] overcame the incompatibility problems by incorporating nonactin directly into a silicone rubber matrix to form a solid state ammonium ion-selective electrode, which can be covered with an enzyme layer. The selectivity of this electrode to ammonium ion is reported to be 750 and 6.5 times higher than those for sodium and potassium ions respectively. A special compensation technique has to be used where the urea concentration is calibrated in a solution of constant potassium ion concentration, and a serum sample has to be diluted so that its potassium ion concentration matches the level of that at which urea calibration was previously performed; an additional uncoated ammonium ion electrode is needed to measure the presence of the interfering ion^[24].

5.4.4 Ammonia Gas-Permeable-Membrane Sensing Electrode.

To overcome the problem associated with the selectivity of ion sensitive electrodes, another approach for monitoring ammonia has been introduced, that is by monitoring ammonia as a gas rather than as an ammonium ion. In a potentiometric gas sensor, the pH electrode and internal solution are separated from the sample solution by means of a hydrophobic gas-permeable membrane. The internal solution employed varies according to the gas of interest, and for ammonia, this is commonly ammonium chloride.

The sample holders are designed in such a way that, when used, ammonia released from the sample solution diffuses across the membrane until the ammonia partial pressure is equal on both sides. The penetration of ammonia disturbs the ammonia-ammonium ion equilibrium already present in the internal solution and causes an increase in the hydroxyl ion concentration. The resulting change in pH, which is proportional to the concentration of the gas present, is measured with the glass pH electrode. The kind of gas sensor is commercially available from Orion.^[25] Because a gas sensor detects the molecular (NH_3) and not the cationic (NH_4) of ammonia from

the sample solution, it provides excellent selectivity which makes this electrode very useful in clinical and laboratory assays. Several urea sensors have been developed using an ammonia gas electrode^[26].

Direct urea measurements in whole blood have been described by Papastathopoulos and Rechnitz^[27] based on an ammonia - gas electrode coupled with a layer of urea solution held on the surface of a gas-permeable membrane. Unfortunately, despite its excellent selectivity, the ammonia gas sensing electrode suffers from several problems. First, a high pH is required for effective conversion of the ammonium ion to ammonia. This can be a serious problem if the enzyme to be coupled to the electrode is not active at high pH. Second, as pointed by Hansen and Ruzicka,^[28] the poor mechanical properties of the membrane and possible clogging of the pores limit its utility. Third, as discussed by Arnold,^[29] response and recovery times are slow, and even slower if the enzyme layer is applied on the surface of gas-permeable membrane. Typical response time are 5 to 10 minutes for low level ammonia, and recovery times as long as 45 to 60 minutes are required when starting from high ammonia levels.

5.4.5 Conductimetric Sensor

A conductimetric sensor measures the ability of a solution electrolyte to carry a current from one electrode to another. Since this ability is determined by the number and type of ions presents in the solution, conductimetric sensors can be used to measure the concentration of ionic species present in a sample.

In its simplest form, the conductimetric sensor can consist of two metals in a solution connected to a voltage source and a current measuring device. The possibility of using this method for the detection of ammonia lies in the equilibrium of ammonia and the positively charged ammonium ion. This equilibrium also proves a convenient way of measuring neutral nitrogenous compounds which release an ionic ammonium ion during their enzymatic reactions.

Chin and Kroontje^[30] pioneered the conduction of urea measurements using a conductimetric sensor. Watson et al.^[31] have developed integrated conductor gold tracks on top of which urea was immobilised by the glutaraldehyde crosslinking method. The system is reported to respond to urea in the range of 0.1 to 10 mM.

Attempts have been made to measure ammonia, instead of the ammonium ion by using a modified conductor employing copper-phthalocyanine,^[32] polypyrrole,^[33] and tetracyanoquinodimethanide (TCNQ).^[34] However, the selectivity of these modified conductors is rather poor.^[35]

5.4.6 Amperometric Ammonia Sensor

In an amperometric sensor, a constant potential is applied between a working and a reference electrode to cause the redox reaction of the analyte to take place, thus generating a net current flow. The current so produced is directly proportional to the analyte concentration.

One important requirement of an amperometric sensor is that an analyte should have redox properties, which ammonia does not have, and thus it is unlikely that ammonia can be measured directly with the use of this technique. However, with certain strategies, the technique has proved to be useful. The first was developed by Suzuki's group in Japan^[36]. They used *Nitrosomonas europaea* techniques to convert ammonia to nitrite which was then converted further to nitrate. The latter conversion was carried out by using *Nitrobacter* sp with the consumption of oxygen. Such consumption was followed by the usual Clark oxygen electrode. The sensor thus developed can be used to determine ammonia in waste waters and is reported to be selective for ammonia, although with a relatively slow response time.

Another method has been introduced by Scheller and co-workers^[37]. This is based on the observation that in the electrochemical oxidation of hydrazine, a linear relationship exists between the logarithm of the current (log I) and the pH of a solution. This dependency was then exploited by these authors to develop an ammonia sensitive

sensor. Urea determinations were carried out after covering the electrode with urea selective membrane. The stability of the signal was reported to be very high, with only two re-calibrations per day needed for routine assays. The main problem with this sensor is obvious, i.e. interferences from any factor which could alter the pH of the solution other than via an enzyme reaction.

A conducting polymer micro-sensor for urea has been described by Pandey and Mishra,^[38] which was based on the gas sensing properties of polypyrrole previously demonstrated by Nylander et al.^[39] The sensor was designed in such a way that the released ammonia gas from urea hydrolysis diffuses through an air gap towards the polypyrrole-coated microelectrode. The resulting current was recorded at a very high potential i.e. 1 Volt with respect to the Ag/AgCl reference electrode. The author of this work reported that the response to urea in the range of 0.1 - 50 mM was good at pH 6.4. This result is quite strange, because the equilibrium between the ammonia-gas and the ammonium ion is in favour of ammonium at low pH. Hence, it is unlikely that the response was due to ammonia released from the sample solution.

An alternative method has been developed by Japanese workers^[40] based on the transferability of the ammonium ion at the interface of nitrobenzene-water and nitrobenzene-PVC/water. This interface was used as an ion selective electrode in an amperometric sensor for detecting the ammonium ion. However, as in potentiometric cation selective electrodes, interference from sodium and potassium are unavoidable. Therefore these authors modified the sensor by covering the electrode with a gas-semi-permeable membrane, to construct an amperometric gas sensor. The measurements were conducted in the stirred solution at various pH values and at a constant potential of 0.37 V vs Ag/AgCl electrode.

Each of the approaches that have been introduced for amperometric ammonia sensing have their own attributes. However, they all equally suffer from several drawbacks. The microbial sensor has a slow response due to the use of several membranes. The life-time of this sensor, as for any microbial sensor, is relatively short, as being based on pH it has a lack of selectivity and is unlikely to be useful for ammonia assays in real

biological fluids. The other two sensors which rely on the partial pressure of ammonia gas have a similar problem to potentiometric gas sensing electrodes, i.e. they require a very high working pH (> 10), which is unfavourable for enzyme reactions.

The optical sensor system developed in the course of this work is aimed firstly at the direct replacement of the existing electrochemical membrane-based sensors in current laboratory use with a latter extension of its application to the area of environmental monitoring. The main advantage of the optical sensor over its electrochemical counterpart is the freedom from electrostatic noise and the ability to use such sensors in applications in which there is a flow of electrical current.

5.4.7 Semiconductor Based Ammonia Sensor.

Semiconductor sensors, as implied by their name, are devices which utilise semiconductor materials as the base sensor. Typically, the sensor consists of two n-type semiconductors, termed a drain and source, separated by a p-type semiconductor called the substrate figure 5.2. This system is then covered with an insulating layer of silicon dioxide.

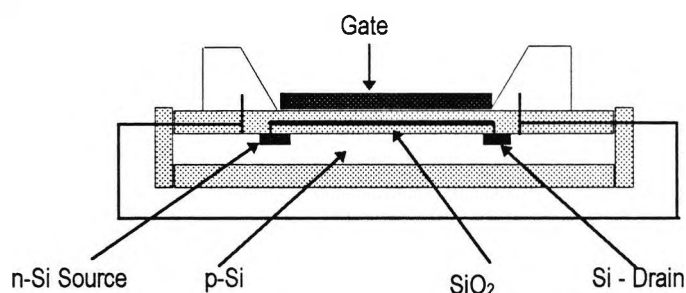


Fig. 5.2: Schematic of a FET Sensor

The area between the source and drain on top of the insulating layer is reserved for a gate which can be switched on or off by applying an external voltage. If the gate is made using metal layer, the system is called a Metal Oxide Semiconductor Field Effect Transistor (MOSFET).

When a positive voltage is applied to the gate with respect to the substrate, electrons in the substrate p-type semiconductor are attracted to the area near the gate-substrate interface and create a conducting channel between the source and the drain, providing a flow of current which will increase or decrease in the presence of a charged dipole layer resulting from the adsorption of gases on the metal gate surface. Therefore, depending on the type of a metal gate employed, the presence of a certain gas on the metal gate can be measured by monitoring the resulting current.

Ammonia gas released from the enzymatic reaction of urea has been detected by using a palladium gate MOSFET,^[41] although the sensitivity is lower with respect to other gases. If an additional thin layer of iridium is incorporated on top of the palladium gate, a higher sensitivity for ammonia is obtained. Winqvist and Danielson reported a further increase in sensitivity and selectivity of such a system by using iridium alone as a gate material.

This so-called iridium thin layer MOS (InMOS) has been used in a flow-through system for analysing ammonia in blood, and has been extended to analysing urea and creatinine in biological samples. Despite of its potential for sensitive and selective ammonia assays, the MOS device suffers from several problems. Firstly, it requires a high operating temperature. Secondly, as is usual for a gas sensing electrodes, its optimum response is achieved at high pH only. These two drawbacks limit its potential to be used as a simple sensor.

5.4.8 IR Methods for Ammonia Analysis

In the near-infrared, using spectrometry, ammonia can be measured directly at wavelengths around 1.53 μm . At this wavelength the LEDs or laser diode light sources available now are relatively expensive. Laser diodes tailored to this wavelength are available but these are very expensive and require expert handling.^[42] IR absorption is still used widely in laboratory-based analysis and the spectrometers employed are very expensive and require careful handling.

5.5 General Comparison of the Techniques

Numerous techniques for sensing ammonia, introduced by many groups all over the world, have been reviewed in the previous sections. However, only a few of these have been developed for commercial purposes. These include:

- * pH indicator based spot test Kits.
- * Glass pH electrode.
- * Cation Glass electrode.
- * Gas sensing electrode.

Although available commercially, such current sensors are not without problems. For example the spot test kits are low in accuracy, and non-specific, the glass pH electrode is not purpose-designed for ammonia, and is therefore not very specific and the ammonia gas sensing electrode has to be operated at high pH and thus is environment incompatible for use with enzymes.

The commercial unavailability of the other potential methods reviewed reflects their limitations, which might be either low selectivity, high cost, inaccuracy, low sensitivity, difficulty of use, low reproducibility, or a combination of these problems. The difficulties associated with an individual sensor are also often associated with problems in the implementation of the technique employed, because each has its own limitations. A brief comparison, reflecting disadvantages and advantages of each technique can be found in the articles written by Rechnitz^[43], Luong et al^[44], Guilbault^[45] and Arnold^[46].

In summary, these highlight that colorimetric techniques are time consuming to employ and usually involve many reagents, and additionally are subject to human error. This means they are difficult to implement in instrumentation for on-line measurement. However, the advantages of these techniques are that they are simple and may be economically employed on a non-routine basis. The conductometric method is said to be inexpensive, but it is non-selective, has a poor signal-to-noise

ratio and is therefore limited to specific applications with controlled chemistry. Further, although semiconductor-based devices have the potential for miniaturisation and mass production, the associated development costs are high compared to the market size, and the lifetimes of devices exposed to uncontrolled analytes, e.g. in river water, are limited. Having said that, the sensing element of these devices normally is very small, which is very promising for *in vivo* measurements.

However, if the present technological developments are used as a basis to judge the status of such devices, the expected advantages seem to lie with fibre optic sensor devices. Miniaturisation with integrated optics is feasible, in principle, to a level similar to that for semiconductor devices, and they suffer from the same difficulties in application where the device has to be used in a flow-through system. Future trends in fibre-optic sensors incorporating micro-tips and solid-phased sensing elements may offer many of the advantages promised by semiconductor devices without the need for an electrical connection to the sensor element.

Presently, however, there are problems with stability, leakage, slow response and non-compatibility with most enzymes, with membrane-based optical sensors. Potentiometric instrumentation is widely available, which is an advantage. In addition, there is no net consumption of reactants in such devices and therefore mass transport in the operation of the instrument is unimportant. However, the method suffers from two main drawbacks. First, because the response is logarithmic, a slight error in the potential will result in a relatively large error in the concentration measured. Secondly, responses are slow due to the time required to establish the equilibrium.

5.6 New Optical Techniques for Ammonia Analysis

In the late 1980s several researchers reported success in measuring ammonia gas by using new techniques based on fibre optics. This type of technique had been described in the literature of the day as a particularly useful because the data would be free of electromagnetic interference with the potential for the use of fibre optic standard

communication cable, rather than conventional copper cable, such as is employed with the electrochemical techniques above.

The development of fibre optic chemical sensors had started in the early 1980s with many research groups around the world reporting their research work. However, most of this work has only provided a beginning and the trend of development of fibre optic chemical sensors is growing very rapidly. Peterson reported the first pH optical sensor^[47]. This new development opened the door for many other researchers. Arnold and co-workers reported the first fibre optic sensor for ammonia gas measurement with this sensor being based on the detection for ammonia in air pollution studies.^[46] However, this sensor suffers from a short life and is sensitive to other species, such as CO₂. The research and development of such technology clearly still needs more exploration. However, this development is a part of a study of such techniques, by which it is aimed to achieve a satisfactory standard for the improvement of previous work on fibre optic chemical and environmental sensor technology.

5.6 Theoretical Aspects of Membrane Based Ammonia Sensor

In this section consideration is given to the development of a computer model that simulates the time-dependent behaviour of ammonia, and other species in chemical equilibrium with ammonia in a sensor. As will be shown, in the experimental section of the next chapter, the dynamic response of the colorimetric dye employed in the sensor system for ammonia is quite complex, prompting the necessity for an appropriate theoretical consideration. The prime goal in developing the model is to aid understanding of the experimental results obtained, in particular the dynamic response of the sensor, and to help in the further design of a sensor.

Three main processes that occur in such sensor systems which need to be included in a model are: chemical equilibrium, diffusion of species in the membrane and sensor cell, and spectrally dependent absorption of light by the various species in the optical cell. More specifically these processes are:

1. Reaction of ammonia with the chloride buffer (NH_4Cl) of 0.001M and the indicator dye (phenol red) in the sensor cell.
2. Diffusion of the ammonia through the membrane and inter-diffusion of the various chemical components NH_3 , NH_4^+ , In^- , InH , H_3O and OH^- in the cell, subject to local charge neutrality.
3. Change in the absorption spectra of the liquid due to changes in the concentrations of the In^- and InH species in the cell which result in access to data on the measured spectra.

These areas will be discussed in turn, with a mathematical description for each form obtained, from which a numerical model that combines the various components and combines these in an overall comprehensive model is developed.

Figure 5.3 shows a construction of the relationship between the analyte, membrane, cell and optical path in the sensor that will be helpful in the above discussion. The figure shows a one-dimensional model of a sensor in which ammonia from the analyte diffuses through a membrane barrier of length X_1 into the sensor cell where it reacts with an indicator which changes the absorption of light which enters the cell from the other end, at $X = X_m$. Changes the colour of the indicator dye can then be inferred from changes in the level of light detected from the reflected light.

In the model the membrane and cell are split into a number of elements of length X_m/m , where X_m is the length of the combined length of the membrane and cell, and m is the total number of elements across the sensor. The problem that needs to be solved in the theoretical model is that given the initial profile, the concentration of each of the chemical species in each of the elements at some initial time $t = 0$, what will the concentration profile be at some later time? To do this, the model considers both the diffusion of the chemical species into and out of each of the elements, in a small increment of time, and then considers the new chemical equilibrium that results from the changed chemical composition in the element.

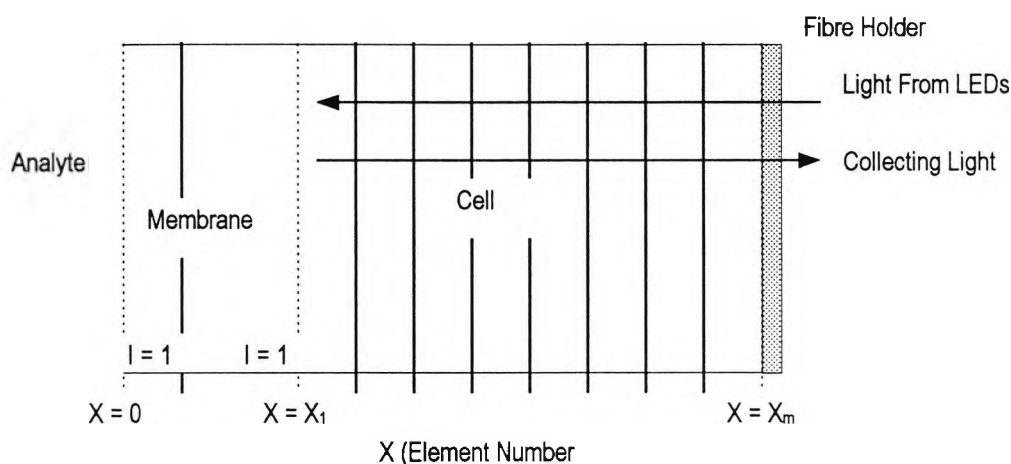


Fig. 5.3: One-dimensional model of sensor. Showing array of elements used in the diffusion-based model of the cell. (showing membrane from $X = 0$ to $X = X_1$, and cell from $X = X_1$ to $X = X_m$). The elements are also defined by the index i , which runs from $X = 0$ to $X = m-1$.

The model assumes that rates of chemical reaction are fast compared to diffusion times and can therefore be ignored. In the model species diffuse from element to element within the membrane-cell depending on the concentration profile at that position and time.

This concentration profile is controlled by the diffusion of NH_3 through the membrane and the chemical activity and diffusion of other species within the cell. Also modelled is the attenuation of green and infra-red light beams that traverse the cell. In the model these impinge on the cell at ($X=X_m$) and are attenuated as they traverse the cell in the 'forward' direction, ($X=X_1$), are reflected from the membrane and are further attenuated on their return to ($X=X_m$), where the remaining light level is recorded. To determine the attenuation, the average values of concentration of each species in the cell are determined and this used with the Beers-Lambert law to determine attenuations, as discussed above.

5.7.1 Chemical Equilibrium Model

Modelling the reaction of ammonia with the buffer and indicator in the cell is the first step to be undertaken. If it is assumed that a local chemical equilibrium exists at every point within the cell, then the following chemical equilibrium equations will describe

the concentrations of the various species present in terms of the appropriate activity constants.

1. The concentrations of the hydronium and hydroxyl ions will be related by:

$$[\text{OH}^-] [\text{H}_3\text{O}^+] = K_w, \quad \text{equ(5.2)}$$

where $[\text{OH}^-]$, $[\text{H}_3\text{O}^+]$, are the hydroxyl and hydronium ion concentrations and K_w is the activity constant for this reaction.

2. Similarly the concentrations of NH_3 and NH_4^+ will be related by:

$$[\text{NH}_3] [\text{H}_3\text{O}^+] = K_{a[\text{NH}_4]} [\text{NH}_4^+]. \quad \text{qu.(5.3)}$$

where $[\text{NH}_3]$ and $[\text{NH}_4^+]$ are the ammonia and ammonium ion concentrations and $K_{a[\text{NH}_4]}$ is the activity constant.

3. Further, for the concentrations of the hydrated indicator and anion species:

$$[\text{In}^-] [\text{H}_3\text{O}^+] = K_{a[\text{InH}]} [\text{InH}] \quad \text{equ(5.4)}$$

where $[\text{In}^-]$ and $[\text{InH}]$ are the indicator ion and indicator species concentrations and $K_{a[\text{InH}]}$ is the activity constant

4. Although it may not be known whether the ammonia in the sample is in the form of NH_3 or NH_4^+ , it is known that the sum gives the total ammonia present: i.e.

$$N_T = [\text{NH}_3] + [\text{NH}_4^+] \quad \text{equ(5.5)}$$

where N_T is the total concentration of ammonia containing species.

5. The same is true for the indicator, where we will know the total combined concentration but not the specific states. i.e.

$$\text{InT} = [\text{In}^-] + [\text{InH}], \quad \text{equ(5.6)}$$

where InT is the total indicator concentration.

6. Finally local charge neutrality will be maintained throughout the cell. This means that the sum of the charge concentrations must be zero;

$$[\text{NH}_4^+] + [\text{H}_3\text{O}^+] - [\text{OH}^-] - [\text{Cl}^-] - [\text{In}^-] = 0 \quad \text{equ (5.7)}$$

7. Equations 1 to 6 form a linear set of equations, which can be solved algebraically by elimination. When all the above equations are combined and the [OH], In-, InH, NH₃, and NH₄⁺ factors are eliminated, a fourth order polynomial in terms of the hydronium ion results. The first real root of this equation gives the hydronium ion concentration at equilibrium and hence the pH of the solution.

$$\begin{aligned} & [\text{H}_3\text{O}^+]^4 + (\text{NT} + \text{Ka}_{[\text{NH}_4]} + \text{Ka}_{[\text{InH}]}) [\text{H}_3\text{O}^+]^3 + (\text{NT} \cdot \text{Ka}_{[\text{InH}]} + \text{Ka}_{[\text{NH}_4]} \cdot \text{Ka}_{[\text{InH}]} - \\ & \text{K}_w - [\text{Cl}^-] (\text{Ka}_{[\text{NH}_4]} + \text{Ka}_{[\text{InH}]}) - \text{InT} \cdot \text{Ka}_{[\text{InH}])} \cdot [\text{H}_3\text{O}^+]^2 + (-\text{K}_w \cdot (\text{Ka}_{[\text{NH}_4]} + \text{Ka}_{[\text{InH}]}) - \\ & [\text{Cl}^-] \cdot \text{Ka}_{[\text{NH}_4]} \cdot \text{Ka}_{[\text{InH}]} - \text{InT} \cdot \text{Ka}_{[\text{InH}]} \cdot \text{Ka}_{[\text{NH}_4]}) \cdot [\text{H}_3\text{O}^+] + -\text{K}_w \cdot \text{Ka}_{[\text{NH}_4]} \cdot \text{Ka}_{[\text{InH}]} = 0 \end{aligned}$$

equ(5.8)

Equation 5.8 can be solved using the Method of Successive Approximations^[21] to obtain the relationship between $\text{pH} = -\log_{10} ([\text{H}_3\text{O}^+])$, and Total Nitrogen concentration, NT. This is done, using the values for the activity constants given in table 5.1, for increasing concentration of total nitrogen ($\text{NT} = [\text{NH}_4^+] + [\text{NH}_3]$) at fixed values of ammonia chloride buffer concentration and optical indicator concentration, as cited in figure 5.4.

$K_{a_{[NH_4]}}$	5.5×10^{-10}
$K_{a_{[InH]}}$	10^{-5}
$K_{a_{[H_2O]}}$	10^{-14}

Table 5.1: Activity constants for the chemical reactions in the simulated ammonia sensor^[16]

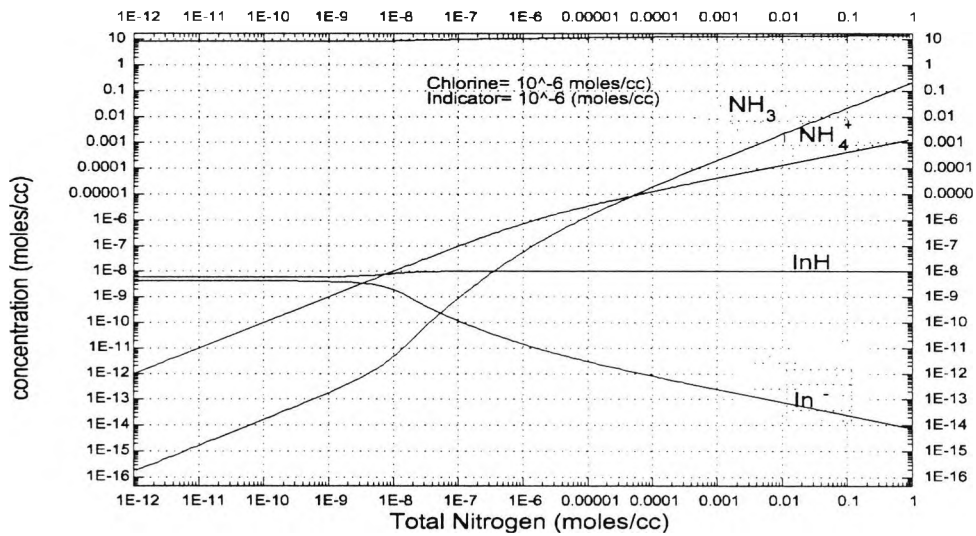


Fig. 5.4: Dependence of the concentration of the various species in the sensor on Total Ammonia concentration.

Once the pH is determined, the concentration of all the other species can then be computed by back manipulation using equations 5.2-5.7. This process results, for example, in the data in Figure 5.4, which shows the relationships obtained for the dependence of the various species concentrations on NT, at fixed concentrations of buffer solution and indicator dye.

Remember, that there are two sources of ammonia in the sensor, the ammonia chloride buffer, and the analyte under analysis. These combine to give a total concentration around the buffer solution concentration, which forms the operating point of the sensor. The most important feature in figure 5.3, for the optical response of the sensor, is how the concentrations of the indicator species InH and In⁻ change. Figure 5.4 also shows that the concentration of total ammonia increases above $\sim 10^{-7}$ moles-cc⁻¹ the indicator changes more and more into the InH form, with the In-

concentration decreasing. It is this change in the In^- concentration that is exploited in the ammonia sensor, via the optical absorption of the species.

5.7.2 Modelling Diffusion in the Sensor Cell.

The concentration of species i in the cell is dependent not only on the chemical equilibrium described above but also the movement of species through the membrane and in the cell must be considered. The important parameters here are the rates of chemical generation (G_i) and removal (R_i), and the flow of species into and out of the region, which are given by dJ_i/dx in a one-dimensional model .

$$\text{where} \quad \frac{dN_i}{dt} = G_i - R_i + \frac{dJ_i}{dx} \quad \text{equ (5.9)}$$

where J_i is the flow of species i , which is related to the diffusion of the species, in one dimension, by Fick's law with G_i and R_i being the rates of chemical generation and removal respectively. This states that the flux of a species J_i is related to the gradient in the density of that species by:

$$J_i = D_i \frac{dn_i}{dx} \quad \text{equ (5.10)}$$

where D_i is the diffusion constant of species (i) and dn_i/dx is the gradient in n_i . In the enclosure of the sensor cell which is being considered, it can be assumed that other major factors, such as net flow, mechanical mixing or electrochemical activity are small compared to the effects of diffusion.

Equations (5.9) and (5.10) combine to form in (5.11) a set of second order differential equation that can be solved by Finite Element Analysis:

$$\frac{dN_i}{dt} = G_i - R_i + D_i \frac{d^2N_i}{dx^2} \quad \text{equ (5.11)}$$

In finite element analysis the continuous second order differential equation is replaced by a difference equation from which approximate solutions for the can be computed

as a function of x and t . The difference forms for the set of equations in equation 5.11 are given in equation 5.12 below:

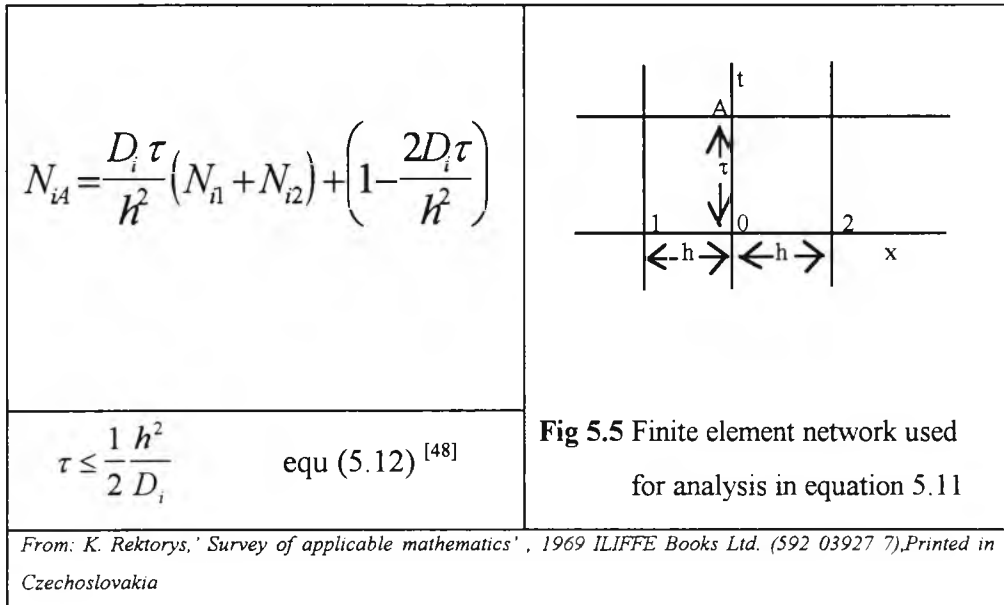


Fig. 5.5 : Finite element network used for analysis in equation 5.11

where x, t are the axes in figure (5.5); h, τ are the increments in x and t ; i is the index for the various species considered, N_{i0}, N_{i1} and N_{i2} are the concentrations at positions 0, 1, 2 of the x axis of figure (5.4), N_{iA} is the concentration at position (A) after time τ and D_i is the diffusion constant. These equation determine the concentration profile at a time $(T_0 + t)$ that results from a known concentration profile at time T_0 .

In practice the solution of the equations in equation 5.12 proceeds in the following manner. The length of the membrane and cell are “sliced” into elements of equal length in the manner described in section 5.8 and shown in figure 5.3.

The simulation then proceeds as follows: The value of the concentration of the ammonia in the analyte at $X=0$, immediately outside the membrane, together with the concentration profile for each of the species in the cell are defined at time $t=0$. From this, new values are then computed for each of the species in the cell after an increment of time τ using equation 5.12. Having computed new values for the

concentrations resulting from diffusion, account must be taken now of any change in chemistry. This done by determining the solution of equation 5.8 to obtain the pH in each element and hence the equilibrium concentrations of each species. One other factor requires addressing to complete an model of the optical sensor. This is the absorbance of light in the cell, discussed in the next section in more detail.

5.7.3 Modelling the Absorbance of light

In order to model the absorption of light in the optical cell, the concentration profiles that result from the above combined chemical equilibrium and finite element must be combined with optical absorption data for the optically active species in the cell to give a model that predicts the absorption spectra expected from a specific of concentration profile. From this the response of the optical sensor signal that results can be simulated.

The actual absorption spectra observed, $A(\lambda)$, will be given by Beer's law applied to a non-homogeneous region.

$$A(\lambda) = \sum_i \int_0^L a_i(\lambda) c_i(\lambda, x) dx \quad \text{equ. (5.12)}$$

where $a_i(\lambda)$ is the absorbtivity of species (i), $c_i(\lambda, x)$ is the concentration of species (i) at x , λ is the spectral wavelength, L is the length of the cell, and x is the distance across the cell. This can be solved by numerical integration using Simpon's Rule (50).

Figure 5.6 shows how the absorption of the two phenol-red indicator species changes with λ for changing concentration

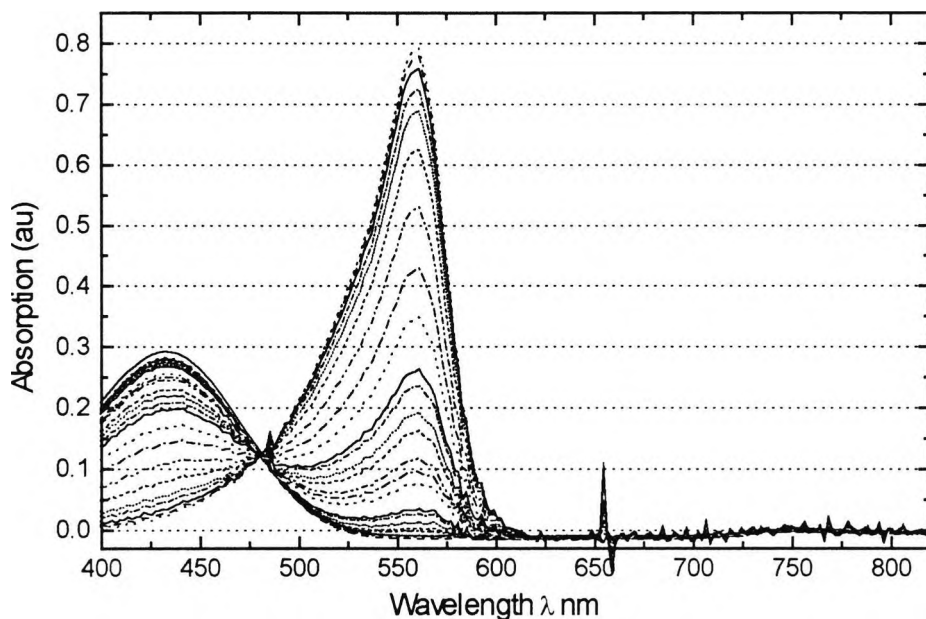


Fig. 5.6: : Absorption spectra of phenol red (2.5%) for various pH values using UV/Vis spectrophotometer

5.8 Simulation of the membrane-based Ammonia Sensor

The simulation brings together the various phenomena discussed in a computer model that predicts the response of the sensor given the dimensions of the sensors, the diffusion constants of the various species, the activation constants of the various reactions, and the concentrations of buffer solution, indicator and the measurand, ammonia.

5.8.1 Main aspects of the Simulation model

The model uses the construction shown in figure 5.2, together with the numerical methods described above for chemical equilibrium, diffusion and optical absorbance. These are combined within one computer model as outlined in the flow diagram in figure 5.7.

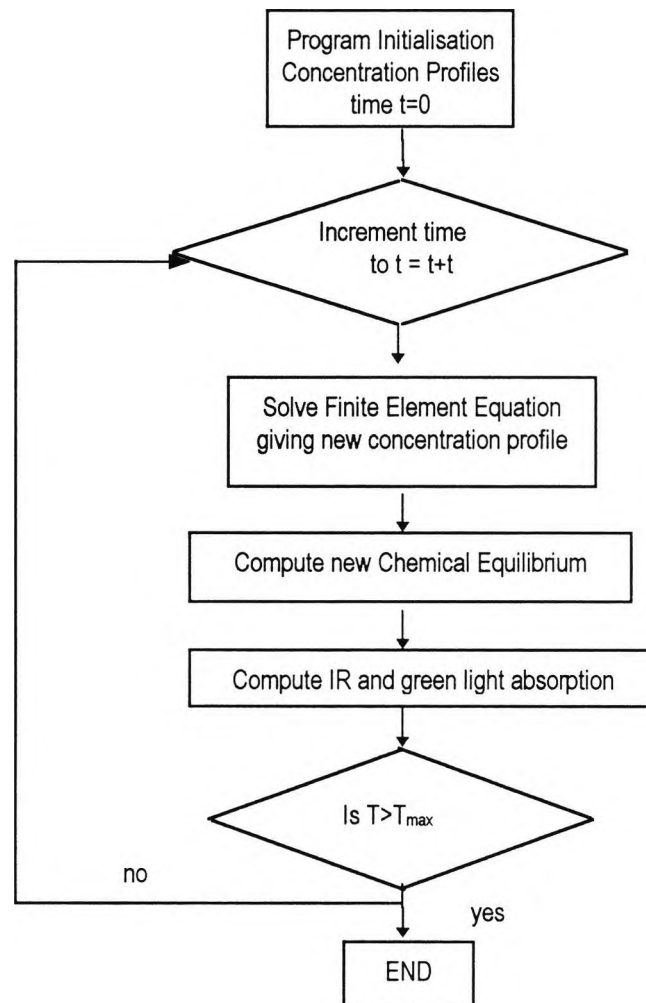


Figure 5.7: Flow Chart for Sensor Simulation Model

The simulation proceeds in the following manner. The concentration profile for the ammonia in the analyte, immediately outside the membrane together with the concentration profile for each of the species in the cell are defined at $t=0$. From this new values are then computed for each of the species in the cell. Figure 5.3 shows a one-dimensional array of elements starting at the analyte-membrane interface at $(X=0)$ through to the membrane-cell interface at $(X=X_1)$ and onto the far cell wall at $(X=X_m)$. In the model species diffuse from element to element within the membrane-cell depending on the concentration profile at any time. This concentration profile is controlled by the diffusion of NH_3 through the membrane and the chemical activity and diffusion of other species within the cell. Also modelled is the attenuation of green and infra-red light beams that traverse the cell.

In the model these impinge on the cell at ($X=X_m$) and are attenuated as they traverse the cell towards ($X=X_l$), are reflected from the membrane and are further attenuated on their return to ($X=X_m$), where the remaining light level is recorded. To determine the attenuation the average values of concentration of each species in the cell are determined and this used with Beer's Law to determine the attenuation, as discussed in the previous section.

5.8.2 Values for diffusion constants in the Membrane and Cell.

Suitable values must be found for the chemical equilibrium and diffusion constants in order to model the chemistry and diffusion of the species present in the measurement cell. Table 5.2 below tabulates the species present in the membrane and the cell along with estimates of diffusion constants at 25°C for these in the membrane and the cell proper. While considering appropriate values for diffusion constants the following were taken in to consideration. Typical value of diffusion constant (D_i) for monovalent anions and cations and small polar molecules i.e. ($\text{CH}_3\text{OH}, \text{C}_2\text{H}_5\text{OH}$), are in the range of $1 - 2 \times 10^{-9} \text{ m}^2\text{s}^{-1}$ and typical values for large molecules,^[49] for example sucrose (m.w.= 342) are in the range of $1 - 5 \times 10^{-10} \text{ m}^2\text{s}^{-1}$. In estimating values of diffusion the following assumptions were made.

1. Rates of reaction for H_2O going to H_3O^+ and OH^- are faster than the diffusion rate of these species. This means that the concentration of these will be determined by local charge neutrality rather than by their concentration gradient.
2. The diffusion-ionic and polar species, like phenol-red, in non-polar, hydrophobic membranes is very low in comparison to other species.
The diffusion constant of IndH in water will be similar to other polar organic molecules like the alcohols and phenols at $\sim 10^{-9} \text{ m}^2\text{s}^{-1}$.
3. (a) The diffusion constant of ionic species is approximately the same as the non-ionised type. For a first guess, a value of $10^{-9} \text{ m}^2\text{s}^{-1}$ is used

(b) The diffusion constant of ionic species is lower than the non-ionised type. Therefore the diffusion constant for Ind^- will be smaller than IndH . For a first guess a value of $10^{-10} \text{ m}^2\text{s}^{-1}$ is used.

4. The rate of reaction for NH_3 going to NH_4^+ is faster than the diffusion rate of these species. This means that the effective diffusion constant of will these species will be the same and their relative concentrations determined by local charge neutrality $\sim 10^{-9} \text{ m}^2\text{s}^{-1}$.

Species	diffusion In membrane $\text{m}^2\text{s}^{-1} \times 10^{-9}$	diffusion In cell $\text{m}^2\text{s}^{-1} \times 10^{-9}$
NH_3	1	1
NH_4^+	0	1
IndH	0	1
Ind^-	0	(a) 1
Ind^-	0	(b) 0.1

Table 5.2: Values of diffusion constant used in the model

5.8.3 Initial Results of Model.

In all the simulations that follow, the sensor modelled consists of a 0.8cm long cell where light is shone through the cell, reflected from the membrane and returns back through the cell to the detector.

Figures 5.8 and 5.9 show a initial simulation results of the response, of otherwise identical sensors, in which one has ammonium chloride buffer while the other has none. In these simulations the diffusion constant for Ind^- and IndH are taken as being the same, corresponding to entry labelled (a) in table 5.2. Experimental results show later that this simulation is somewhat simplified. However, the figures show several important aspects of the response of the sensor.

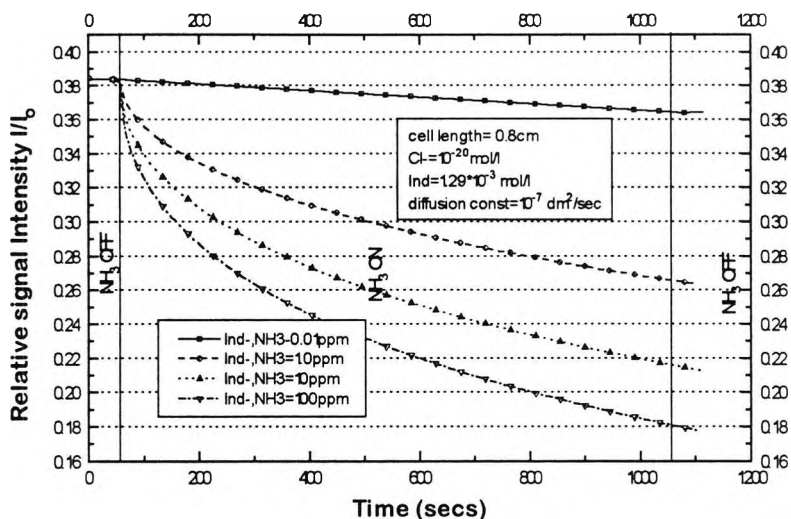


Fig. 5.8: Simulated response of the 'small volume' sensor to ammonia, using unbuffered indicator.

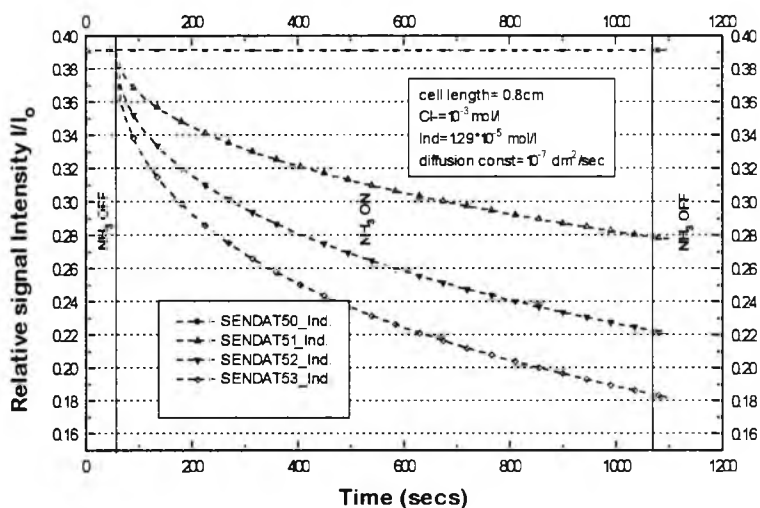


Fig. 5.9: Simulated response of the 'small volume' sensor to Ammonia, using buffered indicator.

Firstly the model indicates a high sensitivity for the sensor to ammonia, as shown in the response of the unbuffered sensor in Fig. 5.8 to 0.01ppm of ammonia. The second observation is the response of the modelled sensor is relatively slow, having not reached equilibrium after more than 1000 seconds. A third observation is that the modelled sensor with ammonium chloride buffer is less sensitive than the unbuffered sensor. It will be shown later that this is borne out in experiment.

When differences in the diffusion of the two indicator species, IndH and Ind⁻ are taken into account by setting the diffusion of Ind⁻ much lower than IndH, as in the entry labelled (b) in table 5.2, the main experimental observations of the sensor, presented and discussed in the next chapter, are simulated more closely.

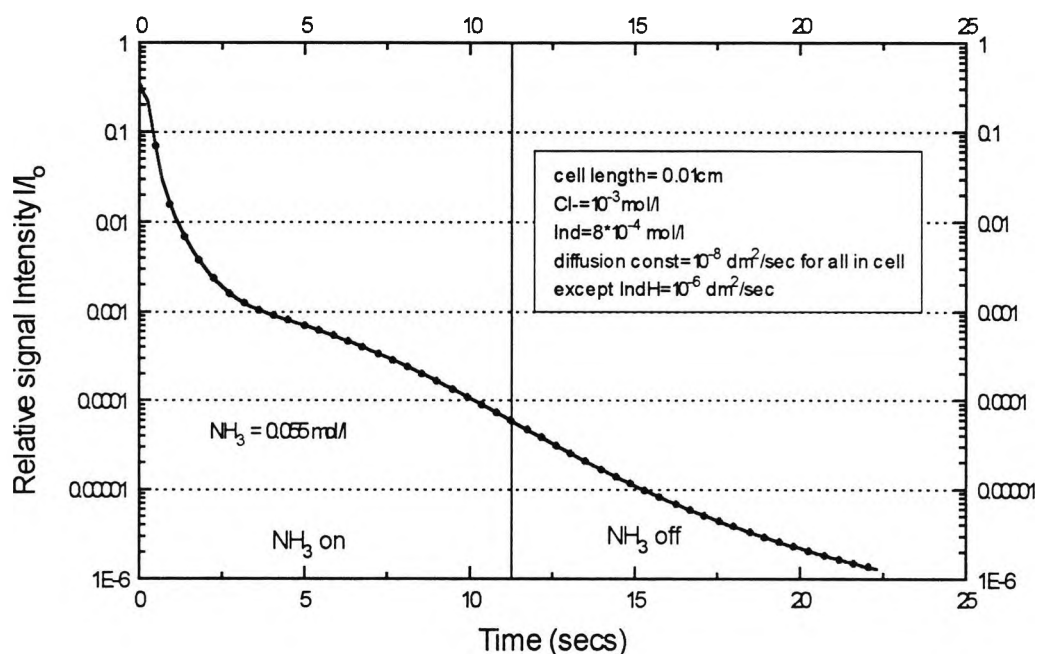


Fig. 5.10: Simulated Response of sensor to step change in ammonia concentration aqueous analyte.

Figure 5.10 shows the response of the modelled sensor with reduced diffusion coefficient for Ind⁻, to a step change in concentration of NH₃ from 0.55 mol l⁻¹ to zero.

There are three main observations in this figure compared to the responses in figure 5.8 and 5.9. Firstly the initial response is quicker, secondly the shape of the response is more complex; and thirdly after removal of the analyte the sensor continues to respond with a strong memory to the removed analyte.

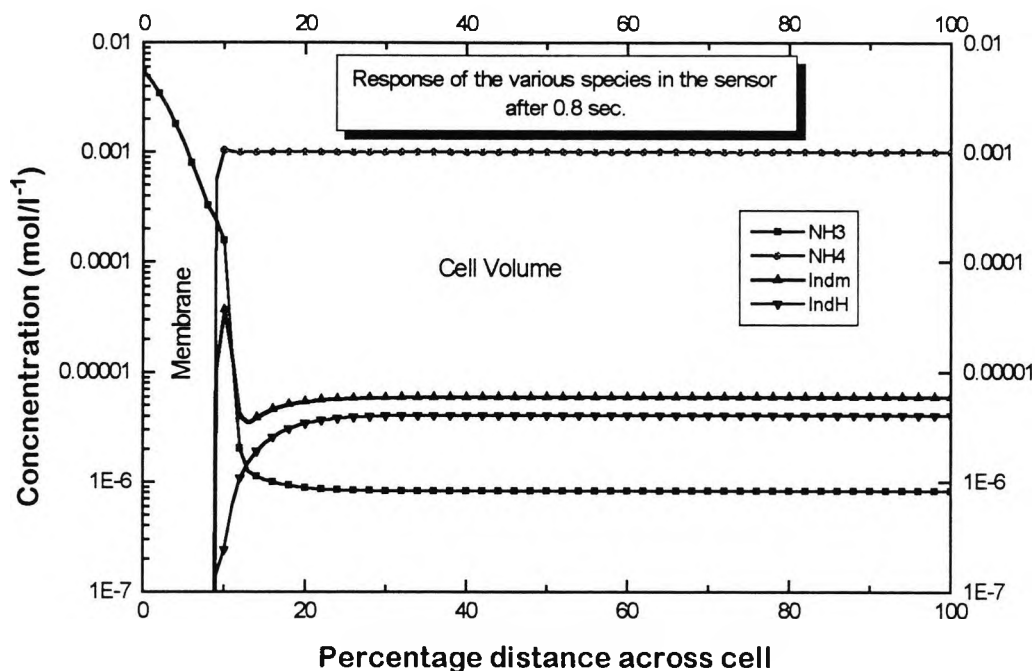


Fig. 5.11 Concentration profiles for the four species after 0.8 seconds of exposure to 0.55 mol/l of ammonia. Other conditions as in fig. 5.10.

The response in Fig. 5.10 is similar to that observed experimentally and is discussed fully in the next chapter. To understand more fully the more complex results in figure 5.10, it is necessary to look into what the model gives about the response of the concentration profile within the cell itself to the ammonia. Fig. 5.11 and Fig. 5.12 show how the concentration profiles for species in the sensor change following exposure to ammonia.

Fig. 5.12 shows the response for NH_3 , NH_4^+ , Ind^- and IndH , after a short time of 0.8 seconds. The most important feature seen in the figure is the accumulation of Ind^- at the membrane-cell interface. This is as observed experimentally, as will be discussed in Chapter 6. In the model this species has a much smaller diffusion constant than its counterpart, IndH , so that once it is formed at the interface, through the transfer of hydrogen to the incoming ammonia, it is much less mobile and moves away from this region at a much reduced rate. The more mobile IndH , on the other hand, finds it easy to move from the cell proper to the interface, therefore there is a build up of indicator at the interface, shown more clearly in Figure 5.12.

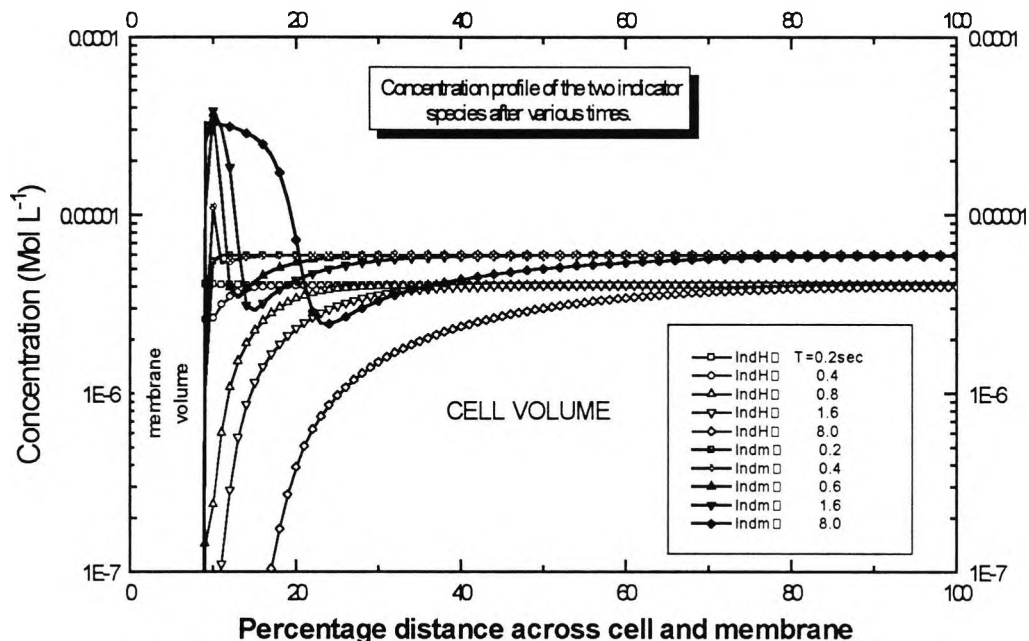


Fig. 5.12: Simulated Response of the Concentration Profile of the two indicator species to prolonged exposure to ammonia. Other conditions as in Fig. 5.11.

5.9 Summary

In this chapter the current position regarding ammonia sensing both in the gas phase and in the aqueous phase has been presented and determined. While significant advances have been made in ammonia sensing in water there are still specific difficulties that limit the range of applicability to electrochemical and optical-fibre colorimetric-based methods. It is also argued that current commercial electrochemical sensors are generally limited in performance and optical fibre methods may offer some improvements. In the final section of the chapter the theoretical basis for an idealised fibre-optic-based sensor design based on gas-selective-membrane barrier and optical measurement of pH has been presented. This theoretical basis serves as a starting point for the development and design of a fibre-based ammonia sensor and as the input to a numerical simulation model with which to evaluate, interpret, and ultimately understand, the actual sensor performance.

In the next chapter, Chapter 6, the development and evaluation of a fibre-based ammonia sensor based on the above theoretical basis will be reported. In the experimental characterisation of the sensor design the performance of an electrochemical sensor will be used as a reference to measure dissolved ammonia concentration. Also, in order to understand the dynamic response of the sensor, the model developed above will be used to simulate the sensor performance.

5.10 References

1. Horton, H.R., Moran, L.A., Ochs, R.S., Rawn, J.D. and Scrimgeour K.G. "Principles of Biochemistry", Neil Publishers, Prentice-Hall, Englewood Cliffs, NJ, (1993).
2. Skoog, D.A., West, D.M., and Holler, F.J. "Fundamentals of Analytical Chemistry", 5th ed, Saunders College Publishing New York, (1988).
3. Crompton, T.R., "Analytical Instrumentation for Water Industry", Butterworth Heineman Ltd., 1st ed., (1991).
4. Toyooki Aoki, Satoshi Uemura, and Makoto Munemori "environ. Sci Technol." 20, pp 515-517, (1986),.
5. Chaney, L.A., and Marbach, E.P., Clin. Chem., 13, p-156 (1960).
6. Horn, D.B., and Squire, C.R., Clin. Chem. Acta., 33, p-592, (1961)
7. Weatherburn, M.W., Anal. Chem., 39, p-971 (1967).
8. J. Assoc. off. Anal. Chem., 56, p-499, (1973).
9. Fleck, A., CRC Crit.Rev. Chem, (Oct. 1974), p-141.
10. Mondzac, A., Ehrlich G.E. and Seegmiller J.E. J. Lab. Clin. Med. 66, p-526, (1965). See also Kaplan, A., In Methods of Biochemical Analysis, Vol. 17, p-311, and the references wherein .
11. Jungers, E., "Spot Test Analysis" John Wiley and Sons, New York, p-36 (1985).
12. Stutts, P. and Fridovich J., Anal. Biochem. 8, p70, (1964).
13. Buck, R.P., in "Ion-Selective Electrodes in Analytical Chemistry" (H. Freiser, ed.) vol. 1, pp-1-141. Plenum, New York, (1978b).
14. Bates, R.G. "pH determination", Wiley, New York. (1975).
15. Vogel's "Quantitative Chemical Analysis" 5th ed., Longman Sci. & Tech. Chapter 15. (1989).
16. Vogels text book of Qantit. Analysis 2nd ed., pp-548., Wiley and Sons Inc. USA. (1984).
17. Nilson, H., Akerlund, A. and Mosbach, K., Biochem. Biophys. Acta., 320, p-529, (1973).
18. Vadgama, P., Kovington, A.K., and Alberti, K.G.M., Anal. Chem. Acta., 136, p-249-256, (1982).

19. Joseph P.J., *Mikrochemica Acta.*, II, p-473-479, (1984).
20. Hansen, E.H. and Ruzicka, J., *Anal. Chem. Acta.*, 353, p-364, (1974).
21. Guilbault, G.G., and Montalvo., J.R., *J. Am. Chem. Soc.* 91, p-2164 (1969).
22. Scholer, R.P. and Simon, W., *Chimia*, 24, p-372, (1970).
23. Guilbault, G.G., and Nagy, G., *Anal. Chem.*, 45, p-417, (1973).
24. Guilbault, G.G., Nagy, G. and Juan, S.S., *Anal. Chem. Acta.*, 67, p-195-201, (1973).
25. Orion Electrode handbook, Model 95-12 (1996).
26. Anfalt, T., Granelli, A., and Jagner, D., *Anal. Lett.*, 6, p-691, (1973) also Guilbault, G.G. and Shu, F.R., *Anal. Chem.*, 44, p-2161, (1972).
27. Papastathopoulos, D.S., and Rechnitz, G.A., *Anal. Chem. Acta.*, 17, p-79, (1975).
28. Hansen, E.H., and Ruzicka J., *Anal. Chem. Acta.*, 72, p-353-364, (1974).
29. Arnold, M.A., and Meyerhoff, M.E., *CRC Crit. Rev., Anal. Chem.*, 20, p-149, (1988).
30. Chin, W.T., and Korontje, W., *Anal. Chem.*, 33, p-1756, (1961).
31. Watson, L.D., et. al., *Biosensors.*, 3, p-101, (1985).
32. Wojltjen, H., et. al., *IEEE, Trans Electron Devices.*, 32, p-1170, (1991).
33. Mtasik, J.J., Hooper, A., and Tofield, B.C., *J. Chem Soc. Faraday Trans.*, A-82, p-1117, (1986).
34. Henrion, L., et. al., *Sensors and Actuators*, 14, p-251, (1988).
35. Lyman, I. "Electronics 60 (1987) 20, p 85.
36. Hikuma, M. et. al., *Anal. Chem.*, 52, p-1020, (1988).
37. Kirstein., D., Kirstein, L. and Scheller, F., *Biosensors*, 1, p-117-130, (1985).
38. Pandey, P.C., and Mishra, A.P., *Analyst*, 113 p-329, (1988).
39. Nylander, C., et.al., in Seiyama, et. al., *Proceedings of the 1st international conference on Chemical Sensors*, Fukuoka, Japan, September 1983, Elsevier, Amsterdam, 1986, p-203.
40. Osakai, T., Kakutani, T. and Senda, M. *Anal. Science*, vol. 3, p-521, (1987).
41. Winqvist, F., and Danielson, B., in Cass., A.E.G., *Biosensors, a practical approach*, IRL, Press, p-173, (1990).
42. W. Gopel, J. Hesse, and J.N. Zemel "Sensors a comprehensive survey", CRC Publisher. vol 3, p-837, (1992).

43. Rechnitz, G.A., Chem. and Eng. News, September (1988), p-24.
44. Luong, J.H.T., Mulchandani, A., and Guilbault, G.G., Tibtech December 1988, vol. 6., 310.
45. Guilbault, G.G., and Luong, J.H. Selective Electrode Review, 1989, vol.11, p-3-16.
46. Arnold, M.A., and Meyerhoff, M.E., CRC Crit. Rev. Anal. Chem., vol.20, p-149 (1988).
47. J.F. Giuliani, and T.W. Barrett, "The effect of ammonia ions on the absorption and fluorescence of an oxazine dye" Spectroscopy Letters 16 (7), pp 555-563 (1983).
48. Peterson, J. I., et.al, "Fibre optic probe for pH measurements" Anal Chem. 52, p-864 (1980).
49. Atkins P.W., 'Physical Chemistry', 5th Edition, Oxford University Press, C26 Table 23.2 and C28 Table 24.7, (1994).

Chapter 6

Design, Construction and Evaluation of a Multi-Wavelength-based Optical Fibre Ammonia Sensor for Water Quality Measurements

Abstract

The design, simulation, construction and evaluation of a novel optical fibre-coupled optrode sensor system for measurement of ammonia concentration is described in this Chapter. The principle of operation of this sensor is based on monitoring the absorption of light at the peak absorption wavelength of the phenol-red cation at 565nm by measuring the transmitted light intensity before and after the dissolved ammonia gas penetrates a gas permeable membrane barrier into the indicator dye buffer solution within the sensor cell.

Optical fibres are used to guide the light from the source to the probe head and back to the detector through the collecting fibre. The system has been evaluated in experiments over a broad operating range using water samples containing ammonia with a known concentration (in the ppm range) prepared in the laboratory and its performance is compared with an existing electrochemical-based ammonia electrode. These sensors are based on similar chemistry and the output of the sensor is compared with the results of a computer simulation.

The essential principle of operation of the optical fibre sensor is similar to that of the existing commercial electrochemical sensor designed for laboratory use and in the first instance the optical sensor is derived from such designs. However, the major innovation is that it is all-optical in operation and represents a step forward in sensor design. Even in the laboratory regime, optical-fibre-coupled sensors can potentially offer such distinct advantages because the measurand containing information will be free from errors arising from electrochemical and electromagnetic interference. A precision of 0.01 ppm NH_3 is achieved with the optical sensor.

The measurement range of this instrument can be varied in measurements made from 0.001 ppm (1 ppb) full scale to greater than 1000 ppm full scale with an appropriate change in ammonia concentration. A stability of $\pm 2\%$ was reached for a testing period of over 48 hours. Final conclusions and recommendations on developments are given at the end of this chapter.

6.1 Data Sampling in the Measurement Process

The measurement of ammonia requires continuous sampling of data to ensure that the species can be detected at a very low concentrations to achieve an accurate result for effective use of the instrument. The optimum period of time between each measurement depends on the nature of the measurement to be made and information to be gathered because each concentration requires a specific time to reach the maximum detecting level of concentration. In some applications it is necessary to measure and update the value of a particular measurand over a short period of time (i.e. 10 to 60 seconds) as an urgent measurement, if required. This is shown in the measurement of the chlorine content in drinking water at a distribution point of a water treatment plant.^[1]

6.1.1 Performance Specification

The Water Research Centre (WRC) has produced a specification for ammonia and chlorine monitors of which the designer should take account, reflecting as it does the needs of UK industry.^[2]

a) The response time of the monitor should not be longer than 20 seconds to achieve 90% of a step change and this should include the reference measurement with which the instrument under test is compared

b) The monitor should be provided with a communication port for monitoring data, control and any signal errors and malfunctions which may occur, for interfacing with a remote control station. It could, in the future, be included as a part of set of monitors for the measurement of different parameters observed by the same station.

c) The monitor should not require attention or supervision, apart from the replacement of components or reagents. The WRC specification in respect of this is for a service interval of at least 30 days.

6.2 Measurement Scheme

The measurement scheme using the wavelength based signal is configured through transmitting two known wavelengths at a very small delay time, e.g. 2 seconds. Then to compare their intensity and to obtain and plot their ratio as the basis of the analytical result. This action can be generated by using a small electronic circuit to control and thus derive the intensity of the emitted light pulses (LEDs) and to collect the receiving light from the reflected mirror surface via a collecting fibre, to the photodetector. This operation takes a few microseconds to measure and monitor this phenomenon which is, in fact, obtaining desirable data. The full description of this small sub-system, which is based on the computer controller, can be found in Chapter 4, (Section 4.1) of this thesis.

6.2.1 Referencing Signal

The reference scheme is provided by an 810nm wavelength infrared LED. This wavelength is not strongly absorbed by the phenol red dye and experiment shows that there is no change in the IR LED intensity during long periods of time if it is run well under the maximum current. The intensity change resulting from the use of a green LED is very sensitive to the external effect of NH_3 on the solution. These effects, caused by ambient light appear as an error in the measurement system and are reflected as a change in the signal output related to the measurand. If no particular precautions are taken to reduce their effect, correcting the final measurement would be a rather difficult task.

6.2.2 Errors in the System

The errors in such a system can be classified as both random and systematic. The random nature of an error can be seen in its uncorrelated aspect with the signal under investigation. Because of this nature, only a full statistical analysis can be used for

complete minimisation of the errors, where the systematic errors are those that can be, to a certain extent, predicted. Such errors are generated in the system because of a specific effect e.g. temperature variations, drift of electronic components etc. Variations in the light source intensity output can be regarded as specific, and compensation can be easily achieved. This is possible by measuring the ratio of the “main” signal to the “reference” signal provided that the variation in the signal is slow compared to the frequency of the measurements. Hence any change in the related measurement, other than that generated by the measurand, may be seen and then compensated.

The adoption of a particular situation for the measurement in this implementation is based on the fact that the phenol red dye does not absorb in the IR and also does not change the background absorption, thus giving the “reference” signal. Additionally the cost of the LED was significantly less when compared with the glass electrode. The type of referencing is preferred because it does not require the use of chemical reagents to alter the absorption in the system. Also, the additional advantage of using this mode of referencing lies in the simplicity of the set-up needed to carry out the measurement of the chemical species of interest, of which ammonia is among the most important.

6.3 The description of the ammonia sensor

The optical fibre ammonia sensor consists of four main systems:

- The optical system
- The electronic system
- The computer controller system
- The chemical analysis unit.

The systems are working as a single instrument and are controlled by a Personal Computer (PC). The electronic system is housed in instrument box to provide electronic screening. The optical system acts as an interface between the electronic

system and the chemical units which are positioned 1.5 m away from the instrument box. The fibres carry the transmitted wavelengths to the solution under test via the sensor head and transmit back the data desired from the chemical unit to the instrument analytical unit. These data are analysed and processed, then displayed graphically.

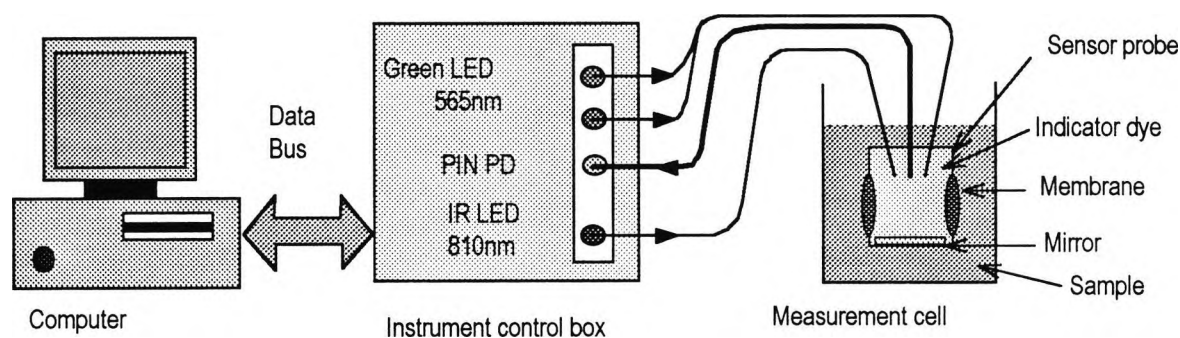


Figure 6.1: Schematic diagram of the experiment set-up

The sensor consists of the following sub-units:

1. A small chamber between the fibres and the mirror surface to fill with the indicator dye and a 0.01M of NH_4Cl as a buffer solution was carefully designed. This chamber is also called an optical cell.
2. A mirror surface was polished to ensure that the maximum transmitted light from the two wavelengths is reflected and received back via the collecting fibre.
3. A two small windows drilled in the both sides of the probe were sealed by the $0.02\mu\text{m}$ thickness ammonia membrane to isolate the internal filling of dye from the outer samples under test. This membrane is exclusively selective to ammonia ions.

The membrane is acting as a communication port between the inner indicator and the outer solution and is selective to only one chemical parameter such as ammonia gas. Experimental results show that only ammonia gas can diffuse through it. The instrument control box which contains the connection and the

electronics is isolated from the liquid unit by 1.5 metre of fibre optic cable.

4. Finally, the whole sensor system is controlled by a Personal Computer (PC).

6.3.1 Optical System

The optical system used consists of 8 single mode transmitting fibres of 600 μ m diameter. Seven of these fibres are coupled to ultra bright green LEDs, with the remaining fibre coupled to an infrared LED to provide the reference signal. The detector was coupled to 1mm diameter plastic fibre which was glued and inserted into the centre of the bundle holder. This fibre was used to guide the optical signal after it had travelled through the sample. All these set of optical fibres are used to guides the radiation to and from the sensor head.

6.3.2 Light Source

The light source was provided by combining the outputs of 5 mm ultra-bright green LEDs. The devices were manufactured from gallium phosphide and gallium arsenide, as visible sources for use where long life and mechanical robustness are required. The intensity of this LED at its peak wavelength of 565nm is 150 mcd, at a current of 20mA. At this wavelength, the experimental results showed that, the peak of the phenol red absorption lies in the same region as the peak of emission of the green LED. The intensity spectrum of the green LED as a function of wavelength is shown in figure 6.2.

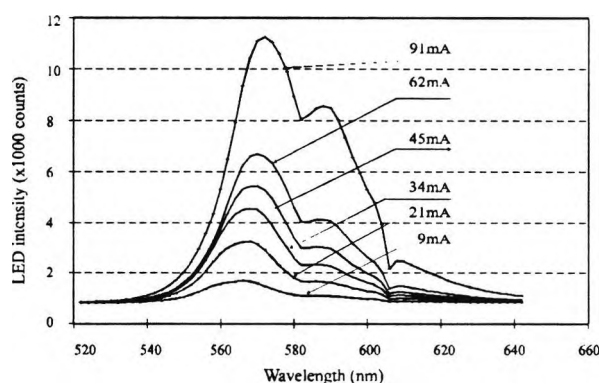


Fig. 6.2: Graph showing the spectrum of the light emitted by a green indicator type LED at various driving current intensities.

6.3.3 Computer Based Controller

The optical fibre ammonia sensor is controlled by a PC, as this can be very useful when handling data from the measurand and plotting the final results. A custom-designed software package written in turbo Pascal was prepared and implemented for this task. This software could be modified at any stage to monitor other chemical species provided the right optical-chemical components are used. The full details of this custom software can be found in Appendix 4. A flow chart of the program is shown in figure 6.3, illustrating the main features.

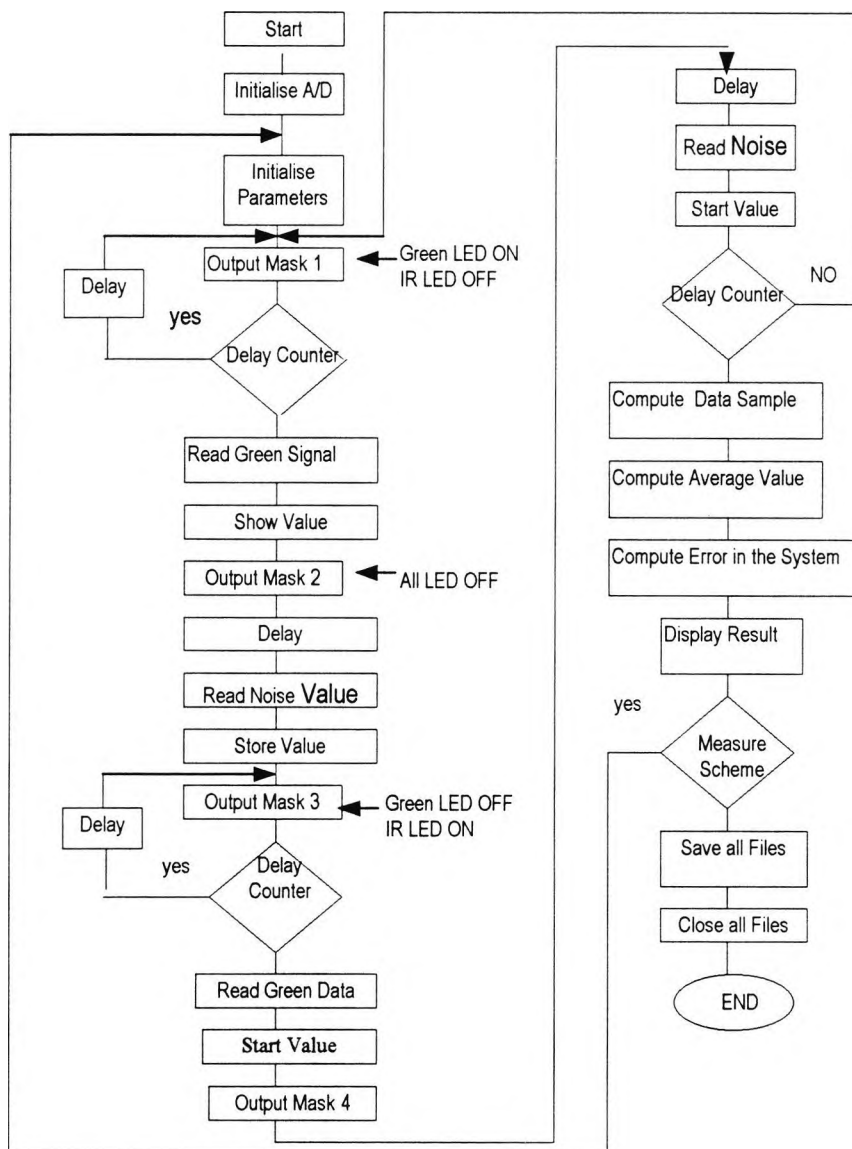


Fig 6.3: Ammonia Sensor software flow chart

6.3.4 Chemical aspects of the optrode

The chemical handling unit is set at 1.5m from the instrument control box. This unit contains the sample under test and, in use, the sensor head is dipped in the sample. The only chemicals sample used are ammonium chloride (NH_4Cl) and sodium hydroxide (NaOH). The NH_4Cl is used to decrease the diffusion time of ammonia in the cell while NaOH is used to maintain the pH of the sample at a pH value greater than 10. Thus the sample which contains ammonium chloride and distilled water will generate ammonia gas. In use, the latter will diffuse through the membrane barrier and react with the indicator dye. The reaction results in a change of the colour of the dye from yellow to red. Under this condition the dye absorbs the light at a wavelength of 565nm, which corresponds to the emission of the green LED.

6.4 Design of the Fibre Optic Probe

Fig. 6.4 shows a schematic diagram of the fibre optic probe used. The fibre holder has nine holes, one of them is positioned at the centre and used to hold the receiving fibre of 1000 μm diameter while the other eight holes around it, at a fixed distance from the centre, are used to hold the transmitting fibre of 600 μm diameter.

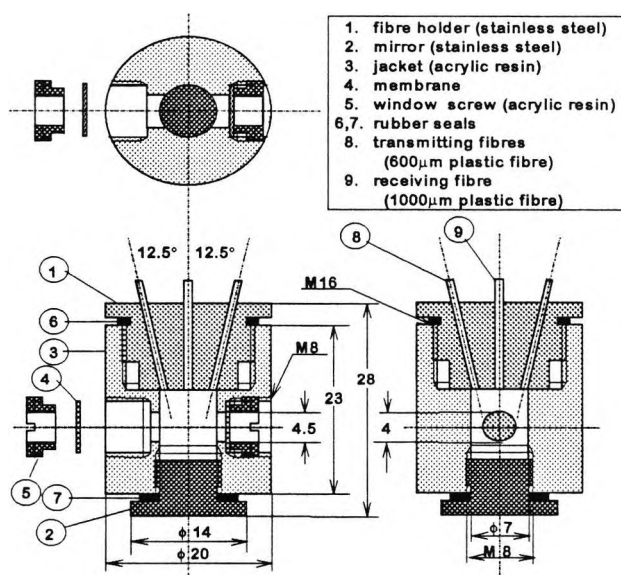


Fig 6.4: Schematic Design of the Fibre Optic Sensor Head

The holes are drilled at an angle of 12.5° with respect to the hole holding the 1mm fibre. The value of this angle is obtained from maximising the amount of light collected by the 1mm diameter fibre. The light emitted from the transmitting fibres is reflected at the surface of the mirror, and collected by the receiving fibre through the indicator solution inside the jacket. The chamber of the jacket was filled with distilled water and the indicator dye (phenol red), in a ratio of 5ml to 1ml. Responding to the change of the concentration of the ammonia in the chamber, the colour of the liquid in the chamber changes accordingly. This change of the colour was measured by using the ratio of the amount of light of wavelength 565nm to that of wavelength 810nm for each state of the measurement e.g. before and after the sample colour has changed.

6.4.1 Sensor Response Function

The following response function has been derived to describe the steady-state response characteristics of the fibre optic ammonia gas sensor.^[3]

$$A = \epsilon b [In] (K_a)_{In} [NH_3] / (K_a)_{amm} C_{amm} - (K_a)_{amm} [NH_3] + (K_a)_{In} [NH_3] \quad \text{equ. (6.1)}$$

Where: A is the measurand absorbance,

ϵ is the molar absorptivity of non-protonated form of the indicator,

b is the effective optical path length of the sensor,

$[In]$ is the concentration of the indicator in the indicator solution,

$(K_a)_{In}$ and $(K_a)_{amm}$ are the acid dissociation constants for the indicator and ammonia respectively,

C_{amm} is the total ammonium ion concentration in the indicator solution and

NH_3 : is the sample ammonia concentration,

This response function is appropriate to an ammonia measurement when a single indicator is employed, and the nonprotonated form of this indicator is monitored colorimetrically

6.4.2 Path Length

The effective optical path length is governed by the geometry of the sensor body. This path length can be approximated to be twice the distance from the ends of the optical fibres to the polished mirror surface. Incident radiation exits the transmitted fibres, travels through the indicator solution, scatters to the membrane, travels again through the indicator solution, and enters the collecting fibre. This constituted the optical path length which relates to the sensitivity of the device response. Longer path lengths correspond to greater sensitivities, but a corresponding weaker optical signal. Additionally, the dye and ammonia ion do not form a homogeneous mixture since there is no mixing effect taking place inside the cell, and hence the dynamic response of the instrument is affected by the volume of the cell i.e. the length of the cell. However, a compromise is required between the path length and the dynamic response of the instrument. It was found that a reasonable response time (1~10 seconds) was obtained for a path length between 2 to 4.5 mm from the fibre end to the polished mirror surface.

6.4.3 The Acid Dissociation

The acid dissociation constant of the analyte is not a parameter that can easily be varied. The concentration of the protonated form of the analyte in the indicator solution, however, must be considered, for analysis reasons, to balance both the acid and alkaline form of the indicator dye and the ammonia gas. The response function in equation (6.1) has been derived on the assumption that the ammonium concentration in the indicator solution remains constant at all ammonia concentrations. The latter condition is maintained, in practice, by adding a high concentration of ammonium chloride to the indicator solution (in the range of 0.1 M).

The most important parameter to consider when designing a fibre optic ammonia sensor for a particular application is the acid dissociation constant of the indicator. Figure 6.5 shows a family of simulated response curves for a range of acid dissociation constants. The indicator dye must be in the form of acid before the sensor head is dipped into the sample under test so as to give the ammonia ion the

opportunity to start to diffuse into the sensor cell via the membrane. The ammonia concentration range used, for these simulated curves, is that corresponding to the anticipated values of interest in wastewater samples.

Low pK_a values result in an initial sharp rise in absorbance with a subsequent levelling off. High pK_a values, on the other hand, produce curves over the full concentration range. The magnitude of the overall absorbance change is much greater with lower pK_a values, whereas intermediate acid dissociation constants gradually go from one extreme to the other.

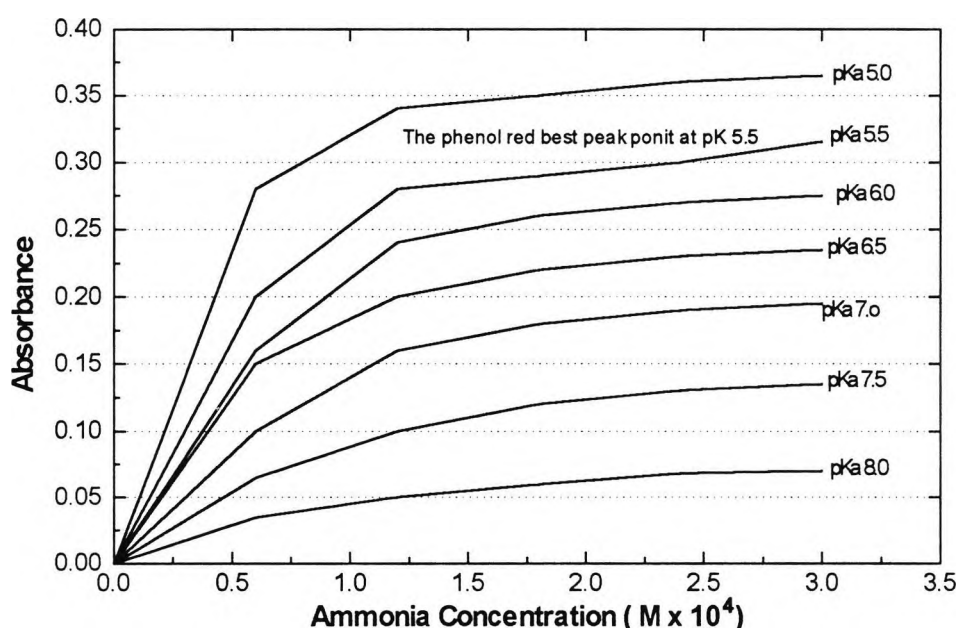


Fig. 6.5 : Effect of Indicator pK_a on the simulation response

6.4.4 Molar Absorptivity of the Indicator

The molar absorptivity and the concentration of the indicator must be considered. For a given indicator acid dissociation constant, the indicator with the largest molar absorptivity provides the greatest sensitivity, because the molar absorptivity is a non-protonated form of the indicator dye. As will be discussed in detail below, a compromise is required with respect to the indicator concentration, and although a high indicator concentration gives a large response, it also requires a longer time to

establish the steady-state condition^[4].

6.4.5 Temperature Effect

Two other parameters that strongly affect the sensor response, but which are not identified in equation (6.1), are temperature and osmolarity. An increase in temperature over 25°C decreases the acid dissociation constant of the indicators and increases the ammonium ion dissociation constant. These changes result in a smaller sensor response.

On the other hand, higher temperatures facilitate diffusion processes which result in a faster sensor response time. A temperature of 30 °C results in responses with reasonable steady-state and dynamic response properties. However, all the measurements in this study were carried out at room temperature (around 20 °C) and at this temperature there was no effect on sensor response to the ammonia measurement. For this the temperature of the dye/sample was monitored throughout the experiment.

6.5 Mathematical Model Simulation

In order to design the fibre optic probe with quick response time and high sensitivity, the use of the ratio of the measured volume inside the probe to the area of the membrane and the relative position of the transmitting fibres to the receiving fibre using were considered, the model of the fibre optic probe, as shown in Fig. 6.6.

The ratio of the measured volume to the area of the membrane strongly influences the dynamic characteristics of the ammonia sensor. As a result of the fact that the change of the concentration of ammonia inside the chamber is caused by the diffusion of the ammonia ion present in the sample through the ion-selective membrane, the surface area of the membrane does affect the rate of diffusion.

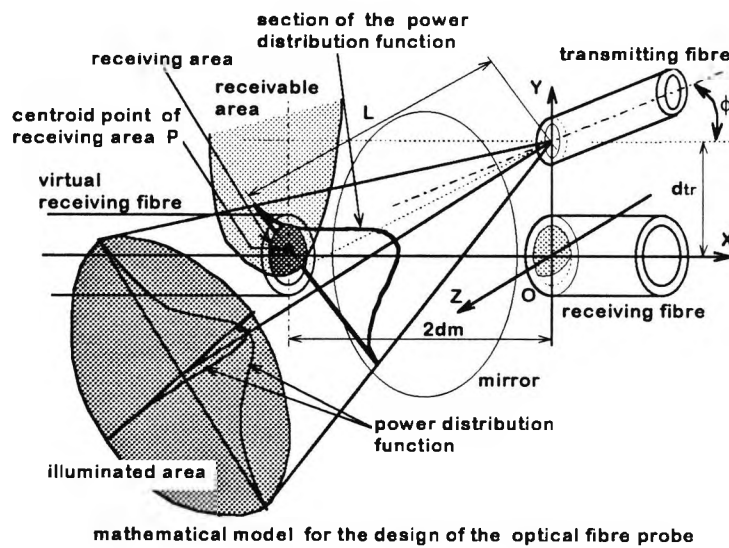


Fig. 6.6 : Mathematical simulation module for the design of optical fibre probe.

Under the condition that the concentration of ammonia and the temperature of liquid are constant, it can be said that the dynamic characteristics of this kind of chemical sensor depend on the ratio (Area of membrane)/(Measured volume). Therefore, the response of the sensor becomes faster, as the above ratio is made large. In order to increase the above ratio, it is necessary to keep the area of membrane large, and to make the diameter of the chamber and the distance between the end of fibres and the mirror small. The diameter of the chamber can be determined by the diameter of fibres used and the distance between the transmitting fibres and the receiving fibre. At the first stage of the design, it was decided that the distance, d_{tr} , between the transmitting fibres and the receiving fibre should be 3mm because of the ease of the manufacture, and as a result of the above dimension the diameter of the chamber was 7mm.

At the second stage of the design, ϕ is the angle between the receiving fibre and the transmitting fibres. This angle, ϕ , decides the illuminated area in the chamber, and it is expected that a larger angle relates to increases in the illuminated area, and that the received power will be increased. Furthermore this angle influences the reflecting condition at the ends of the transmitting fibres, and the angle of the axis of the cone which shows the illuminated area becomes larger than the angle, ϕ . This effect is an advantage for the design of the probe, and the distance between the fibre and the mirror could then be made shorter. The received power, at the receiving fibre in the

proposed probe could be calculated using the above mathematical model.

6.5.1 Model Assumption

In this model, the following points were assumed:

- a) The receiving area on the end of the virtual receiving fibre is essentially determined by the N.A. (numerical aperture) of the receiving fibre and the distance between the virtual receiving fibre and the transmitting fibre, regardless of the portion of the transmitting fibre.
- b) The power distribution is approximated by the two dimensional Gaussian function which has an elliptical base.
- c) The major and minor axes of the elliptical base vary in proportion to the distance , L , between the transmitting fibre and the intersection of the axis of the illuminated cone and the perpendicular from the centroid of the receiving area on the end of the virtual receiving fibre on it.
- d) The proportional constant of the major axis is larger than that of the minor axis because of the reflecting condition at the end of the transmitting fibre.
- e) The power reduction caused by the absorption would be very small.

6.5.2 Simulation Results

The results of the simulation are shown in figure. 6.7. From these results, it has become clear that the received power was maximum at an angle $\phi=12.5$ degrees. In the case of a smaller angle than 12.5 degree, the received power was less, because the centre area of the power distribution was not received by the receiving fibre.

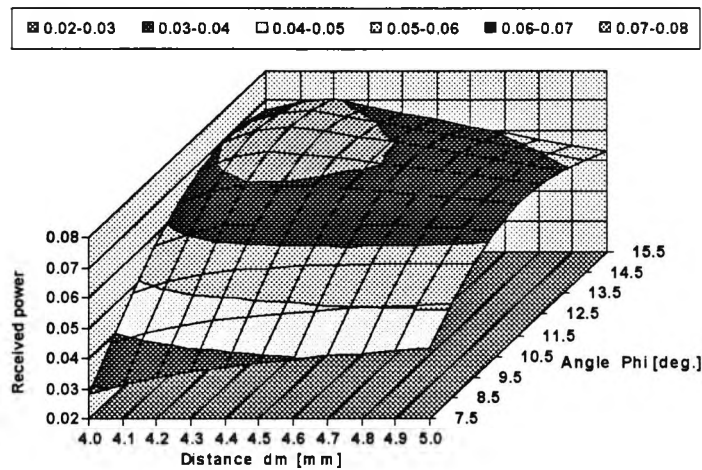


Fig. 6.7: Received power by the receiving fibre in proposed probe

On the other hand, in the case of a larger angle than 12.5 degrees, the received power became less, because the distance from the transmitting fibre to the receiving fibre became longer, although the centre area of the power distribution was received. In addition to above discussion, a much large angle could cause difficulty in the manufacturing, and therefore the angle, $\phi = 12.5$ degrees was determined as the most suitable for use. Under this condition, it became clear that the angle of the axis of the illuminated cone was 14 degrees, from the results of the simulation. At the final stage of the design, the distance, d_m , between the fibre and the mirror was considered. The change of the received power is shown in figure. 6.8, in terms of the increase of the distance between the mirror and the receiving fibre.

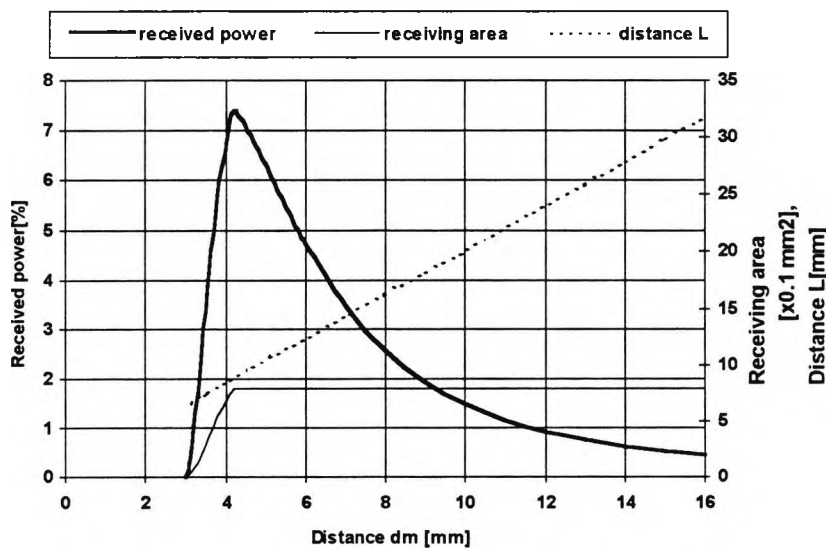


Fig. 6.8: Simulation results of the received power

From the simulated results, it became clear that the distance, d_m , between the transmitting fibre and the mirror strongly influenced the received power, and that the condition $d_m = 4.3$ mm would offer the maximum received power. However, the region around $d_m = 4.3$ mm is very critical and therefore the received power would be greatly changed by any small change of the reflective index of the liquid. At a shorter distance than 4.3 mm, an increase of the receiving area caused increase of the received power, and the receiving area was approximately equal to the area of the receiving fibre at a distance, $d_m = 4.3$ mm.

On the other hand, the distance, L , from the transmitting fibre to the receiving fibre was continuously increased in terms of the increase of the distance, d_m . The increase of the distance, L , reduced the received power, even if the received area was not so different from that seen previously. In the manufacturing of a probe, the angle, ϕ , was changed from 12.5 degree to 6 degree, because the larger angle caused a problem in the fabrication process. Therefore, the received power under the condition that the angle, $\phi = 6$ degrees is shown in Figure 6.9. The distance, d_m , is optimised at 3.2 mm from these results.

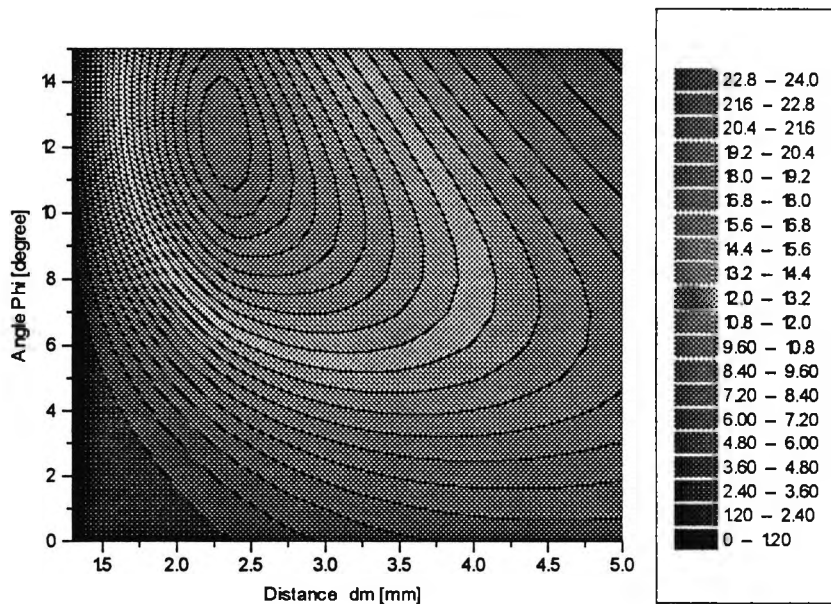


Fig. 6-9 : Contour map of received power

6.6 Manufacturing The Sensor Head

The sensor head was manufactured from clear acrylic resin plastic tube and drilled and fitted with two membrane windows. The advantage of such material is the ability to monitor ammonia diffusion through the membrane with the naked eyes. The whole sensor probe can be disassembled in a few minutes for cleaning or refilling of a new indicator dye without the need for expert intervention.

An adjustable mirror is fixed at a maximum signal peak distance from the transmitting and collecting fibres. This mirror was made from stainless steel, which does not react with indicator dye or the internal buffer solution. The mirror was polished and placed at a distance where the maximum reflected signal can be achieved. In order to keep the probe head free of bubbles, the windows were threaded and the cell filled with the dye and then the window was screwed in. (The sensor geometry used can be found in Appendix 1). The advantage of this design is that potentially it can be used in both laboratory and field measurements. However, in the production of the sensor head there was a small change in the dimensions due to the manufacturing tolerances. This change does not effect the sensor response or performance but only was included to make it easier to produce.

6.7 Experimental Procedure

A set of ammonia samples at different concentrations was carefully prepared and maintained at a room temperature. Also a second set of water samples from different parts of the country was collected and tested using the optical ammonia sensor. During the measurement each sample was placed in a small glass cup, then the probe was dipped into the sample. The sample and the probe are both covered by a plastic film to protect them from the ambient species e.g. CO₂. The sample was then placed over magnetic stirrer to make sure that the ammonium ion and the water are mixed properly.

6.7.1 Sample Preparation

This preparation consisted of repeated dilution of 0.594 grams of NH₄Cl in 200ml of

distilled water corresponding to 1000ppm of NH_3 down to 0.01 ppm. Measurements of weight were done using a (Electronic Balance WA310) microbalance accurate to $\pm 0.5\mu\text{g}$. Measurement of volume were done using a analytical measurement cylinder calibrated in steps of 10ml to 200 ml, with an accuracy of 1% of full volume. Samples were diluted down using a 5ml volume Watman automatic pipette accurate to 2% of full volume. The dilution scheme is a shown in table 6.1. Error resulting from this procedure are considered minimal. This is because any errors introduced in volume measurement are minimised by later dilution. For example, the introduction of a 10% error in concentration at the beginning of the repeated dilution scheme will only result in a 10% error in the error of the 0.01ppm reading. Such an error is well within the tolerances of the experiment, considering the dynamic range of the concentration. Using the equipment discussed above, an error in dilution of less than 3% is achieved. The calculation of the concentration of ammonia in the sample was carried out by using the following procedure:

1 gram per litre = 1000 ppm for water

1000 ppm NH_4Cl = 1g NH_4Cl in 1 litre.

1g per litre NH_4^+ (molecular wight of NH_4^+ = 18.04)

Using NH_4Cl

1g x Molecular weight. (NH_4Cl) / m.w. of water.

= 1g x 53.49/18.04 =2.97g

therefore 2.97g/5 = 0.594g1000ppm NH_3

From this calculation a set ammonia samples was prepared as follows:

200ml of distilled water add to 0. 594g of NH_4Cl \Rightarrow 1000ppm of NH_3 sample (1)
20ml of sample (1) added to 180 ml of distilled water \Rightarrow 100ppm of NH_3 (2)
20ml of sample (2) added to 180 ml of distilled water \Rightarrow 10ppm of NH_3 (3)
20ml of sample (3) added to 180 ml of distilled water \Rightarrow 1ppm of NH_3 (4)
20ml of sample (4) added to 180 ml of distilled water \Rightarrow 0.1ppm of NH_3 (5)
20ml of sample (5) added to 180 ml of distilled water \Rightarrow 0.01ppm of NH_3 (6)

Table 6.1: The set of Ammonia samples

A large number of water samples with different ammonia concentrations was tested, using an optical fibre probe. The aim of this part of the work was to detect the lowest concentration of ammonia in the water samples. The lowest measurement achieved is 0.001ppm NH_3 . For each of the calibration experiments, a fresh sample of water containing ammonia was made available, shortly before the start of each experiment, from an ammonium salt (Fisher chemical) at concentration of 100% measured as NH_3 . A 1000ppm ammonia concentration was prepared as the highest concentration used in the work. The method used in this process was as follows.

6.7.1.1 pH Adjuster

In the electrochemical probe, a blue dye containing sodium hydroxide was used to raise the pH and allow diffusion to take place into the cell via the membrane. However, the same principal was used in this investigation to raise the pH level to a pH value greater than 10 to achieve ammonia diffusion through the membrane. This increase in the pH value was gained by using laboratory grade sodium hydroxide (which is very cheap compared to the blue dye supplied by Orion with their ammonia electrode).^[5]

The use of sodium hydroxide to increase the pH value is however, a disadvantage because the chemical principle used in the measurement is tied to the presence of sodium hydroxide in the sample. The other investigation carried out was to model the optical fibre ammonia sensor by using two electrodes. One electrode should be dipped in the sample and the other one placed next to the membrane. However, very good results were obtained and the pH level was successfully brought up to a pH value of 14 without adding sodium hydroxide to the sample^[6].

6.7.1.2 The Internal Filling Solution

The internal filling solution was carefully investigated in the experiment. It was found that the sulphonphthalein (phenol red) is the most suitable indicator dye for this work. The chemistry, related to the study of this dye, was illustrated in Chapter 3. As the phenol red indicator was supplied commercially it was usually at a very high concentration. However, in this experiment, the phenol red concentration was diluted

by adding distilled water. The ratio of this mixture is 40 : 1. This dilution was found to be very suitable for fast response and the colour of the indicator became very bright yellow in the acid region. Further, it makes the monitoring of the ammonia diffusion very easy and fast.

6.8 The Electronic System

The electronic system used in this work incorporates custom-build circuitry that contains analogue and digital electronics. A full explanation of the electronic design was illustrated in Chapter 4, for the pH optical fibre sensor. However, a small modification was made in the case of ammonia sensor, with the use of an analogue to digital conversion (A/D) card supplied by Keithley Electronic.^[6]

6.9 Sensor calibration

The sensor calibration was carried out using the same procedure as the pH calibration in Chapter 3. This initial calibration is necessary before the first measurement with the sensor, to make sure that all the measurements are carried out simultaneously time as the pH calibration. This calibration is also compared with that using a conventional pH electrode. The procedure of the calibration method was carried out by placing the optical head and the pH electrode in 250 ml of distilled water at the same time. A 0.5 ml sample of phenol red was added to the water, and the sample placed over a magnetic stirrer to ensure that it mixes sufficiently.

The calibration process was begin using alkaline solution sodium hydroxide (NaOH) to increase the pH of the water to a value of pH 10. The reverse part of the calibration curve was obtained by using very dilute quantity hydrochloric acid (HCl) to reduce the pH to the initial pH value. However, the calibration result obtained is seem to be accurate, when compared to that from the conventional pH electrode result. The most sensitive area is from pH 6.5 to pH 8.5, as shown in fig 6.10.

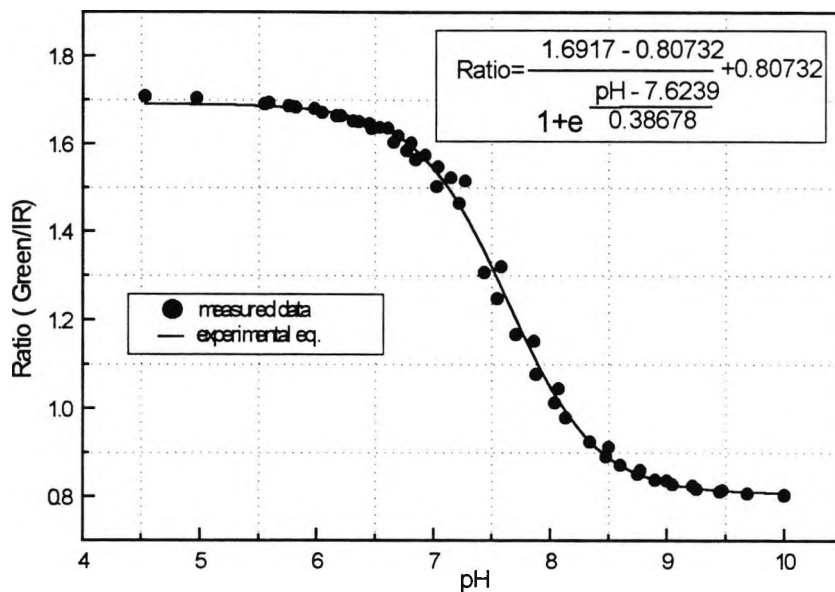


Figure 6.10: Ammonia sensor calibration to pH as an early procedure to ammonia measurements

The calibration is not a routine procedure but it is only required once, in the early stage of sensor use. One of the many advantages of the optical sensor approach, unlike that of the conventional electrode, is that it does not require storage in a solution, but it can be stored in a dry state at a maximum of 3 months without affecting the membrane life. Storage in 0.1M of ammonia solution can ensure the life of the membrane remains constant ^[8]. The sensor can be disassembled and a new filling solution added in a few minutes without need of new calibration, as long as the indicator dye is in the same concentration of 40:1.

The error in the measurement from the system was estimated to be approximately 3.5% and this mainly resulted from the noise in the detection system. However, the data were analysed using the computer program discussed previously and a number of invalid data were eliminated, which resulted in a reduction of the overall error in the system. In comparing the experimental results with those of the simulation, a similar type of response, to that shown in Figure 6.11 resulted.

6.10 Experimental Assessment and Optimisation of Sensor Design

In this section the performance of the sensor head design, as part of the overall system, is assessed. This is done with the aid of a simultaneous measurements of the ammonia concentration with the optical probe and a commercial electrochemical sensor. In the assessment, the response time of the sensor head found to be comparable to the response of the electrochemical sensor, but however more complex than was originally envisaged.

The main reason for the complex response was found to be due to the poor mixing of the ammonia and the indicator in the cell, as indicated by the formation of two coloured regions with a distinct boundary between them. The computer simulation model, outlined in Chapter 5, shows how this can be explained by the lower diffusion coefficient of the Ind^- species compared to the InH species. This results in a build up of a Ind^- rich layer at the membrane wall, through which the ammonia must diffuse to reach the InH .

With the resulting understanding of the dynamics underlying the sensor behaviour, the design of the sensor is changed from that initially considered to address the problem. The most important modification was to reduce the cell volume and hence the response time. This was accomplished in a new sensor head cell in which the specular mirror was replaced by a gas permeable membrane. An assessment of the optimised sensor was made and discussed below.

6.10.1 Assessment of the original designed sensor

In a preliminary assessment of the sensor designed and discussed in Section 6.4, its dynamic response to increasing concentrations, up to 1000ppm, was considered. In the assessment, the performance of the optical sensor was compared to that of a commercially available electrochemical sensor. In the experiments carried out, the procedures recommended by the manufacturers for the use of the electrochemical sensor were adapted, as described in Section 6.7, for use also with the optical sensor.

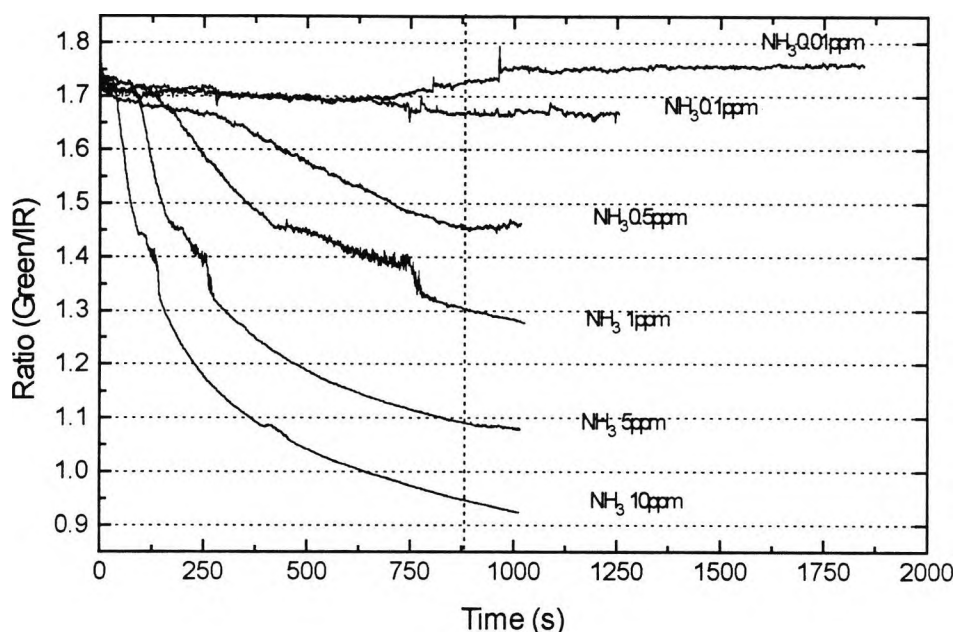


Figure 6.11: Original Fibre Optic Ammonia Sensor Response (Design: Ratio of Green to IR light signal intensities with increasing concentrations of ammonia).

The resulting response of both the optical and the electrochemical sensors to increasing concentrations of ammonia are shown in figure 6.11 and figures 6.12 respectively. These responses are then compared where their calibration graphs are given in figure 6.13 and figure 6.14. These show a similar linear response, between the signal and the log of the ammonia concentration, taken after a 750 second exposure to ammonia.

The calibration of the optical sensor is shown in figure 6.13. The figure shows that the sensor has excellent sensitivity to ammonia, where a lower limit of 0.01ppm of ammonia can be easily discerned. However, the figure also shows several limitations which require further investigation to optimize the system. These include the non-linear response of the sensor at high concentrations, and a large “dead-time” before the sensor responds in a usable way and shows a diffusion limited response.

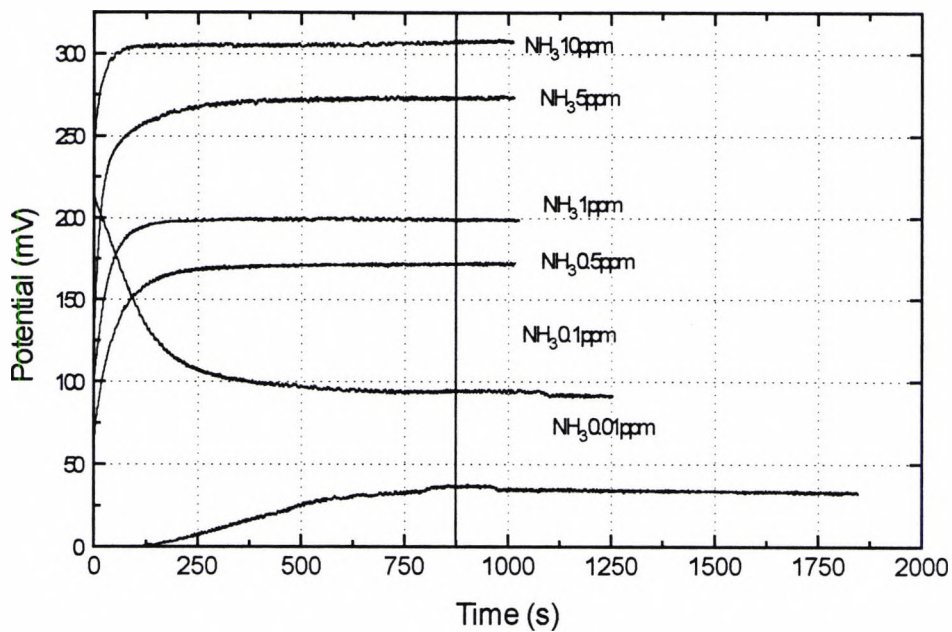


Figure 6.12: Original Sensor Design: Response of the electrochemical potential of commercial ammonia sensor with increasing concentrations of ammonia

However the response of the electrochemical sensor in figure 6.14 shows that this delayed response is also found, as a consequence of using a membrane barrier. The graph of optical signal ratio versus ammonia concentration shown in figure 6.13 and that of the electrochemical potential versus ammonia concentration shown in figure 6.14 illustrate that the optical sensor gives a similar linear response to ammonia when used under the conditions specified for the electrochemical sensor. This confirms the suitability of the optical sensor as a replacement for the electrochemical sensor, possibly in application areas that preclude the use of an electronically based system i.e. where there are strong electrical fields or electric currents in the regions where the sensor is used.

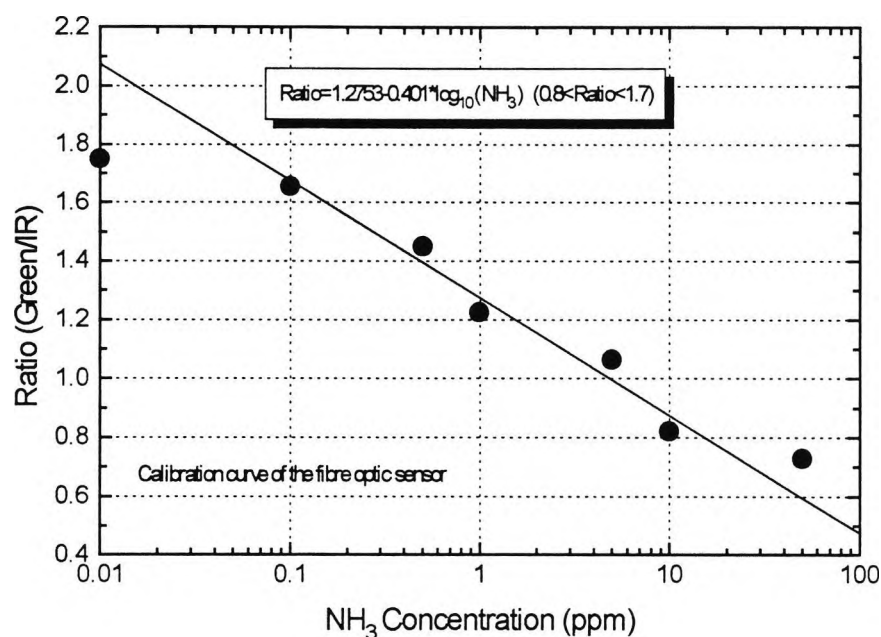


Figure 6.13: Calibration of the fibre optic ammonia sensor

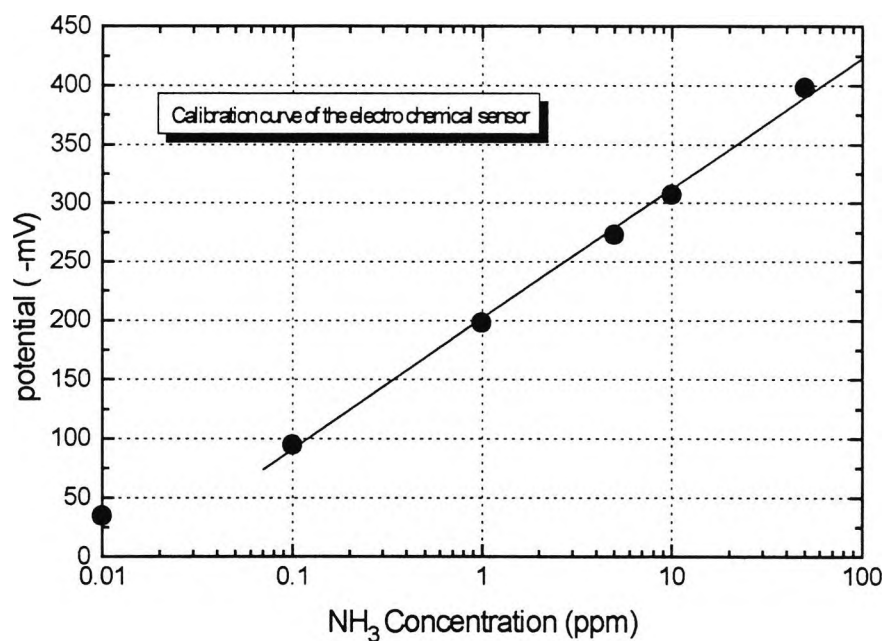


Figure 6.14: Calibration of the electrochemical ammonia sensor

A linear relationship between the electrochemical potential and log (concentration) after the sensor signal approaches equilibrium at 750 seconds is seen for different ammonia concentrations. The above comparison of the optical and electrochemical

sensors shows that the optical sensor is capable of measuring the ammonia concentration over a wide dynamic range and has a comparable response to the widely used membrane-based electrochemical sensor.

6.11 Assessment of the modified sensor design

The relatively complex and slow dynamic response of the sensor shown in figures 6.11 is addressed in a modified sensor design. In order to solve these problems, the most important modifications made were to reduce the cell volume and increase the membrane area, and hence improve the response time. This design also has the advantage of cylindrical symmetry around both the optical axis and that of the chemical membrane, as shown in figure 6.15.

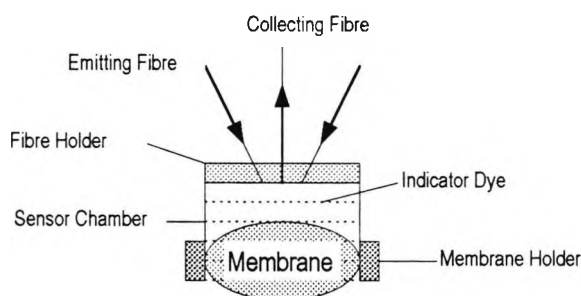


Fig. 6.15: The new sensor head after several modifications

The design offers several advantages over the original design. These include the potential for simplified one-dimensional modelling of the sensor performance, simpler construction and a smaller sensor, volume. With the new sensor the research work could then progress more easily on two fronts-mathematical modelling of the sensor behaviour, as developed and discussed in Chapter 5, and the construction and assessment of a simplified sensor, as depicted above. This sensor is physically very similar to the commercial electrochemical sensor used in the study, being geometrically closely matched to that design.

6.12 Validation of the new sensor head

A validation of the probe performance was obtained using the fibre optic sensor at a concentration of 100 ppm of NH_3 . Following that, the concentration was reduced in various steps down to a concentration of 0.001ppm NH_3 . The set of results obtained was used to assess the minimum detectable concentration of ammonia using this optical technique and the experimental work started without the addition of a buffer solution to the indicator dye in the sensor cell. The response of this sensor is shown in fig 6.16.

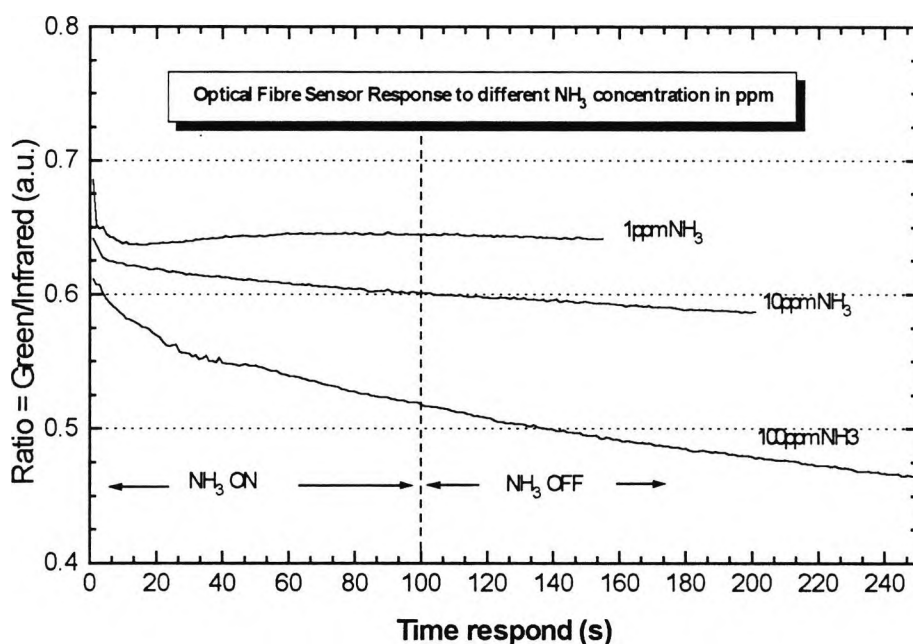


Figure 6.16: Optical fibre sensor response to ammonia concentration (without buffer)

Further work was carried out with this new design to investigate its characteristics further. The sensor volume was filled with a buffered solution containing ammonium chloride buffer and 0.02% phenol red solution, whose pH value was set at a value of 4.5. Three samples of ammonia at various concentration levels in the range from 1ppm to 100ppm have been used to assess the response time of the sensor, which is shown in Figure 6.16. For the 100ppm sample, the measurement was carried out at two pH values, namely 4.5 and 6.8. These two graphs were shown to overlap after 200 seconds.

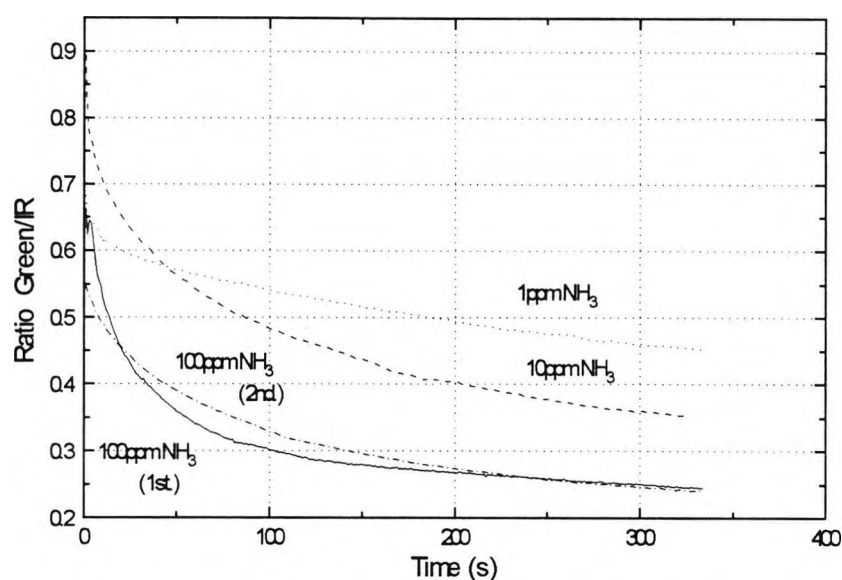
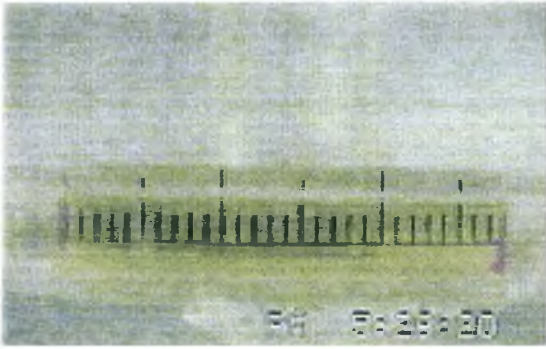


Figure 6.17: Fibre optic sensor response to ammonia (using buffer)

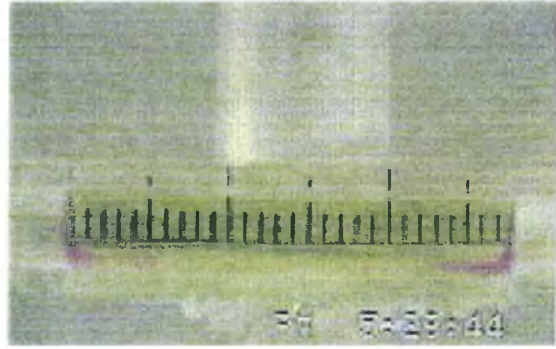
The sensor response thus obtained is faster than that of the original design, shown in figure 6.11. The response is still somewhat slower than that of the electrochemical sensor by around 2%. This difference is attributed to the reduced diffusion due to the segregation of the optical dye inside the sensor cell. The source data for figure 6.17 are given in Appendix 3.

6.13 Separation of the optical dye

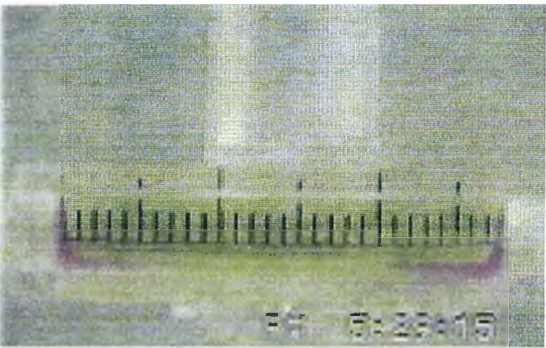
This separation of the optical dye in the membrane cell was investigated further in an experiment using a calibrated measurement tube of length 5.4cm and 1.0cm diameter, sealed with a membrane at each side and placed in an ammonia sample, of 50ppm. Figure 6.18 (a-t) shows the temporal response over a period of 40min, illustrating clearly the exclusion of the dye into separate coloured regions which control the response of the cell.



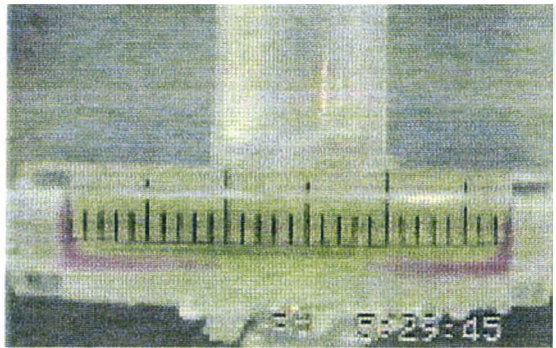
(a) 0 min



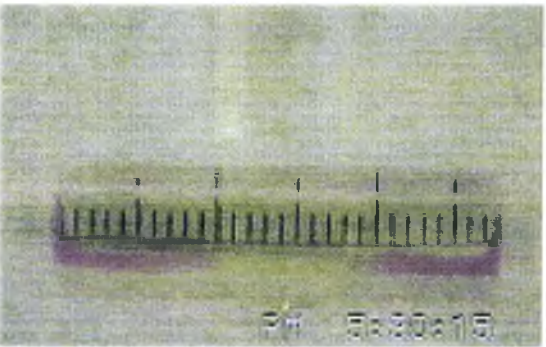
(b) 0.5 min



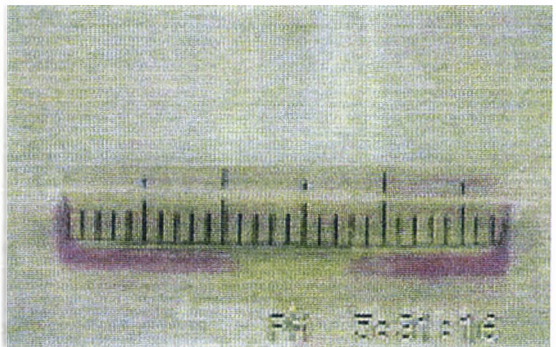
(c) 1 min



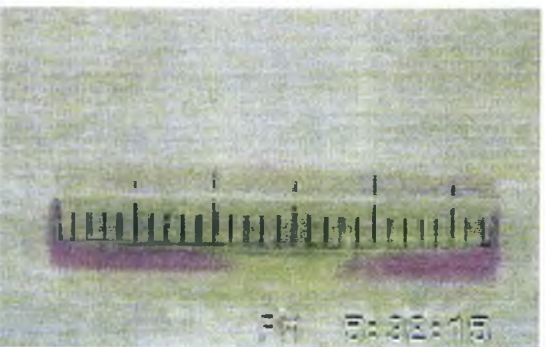
(d) 1.5 min



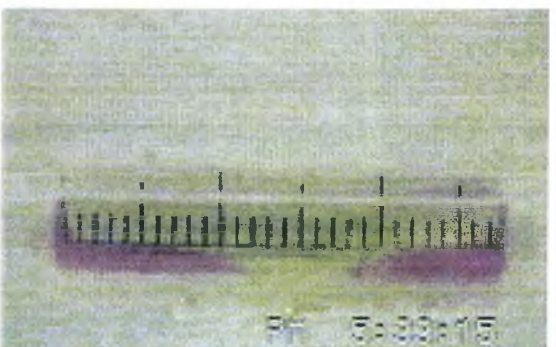
(e) 2 min



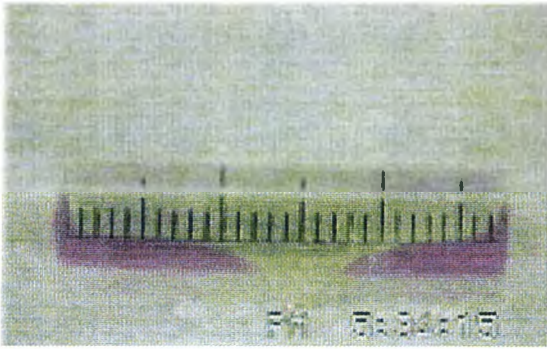
(f) 3 min



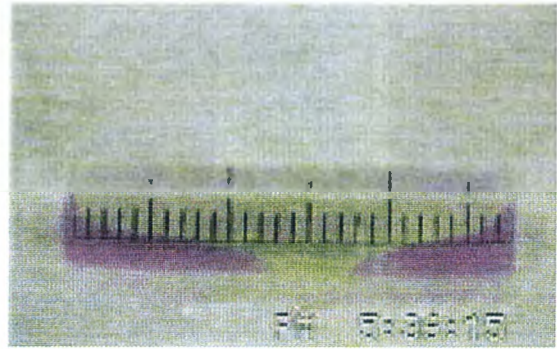
(g) 4 min



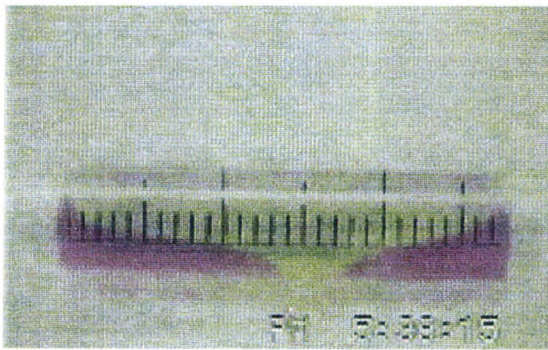
(h) 5 min



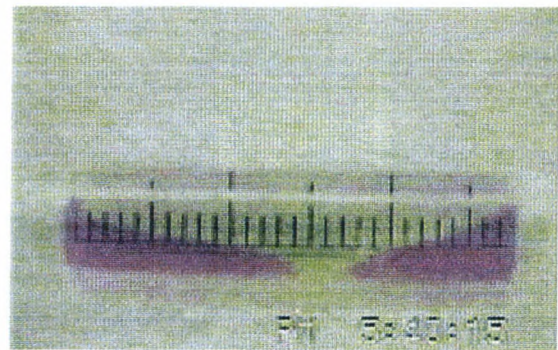
(i) 6 min



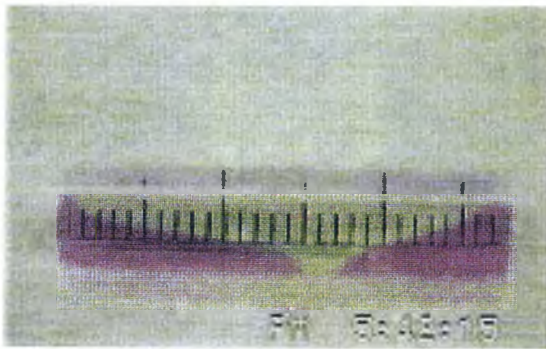
(j) 8 min



(k) 10 min



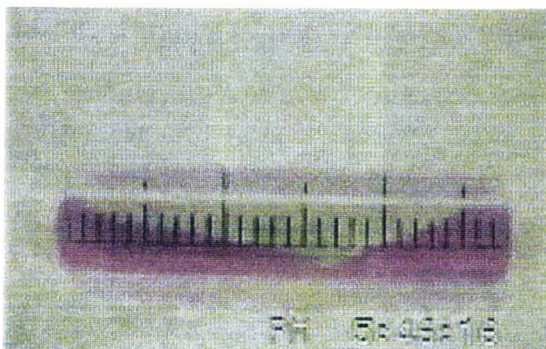
(l) 12 min



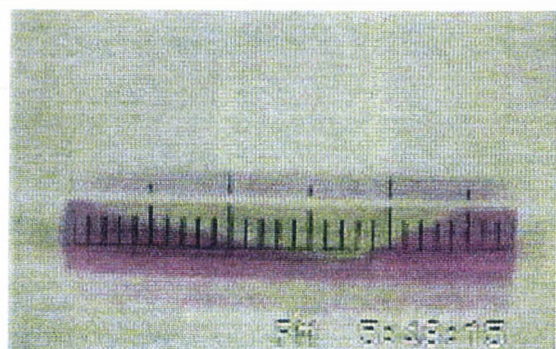
(m) 14 min



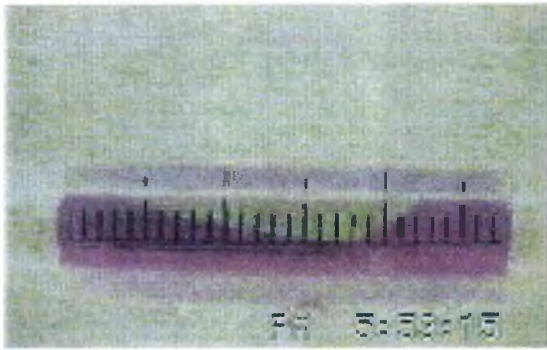
(n) 16 min



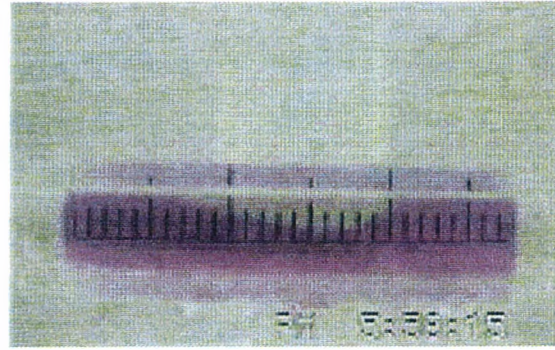
(o) 18 min



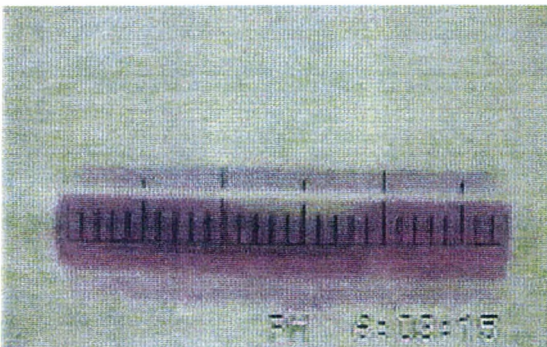
(p) 20 min



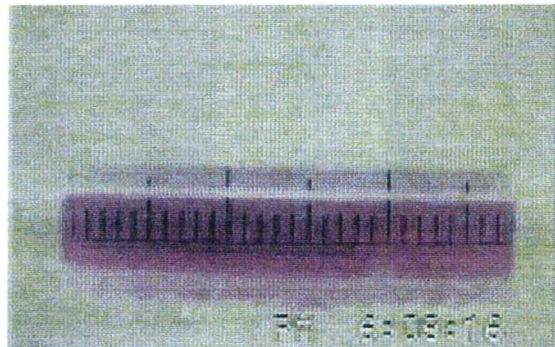
(q) 25 min



(r) 30 min



(s) 35 min



(t) 40 min

Fig. 6.18: (a-t) Showing the temporal response over a period of 40 min.

6.14 Long term Running and Dynamic Response

To investigate further the response of the optical probe which determines the overall performance, the sensor was used in a long term experiment that carried out over a two week duration. Apart from showing the long term response of the sensor this experiment also shows the reliability and stability of the sensor system. In this experiment, the response of the probe was measured until it reached equilibrium at 0.01ppm NH_3 , which required less than five minutes (300 s).

The response is shown in figure 6.19. The sensor was then moved to a 200ml distilled water sample where its response was followed until the sensor had reached a “recovering point,” which took less than 7 hours. This slow return to equilibrium is due to the conversion of the NH_3 to NH_4^+ in the sensor, the segregation of the dye and the diffusion limited effects in the sensor. In this satisfactory response however, the sensor still needs some modification to the ammonia dye mixture as this will speed the recovery. Although not covered in detail in this work, initial trials which were carried out where the internal mixture was agitated by ultrasonic vibration, heat, or light, showed their effects had an marked influence on sensor response time. Further work to address this partially irreversible behaviour is discussed in Chapter 7.

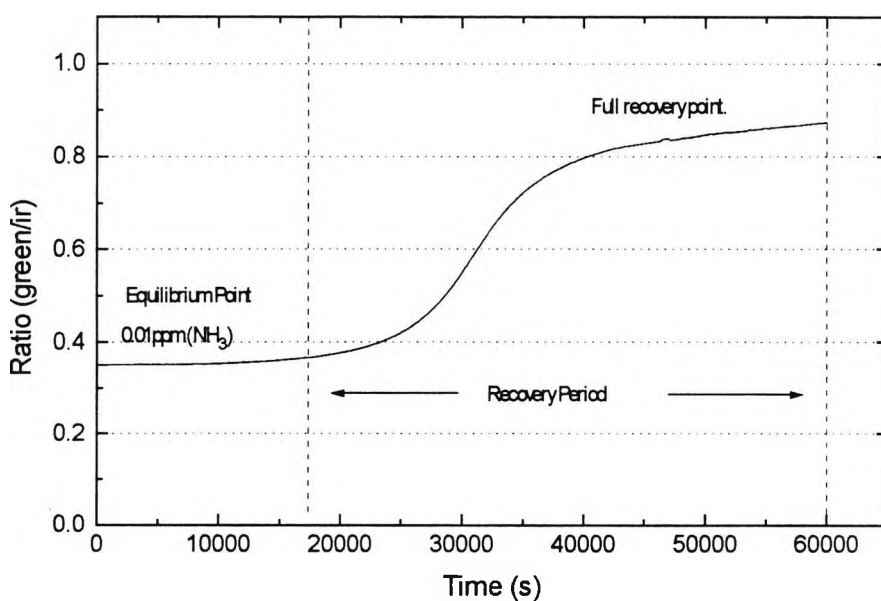


Figure 6.19 : Long time running and sensor recovery

6.15 SUMMARY

In this section the performance of the sensor head design has been assessed and discussed. This was done with the aid of simultaneous measurements of ammonia concentration with the optical probe and a commercial electrochemical sensor. In the assessment, the response time of the sensor head was found to be comparable to the response of the electrochemical sensor, however, being more complex in behaviour than originally envisaged.

The main reason for the complex response was found to be due to poor mixing of the ammonia and the indicator in the cell, illustrated by the formation of two coloured regions with a distinct boundary between them as shown in figure 6.18 (a to t). The computer simulation model, outlined in Chapter 5, shows that this can be explained by the lower diffusion coefficient of the Ind^- species compared to the InH species. This results in the build up of a Ind^- rich layer at the membrane wall through which the ammonia must diffuse to reach the InH .

With the resulting understanding of the dynamics underlying the sensor behaviour, the design of the sensor was changed to address the problem. The most important modification was to reduce the cell volume and hence the response time. This was accomplished in a new sensor head cell in which the specular mirror was replaced by a gas permeable membrane. The section ends with an assessment of the optimised sensor.

The partial irreversibility of the response of the sensor was investigated in some detail. This was not thought to limit the potential of the sensor only to laboratory use, as the addition of agitation of the dye decreases the response time markedly.

6.16 References

1. Marino, D.F. and Ingle, J.D., "Determination of Chlorine in Water by Luminol Chemiluminescence", *Anal. Chem.*, 53, p-455-458, (1981).
2. Montgomery, J.M., *Water Treatment Principles and Design*, John Wiley & Sons, Inc. USA, (1985).
3. P.W. Atkins "Physical Chemistry", 2nd Edition, Chapter 11, Oxford University Press, (1982).
4. Bishops, E., *Indicators*, Chapter 3, Pergamon Press, Oxford, (1972).
Orion Analytical Division USA, "Orion Ammonia Electrode data sheet" (1995).
5. Bourilkov J., Fneer M., Boyle W.O.J, Grattan K.T.V., and Palmer A.W. "Dissolved Gas Sensing Based Composite Optical Fibre and Electrochemical Techniques" *Proceeding of the Applied Optics and Optoelectronics, Conference Reading* (1996).
6. Keithley Electronics Technical Data Sheet, (1997).

Chapter 7

Conclusions

7.1 Summary.

This thesis reports on the specification, development, construction and assessment of an optical fibre-based sensor for dissolved ammonia in solution. The measurement method used for the sensor is based upon optical measurement of pH, modified by the presence of ammonia. In operation, the pH sensitive test solution is isolated from the analyte by a gas permeable membrane. Ammonia from the analyte, outside the sensor, diffuses through the membrane and into the test solution in the measurement cell where the change in pH is monitored colorimetrically by measuring the corresponding change in optical absorption of a pH sensitive dye.

The work of the thesis commenced with the assessment and modification of an existing colorimetric based pH sensor system discussed in an earlier research programme^[1]. This work involved the design of the appropriate optics, electronics and the computer hardware and software for the specific applications. Having assessed and ascertained the ability of the resulting system to measure pH it was employed in an initial assessment of monitoring ammonia, measuring the pH change induced by the addition of ammonia to buffered solutions.

Here, a simple and inexpensive fibre optic pH sensor for use in liquid solutions, incorporating a second wavelength reference channel, is demonstrated. The measurement of pH is based on the Beer-Lambert law which is used to relate the concentration of the chemical species to its absorption of light at a convenient wavelength. This approach was based on an indirect monitoring of the chemical species and was implemented using phenol red indicator dye to measure the concentration of the hydrogen ions.

The objective of demonstrating the feasibility of using solid state optoelectronic components was achieved in a satisfactory way through the use of two LEDs for 'signal' and 'reference' light channels and a Si p-i-n diode as detector. In addition, simple logic circuitry was built and used to control the device. As a result a rapid response, safe and reliable system, incorporating an optical bundle was illustrated.

The main work of the thesis presented in the second part describes the development of an optical fibre based ammonia sensor for monitoring water quality parameters. The measurement procedure is based upon familiar colorimetric tests, and a sensor response to ammonia concentration as low as 0.01 ppm was achieved. This limits of detection were below the EC guideline concentrations 0.5~0.05ppm.

Fibre optics were used as an essential part of the sensor to provide flexibility in the design, the possibility of monitoring the ammonia species remotely and to offer a decrease in interferences effects that could affect the measurement. Additionally, the transducing effect was purely optical, hence no electrical connection to the sample is required. This is a major advantage, especially for any further development for medical and potentially hazardous applications, such as measurements in sewers in presence of explosive gases.

The advantage of the indirect method used was shown to lie with the high sensitivity of the measurement as a result of the value of the absorption coefficient of extinction of the dye. Additionally, the hydronium ion concentration cannot be measured directly because it does not absorb in the visible part of the spectrum but it was possible to use the same part of the spectrum in order to monitor it indirectly, through the discussed method. However, when the indirect method was used to measure the pH of the sample, it showed a distinct disadvantage, namely a limited range of the measurement e.g. ± 1 pH units. This is not attributed to the method used but rather to the logarithmic relationship between the pH and absorption of light by the indicator. However, the measurement range can be extended by using a universal indicator dye combination, but multiple light sources would then be required.

Another drawback of this particular application resides in the non-linearity of the measurement which made the use of a calibration curve difficult, although this was overcome by having such information held in the computer memory and relating the ratio measurement by comparing it with the data stored in memory. The other advantage is using the computer to control and store all the measurement data. Also the calibration curve could be shown to be capable of being approximated to a linear curve when the measurement occurred around the inflexion point where the error due to non-linearity of the response of the instrument was minimal.

The analysis made in Chapter 3 showed that the resultant error in this type of measurement could be as low as 0.001 pH units under certain circumstances. This could be achieved with a signal to noise ratio in the order of 40 to 50 dB. However, an additional error has been introduced in the system because the measurement was affected by the ionic strength of the sample. Although this error is negligible when the sample is dilute, it can be as large as 0.02 pH units in concentrated samples. Consequently, the absolute measurement of pH would not be as accurate as the relative measurement. However, it is the measurement of the variation of pH that is more important in practical situations.

Having verified the feasibility of this approach to ammonia monitoring, a sensor system which incorporated a gas permeable membrane to separate the test solution from the analyte was designed, constructed and evaluated. Assessment of this sensor showed problems with its dynamic response which appeared to be linked to poor mixing of the ammonia diffusing through the membrane mixing with the solution in the sensor volume. This poor mixing could be seen visibly through distinctly different coloured regions in the sensor volume corresponding to regions of different pH.

In the ammonia sensor implementation a buffer solution of ammonium chloride of 0.01M was incorporated and mixed with the phenol red dye inside the sensor chamber. The result was obtained with and without adding the buffer solution to the indicator dye. This was discussed in Chapters 4 and 6.

The results obtained were compared with those from a commercially available Orion ammonia electrode. Thus the fibre optic ammonia sensor was seen to produce a very competitive set of results when compared with those from the electrode system. The work also showed that the practicability of a method for the basic design of the sensor was largely dependent on the dye species involved and the value of their coefficients of extinction. Moreover, the use of appropriate dyes can enhance the sensitivity aspect but it does introduce an additional error caused by interfering molecules. This effect was shown to be very small with the use of an ion-selective membrane for dissolved ammonia monitoring.

A computer model of the diffusion, chemical and optical processes in the sensor was then employed to simulate behaviour and to gain more insight into the above behaviour. The model showed that the problem with mixing resulted from the different diffusivities of the ionic and hydrogenated forms of the optical indicator dye, leading to a build up of the ionic form in the region of the membrane barrier. The model showed that several factors required addressing in the further design of the sensor, including that the sensor should have a minimum volume and maximum membrane area; it should have some methods for mechanically mixing the buffer solution; and it would be helpful for the sensor to have a simpler geometry with cylindrical symmetry.

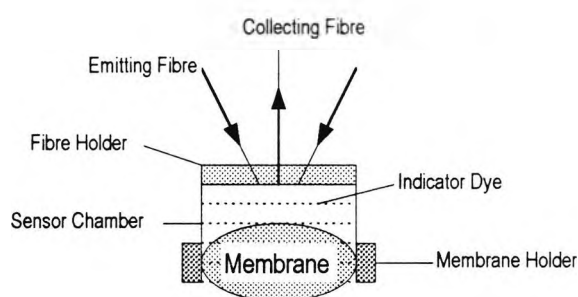


Fig. 7.1: The second design and improvement of the sensor head

In a second redesigned system, the test solution volume was reduced and the mirror of the original sensor design replaced by the white membrane which served as an optical reflector. This redesigned sensor had similar geometry to existing electro-

electrochemical-based chemical sensors and gave superior performance to that originally achieved.

7.2 Further Work

Apart from the improvements in the spectral fibre performance required, and the implementation of a practical instrumentation system, further work needs to be aimed at producing optical sensors for other measurands. The use of a pH indicating dye for the detection of ammonia, whilst demonstrating the principle of the sensor, is not ideal with respect to selectivity; any airborne chemical species that changes the pH of water will cause interference. Also, the demand for ammonia sensors is not as great as for other gases, e.g. oxygen, carbon dioxide, various organic molecules, etc.

In order to produce new and better sensors, measurand-specific molecules which change their optical spectra with measurand concentrations are required. In searching for such molecules it is instructive to study the way in which biological systems perform molecular recognition.

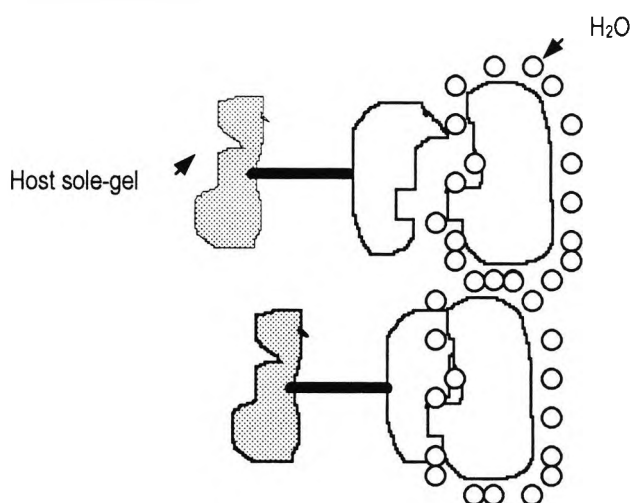


Fig 7.2 Shape recognition and hydrophobic bound in biological system

This is carried out in living organisms for a variety of tasks, ranging from providing a sense of smell to the use of antibodies in attacking foreign bodies; the mechanism is however always the same. It is based upon *shape recognition* and the *hydrophobic bond*, shown schematically in figure 7.2.

The reagent molecule is an exact replica of the analyte molecule to be detected. Both of the molecules (or sites) are hydrated with a layer of water molecules, some of which are eliminated when the molecules bond. It is the elimination of the water molecules which is the major factor in changing the free energy of the system (due mainly to changes in entropy), hence driving the reaction.

The reaction thus only occurs if the analyte molecule is an exact fit to the reagent molecule (or site), thus eliminating the water. This reaction is specific to a very high degree. The incorporation of such molecules into the sol-gel host film could lead to production of very specific sensors. Since the mechanism only occurs in the aqueous environment, the "guest-host" system described here is ideal; polymer immobilization methods with incorporated sol-gels could be used.

Reference

1. Grattan, K.T.V., Mouaziz, Z., Palmer, A.W., "Dual Wavelength Optical Fibre Sensor for pH Measurement" *Biosensors*, 3, pp 17-25, (1987).
2. Fneer, M., Grattan K.T.V., Boyle J.W.O., Kurata J. "Optical Fibre Ammonia Sensor for Water Quality Measurements", *Procedure of FOS 11 Sapporo Japan* (1996).

List of Publications

1. Fneer, M., Boyle, W.J.O., and Grattan, K.T.V. "Development of an Optical Fibre-Based Calorimetric Ammonia Sensor", Proceeding of the Sensor and their Applications to the 7th., Dublin, September 1995. Pp (236 - 240).
2. Fneer, M., Kurata, J., Boyle, W.J.O., and Grattan, K.T.V., " Optical Fibre Ammonia Sensor for Water Quality Measurements", Proceeding of Optical Fibre Sensors 11th, Sapporo Japan, May 1996, pp (438 - 441)
3. Bourilkov, J., Fneer, M., Boyle, W.J.O., Grattan, K.T.V., and Palmer, A. W., "Dissolved Gas Sensing Based Composite Optical Fibre and Electrochemical techniques". Proceeding of the Applied Optics and Opto-Electronics., Reading September 1996., pp (449 - 454)
4. Fneer, M., Grattan, K.T.V., Kurata, J., and Boyle W.J.O. "Modelling The Fibre Optic Ammonia Sensor" Paper accepted for Publication on Sensor and their Applications 8th Glasgow September 1997.

Some of these publications are listed in appendix No. 6, at the end of this thesis.

Appendix 1

Drawings And Notes For the Fibre Optic Probe Design

General

The drawings of figures 1 to 8 show the probe assembly and all individual components. The main probe parts are made from clear acrylic and rigid polyurethane. Although these are reasonably strong materials, care should be taken in use of the probe. This applies particularly to the tightening of screw threads as follows:

1. The fibre holder screws should be tightened evenly and only tightly enough to lightly compress the o-ring which will then provide a good seal. The o-ring can be seen through the jacket as it starts to compress.
2. The wall thickness of the window screws is only 0.75mm. They should therefore be tightened very carefully.
3. A seal can be achieved at the lower o-ring by tightening the sealing plug by hand. Again, the o-ring can be seen through the jacket as it starts to compress.

During assembly of the cell, the space between the mirror and the sealing plug could first be filled with the same fluid as the rest of the cavity in order to remove the possibility of air passing the mirror thread into the test volume.

Tooling

The following tools are required to dismantle and assemble the probe:

Fibre holder mounting screws - No. 1 phillips screwdriver

Mirror adjustment - 4mm AF allen key

Window screws - 8mm parallel tip screwdriver

Cell dimensions

The internal cell length (between the fibre ends and the mirror) can be adjusted by turning the mirror screw after removing the sealing plug. The range of adjustment is from 7mm to 13mm. The cell and window diameters are 7mm and 4mm respectively.

Drawings

The scale of all drawings is 1:1.5

All dimensions shown are mm.

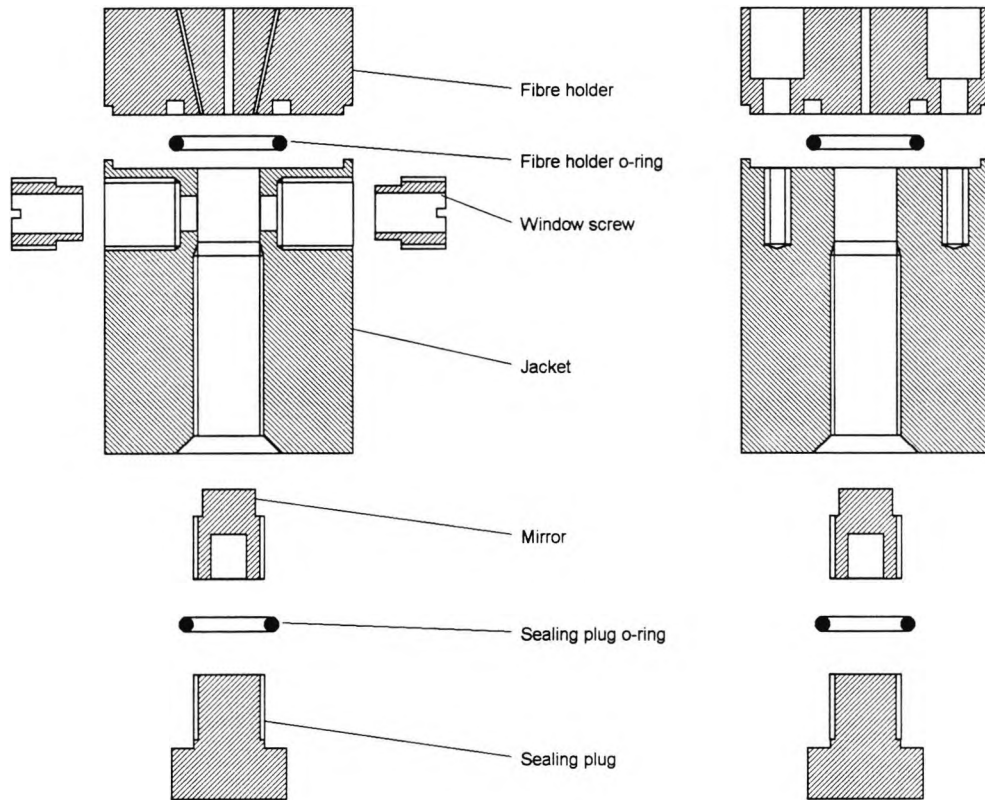


Figure A1.1
Exploded views of components

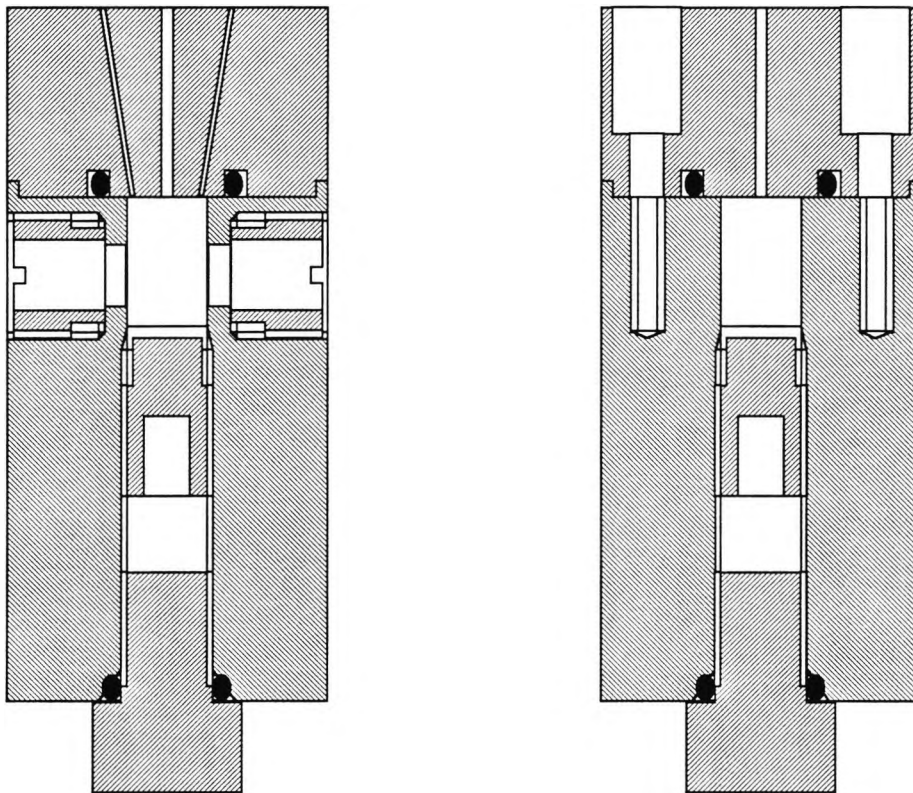
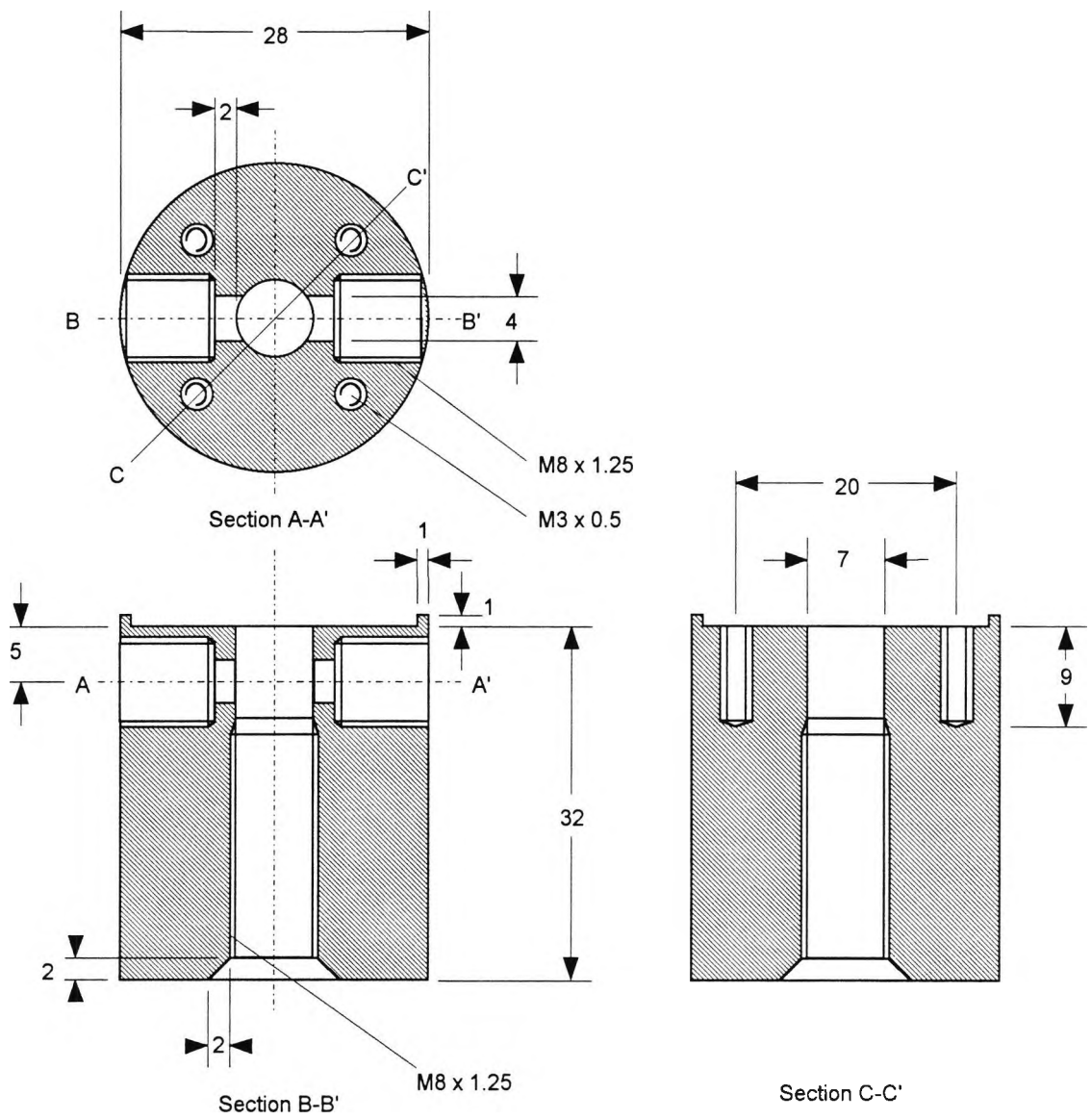
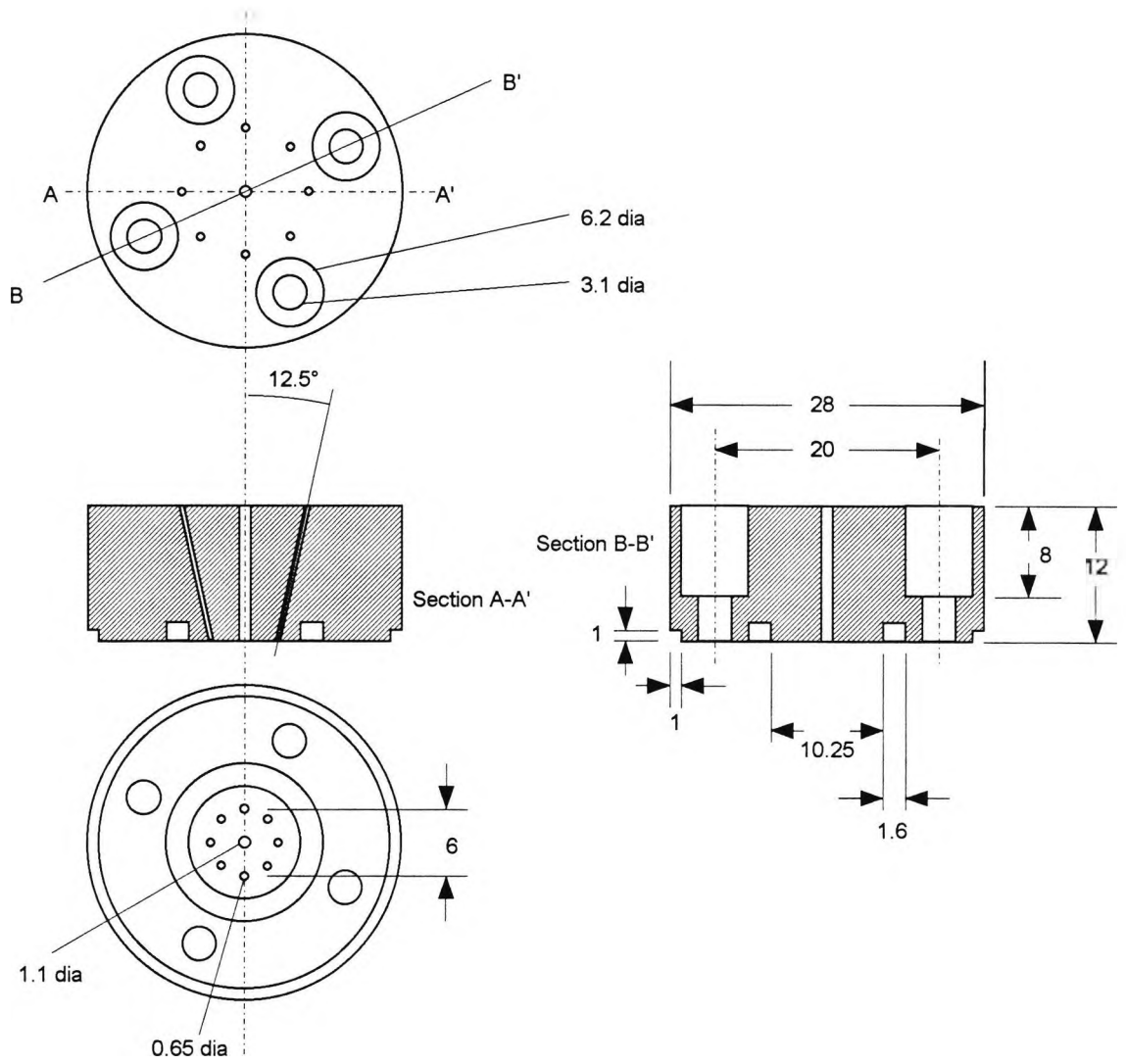


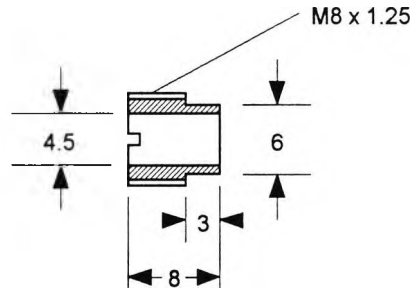
Figure: A1 .2 Assembly Views



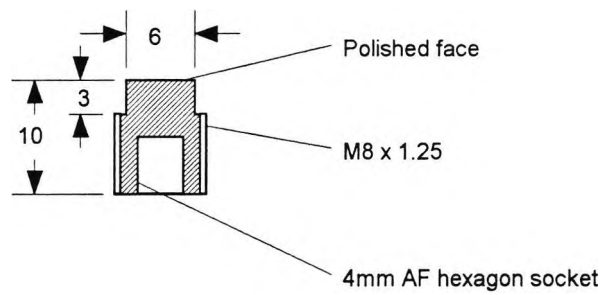
Jacket
 Material: clear acrylic
 Figure : A2.3



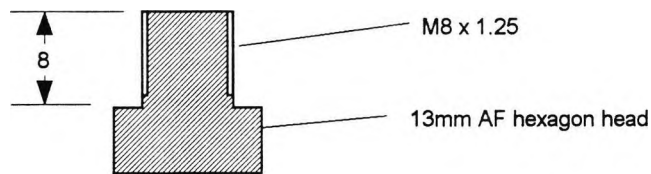
Fibre Holder
 Material: rigid polyurethane
 Figure: A2.4



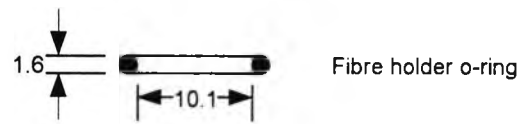
Window Screw
 Material: rigid polyurethane
Figure: A1.5



Mirror
 Material: A2 stainless steel
Figure: A1.6



Sealing plug
 Material: A2 stainless steel
Figure: A1.7



O-rings
Material: medium nitrile
Figure: A1 .8

Appendix 2**Calculation of the Inflexion Point**

The calculation of the position of the inflexion point is carried out by taking the second derivative of the relationship between light transmission and the variation of pH values of the dye. Mathematically, the inflexion point denotes the point for which the derivative of the curve changes sign and solution of the equation $\frac{d^2 x}{d\delta^2} = 0$

provides a value at which the most linear part of the calibration curve occurs. For this, a simplification of the initial relationship between the light intensity and the pH as described in the system response, (e.g. Equation A2.1) is necessary for simplicity e.g. $x = P/P_0$.

$$\log(x) = -\frac{m}{10^{-\delta} + 1} \quad [\text{A2.1}]$$

$$x = 10^{-m/(10^{-\delta} + 1)} \quad [\text{A2.2}]$$

Initially the first derivative of equation A2.2 is obtained in the following manner (Eq.A2.4):

$$\frac{dx}{d\delta} = -m \ln 10 \cdot 10^{-m/(10^{-\delta} + 1)} \frac{d}{d\delta} \left(\frac{1}{10^{-\delta} + 1} \right) \quad [\text{A2.3}]$$

$$\frac{dx}{d\delta} = -m(\ln 10)^2 \frac{10^{-\delta}}{(10^{-\delta} + 1)^2} 10^{-m/(10^{-\delta} + 1)} \quad [\text{A2.4}]$$

The second derivative as a function of the same variable is computed and is presented in a simplified manner by splitting the numerator and denominator as follows:

$$\frac{d^2 x}{d\delta^2} = \frac{A - B}{(10^{-\delta} + 1)^4} \quad [\text{A2.5}]$$

$$A = -m(\ln 10)^2 (10^{-\delta} + 1)^2 \frac{d}{dx} (10^{(-m/10^{-\delta} + 1) - \delta}) \quad [\text{A2.6}]$$

$$B = (-m \ln 10^2) (10^{-m/10^{-\delta} + 1} - \delta) (-2 \ln 10) (10^{-\delta}) (10^{-\delta} + 1) \quad [\text{A2.7}]$$

$$\frac{d}{d\delta} 10^{(-m/10^{-\delta} + 1) - \delta} = \left(\frac{m \ln 10 * 10^{-\delta}}{(10^{-\delta} + 1)^2} - 1 \right) * 10^{(m/10^{-\delta} + 1) - \delta} \ln 10 \quad [\text{A2.8}]$$

$$\frac{d^2 x}{d\delta^2} = (m \ln 10^3) \left(\frac{10^{(-m/10^{-\delta} + 1) - \delta}}{(10^{-\delta} + 1)^3} \left\{ (10^{-\delta} + 1) \left(\frac{m \ln 1 * 10^{-\delta}}{(10^{-\delta} + 1)^2} - 1 \right) + 2 * 10^{-\delta} \right\} \right) \quad [\text{A2.9}]$$

The value of δ , satisfying the inflexion point condition, is then calculated by solving

$$\frac{d^2 x}{d\delta^2} = 0 \text{ hence, only the part between brackets is used for the calculation of the}$$

solutions, since the first part cannot be zero.

$$(10^{-\delta} + 1) \left(\frac{m \ln 10 * 10^{-\delta}}{(10^{-\delta} + 1)^2} - 1 \right) + 2 * 10^{-\delta} = 0 \quad [\text{A2.10}]$$

This equation can be rewritten as the following:

$$10^{-2\delta} + m \ln 10 * 10^{-\delta} - 1 = 0 \quad [\text{A2.11}]$$

The solutions to this equation are determined following a normal procedure. This specific determination of Eq. A2.11 is $\Delta = (m \ln 10)^2 + 4$ is always positive and hence two solutions exist.

$$10^{-\delta} = m \ln 10 \pm \sqrt{(m \ln 10)^2 + 4} \quad [\text{A2.12}]$$

Only the positive result will be taken since the part under the square root is always larger than the first factor. Hence the coordinate of the inflexion point are given below:

$$\delta = -\log(-m \ln 10 + \sqrt{(m \ln 10)^2 + 4}) \quad [\text{A2.13}]$$

As a result, the value of $\delta = \text{pH} - \text{pK}$, is a function of the parameter m as was already shown graphically in Chapter 3. The negative sign of the solution shows that the inflexion point occurs at a pH value smaller than the pK value of the dye.

Appendix 3

Data for figure 6.17.

<i>100ppm 1st.</i>	
Time (s)	Ratio (g/ir)
0	0
50	0.35
100	0.27
150	0.26
200	0.25
250	0.25
300	0.25
350	0.25
400	0.25

Data of figure 6.17: ammonia concentration 100ppm 1st graph

<i>100ppm 2nd.</i>	
Time (s)	Ratio (g/ir)
0	0
50	0.38
100	0.36
150	0.3
200	0.28
250	0.27
300	0.27
350	0.27
400	0.27

Data for figure 6.17: Ammonia Concentration 100ppm 2nd graph

<i>10ppm</i>	
Time (s)	Ratio (g/ir)
0	0
50	0.55
100	0.48
150	0.45
200	0.40
250	0.38
300	0.35
350	0.35
400	0.35

Data of figure 6.17: ammonia concentration 10ppm.

<i>1ppm.</i>	
Time (s)	Ratio (g/ir)
0	0
50	0.58
100	0.56
150	0.26
200	0.54
250	0.50
300	0.44
350	0.40
400	0.40

Data for figure 6.17: ammonia concentration is 1ppm.

Appendix 4**The Ammonia Sensor Control software for both sensors Optical and Electrochemical**

```

{*Optical and Electrochemical sensor Time series control }
{updated on the 20.08.1995 *}

{*****}

PROGRAM monitor_control(input,output);

{$R+} { RANGE CHECK ON }
{$I+} { IO CHECK ON   }
{$N+} { CO PROCESSOR }
USES dos,crt,winttt5,fastttt5;

CONST
sample_end=1;
sample_beg=3;
pulse_on=5;

VAR  printer,ad_board,out_ad_no,inp_ad_low,inp_ad_high, clear_ad_reg,
     ad_conv_loop_low,ad_conv_loop_high,out_da_low, out_da_high:word;
     green_sig,ir_sig,AmEl_sig,phvalue,ratio:real;

     i,num_of_sam,TIME,samp_rate,SAMP_TIME,delay_time:integer;

     green_sig_arr:array[1..512] of real;
     ir_sig_arr:array[1..512] of real;
     ir_avr,green_avr,AmEl_avr: real;
     AmEl_sig_arr:array[1..512] of real;

     newfile:string;
     datafile,tempfile:text;
     is_key,quit,wrtdata,fldata,trace,graphics:boolean;
     key:char;

{*****}

```

```

PROCEDURE BEEP;
BEGIN
  SOUND(400);
  DELAY(100);
  SOUND(100);
  DELAY(50);
  NOSOUND;
END;

```

```

PROCEDURE set_up_variable_values;
BEGIN
  printer:=$3bc;
  ad_board:=$278;
  out_ad_no :=ad_board;    { 4 bits channel no  }
  inp_ad_low :=ad_board+1; { 8 bits A-D low data  }
  inp_ad_high :=ad_board+2; { 4 bits A-D high data  }
  clear_ad_reg :=ad_board+3; { clear A-D register  }
  ad_conv_loop_low :=ad_board+4; { A-D conv loop low  }
  ad_conv_loop_high :=ad_board+5; { A-D conv loop high  }
  out_da_low :=ad_board+6; { 8 bits D-A low data  }
  out_da_high :=ad_board+7; { 4 bits D-A high data  }
  delay(100)
END;

```

```

function a_d(channel:byte):integer;
var loop:integer;
    a,low_byte,high_byte:byte;
BEGIN
  port[clear_ad_reg] := 0; { set up ready for conversion }
  port[out_ad_no] := channel;
  for loop := 1 to 7 do A := port[ad_conv_loop_low];
  for loop := 1 to 7 do A := port[ad_conv_loop_high];
  delay(1);
  low_byte := port[inp_ad_low];
  high_byte := port[inp_ad_high] and 15;
  a_d:= low_byte + high_byte shl 8;
END;

```

(*****)

```

function channel_in(channel:byte):byte;
var mask,din,chn:byte;
BEGIN
  if (channel<1) or (channel>8) then exit;
  mask:=1;
  din:=port[printer];

```

```

chn:=channel-1;
channel_in:=(din and (mask shl chn)) shr chn;
END;

```

```
(*****)
```

```

PROCEDURE channel_set(channel:byte);
var mask,chn:byte;
BEGIN
  if (channel<1) or (channel>8) then exit;
  mask:=1;chn:=channel-1;
  port[printer]:=port[printer] or (mask shl chn);
END;

```

```
(*****)
```

```

PROCEDURE check_pause;
BEGIN
  is_key:=keypressed;
  if is_key then key:=readkey;
  if (key='p') or (key='P') then      {if q is pressed}
  BEGIN
    mkwin (30,9,60,14,red,white,1);
    writeat(35,11,yellow,red,'THE PROGRAM IS STOPPED');
    writeat(35,12,yellow,red,'PRESS SPACE TO CONTINUE');
    gotoxy(59,9);
    BEEP;
    repeat
      BEGIN
        key:=readkey;
      END;
    until key=' ';
  END;
END;

```

```
(*****)
```

```

PROCEDURE channel_reset(channel:integer);
var mask,chn:byte;
BEGIN
  if (channel<1) or (channel>8) then exit;
  mask:=1;
  chn:=channel-1;
  port[printer] := port[printer] and (not (mask shl chn));
END;

```

```
(*****)
```

```
Function Fmade(var Thefile: text; Fname: string): boolean;
```

```
{create a new file and does all necessary checking, returns true if the file has been
successfully created}
```

```
BEGIN
  ASSIGN(Thefile, Fname);
  (*$I-*)
  rewrite(Thefile);
  (*$I+*)
  if ioresult=0 then
    fmade:=true
  else fmade:=false;
END;
```

```
(*****)
```

```
PROCEDURE initialise;
BEGIN
  set_up_variable_values;
  port[printer]:=0;
END;
```

```
(*****)
```

```
PROCEDURE ask_4_ph;
BEGIN
  mkwin (25,9,60,14,red,white,1);
  writeat(27,11,yellow,red,'ENTER THE VALUE OF THE pH');
  GOTOXY(54,11);
  READLN(phvalue);
END;
```

```
(*****)
```

```
PROCEDURE ask_4_file;
BEGIN
  mkwin (25,9,60,14,red,white,1);
  writeat(30,10,yellow,red,'ENTER THE NAME OF THE FILE');
  GOTOXY(35,12);
  READLN(newfile);
END;
```

```
PROCEDURE check_4_quit;
  VAR newans:CHAR;
BEGIN
  CLRSCR;
  WRITELN('enter N for new pH value or Q to quit :');
  READ(key);
  IF (key=#113) OR (key='Q') THEN {if q is pressed}
```

```

BEGIN
  mkwin(20,9,65,15,red,white,1);
  writeat(22,11,yellow,red,'YOU ARE SURE YOU WANT TO QUIT (Y/N) -
>');
  GOTOXY(61,11);
  READ(newans);
  REPEAT
    GOTOXY(61,11);
    READ(newans);
    IF (newans='Y') OR (newans='y') THEN
      BEGIN
        port[printer] := port[printer] and 0;
        flush(datafile);
        flush(tempfile);
        close(datafile);
        CLRSCR;
        halt;
      END;
    UNTIL (newans='Y') OR (newans='y') OR (newans='n') OR (newans='N') ;
  END;
  CLRSCR;
  IF (key='N') OR (key='n') THEN {if N is pressed}
  BEGIN
    mkwin (20,9,60,14,red,white,0);
    writeat(22,11,yellow,red,'ENTER THE NEW VALUE OF pH');
    GOTOXY(54,11);
    READLN(phvalue);
    CLRSCR;
  END;
END;

```

(*****)

```

PROCEDURE DRIVELED;
BEGIN

```

```

  channel_set(1);
  delay(sample_beg);
  channel_set(5);
  delay(pulse_on);
  channel_reset(5);
  delay(sample_end);
  channel_reset(1);
  delay(pulse_on);
  channel_set(7);
  DELAY(pulse_on);
  channel_reset(7);
  delay(pulse_on);

```

```

channel_set(2);
delay(sample_beg);
channel_set(6);
delay(pulse_on);
channel_reset(6);
delay(sample_end);
channel_reset(2);
END;

PROCEDURE backframe(A:STRING);
BEGIN
mkwin(1,1,80,4, yellow,blue,2);
GOTOXY(2,2);
TEXTCOLOR(WHITE);
TEXTBACKGROUND(BLUE);
writeln(' SAMPLING TIME IS ',samp_rate:3,' SECONDS    NUMBER OF
TOTAL SAMPLES/READING IS: ',NUM_OF_SAM:4);
GOTOXY(4,3);
TEXTCOLOR(YELLOW);
writeln('TIME(S)   GREEN/IR   AVERAGE IR   AVERAGE GREEN
AVERAGE mV');

mkwin(1,23,80,25,white,red,2);
TEXTCOLOR(YELLOW);
TEXTBACKGROUND(RED);
GOTOXY(10,24);
writeln(A);
END;

BEGIN
CLRSCR;
backframe('    COMBINED OPTICAL AMMONIA AND PH SENSOR');
TEXTBACKGROUND(0);
TEXTCOLOR(15);
ask_4_file;
ASSIGN(datafile,newfile);
REWRITE(datafile);
repeat
REPEAT
{CLRSCR;}
mkwin(20,9,65,14,red,white,1);
writeat(22,11,yellow,red,'ENTER THE SAMPLING TIME (SECONDS) ');
GOTOXY(60,11);
READLN(samp_rate);
IF samp_rate<=0 THEN
BEGIN
beep;
writeat(22,11,yellow,red,' INVALID VALUE RE-ENTER A NEW VALUE ');

```

```

    GOTOXY(22,60);
    READLN;
    END;
UNTIL samp_rate>0;
initialise;
mkwin(20,9,65,14,white,BLACK,1);
writeat(27,11,yellow,red,'ENTER THE SAMPLE NUMBER <512');
GOTOXY(57,11);
READLN(num_of_sam);
WHILE (num_of_sam <1) OR (num_of_sam>512) DO
BEGIN
    mkwin(20,9,60,14,YELLOW,BLACK,1);
    writeat(32,11,yellow,red,'VALUE OUT OF RANGE');
    BEEP;
    WRITEAT(27,13,YELLOW,BLUE,'ENTER VALUE (1,512) ');
    GOTOXY(48,13);
    READLN(num_of_sam);
    CLRSCR;
END;
delay_time:=samp_rate*1000-num_of_sam*36;
if delay_time<0 then
begin
writeat(32,11,yellow,red,'sample time required greater than time between sampling');
BEEP;
delay(1000);
end;
until delay_time>0;
CLRSCR;
backframe('    COMBINED OPTICAL AMMONIA AND PH SENSOR');
WINDOW(1,5,80,22);
writeln(datafile, 'TIME= ',SAMP_TIME,' SECONDS');
writeln(datafile, 'TIME(S)  GREEN/IR    AVG IR    AVG GREEN
AVGmV');
REPEAT
    green_avr:=0;
    ir_avr:=0;
    AmEl_avr:=0;
    FOR i:=1 TO num_of_sam DO
    BEGIN
        driveLED;
        green_sig_arr[i]:=a_d(1);
        ir_sig_arr[i]:=a_d(3);
        AmEl_sig_arr[i]:=a_d(6);
        green_avr:=green_avr + green_sig_arr[i];
        ir_avr:=ir_avr + ir_sig_arr[i];
        AmEl_avr:=AmEl_avr+AmEl_sig_arr[i];
    END;
IF ir_avr <>0 THEN

```

```
BEGIN
  ir_avr:=ir_avr/num_of_sam;
  AmEl_avr:=AmEl_avr/num_of_sam;
  green_avr:=green_avr/num_of_sam;
  ratio:=green_avr/ir_avr;
  DELAY(delay_time);
  TIME:=TIME+samp_rate;
  WINDOW(2,3,20,79);
  writeln(datafile, TIME:5,'      ',ratio:7:5,'      ',ir_avr:7:1,'      ',green_avr:7:1,'
',AmEL_avr:7:1);
      writeln(TIME:5,'      ',ratio:7:5,'      ',ir_avr:7:1,'      ',green_avr:7:1,'
',AmEL_avr:7:1);
  END;
  UNTIL keypressed;
  close(datafile);
END.
```

Appendix 5**Cost Estimation of Fibre Optic Based Ammonia Sensor Implementation**

List of component used in the implementation of the fibre optic based ammonia sensor and their price based on a single unit purchase.

Company	Item	Price	Address
BDH through Merck	Ammonium chloride 1044-5Q	£05.20	100 Boulevard Magnapark, Lutterworth, Leicester LE17 4XN
RS	6 Ultra Bright Green LEDS of 565 nm	£06.00	The Fairway Estate, Green Lane, Hounslow Middlesex TW4 6BU
	6 Infrared LEDs at 810 nm	£08.00	
	3 Si p-i-n Photodiode	£28.00	
	3 Volts Regulator	£02.00	
	4 LF 309H RS(307- 086)	£28.98	
	8 Transistors BC 183L	£04.82	
	28 Resistors	£02.98	
	8 Capacitors 0.1µF	£03.97	
	RS Instrument Plastic Box (Sensor Housing)	£37.98	
Tech Optics	Amphenol Connectors	£20.00	Unit 6 Cala Industrial Estate, Tannery Road Tunbridge, Kent TN9 1RF
	4 x SMA 905-150-5005 LEDS Housing	£48.99	
	10 m Quarts Optical Fibre	£78.00	
Kettely Electronics	8 bit AD Converter	£135.00	Kettely Electronics 128, Hays Lane Colchester, Essex
Fisher Chemical	phenol red Indicators	£10.00	Fisher Chemical Ltd Laghbrah, England
TOTAL AMOUNT		£419.92	

Appendix 6

Some of the early publication out of this thesis

DEVELOPMENT OF AN OPTICAL FIBRE BASED COLORIMETRIC AMMONIA SENSOR.

M. Fneer, W. J. O. Boyle and K.T.V. Grattan.

Measurement and Instrumentation Centre Department of Electrical, Electronic and Information Engineering, City University, Northampton Square, London EC1V 0HB, UK.

Abstract

The construction and performance characteristics of a novel optical fibre-coupled optrode for ammonia concentration measurement are described. The operation of the optrode is analogous to the common electrochemical ammonia sensor, where changes in the concentration of ammonia that arise from its diffusion through a gas permeable membrane are monitored by their effect on the pH of an ammonium sulphide buffered solution. In the optrode, changes in pH are measured optically rather than electrochemically. These alterations in the optical absorption characteristics of the pH indicator dye (phenol red) which result from the changes in ammonia concentration are observed using a dual optical wavelength scheme to provide a reference channel. The buffer solution of the optrode is isolated from the solution under test by a Teflon membrane, and results obtained from the optically addressed colorimetric sensor for ammonia are described and discussed.

Key words: Fibre optic ammonia sensor, phenol red, membrane, pH, colorimetric, optical probe.

Introduction

The measurement of ammonia is of a particular importance, not only in biomedical science but also in environmental, forensic, food sciences as well as in the study of enzymatically degradable nitrogenous compounds. Numerous methods for this purpose have been introduced, and some of them are commercially available⁽¹⁾. However, so far none of these methods satisfies all the common needs for a simple, reliable, cheap and stable ammonia sensor. During the same development period similar needs for a glucose sensor have been fulfilled by the production of a device based on the amperometric method. This kind of sensor is now commercially available as a disposable sensor strip, equipped with a pen-sized potentiostat⁽²⁾. This shows the adaptability of an amperometric method for miniaturisation and mass production. The extension of this technology for the development of multi-functional sensors is easily envisioned. Bearing these facts in mind, it is useful to explore the use of colorimetric techniques for the development of optical fibre-based sensors for the measurement of the concentration of different chemical species, of which ammonia is among the most important.

Ammonia sensors

The detection of ammonia, either as a vapour or in aqueous solution, may be carried out in a similar manner to the measurement of pH, i.e. based on the use of pH indicators. Shahriari et al.⁽³⁾ and Zhou et al.⁽⁴⁾ have constructed sensors as shown in figure 1, based upon optical absorption by the ammonia indicator bromocresol purple, suitable for ammonia detection.

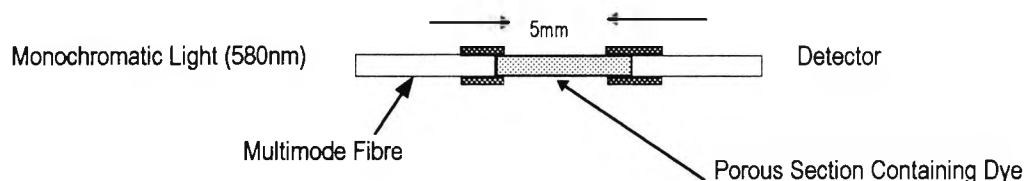


Fig.1.: Ammonia sensors of Shahriari et al. and Zhou et al.

The dye is adsorbed into a section of porous fibre, into which the NH_3 enters and interacts with it. For this reaction to occur, adsorbed water must be present to create NH_4OH , and so the devices are sensitive to humidity as well as ammonia. Shahriari's device uses porous glass made by heat treating and etching the borosilicate glass, giving a pore size of 80 - 150 nm. It can detect an ammonia level down to 0.7ppm, and shows a linear relationship between adsorption coefficient and concentration up to 3ppm. Zhou's sensor is less sensitive, working in the range 10 - 90ppm, utilising a porous plastic (a treated polymethylmethacrylate) with a pore size of $\approx 10\text{nm}$. Besides the sensitivity to humidity, both devices have the major disadvantage of very long response time, typically 20 minutes.

In recent years, some investigations on coated optical waveguide spectrophotometric and fluorescence sensors for ammonia vapour have been described^(5,6). Each of these investigations has followed a different technique in measuring the ammonia vapour concentration. Further development to an earlier work on pH optical fibre sensors,⁽⁷⁾ in a new scheme to measure ammonia concentration in water using a fibre optic probe, is described here.

The work presented lies within the context of continuing development of an ammonia optical fibre sensor, based on the pH change induced by dissolved ammonia. In this sensor, ammonia changes the equilibrium balance of a buffer solution (NH_4SO_2) causing H^+ ions to diffuse through a gas permeable membrane, hence modifying the H^+ concentration and the colour of the phenol red indicator. This work reports on the development of the optical and data acquisition system, and the evaluation of this system in measuring pH. Thus the sensor is analogous to the electrochemical sensor of the Severinghaus electrode⁽⁹⁾.

The separation between the water sample and the phenol red dye is achieved by the use of a Teflon membrane⁽⁸⁾. The response of the probe is dependent on the variation in the concentration of the ammonia in water.

Instrument Aspects

A schematic diagram of the experimental instrumentation employed is shown on figure 2. The absorption change of the dye solution used, phenol red, is monitored using the change in its absorption spectrum at 565nm, using light from an ultra-bright green LED (40 nm FWHM) of output intensity 120 mcd. The diode is housed in a standard SMA fibre optic housing connector. The reference wavelength is provided by light from an infrared (IR) LED at 810nm (40 nm FWHM) as, at this wavelength, there is very small absorption by the indicator dye, and tests carried out showed that it is not dependent on pH value at this wavelength. The LEDs are operated at room temperature with a fixed current to allow equalisation of their temperature. More active stabilisation of temperature and thus the spectral characteristics of LEDs is an aspect of the requirement of the system.

Light from the green LEDs was coupled into 6 x 600 μm diameter plastic clad silica fibre (PCS) of which three fibres were coupled into each green diode. The infrared LED was coupled to a single fibre of 600 μm diameter. This bundle of fibres led to the sensor head (or probe), which was approximately 1.5m from the instrument control box. The probe was manufactured from a solid plastic core of internal length 2cm, the ends of which were made from stainless steel and closed and demountable for easy cleaning and re-polishing, if necessary. One end was polished to provide a reflective surface, and the other end was drilled with 7 small holes at an angle of 7.1 degrees to the Centre. The fibres were inserted and glued to the holes and the ends could also be polished. The materials used are such that they can easily be polished if necessary and re-calibration with respect to standard buffer solutions can be easily performed. At the fibre input end, the light which had travelled across the solution and had been reflected was received by one fibre of 1000 μm (1mm) diameter which was surrounded by the other transmit fibres. This fibre was connected to a silicon light detector PIN diode where the intensities of the signals on each wavelength band were determined. For all the fibre couplings, expanded, but otherwise standard, SMA - compatible stainless steel connections were used. Fibre bundles were made from individual fibres stripped of the plastic coating, then fixed with epoxy resin and polished. This combination is inert and resistant to strongly acid or alkaline solutions.

The device was tested by placing the probe in a solution containing ammonium sulphide (NH_4SO_2) and the indicator dye is separated by a membrane in the probe chamber and its absorption, integrated over the emission spectrum of the green LED, is measured as being indicative of the pH.

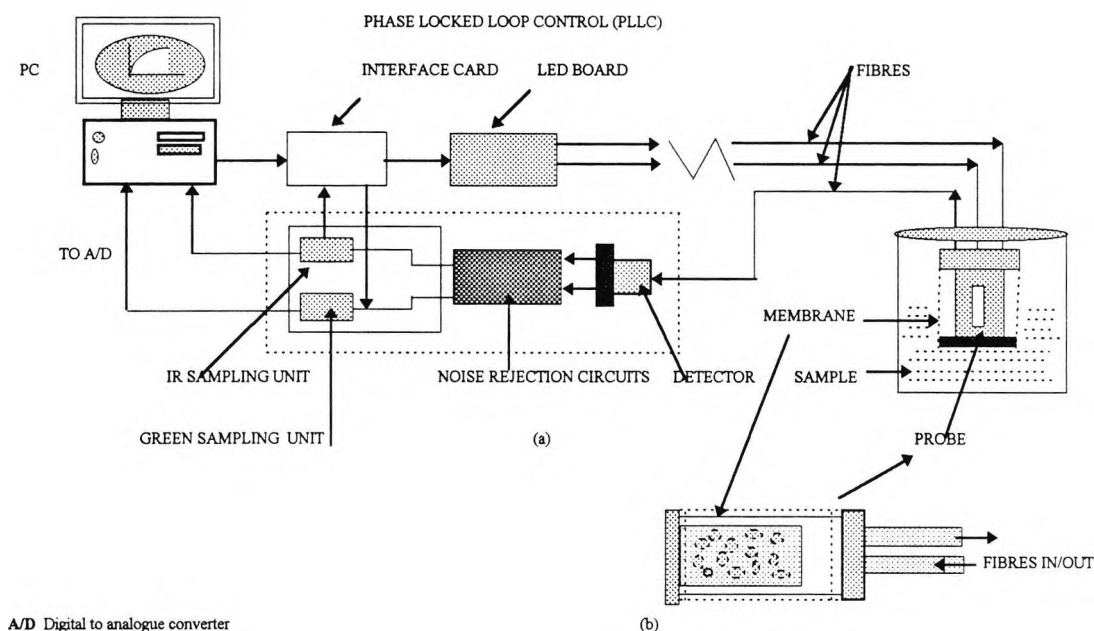


Figure 2. (a) Schematic of the ammonia sensor showing the electronic system and the fibre optic Probe construction. (b) Expanded view of probe.

Electronic Aspects.

As shown schematically in fig.2, the hardware system is controlled by a PC. The interface consists of two units, one to control the LEDs and the other to control the 8 bit analogue-to-digital (A/D) converter which is connected to the PIN diode detector. The interface to the LEDs is controlled via the parallel printer port, whilst the A/D converter is located in the PC on a bus interface card.

This hardware is controlled by software written in Turbo Pascal. This software provides a train of pulses that alternately turn on-and-off the green and the infrared LEDs, and it also reads the digital values generated by the A/D converter from the signal produced by the optical detector. With the present software configuration, details of the pulse timing can be controlled and the time-varying signal from the detector can be displayed graphically and recorded to file, for later analysis by spreadsheet software. With the system as it is, the dynamic response of the sensor to changes in ambient chemistry can be expected to be recorded. With further development of the sensor systems, the computer hardware and software may be simplified to be suitable for a single chip microprocessor controller solution.

The detector circuit used is based on a silicon PIN diode with integral amplifier (RS type 308067). Such a device is low noise and of adequate bandwidth for this application (linear to a few kHz). Additionally a three-stage, low noise amplifier is used further to boost the small signal level. Three simple type 071 operational amplifiers were used with the gain selected by appropriate resistors. The phase selective detector circuit, through the use of sample and hold elements (LF398H), synchronised with the LED signals rejects the d.c. level and enables the intensities of the infrared and green signals to be measured. These outputs (green and infrared outputs) were then measured and displayed and the ratio of the infrared to green signal intensity obtained. This parameter is directly related to the pH of the solution via a pre-determined calibration, which is performed prior to be used of the system.

Indicator and reagent.

Phenolsulfonphthalein (phenol red) was the indicator dye employed in this work as it can be used to measure pH and thus ammonia concentration over a wide range. It exists in two tautomeric forms, each having a significantly different absorption spectrum.

As the characteristics of the solution vary, the relative size of the optical absorption of each tautomer varies in response to the changing relative concentrations of the acid and base forms of the indicator. This can conveniently be monitored at the peak of the absorption at 565nm, corresponding to the green LED emission while the small infrared absorption is independent of that change. Fig 3 show the absorption spectra of the indicator dye for sample solutions of varying pH, obtained in a conventional spectrophotometer in 1 cm sample cell.

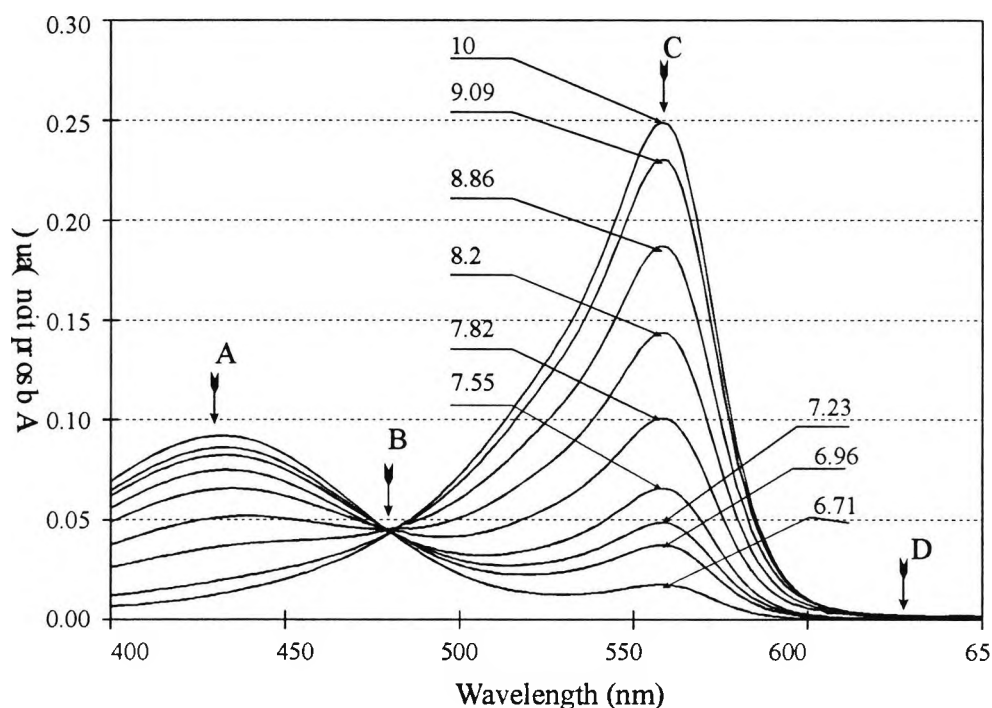


Figure 3: Absorption Spectra of phenol red as a function of wavelength for different pH values, related to ammonia concentration in water.

Calibration.

The response of the device, i.e. the ratio of the signals from the two LEDs, is plotted as a function of the output from an electrochemical pH meter which itself was referenced to standard buffer solutions, carefully prepared in the normal way. A typical set of calibration curves is shown on fig.4 over the pH range from 6 to 10 for solutions which were prepared containing ≈ 0.5 ml indicator and stirred continuously.

The accuracy of the sensor as used is 0.05 pH, this arising from the error in the measurement of the peak at 565nm, due to the electronic background noise in the system, which corresponds to an error in the reading of approximately $\pm 1\%$. The stability of the reading is very satisfactory showing a negligible change over 1h for a solution of constant pH. The temperature stability of the device is very good, corresponding to 0.04pHK^{-1} over the range 22°C to 50°C , in the pH region around 7.8 units.

The response of such a device is very fast and diffusion limited only, due to the rapid responses from the modulated LEDs and the electronic processing. This compares with a conventional electronic meter which may require several seconds to re-stabilise after the pH of the solution is changed.

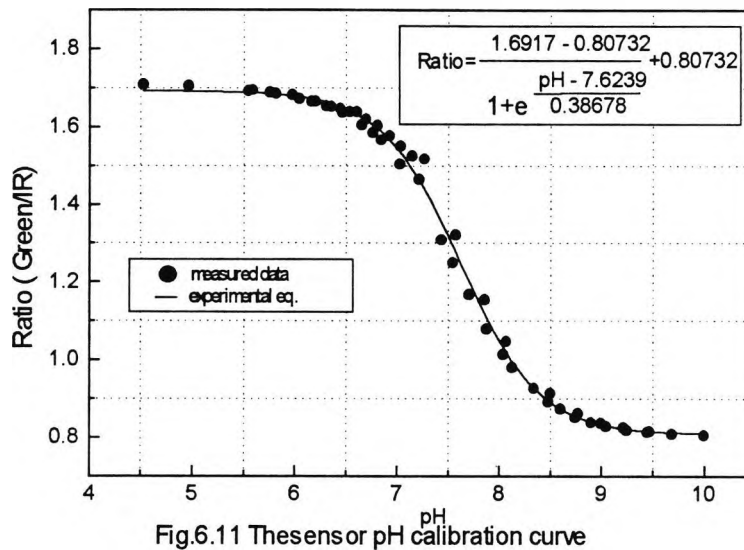


Fig 4 : Calibration curve of the device, over the pH range 6 to 10.

Discussion.

The preliminary stage in the development of fibre optic ammonia sensor, for use in aqueous solutions, has been described. The first stage of construction of the sensor has been evaluated by measuring the performance in measuring pH. Further work on the development of the sensor in which it is evaluated with various gas permeable and ammonia selective membranes will be presented. The objective of demonstrating the use of optical and data acquisition was achieved through the use of two LED emitting at 565 nm and 810 nm, for the signal and reference light channels and PIN diode as a detector. Further, a software program was used to control the device with a PC.

References.

1. Manufactured by Medicines inc., Abingdon, England and Cambridge, Mass., USA. Cooper A.J.
2. Plum F. "Physiol Rev.", 61, 440 519. (1987).
3. Shahriari et. al., "Porous optical fibres for high sensitivity ammonia vapour sensors", Op.Lett. 13, 407 (1988)
4. Zhou et. al. "Porous plastic optical fibre sensors for ammonia measurement", Appl. Op.28, (2022 (1989).
5. Giuliani et. al., "Reversible optical waveguid sensor for ammonia vapours", Op. Lett. 8, 54 (1983).
6. Day, R. A., and A. L. Underwood: "Quantitative Analysis," 6th ed., Prentice-Hall, Englewood Cliffs, NJ, (1991).
7. Grattan, K.T.V., Mouaziz, Z. and Palmer, A.W. " Dual wavelength optical fibre sensor for pH Measurement" Biosensor 3, 17-25, (1987).
8. Day, R. A., and A. L. Underwood: "Quantitative Analysis," 6th ed., Prentice-Hall, Englewood Cliffs, NJ, (1991).
9. Janata, J. "Principal of Chemical Sensors" chapter 4, Plenum Press 1990.

Optical Fiber Ammonia Sensor For Water Quality Measurement

M. Fneer ^(*), J. Kurata ^(**), W. J. O. Boyle ^(*) and K. T. V. Grattan ^(*),

^(*) Measurement and Instrumentation Centre
Department of Electrical, Electronic and Information Engineering
City University, Northampton Square, London EC1V 0HB

^(**) Department of Mechanical Engineering
Kansai University, 3-3-35 Yamate-cho, Osaka 564, Japan

Abstract

The construction and performance characteristics of a novel optical fibre-coupled optrode for ammonia concentration measurements are described. The principle of operation of the optrode represents a development from the principle in the electrochemical sensor used commercially.

Introduction

Optical fibre chemical sensors offer several advantages over the conventional sensors, as such sensors can be used to measure the concentrations concerned without significantly perturbing the sample, and they can be used for continuous sensing. The use of optical fibre sensors (optodes) for chemical species such as ammonia determination has also revealed their considerable potential owing to their inherent advantages such as the elimination of the internal electrodes, which are expensive, bulky, and require careful handling. Optical fibre sensors can potentially be more robust and with the state of knowledge of the appropriate chemistry, progress in the field of chemical sensors based on optical fibres is limited only by the development of appropriate sensor schemes themselves. These sensors may be classified as reversible, in which the reagent phase is not consumed by its interaction with the analyte, or non-reversible, in which the reagent phase is consumed. This work describes the design and construction of an optically based development of a commercial electrochemically based ammonia sensor which has future application in ion-selective sensing. [1]

Experimental development

A schematic diagram of the experimental instrumentation employed is as shown figure 1. The absorption change of the dye solution used, phenol red, is monitored using the change in its absorption spectrum at 565nm, using light from an ultra-bright green LED (40 nm FWHM) of output 120 mcd. The diode is housed in a standard SMA fibre optic housing connector. The reference wavelength is provided by light from an infrared (IR) LED at 810nm (40 nm FWHM) as, at this wavelength, there is very small absorption by the indicator dye, which is not dependent on pH value at this wavelength. The LEDs are operated at room temperature with a fixed current to allow equalization of their temperature. Active stabilization of

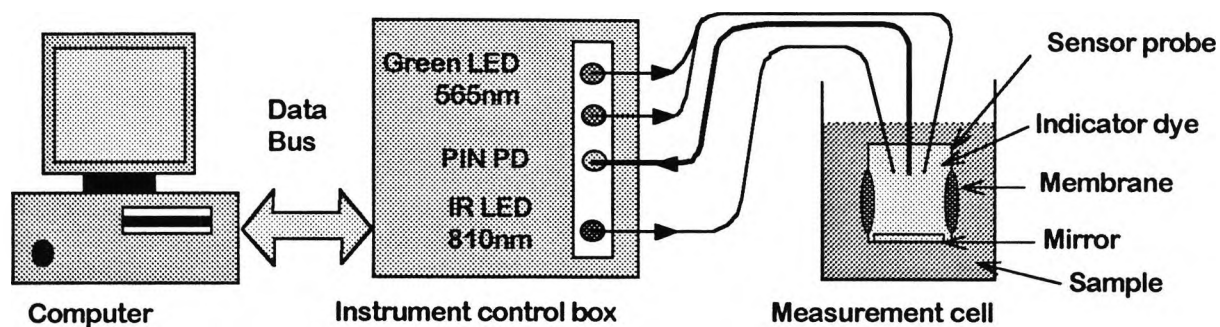


Fig.1 Schematic diagram of the experiment setup

temperature and thus the spectral characteristics of LEDs is an important aspect of the requirements of the system. Light from the green LEDs was coupled into 6 x 600 μ m diameter plastic clad silica fibres (PCSs) of which three fibres were coupled to the output of each green diode. The infrared LED was coupled two fibres of 600 μ m diameter. This bundle of fibres which was approximately 2m long led to the sensor probe, from the instrument control box although the length of this optical cable could be increased considerably without problems. Custom design software determines the sequences of the light pluses and the phased locked loop (PLL) synchronization used. The measured data are acquired, averaged of achieve noise reduction and presented in a suitable graphic format [1]. With further development of the sensor systems, the computer hardware and software could be simplified to be suitable for a single chip microprocessor controller device.

Design of the optical fibre probe

In figure 2, the dimensional schematic of the optical fibre probe is illustrated. The light emitted from the transmitting fibres is refracted at the surface of the mirror, and received by the receiving fibre through the liquid inside the jacket. According to the change of the concentration of the ammonia in the chamber, the colour of the indicator liquid in the chamber after. In order to design the probe with quick response and high accuracy, the ratio of the measured volume inside the probe to the area of membrane was carefully considered, and the relative position of the fibres optimized by using an appropriate model.

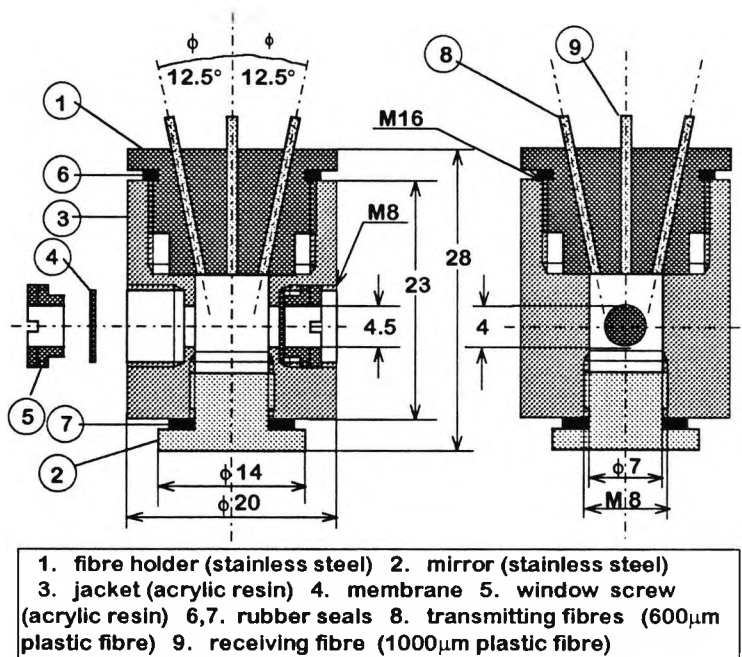


Fig.2 Dimensional schematic of the probe

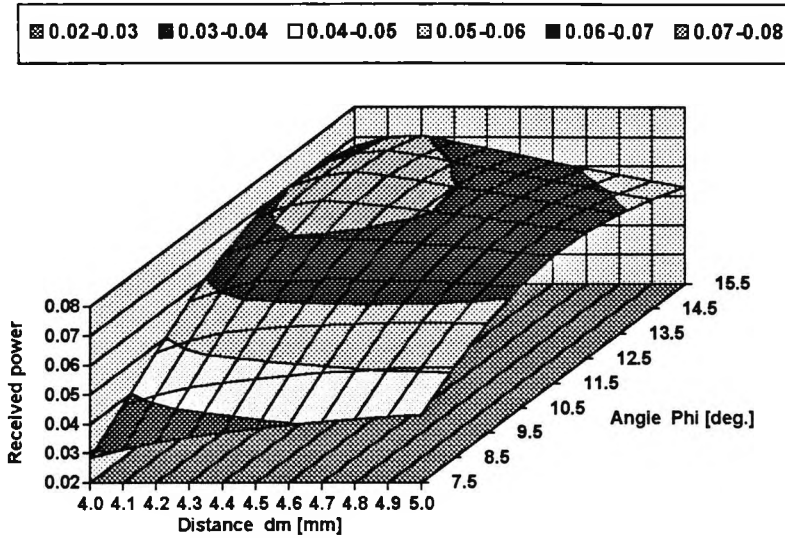


Fig.3 Received power by the receiving fibre

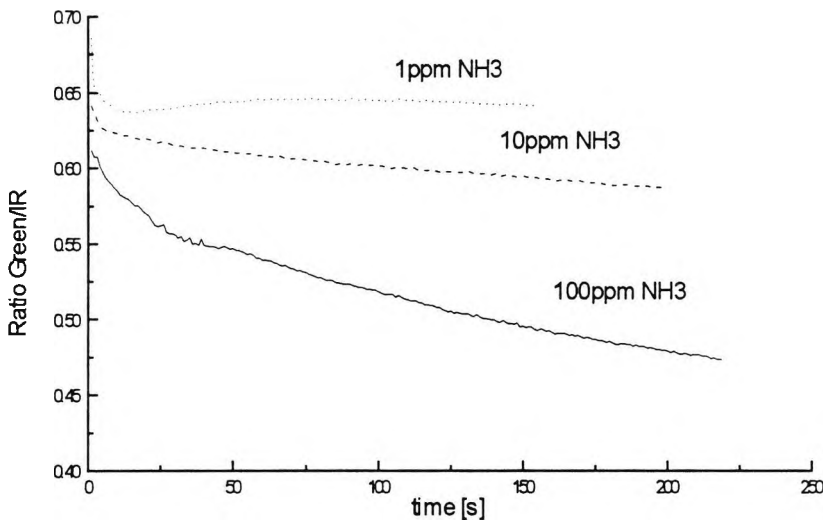


Fig.4 Experimental results using the ionalyzer and phenol red

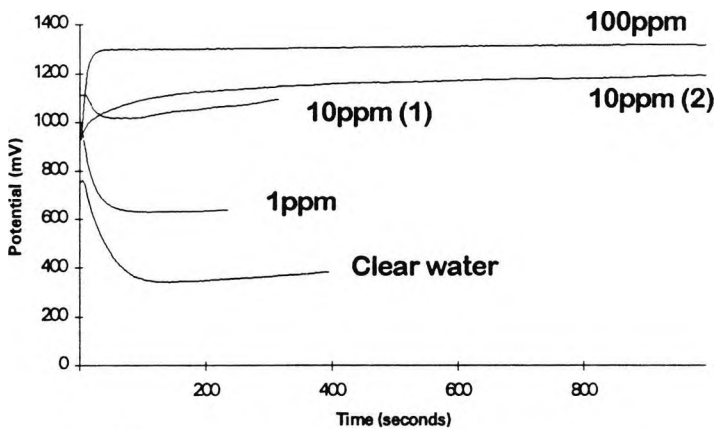


Fig.5 Response of electrochemical sensor to NH3

From the results of a simulation shown in figure 3, it was become clear that the received power was maximum at an angle, $\phi=12.5$ degree for the fiber, as shown in figure 2. As a result, it was clear that the angle of the axis of the illuminated cone of light was approximately 14 degrees from the simulation.

The distance , d_m , between the transmitting fibre and the mirror, strongly influenced the received power, and it become clear from the calculation that a value of $d_m=4.3$ mm would offer the maximum received power. It can be shown that the fixing of this value is particularly important as in the region around $d_m=4.3$ mm the received power would be greatly changed by a small change of the refractive index of the liquid.

Response of the sensor

In operation the sensor volume was filled with a bufered solution containing Ammonia Sulphide buffer and 0.02% phenol red solution which a starting pH of 4.5. Figure 4

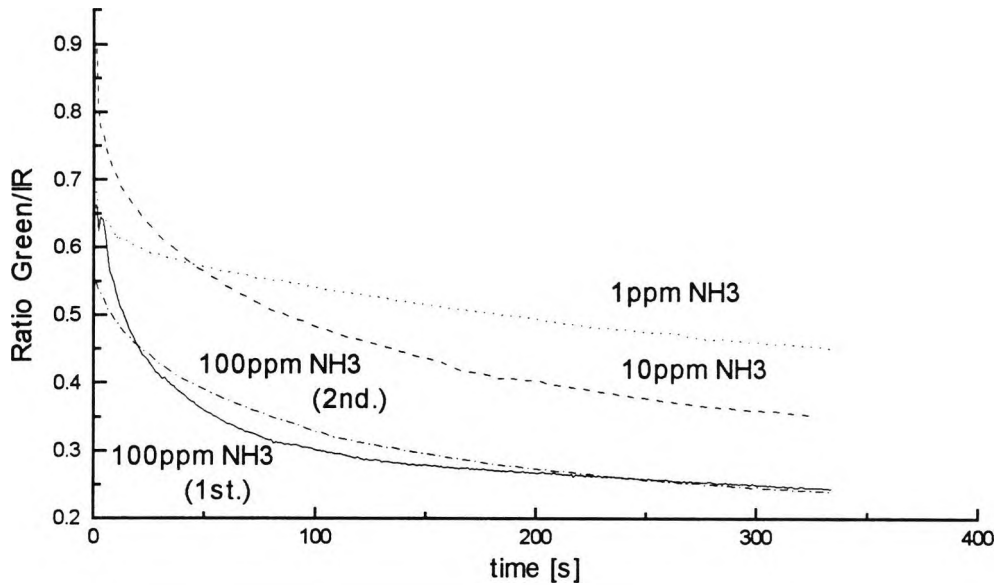


Fig.6 Experimental results using water and phenol red

shows the response of this sensor to three solutions of ammonia in the range 1ppm to 100ppm. It can be seen that compared to the response time to ammonia the response is mainly irreversible, or slowly reversible. Figure 5 shows the response of the electrochemical sensor with similar internal solution other than the dye to the same range in pH. As can be seen the optical probe shows similar response characteristics.

Of some concern is the initial value of pH. For the measurements in figure 4, the initial value of pH=4.5 for the buffered solution, is low compared with the range of the phenol red indicator pH=6.8. Figure 6 shows the two repeated measurements of the response of the sensor and three response to three solutions in the range 1ppm to 100ppm without the buffer, where the internal solution is at a more appropriate starting pH=6.3. The initial values were different from each other because of the change of the pH value of the indicator dye, and the response became stable about 200sec. later from the starting of the measurement.

Conclusion

The response of this sensor was very similar to that of the conventional electrochemical sensor. The ammonia concentration was measured directly without mixing other chemical to the sample. The advantage of this development is that this sensor can be used in the ammonia measurement at different applications such where the electrode would interfere with the measurements.

Reference

[1] M.Fneer, W.J.O. Boyle and K.T.V. Grattan, Development of an optical fiber based colorimetric ammonia sensor, Proc. of Sensor and their Application 7th, pp.236/240, Dublin (1995).

Time Multiplexed Dual Wavelength Fibre Optic Ammonia Sensor

M. Fneer ^(*), K. T. V. Grattan ^(*), W. J. O. Boyle ^(*) and J. Kurata ^(**).

^(*) Measurement and Instrumentation Centre
Department of Electrical, Electronic and Information Engineering
City University, Northampton Square, London EC1V 0HB

^(**) Department of Mechanical Engineering
Kansai University, 3-3-35 Yamate-cho, Osaka 564, Japan

Abstract. A rapid response, inexpensive, fibre optic ammonia sensor which uses a two wavelength time division multiplexed system to measure the change in absorption of an indicator dye with it and providing a reference channel for other losses in the light path has been constructed and described, for use in solution, with solid state LED light source and P-i-n photodetector being employed. The aim has been to investigate the measurement of dissolved ammonia in aqueous solutions, comparing the optical with an electrochemical approach to the measurement.

1. Introduction

The measurement of ammonia in solutions usually requires continuous sampling of data to ensure that the species can be detected at very low concentrations, to achieve an accurate result for effective use of the instrument and the monitoring process. The optimum period of time between each sample analysis depends on the nature of the measurements to be made and the information to be gathered, because each concentration requires a specific time to elapse to reach the maximum detectable level of concentration. In some applications, it is necessary to measure and update the value of a particular sample over a short period of time (i.e. 10 to 60 seconds) as an urgent measurement may be required. An example of this is shown in the measurement of the chlorine content in drinking water at a distribution point in a water treatment plant.^[1]

The authors have previously explored the use of fibre optic based ammonia sensor using colorimetric techniques for water quality measurements^[2], and in this research work the measurement of ammonia in aqueous solution was made using a very simple and cheap method of analysis offering good accuracy yet reasonable cost.

As again, ammonia absorbs at a wavelength of $\lambda = 1600\text{nm}$ ($1.6 \mu\text{m}$) and at this wavelength range only via an Infrared Spectrophotometer that the ammonia concentration can be directly measured. However, this method of analysis is still very expensive to employ and needs an expert technician to make good use of the equipment. Also this method is only a laboratory based approach. At the present time the market needs more field measurements and mobile sensors, which can only realistically be achieved by further development of new sensors and analytical instrumentation.

2. Experiment Arrangement

The schematic diagram of the dual wavelength scheme, with external referencing, is depicted in Figure 1. The basis of the implementation relied on generating two wavelengths i.e. at 565nm and 810nm, using two indicator type LEDs. The first LED was used to monitor the behaviour of the phenol red indicator dye, through the change of the transmitted light intensity, and the second LED was used for the measurement of background absorption and other external interferences, to provide compensation.

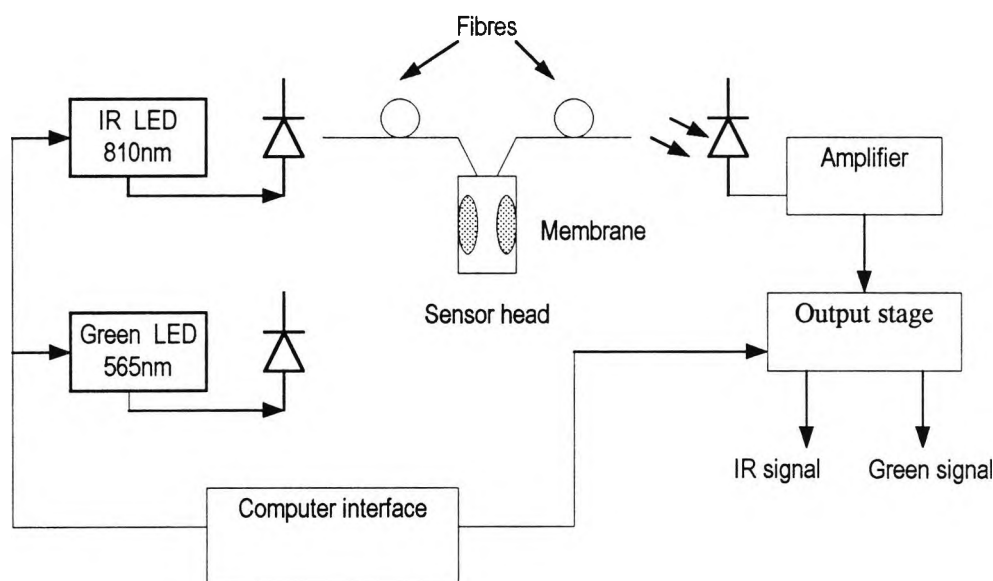


Figure 1: Set-up of the time multiplexed dual wavelength fibre optic ammonia meter

The two optical signals i.e. from both the green and infrared LEDs were time multiplexed using a square wave modulation scheme. The optical signal thus generated was guided through two short lengths of optical fibres to the sensor head via a fibre bundle to the probe head. A reflecting mirror, positioned at the opposite end of the probe head, facing the emitting fibre, was used to reflect the light often passed through the solution. A bundle of fibres positioned around the emitting fibre was used to guide the reflected light back to the detector. Processing of the acquired signal was carried out in order to demodulate the individual signals corresponding to the green and infrared optical channels respectively and to remove the effects of ambient light and other interference effects. Separate outputs for the two signals i.e. absorption and reference signals, were provided and a subsequent ratio was then performed.

3 The Sensor Head Design and Construction

The probe was designed so that the fibre probe head could be easily dipped in to a sample solution. The head probe was made of separate parts, to ensure ease of construction and so that it could readily be taken apart for cleaning when necessary. Due to the acidic nature of the environment where the probe head is being used, it was made from stainless steel to prevent long term effects of corrosion.

A schematic of the probe is shown in figure 2. The first part was made to connect the fibre to the probe head, while the second consisted of a hollow cylindrical body into which large holes were machined along its longitudinal side and sealed with an

ammonia ion selective membrane so that the ammonia ion present in the sample liquid could flow in and out without restriction. The large diameter of the holes was also used to help reduce the chances of air bubbles being trapped inside the optical probe cell, as such air bubbles could cause larger errors in the measurement by disturbing the path of the light beam. If this were to happen, the light intensity being reflected by the mirror and reaching the detector would not necessarily provide a true measurement of the absorption of the light by the dye.

The third part of the probe head consisted of a threaded metallic end whose front surface, facing the fibres, was well polished to produce a highly reflecting surface which was used as a mirror. Its distance from the fibre end was designed to be the path length of the optical cell. A facility for changing this distance was provided through a thread which was machined onto the body of the mirror. The path length with such a system was approximately twice the distance between the fibres end and the polished mirror surface.^[3] work has shown that there was an optimum position of the mirror where maximum light intensity was reflected, which was found experimentally to be around 20mm in this implementation.

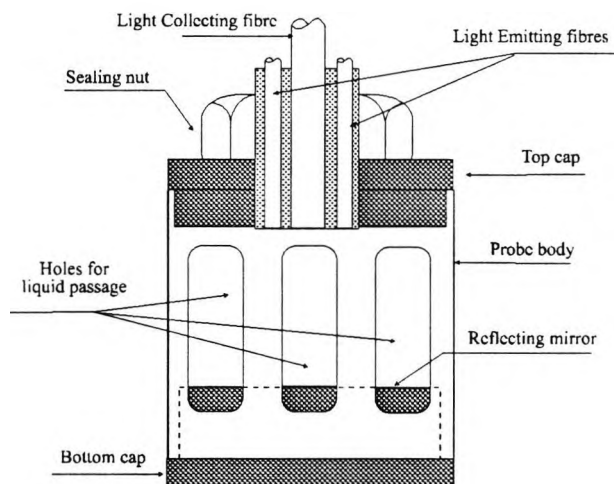


Figure 2 : Schematic design of the sensor head.

4 Membrane Employed

A very thin ($0.2\mu\text{m}$) hydrophobic ion selective-membrane for ammonia gas was incorporated. The life of this membrane was estimated to be about two to three months if the sensor head is stored under dry conditions, and if the sensor head is left with the indicator dye outside the ammonia sample or any other stored solution for a period of time the dye will leave the sensor cell, through the membrane and thus may cause a shorter life time to be seen for the membrane. To maximise the life of the membrane, manufacturer recommendations to store the sensor head, after the measurement, in a prepared 0.01M of ammonia solution should be adhered to.^[4]

5 Results and Discussion.

A sensing test was carried out on the sensor. the first result was obtained using fibre optic sensor at a 100 ppm of NH_3 , going down to 0.001ppm. The aim of this work is to find the lowest detection limit possible of the ammonia concentration that could be measured, i.e. where it was 0.001ppm or less. A further aim was to eliminate the

addition of the chemical reagents in the sensor scheme such as occur in the use of other conventional sensors.

The initial experimental work was carried out without adding a buffer solution to the indicator dye in the sensor cell. This result was obtained and is compared with that for an electrochemical sensor as shown in figure 3.

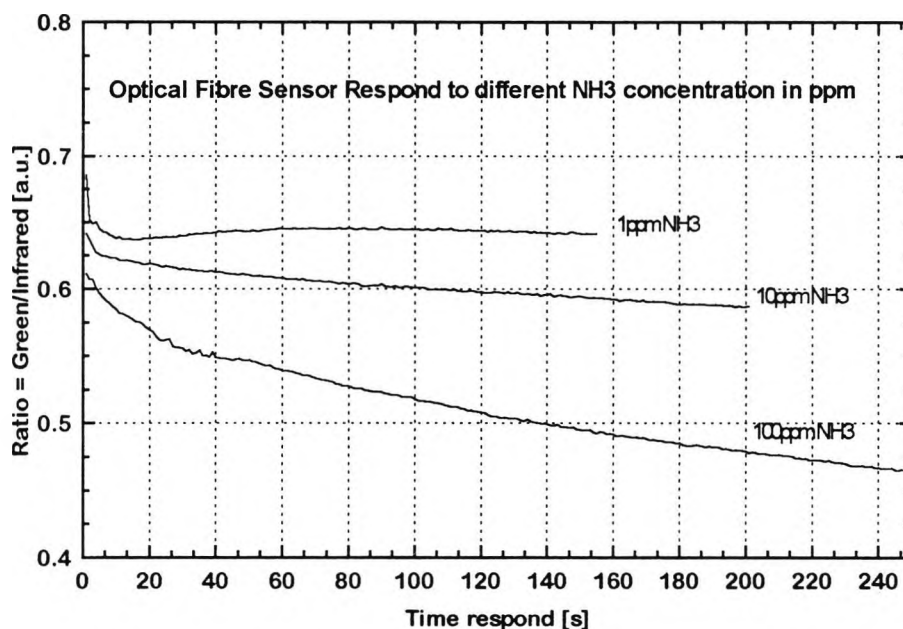


Figure 3: Experimental result for Optical Fibre Sensor response to different concentrations of NH₃.

The sensor response shown was relatively slow compared to the result obtained using an electrochemical electrode. This was thought to result from the belief that the mixing of the ammonia ions inside the sensor cell during the diffusion time, was not uniform at this stage of the measurement. A further experimental test was carried out to improve the sensor dynamic response. However, with diluting the phenol red concentration and reducing the optical path (sensor cell volume), an improvement to the dynamic response of the sensor system was seen.

A further experiment were carried out after a reduction of the cell volume. The sensor volume was filled with a mixture of 0.01M of ammonium chloride (NH₄Cl) as a buffer solution and 0.02% phenol red solution which had a starting pH of 4.5.

Figure 4 shows the response of the sensor to three solutions, of differing ammonia concentrations, in the range 1ppm to 100ppm. It can be seen that, compared to the response time to ammonia, the response is mainly irreversible, or slowly reversible.

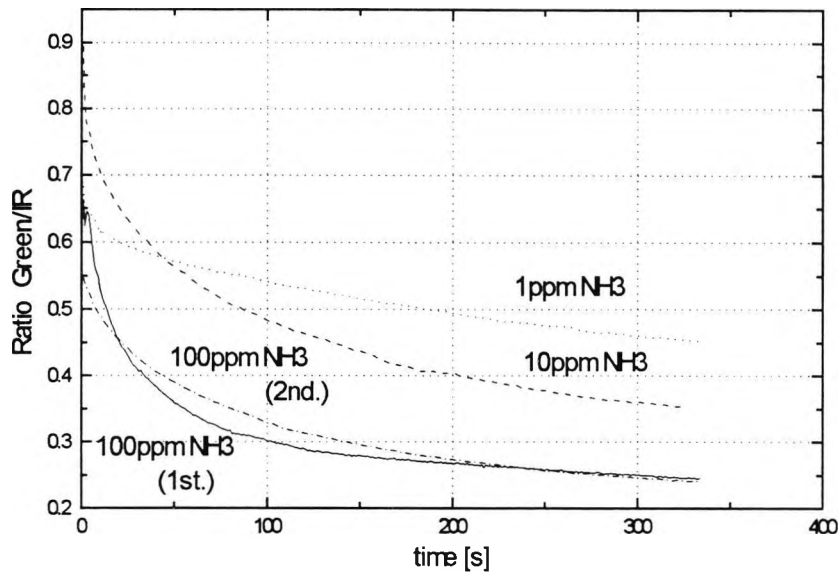


Figure 4: Experimental results using water and phenol red (without buffer)

6 Simulation results

From the experimental results and the simulation results in figure 5 and 6 it is clear that both results, experimental and theoretical agree in the measurement principle. The success of the sensor operation is a first step towards new exploration in the field of fibre optic technology to trust and implement in the water industry of fibre optic technology to trust and implement in the water industry.

All the obtained results was compared with the commercially available Orion ammonia electrode. The work also showed that the practicability of a method for the basic design of the sensor is largely dependent on the dye species and the value of their coefficient of extinction. Moreover, the use of dyes can enhance the sensitivity aspect but does introduce additional error because of the possibility of interfering molecules such as CO_2 . This effect was shown to be very small with the use of ion-selective membrane for the dissolved ammonia monitoring.

A computer model of the diffusion, chemical and optical processes in the sensor was then employed to simulate the behaviour of the sensor and gain more insight into the above behaviour. The model showed that the problem with mixing result from the different diffusivities of the ionic and hydrogenated forms of the optical indicator dye, leading to a build up of the ionic form in the region of the membrane barrier. The model indicated that several factors required addressing in further design of the sensor. These include that the sensor should have a minimum volume and maximum membrane area; it should have some methods for mechanically mixing the buffer solution; and it would be helpful for the sensor to have a simpler geometry with cylindrical symmetry.

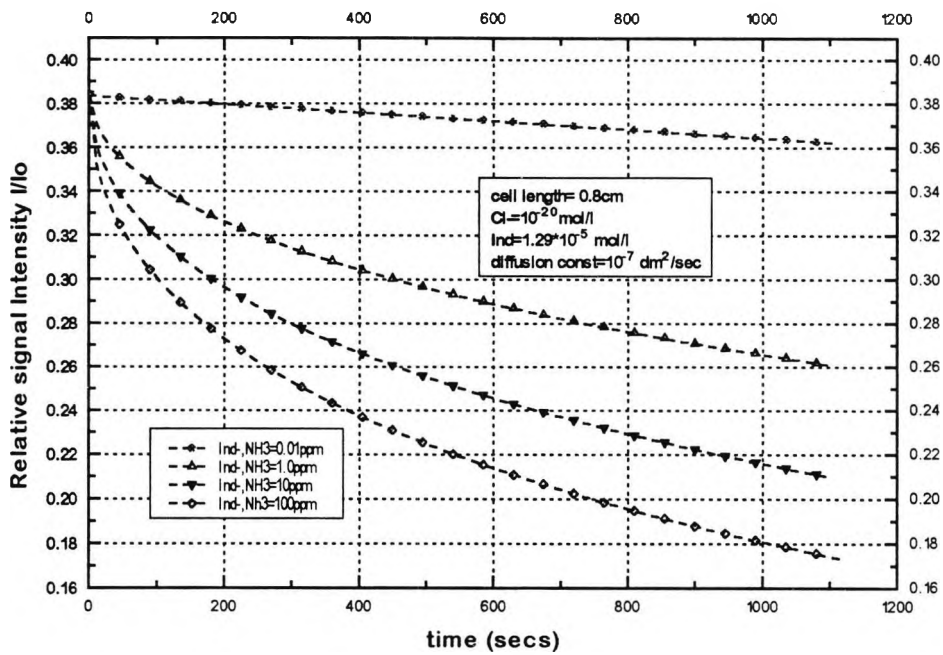


Figure 5: Simulated response of the 'small volume' sensor to ammonia, using unbuffered indicator.

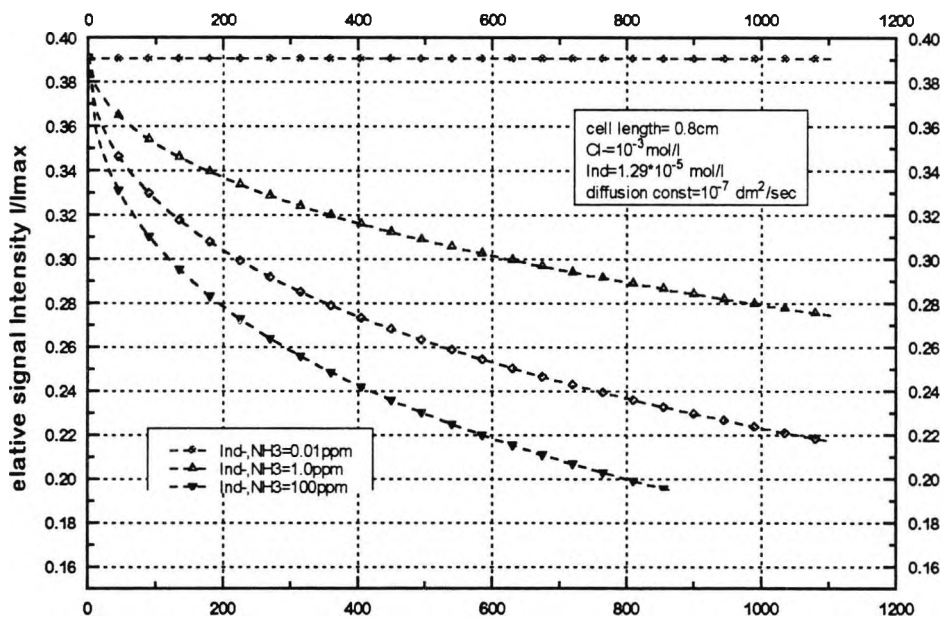


Figure 6: Simulated response of the 'small volume' sensor to Ammonia, using buffered indicator.

7 Discussion

The set of the above experiments carried out in order to calibrate the fibre optic based ammonia sensor was conducted with a variety of water samples. Multiple calibration graphs were then computed from data obtained in different experiments. It was found that the measured optical properties of ammonia were slightly modified by different types of waters. A set of additional experiments led to the following conclusions:

Information about the type of water was needed in order to establish the appropriate calibration curve to use for a particular type of water. Although all the computed calibration curves had a common point (at zero concentration), the curves of these calibration graphs were different. The overall error for each particular type of water was found to be no more than 3%.

The effect of long term running of the sensor was also conducted over a period of three weeks. This was carried out in order to look at the different problems that might arise from such long use and it was found that distilled water did not create any problem. The calibration graphs of the fibre optic sensor were very similar to the conventional ammonia electrode sensor results for the range of concentration from 100 to 0.01ppm.

8 Reference

1. Mouaziz, Z., Briggs, R., Hamilton, I., and Grattan, K.T.V., (1993), "Design and Implementation of a Fibre-Optic-Based Residual Chlorine Monitor", *Sensors & Actuators B- Chemicals*, Vol. 11, p-431 - 440.
2. Fneer, M., W.J.O. Boyle and Grattan K.T.V., "Development of an Optical Fibre Based Colorimetric Ammonia Sensor", *Proceeding of the seventh conference on Sensors and their Applications*, Dublin, (Sept. 1995) pp 236 - 240.
3. Fneer, M., Kurata, J., Boyle, W.J.O., Grattan, K.T.V. "Optical Fibre Ammonia Sensor for Water Quality Measurement", *Proceeding of FOS 11* (May 1996) pp 438 - 441, Sapporo, Hokkaido, Japan.
4. Koryta, J., and Stulik, K., " Ion-Selective Electrode", (1983), Cambridge University Press, Chapter 6.